

P-209
NASA Contractor Report 172587

Critical Joints in Large Composite Primary Aircraft Structures

Volume II — Technology Demonstration Test Report

B. L. Bunin

Douglas Aircraft Company
Long Beach, California 90846

Contract NAS1-16857
June 1985

(NASA-CR-172587) CRITICAL JOINTS IN LARGE
COMPOSITE PRIMARY AIRCRAFT STRUCTURES.
VOLUME 2: TECHNOLOGY DEMONSTRATION TEST
REPORT (Douglas Aircraft Co.) 209 p

N88-28915

Unclas
CSCL 01C G3/05 0164885

Date for general release (shall be 3 years from date of report).



National Aeronautics and
Space Administration

Langley Research Center
Hampton, Virginia 23665

PREFACE

This test report was prepared by Douglas Aircraft Company, McDonnell Douglas Corporation, under contract NAS1-16857, "Critical Joints in Large Composite Aircraft Structure." This program was conducted as part of the NASA Aircraft Energy Efficiency (ACEE) program.

The research program was monitored by Andrew J. Chapman, ACEE Composites Project Office, Langley Research Center, NASA. Bruce L. Bunin was the Douglas Project Manager.

In addition to the author, Douglas personnel contributing to this program included D. J. Watts and W. D. Nelson, prior Project Managers, L. J. Hart-Smith and J. B. Black, Stress Analysis, L. P. Marius, Design, J. V. Walker, and E.P. Moenning, Materials, G. C. Janicki and P. J. Marra, Manufacturing R&D, and R. L. Oswald, Program Administration.

PRECEDING PAGE BLANK NOT FILMED

THE
FEDERAL BUREAU OF INVESTIGATION
UNITED STATES DEPARTMENT OF JUSTICE
WASHINGTON, D. C. 20535

10

RECEIVED FOR THE DIRECTOR

CONTENTS

Section		Page
1	INTRODUCTION	1
2	STRINGER TRANSITION TEST	
	2.1 Test Article	3
	2.2 Instrumentation	16
	2.3 Test Setup	22
	2.4 Test Program - Procedures and Results	25
3	TECHNOLOGY DEMONSTRATION SUBCOMPONENT TESTS	
	3.1 Test Articles	40
	3.2 Instrumentation	46
	3.3 Test Setup	50
	3.4 Test Program - Procedures and Results	56
4	TECHNOLOGY DEMONSTRATION TEST PROGRAM	
	4.1 Test Article	62
	4.2 Instrumentation	72
	4.3 Test Setup	78
	4.4 Test Program - Procedures and Results	84
5	TECHNOLOGY DEMONSTRATION ARTICLE - REBUILD AND TEST	91
6	CONCLUSIONS	104
7	REFERENCES	107

PRECEDING PAGE BLANK NOT FILMED

LIST OF ILLUSTRATIONS

<u>Figure</u>		<u>Page</u>
1	Joint Transition Specimen	4
2	Stringer Transition Concept	5
3	Stringer Tool and Fabrication Concept	6
4	Skin/Stringer Prior to Machining	7
5	Stringer Transition Joint - Plan View	9
6	Stringer Transition Joint - Side View (with Lower Splice)	10
7	Stringer Transition Cross-Sections	11
8	Stringer Joint Specimen - Thickness Transitions	12
9	Stringer Joint End Fitting - Plan View	13
10	Stringer Joint End Fitting - Side View	14
11	Stringer Joint Test Specimen	15
12	Stringer Transition - Strain Gage Locations	17
13	Stringer Transition - Strain Gage Locations	18
14	Stringer Transition - Strain Gage Locations	19
15	Data Acquisition System	21
16	Stringer Joint Test Setup	23
17	Stringer Transition Specimen Installed in Test Machine	24
18	Stringer Transition Test - Failed Specimen	26
19	Stringer Transition Test - Failed Specimen	27
20	Stringer Transition Test - Failed Specimen	28
21	Stringer Transition Test - Failed Specimen	29
22	Stringer Transition Test - Failed Specimen	30
23	Stringer Transition Test - Failed Specimen	31
24	Photo-Elastic Survey - Stringer Blade Applied Load = 40,000 Pounds	35
25	Photo-Elastic Survey - Stringer Blade Applied Load = 60,000 Pounds	36
26	Photo-Elastic Survey - Stringer Blade Applied Load = 80,000 Pounds	37
27	Photo-Elastic Survey - Upper Splice Applied Load = 40,000 Pounds	38
28	Photo-Elastic Survey - Upper Splice Applied Load = 80,000 Pounds	39

LIST OF ILLUSTRATIONS (Cont.)

<u>Figure</u>		<u>Page</u>
29	Demonstration Subcomponent Concept	41
30	Subcomponent #1 - Plan View	42
31	Subcomponent #1 - Side View	43
32	Subcomponent #2 - Plan View	44
33	Subcomponent #2 - Side View	45
34	Subcomponent #1 - Strain Gage Locations	47
35	Subcomponent #2 - Strain Gage Locations	48
36	Demonstration Subcomponent #1	51
37	Demonstration Subcomponent #2	52
38	Side Restraint System - Subcomponent #1	53
39	Side Restraint System - Subcomponent #1	54
40	Side Restraint System - Subcomponent #2	55
41	Subcomponent #1 - Failed Specimen	58
42	Subcomponent #1 - Failed Specimen	59
43	Subcomponent #2 - Failed Specimen	60
44	Subcomponent #2 - Failed Specimen	61
45	Technology Demonstration Joint	63
46	Technology Demonstration Specimen Assembly	64
47	Technology Demonstration Article - End Fitting	65
48	Technology Demonstration Article - Cross-Sections	66
49	Technology Demonstration Specimen Assembly	68
50	Technology Demonstration Specimen Assembly	69
51	Technology Demonstration Specimen Assembly	70
52	Technology Demonstration Specimen - Test Section	71
53	Technology Demonstration Article - Strain Gage Locations	73
54	Test Article After Instrumentation - Spar Cap Side	74
55	Test Article After Instrumentation - Spar Cap Side	75
56	Test Article After Instrumentation - Skin Side	76
57	Test Article After Instrumentation - Skin Side	77
58	Technology Demonstration Test Setup	79
59	Technology Demonstration Test Setup	80
60	Technology Demonstration Test - Load Actuators	81
61	Technology Demonstration - Lower End Fitting	82

LIST OF ILLUSTRATIONS (Cont.)

<u>Figure</u>		<u>Page</u>
62	Technology Demonstration - Upper End Fitting	83
63	Technology Demonstration - Side Restraint	83
64	Technology Demonstration Test #1 - End Fitting Failure	85
65	Technology Demonstration Test #1 - End Fitting Failure	86
66	Technology Demonstration Test #1 - End Fitting Failure	87
67	End Failure Representation	89
68	C-Scan Results - Spar Cap Member	90
69	Joint Re-Test with Aluminum Replacement Part	92
70	Joint Re-Test with Aluminum Replacement Part	93
71	Joint Re-Test with Aluminum Replacement Part	94
72	Joint Re-Test Setup	95
73	Demonstration Joint Test Section	98
74	Demonstration Side Restraint System	99
75	Technology Demonstration - Test Section Failure	100
76	Technology Demonstration - Test Section Failure	101
77	Technology Demonstration - Test Section Failure	102
78	Technology Demonstration - Test Section Failure	103

~~PRECEDING PAGE BLANK NOT FILMED~~

SUMMARY

A program was conducted to develop and demonstrate the technology for critical structural joints of a composite wing structure that meets all the design requirements of a 1990 commercial transport aircraft.

The program was divided into two phases. Phase I was completed in September of 1983, during which the procedures for bolted composite joint design and analysis were developed. Tests were conducted at the element level to supply the empirical data required for methods development (Reference 1). Large composite multirow bolted joints were tested to verify the selected design concepts and for correlation with analysis predictions (Reference 2). The Phase I summary is reported in Reference 3. The Phase II program included additional tests to provide joint design and analysis data, and culminated with several technology demonstration tests of a major joint area representative of a commercial transport wing.

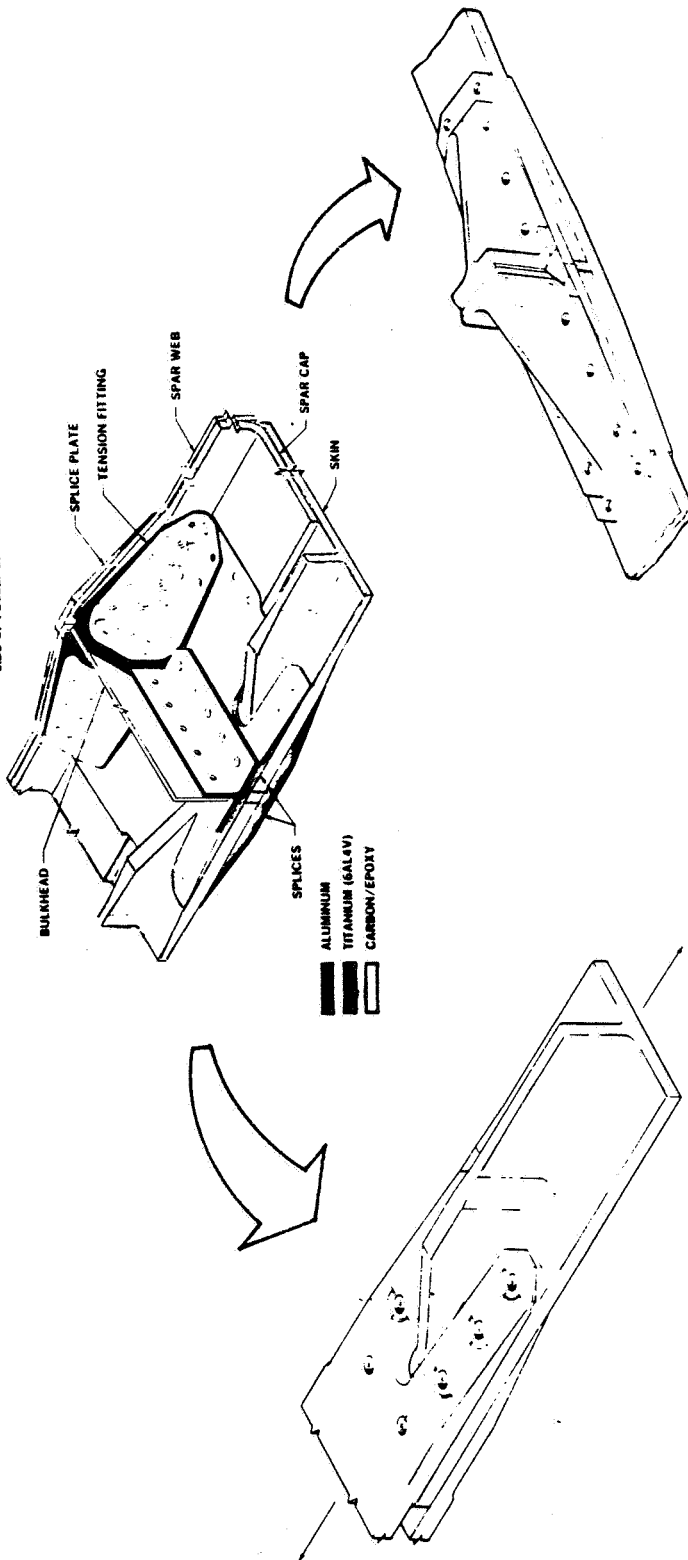
The region selected for the Phase II test program was the wing root splice at the lower rear spar at the side of the fuselage. Because of the complexity of this region, the test program was formulated to investigate portions of this area individually. The stringer transition joint was tested as a separate specimen, while portions of the corner joint representing the skin, spar cap and spar web splices were tested as subcomponents. The test program, as illustrated on the following page, culminated with the testing of a large specimen representing the skin and spar cap corner splice with the skin terminating just aft of the first stringer.

PRECEDING PAGE BLANK NOT FILMED

SECRET TOP SECRET

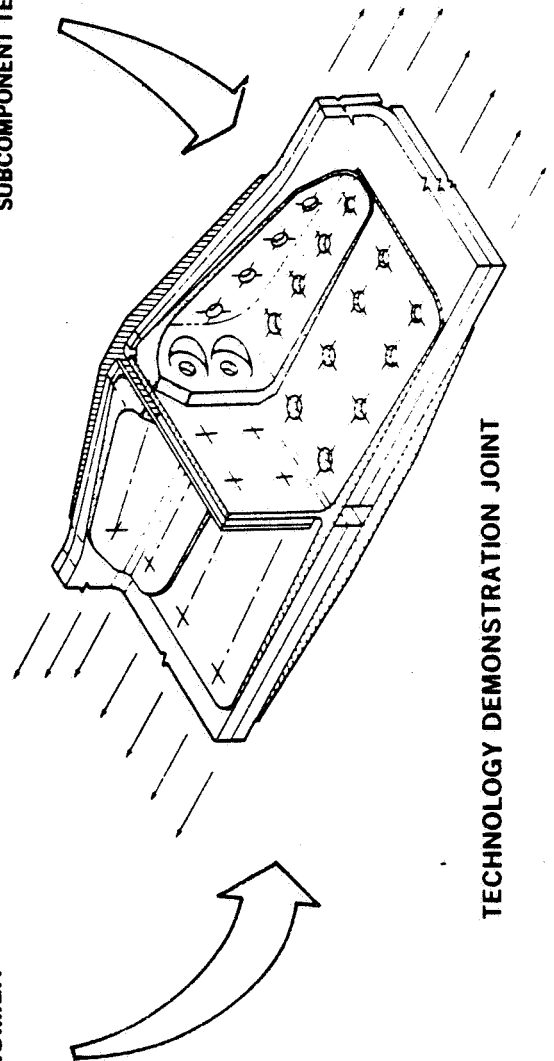
COMPOSITE WING STRUCTURE LOWER REAR SPAR AND STRINGER CONCEPTUAL JOINT

DHEDRAL AND SWEEP ANGLES AT
SIDE OF FUSELAGE BULKHEAD NOT SHOWN



JOINT TRANSITION SPECIMEN

SUBCOMPONENT TEST SPECIMEN



TECHNOLOGY DEMONSTRATION JOINT

SECTION 1

INTRODUCTION

This report contains the results of several design verification and technology demonstration tests conducted during Phase II of the Critical Joints Program. The major objective of this investigation was to develop and demonstrate the technology for critical structural joints of a composite wing structure that meets all the design requirements of a 1990 commercial transport aircraft. The specific objective of the test program described in this report was to verify the structural integrity of selected design concepts and to provide data for correlation with analytical predictions.

The procedures and results for four large multirow bolted joint tests are presented. The first to be tested was a wing skin/stringer transition specimen representing a stringer runout and skin splice on the wing lower surface at the side of the fuselage attachment. The second and third specimens to be tested were referred to as "technology demonstration subcomponents." These two specimens were tested as representative sections of the upcoming technology demonstration article which was the fourth and final specimen to be tested in Phase II of the program. The technology demonstration article consisted of a large bolted joint representing the lower wing skin and rear spar joint at the side of the fuselage joint. The specimen extended forward from the rear spar up to but not including the aft stringer.

All tests were static tension tests. In some cases, the joint specimens were loaded to what was considered a "limit load" level and, following a return to zero load, were visually inspected for any damage or flaws that may have propagated under load. In each case, the joint elements representing the wing structure to be attached were made of fibrous composite laminates. The Ciba-Geigy 914/T300 material system was used in 10-mil tape form. All laminates used a (37.5% 0°, 50% ± 45°, 12.5% 90°) fiber pattern. The splice members in each case were metallic, using combinations of aluminum and titanium materials.

This report is divided into three separate sections. Each section includes a discussion of the test article, instrumentation, test setup, test procedures, and test results for each of the four specimens. Because of their similarity, the two demonstration subcomponent tests are discussed in a single section.

SECTION 2.1
STRINGER TRANSITION TEST
TEST ARTICLE

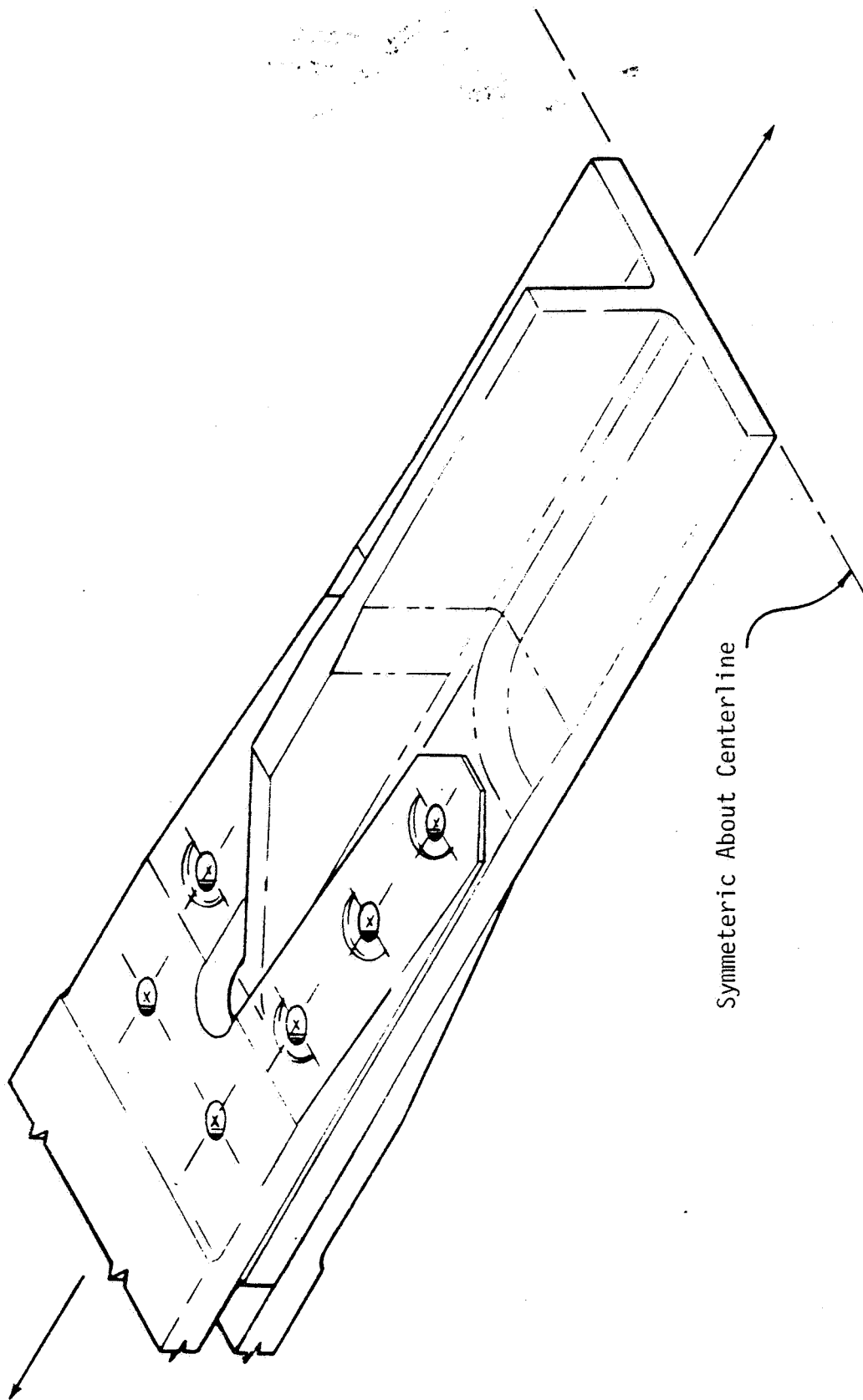
The stringer transition specimen was the first of several large multirow bolted joints to be tested in Phase II. The concept, shown in Figure 1, consists of an integral wing skin and blade stringer, representative of the lower wing surface. The selected design approach transitions the stringer into the skin as it meets the bolted shear joint at the side of the fuselage, as opposed to providing a bolted connection through the stringer itself to the center wing box. The stringer blade is scarfed along the length of the bolted joint while a thickness buildup occurs in both the skin and the stringer.

Several concepts for the fabrication of the integral skin and stringer were evaluated from both a manufacturing and structural integrity standpoint. The design objective was to provide a smooth transition from the skin structure to the bolted joint with a minimum of complexity in the fabrication procedures without sacrificing any structural requirements. Of primary concern was the tip of the stringer transition, where high load transfer combined with stress concentration effects could lead to critical out-of-plane forces. Thus, the selected concept maintained continuous plies wherever possible and thickness transitions were achieved with taper angles that were shallow enough to reduce peel forces below critical levels.

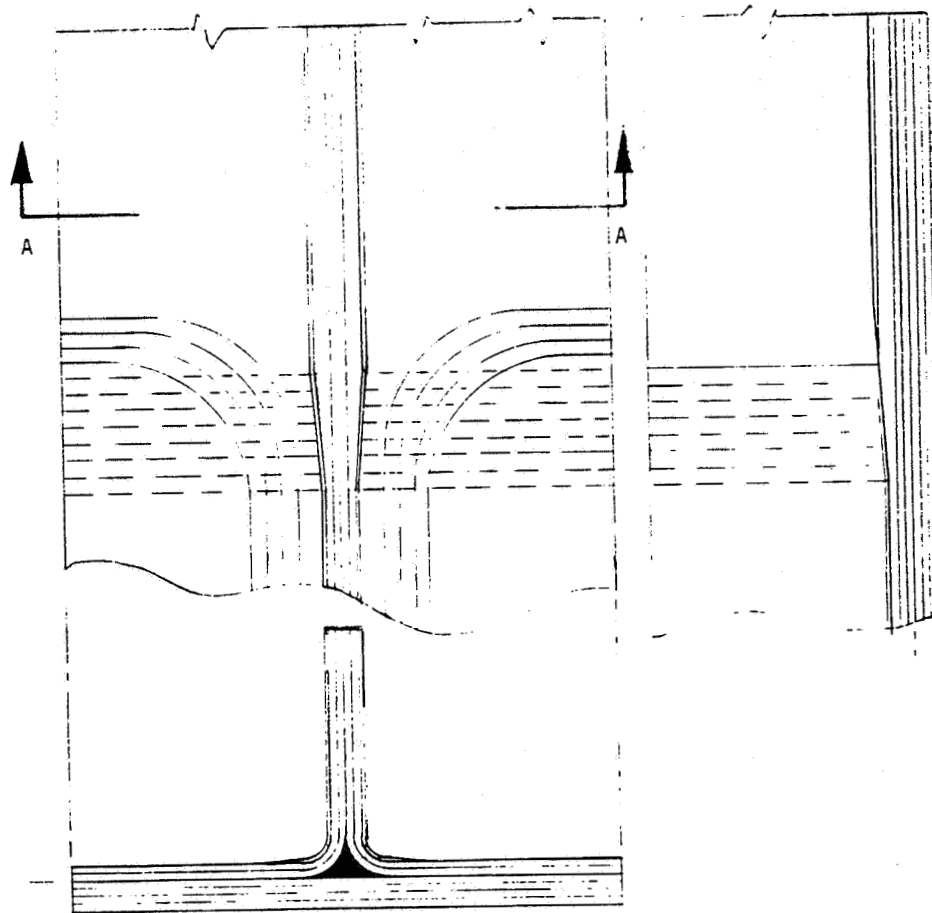
The skin buildup at the stringer end was accomplished by interspersing 8 plies among the 16 plies which form the upper portion of the skin (and turn up to form the stringer blade). The blade end is then thickened along with the skin, as shown in Figure 2. Four additional plies were added on each side of the basic blade to buildup the required blade thickness and are fanned out at the skin buildup. These additional plies are on the external surface and are not interspersed. The tooling concept for the specimen is illustrated and explained in Figure 3. This specimen

FIGURE 1

JOINT TRANSITION SPECIMEN



ORIGINAL PAGE IS
OF POOR QUALITY



BASIC SECTION

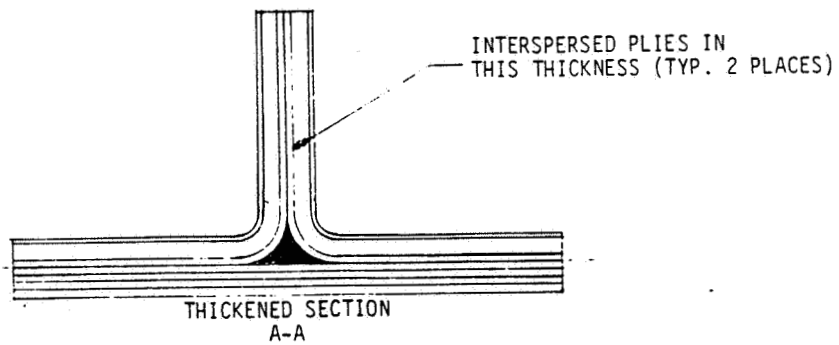
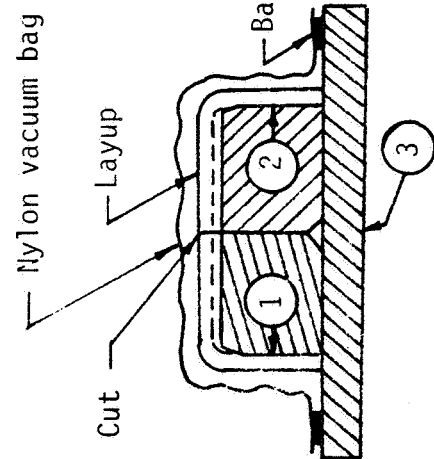
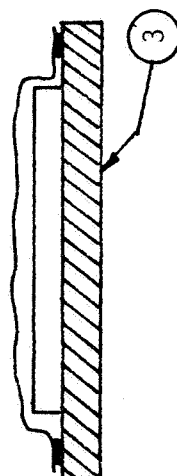


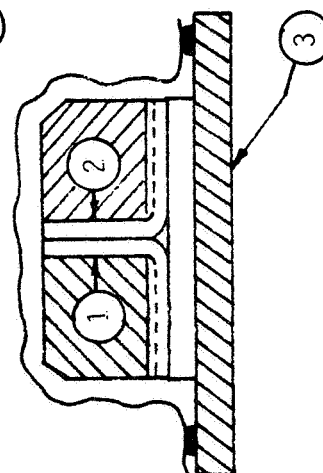
FIGURE 2 STRINGER TRANSITION CONCEPT



Steps
a, b



c.

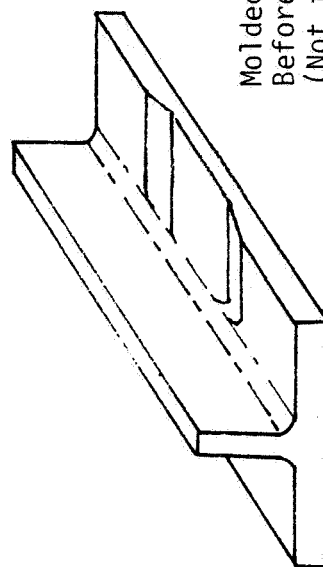


d, e.

Tools: (1), (2) 7075-T6 Aluminum mandrels.
(Densification and curing tools).
(3) 7075-T6 Aluminum caul plate

Fabrication:

- Mandrels (1), (2) are placed together for layup of variable thickness channel.
- Plies densified under vacuum bag.
- 32 plies of flat skin laid up and densified on caul plate (3).
- Densified channel is cut and two mandrels with layups repositioned on 32-ply skin layup with structural adhesive in joints.
- Assembly is bagged, autoclave cured and trimmed to final dimensions.



Molded Stringer
Before end trim
(Not to scale)

FIGURE 3 STRINGER TOOL AND FABRICATION CONCEPT

was fabricated, as shown in the figure, by laying up a channel section, cutting the section in half, and placing these sections back to back to form the blade and upper portion of the skin. This assembly is then placed on top of additional plies to form the required skin thickness and the part is cured. The fabrication concept was developed with a complete cover panel in mind, extending from leading edge to trailing edge. The procedure would consist of laying up several channel sections and placing them back to back (without cutting the section in half). The cured laminate is shown in Figure 4, prior to being machined to final dimensions.

Details of the stringer transitions test article are presented in Figures 5 through 10. These figures indicate all the pertinent specimen dimensions including laminate thicknesses and fastener sizes. The specimen was fabricated with a stringer transition at each end, and the titanium splice plates were extended to form the points of attachment to the test machine. This approach greatly simplified the specimen and its assembly by combining the test section joints with the end fittings. The splice plate was machine tapered and spotfaced at the fastener holes. All fasteners were made of titanium. A close-up view of the unbroken end of the specimen after testing is shown in Figure 11.



ORIGINAL PAGE IS
OF POOR QUALITY

ORIGINAL PAGE IS
OF POOR QUALITY

FIGURE 4 SKIN/STRINGER PRIOR TO MACHINING

ORIGINAL PAGE IS
OF POOR QUALITY

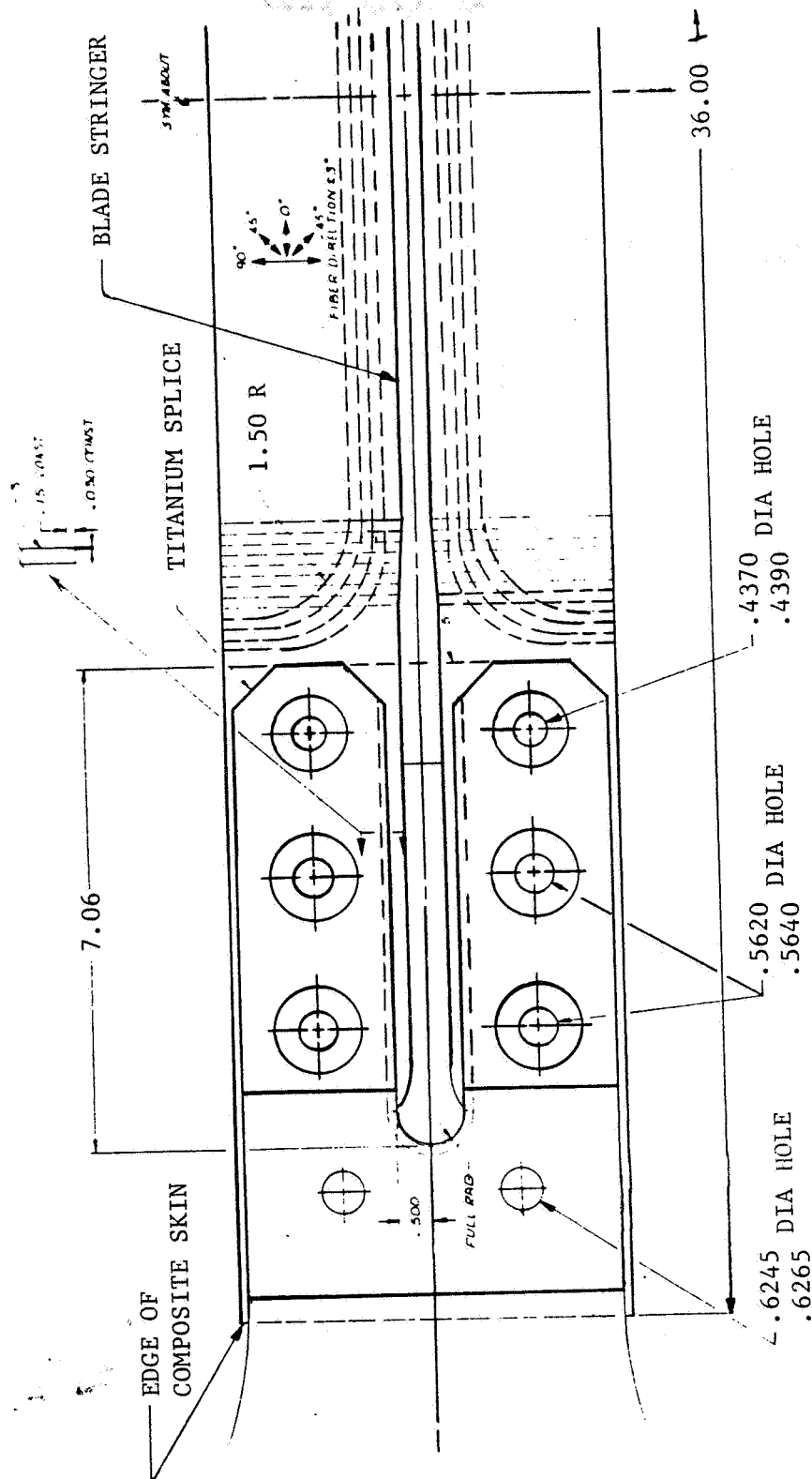


FIGURE 5 STRINGER TRANSITION JOINT - PLAN VIEW

ORIGINAL PAGE IS
OF POOR QUALITY

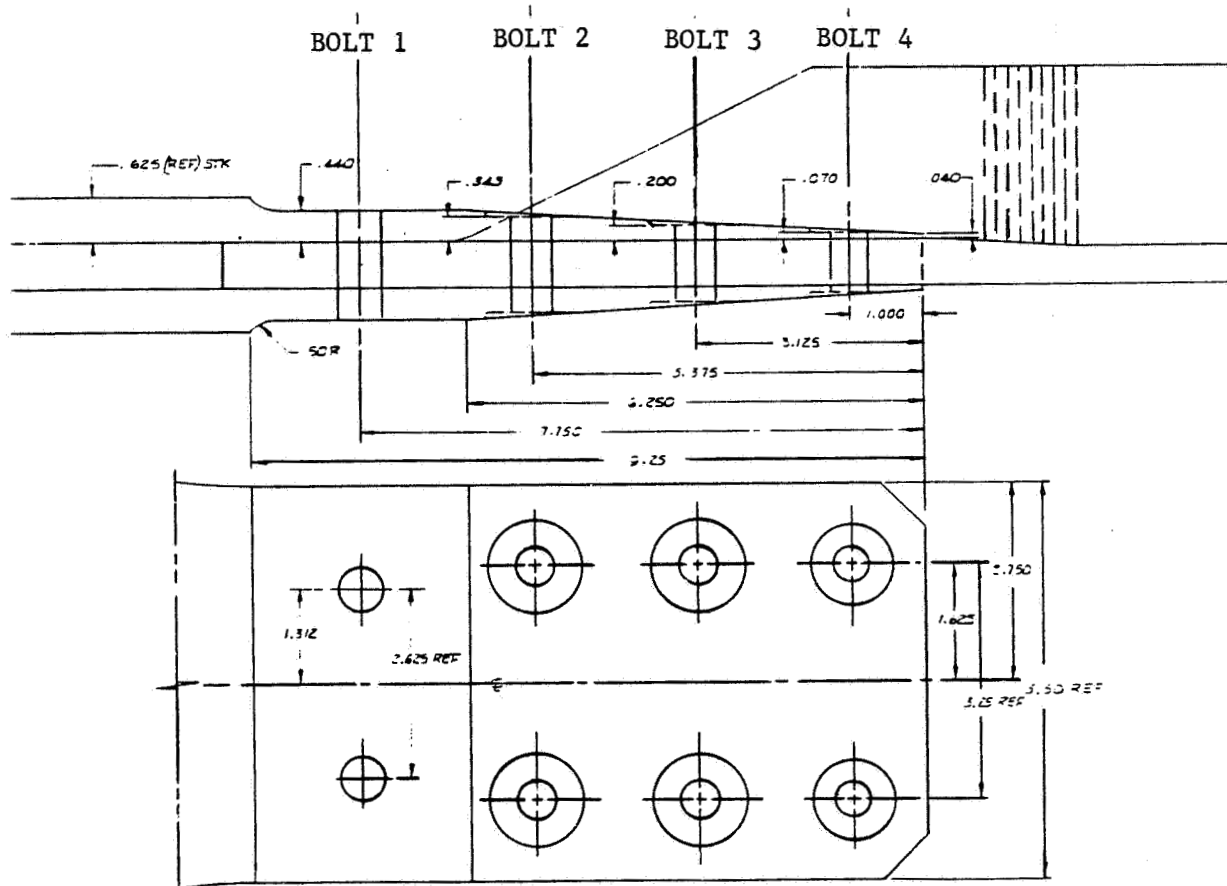
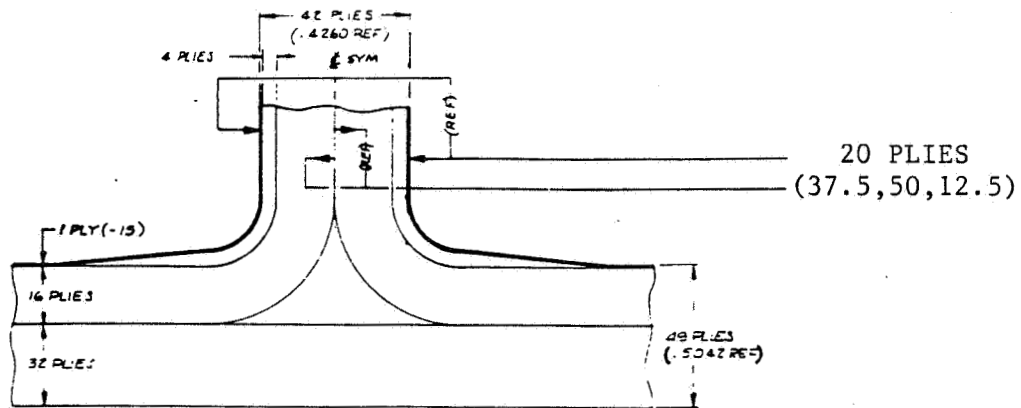


FIGURE 6 STRINGER TRANSITION JOINT
- SIDE VIEW (WITH LOWER SPLICE)

ORIGINAL PAGE IS
OF POOR QUALITY

CONSTANT
SECTION



JOINT
AREA

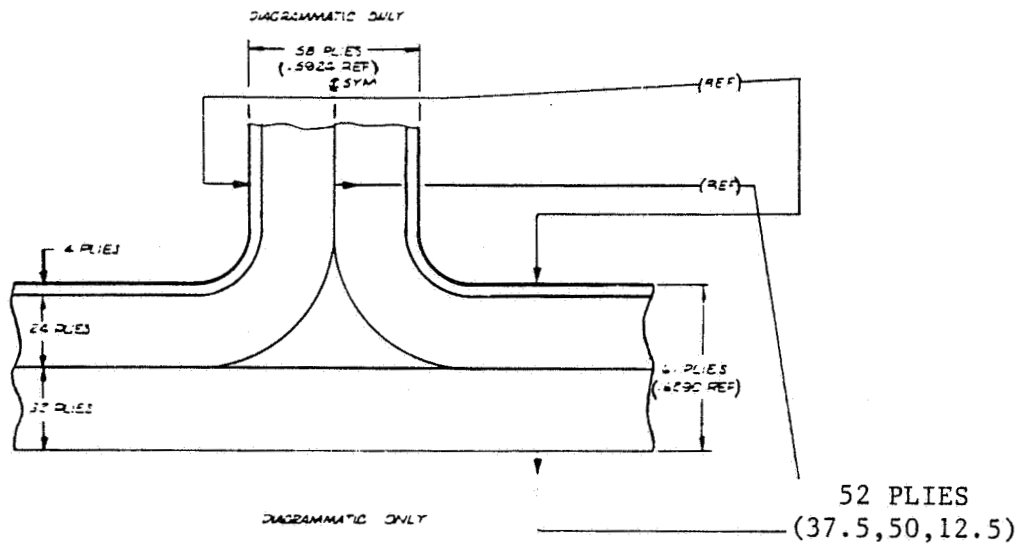


FIGURE 7 STRINGER TRANSITION
CROSS-SECTIONS

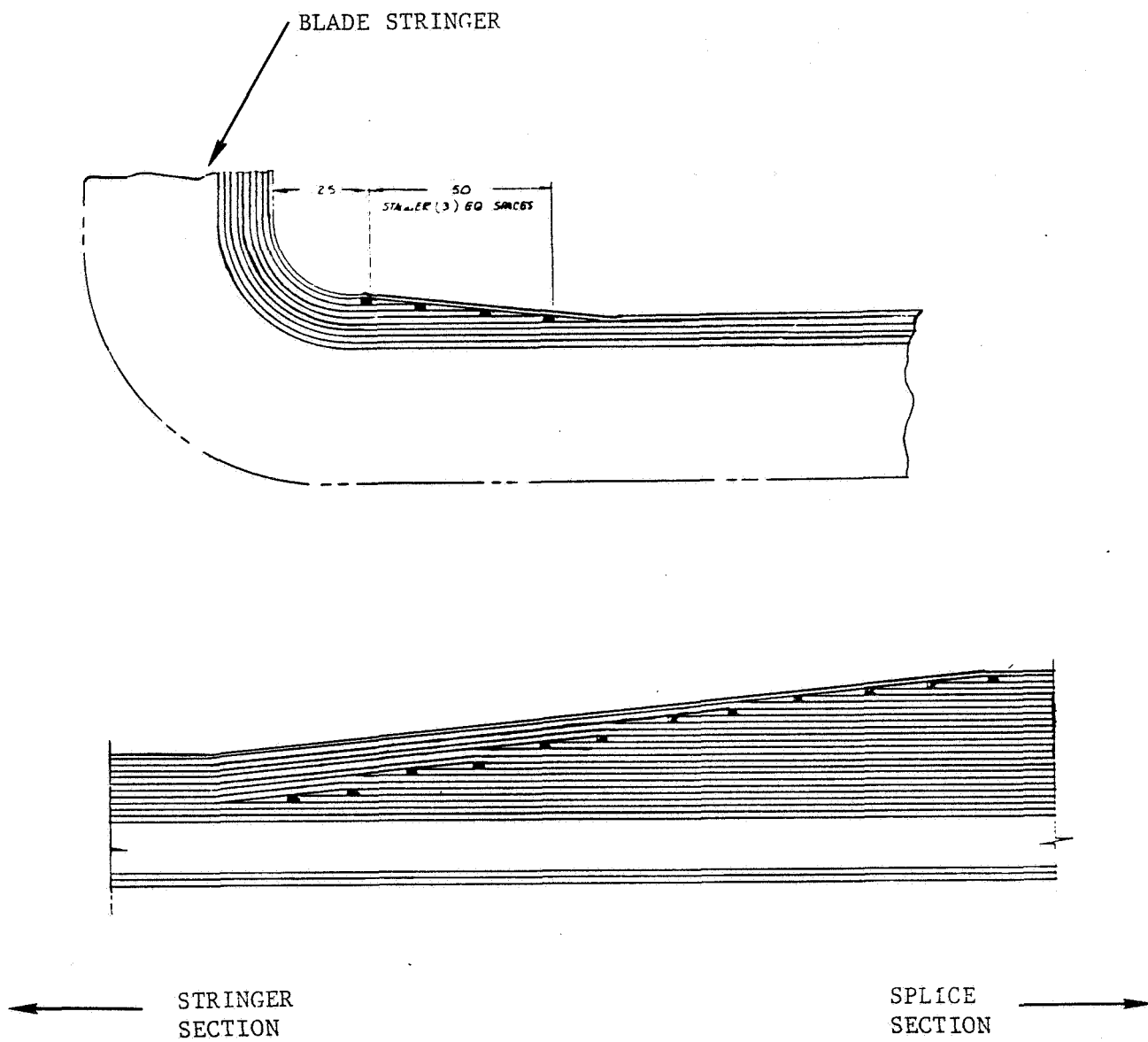
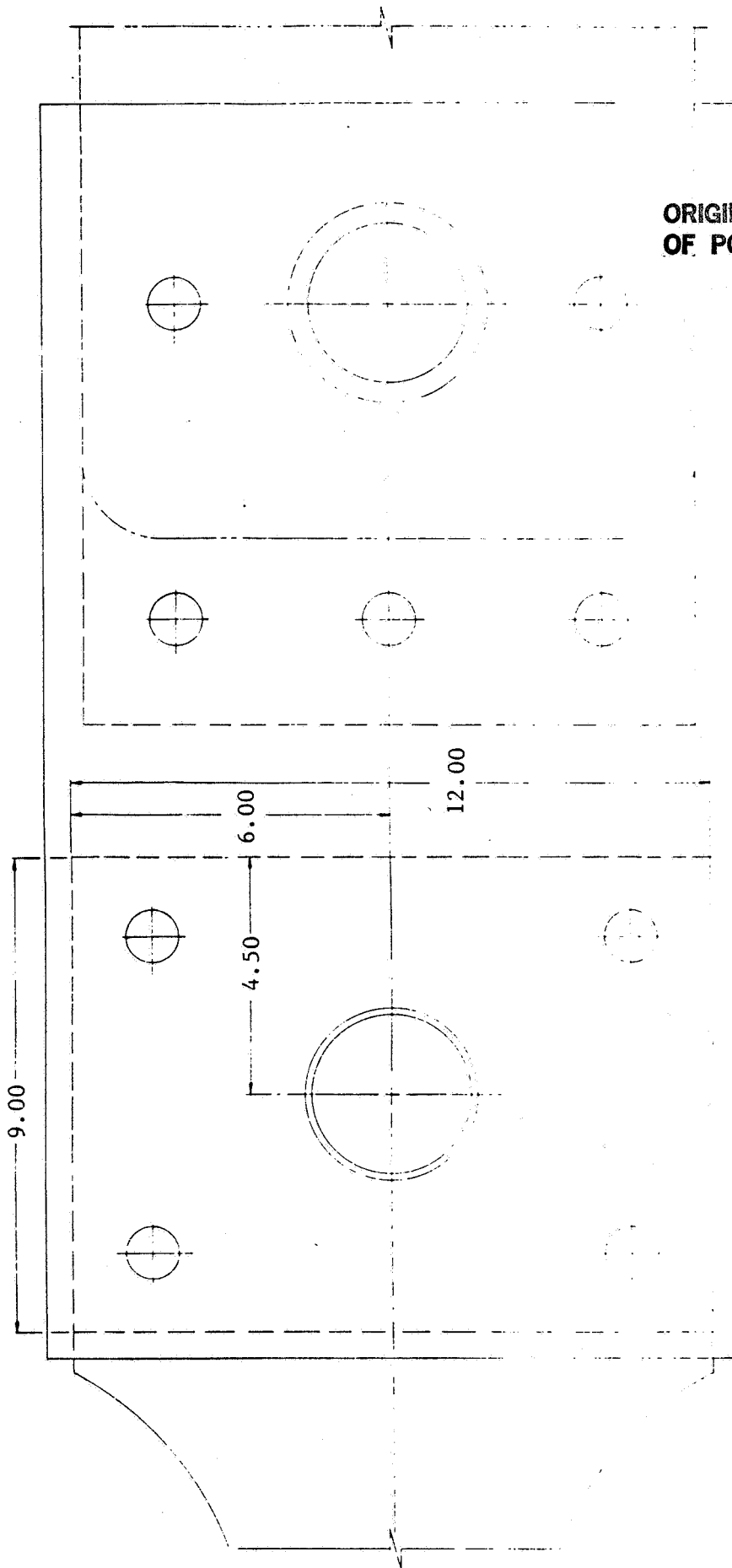


FIGURE 8 STRINGER JOINT SPECIMEN -
THICKNESS TRANSITIONS



ORIGINAL PAGE IS
OF POOR QUALITY

FIGURE 9 STRINGER JOINT END FITTING - PLAN VIEW

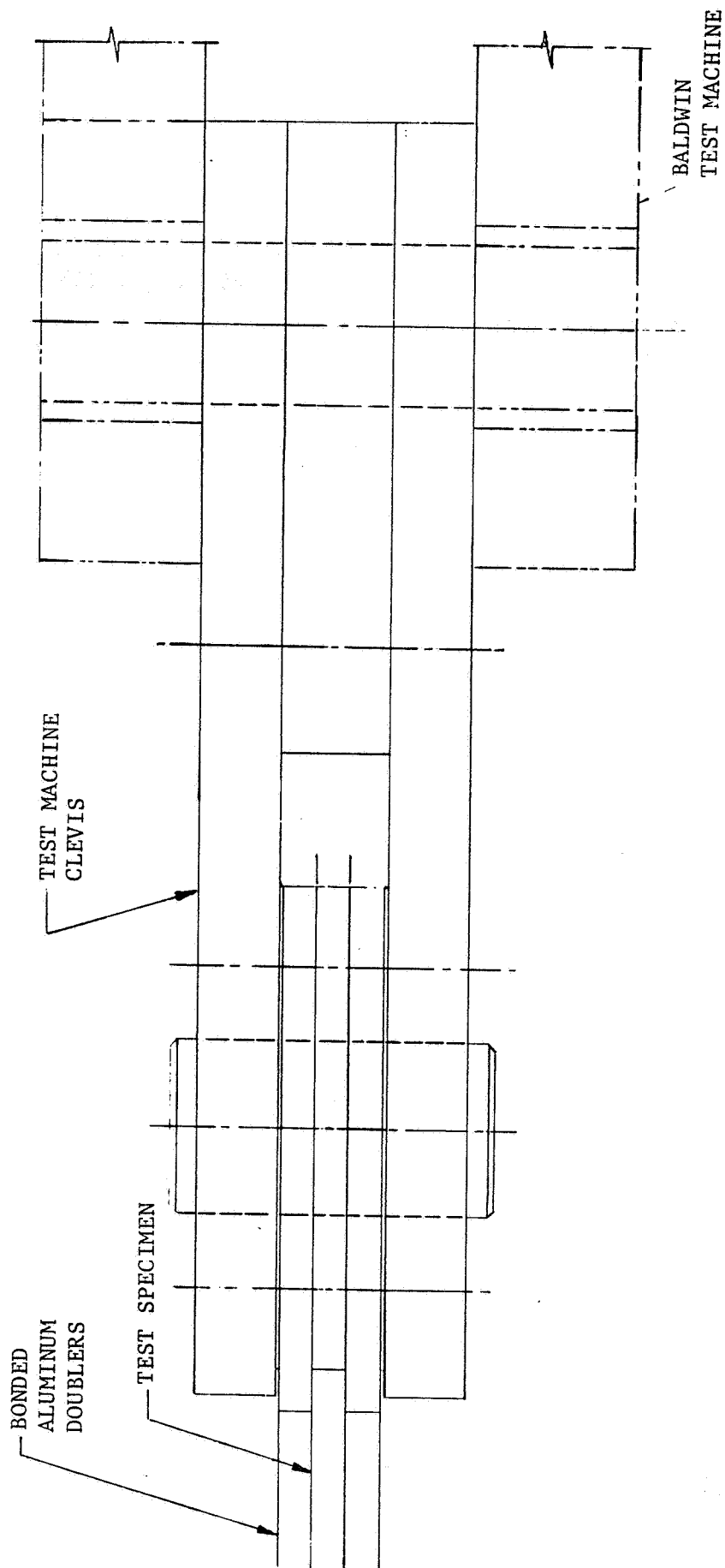


FIGURE 10 STRINGER JOINT END FITTING - SIDE VIEW

ORIGINAL PAGE IS
OF POOR QUALITY

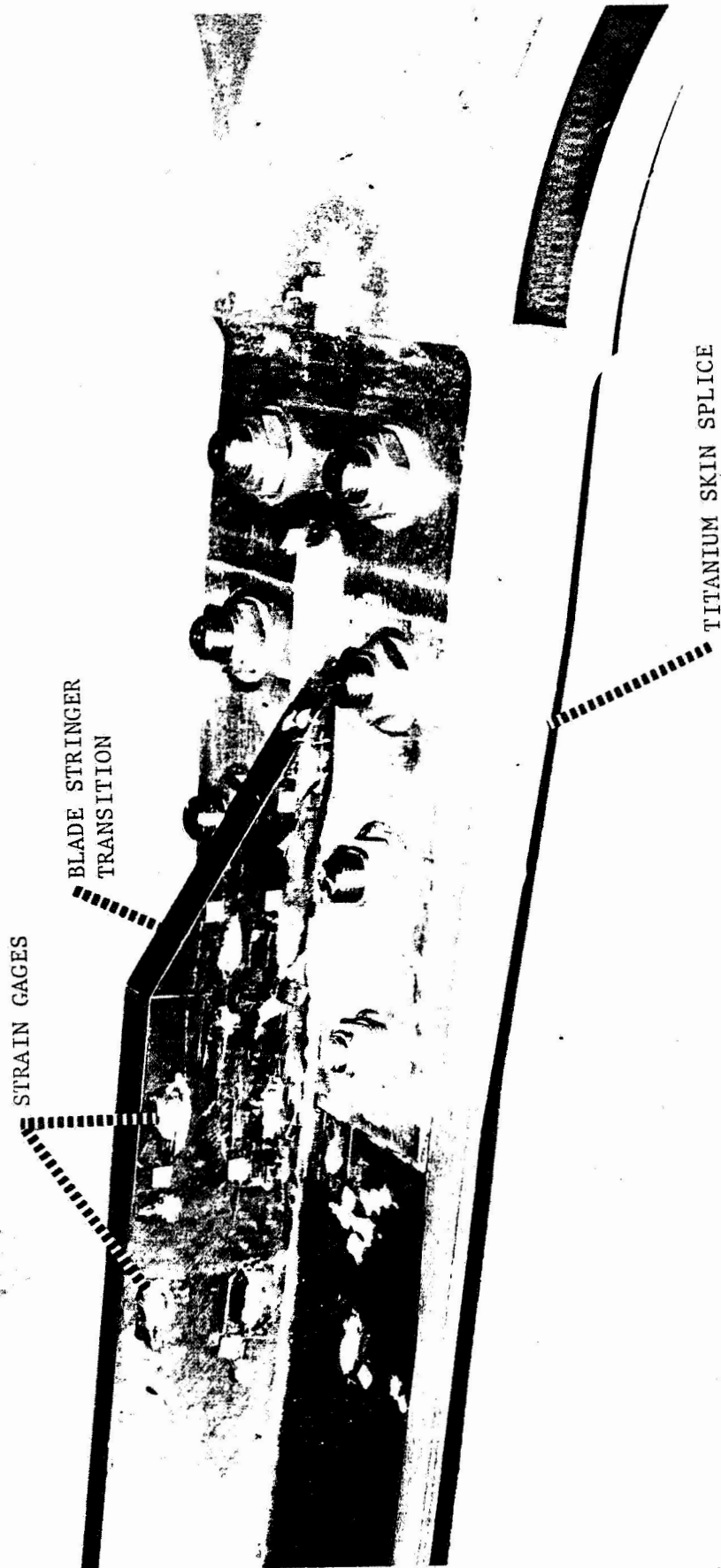


FIGURE 11 STRINGER JOINT TEST SPECIMEN

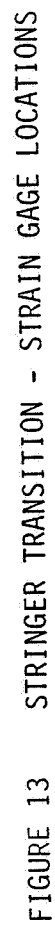
SECTION 2.2
STRINGER TRANSITION TEST
INSTRUMENTATION

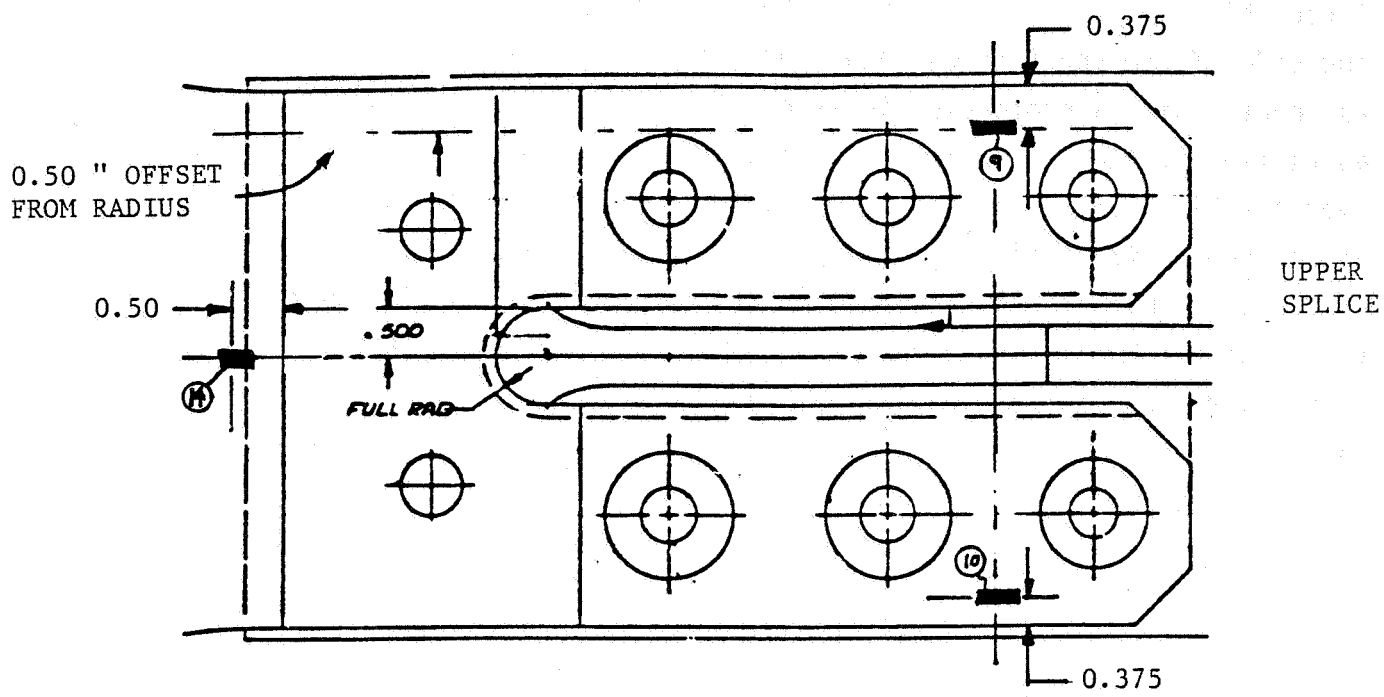
The stringer joint specimen was equipped with 15 axial strain gages to monitor the performance of the bolted joint and the basic skin/stringer section. The selected strain gage locations are shown in Figure 12 through 14 (taken from Douglas TAD - ZCA10200).

The gage locations shown in Figure 12 were selected to measure the load levels in the stringer blade as it is increased in thickness and is scarfed into the skin. Gages 3 and 6 in Figure 13 were located to monitor the strain levels in the skin prior to and immediately following the build up in thickness, providing the gross-section strain levels outside the bolted joint. The tip of the stringer transition was identified as a potentially critical location because of the high load transfer occurring at that point combined with the local stress concentration effects. Gage 13 was placed as close as possible to the blade/skin intersection point. The remaining gages shown in Figure 14 were used to monitor loads in the titanium splice plates away from the joint and at a point one bolt row removed from the predicted failure location.

All axial gages used were type EA06-125AC-350. The gage mounting surfaces were prepared using GA2 epoxy as a base filler material. Light sanding was used to smooth mounting surfaces as required. All gages were bonded to the prepared surface with MBOND 200 adhesive and sealed with clear RTV silicone. The side restraint used to react out-of-plane kick forces (see discussion in Test Setup section) was equipped with a 10,000 pound capacity load cell to monitor these forces throughout the test.

The data acquisition system used for the test consisted of a Tektronix 4054 Graphics and Data Acquisition System, capable of single point or continuous read of strain gage and load cell output. The system is shown in Figure 15 along with a Tektronix printer which provided hard copies of the test data as required during the test. Also shown is the load control system for the mechanical test machine used to apply test loads.





GAGES 9 THROUGH 11 LOACTED MIDWAY BETWEEN BOLT ROWS, .375 " FROM EDGE.

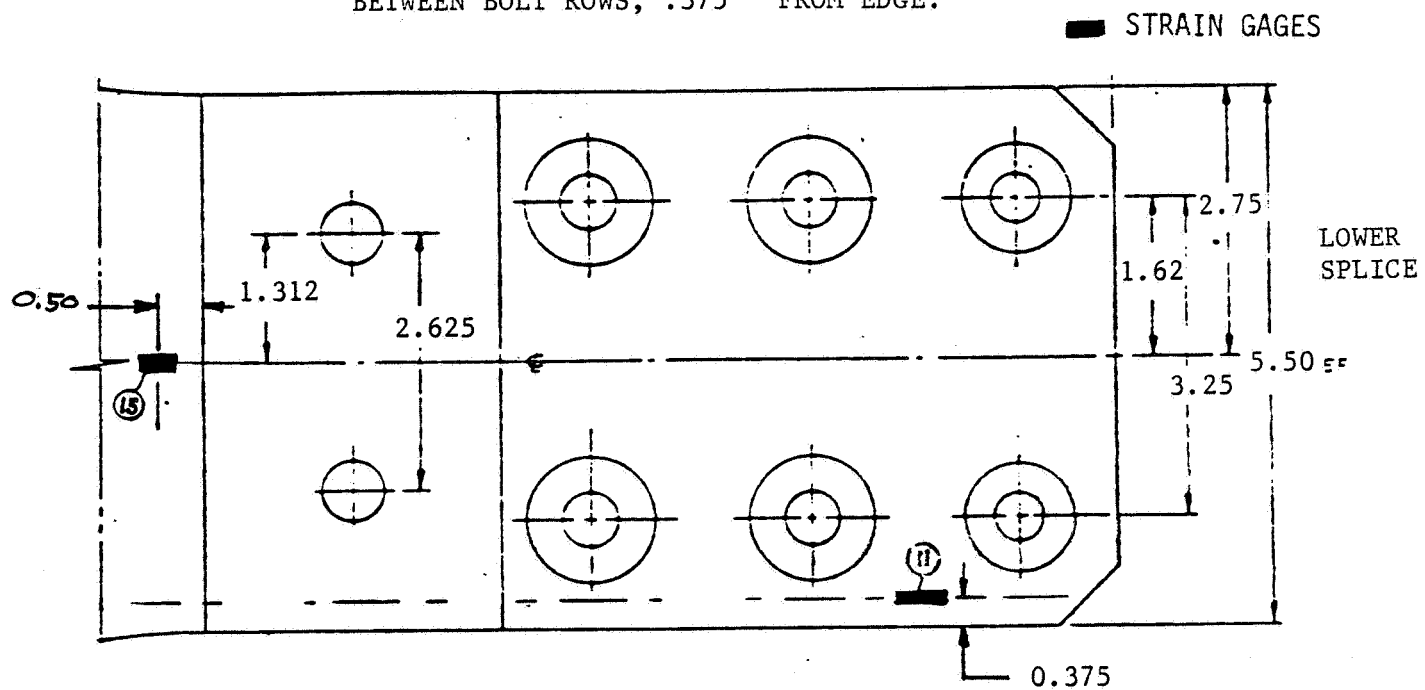


FIGURE 14 STRINGER TRANSITION - STRAIN GAGE LOCATIONS

Since this specimen was designed with a "test section" at each end, only one side of the specimen was equipped with strain gages. The other side was coated with a photo-elastic material to provide a qualitative assessment of the structural response. The composite member was coated over the blade and skin to a point sufficiently beyond the bolted joint and thickness transitions. The upper titanium splice plate was also coated to examine the hole shadowing and stress concentration effects. (See Section 2.4 on Test Results for photographs of the photo-elastic material response.) The coating used for this specimen consisted of Ciba-Geigy 502 resin with Furane 951 hardner photo-elastic material.

ORIGINAL PAGE IS
OF POOR QUALITY



FIGURE 15 DATA ACQUISITION SYSTEM

SECTION 2.3

STRINGER TRANSITION TEST

TEST SETUP

The stringer transition specimen was tested in a 1,100,000 pound capacity Baldwin test machine. The specimen was mounted vertically in the test machine with the specimen end fittings attached to the machine clevises through a standard pin loading arrangement. The overall test setup is shown in Figure 16. The asymmetry of the specimen required that a side restraint be used to restrict out-of-plane deflections. The side restraint system consisted of an aluminum beam which spanned across to the test machine support towers and was rigidly clamped. A 10,000 pound capacity load cell was mounted to the beam with a load block that contacted the outer skin side of the specimen. The shifting center of gravity of the specimen caused deflections to occur which would place additional tension load on the skin side. Thus, the load cell need only react compression forces. The specimen was given enough length to allow the reaction point to be representative of the first outboard rib in a typical wing structure, so that restricting the out-of-plane deflection at that point was not unrealistic. A close-up view of the specimen installation including the side restraint is shown in Figure 17.

ORIGINAL PAGE IS
OF POOR QUALITY

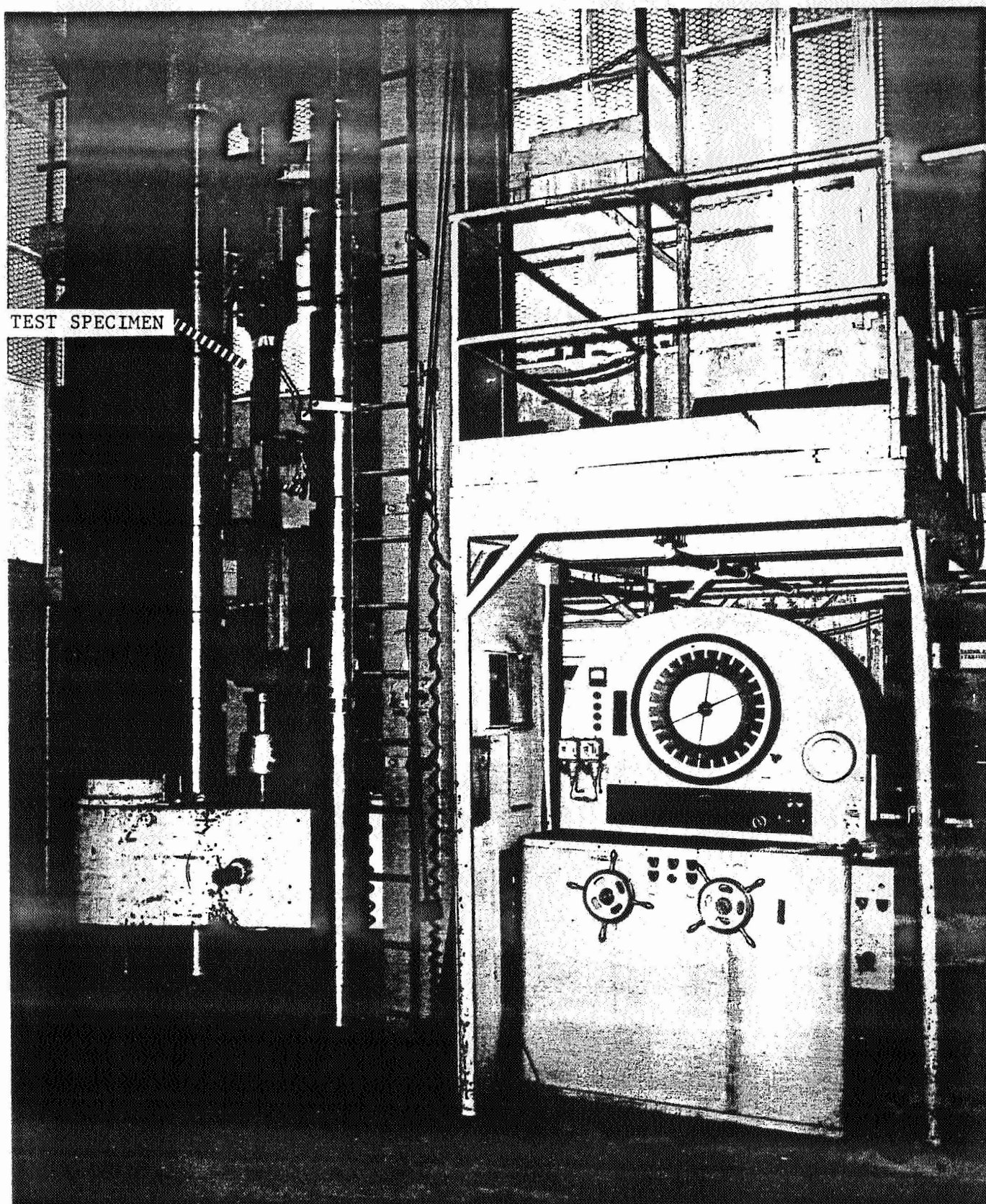


FIGURE 16 STRINGER JOINT TEST SETUP

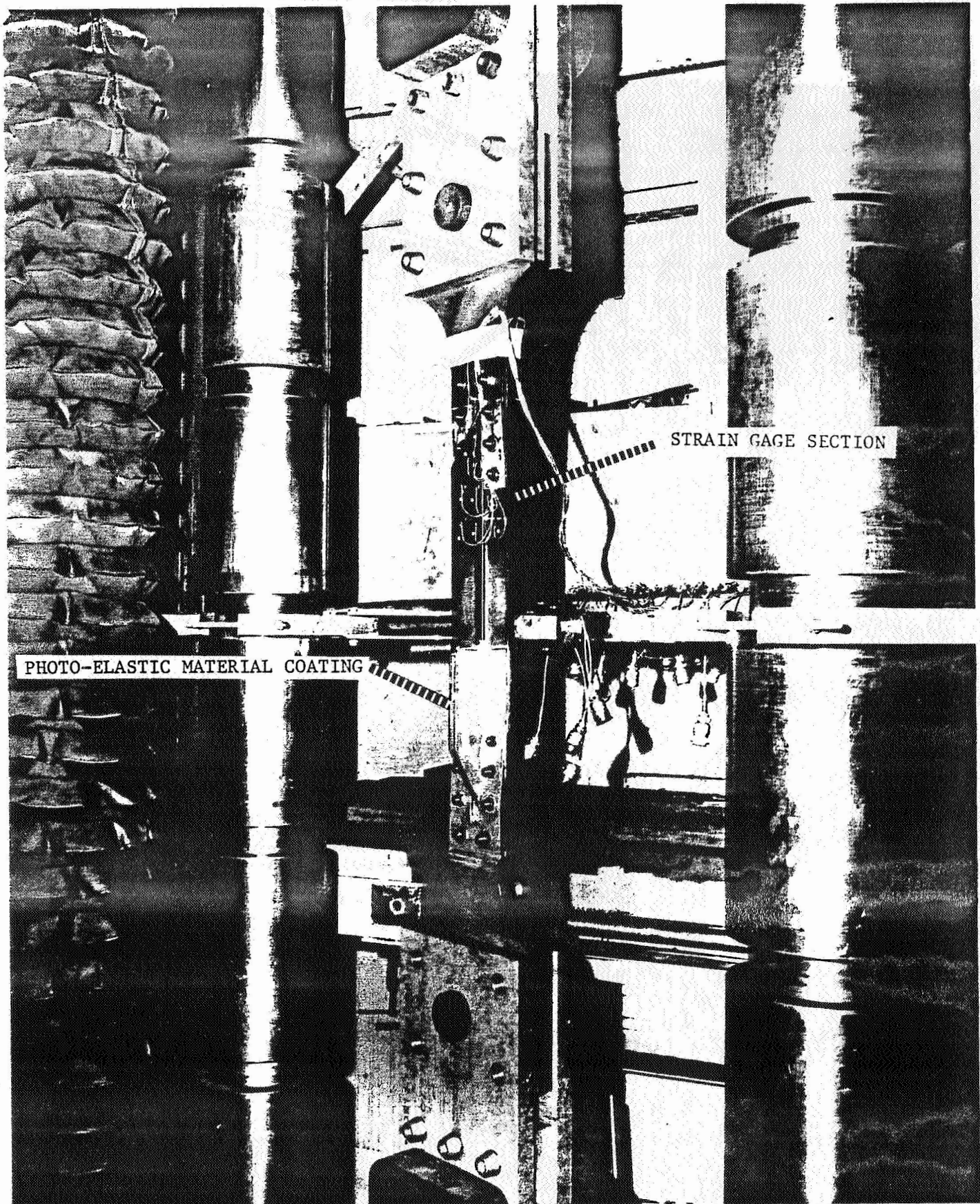


FIGURE 17 STRINGER TRANSITION SPECIMEN INSTALLED IN TEST MACHINE

SECTION 2.4

STRINGER TRANSITION TEST

TEST PROGRAM - PROCEDURES AND RESULTS

The intent of the stringer transition joint test was to determine the static tension strength of a bolted splice and stringer runout concept for the side of the fuselage attachment, and to correlate these results with analysis predictions. The objective was to maximize the bolted joint strength while avoiding a premature failure of the stringer transition.

After the photo-elastic coating was completed the specimen was installed in the test fixture and loaded to approximately 40,000 pounds. The strain distributions indicated by the coating were visually examined to assist in the final selection of strain gage locations. The specimen was then removed from the test fixture and strain gages were applied.

After re-installing the specimen in the test fixture, the load application and data acquisition systems were checked to ensure proper operation. The static test then began with axial tension load applied to the specimen in increments of 10,000 pounds. Strain readings were taken at each load increment up to 120,000 pounds of applied load. Photographs of the photo-elastic material were taken at increments of 20,000 pounds up to the 80,000 pound load level. The specimen was then loaded at a constant rate to static failure with the data acquisition system taking continuous data samples at approximately 0.6 second intervals.

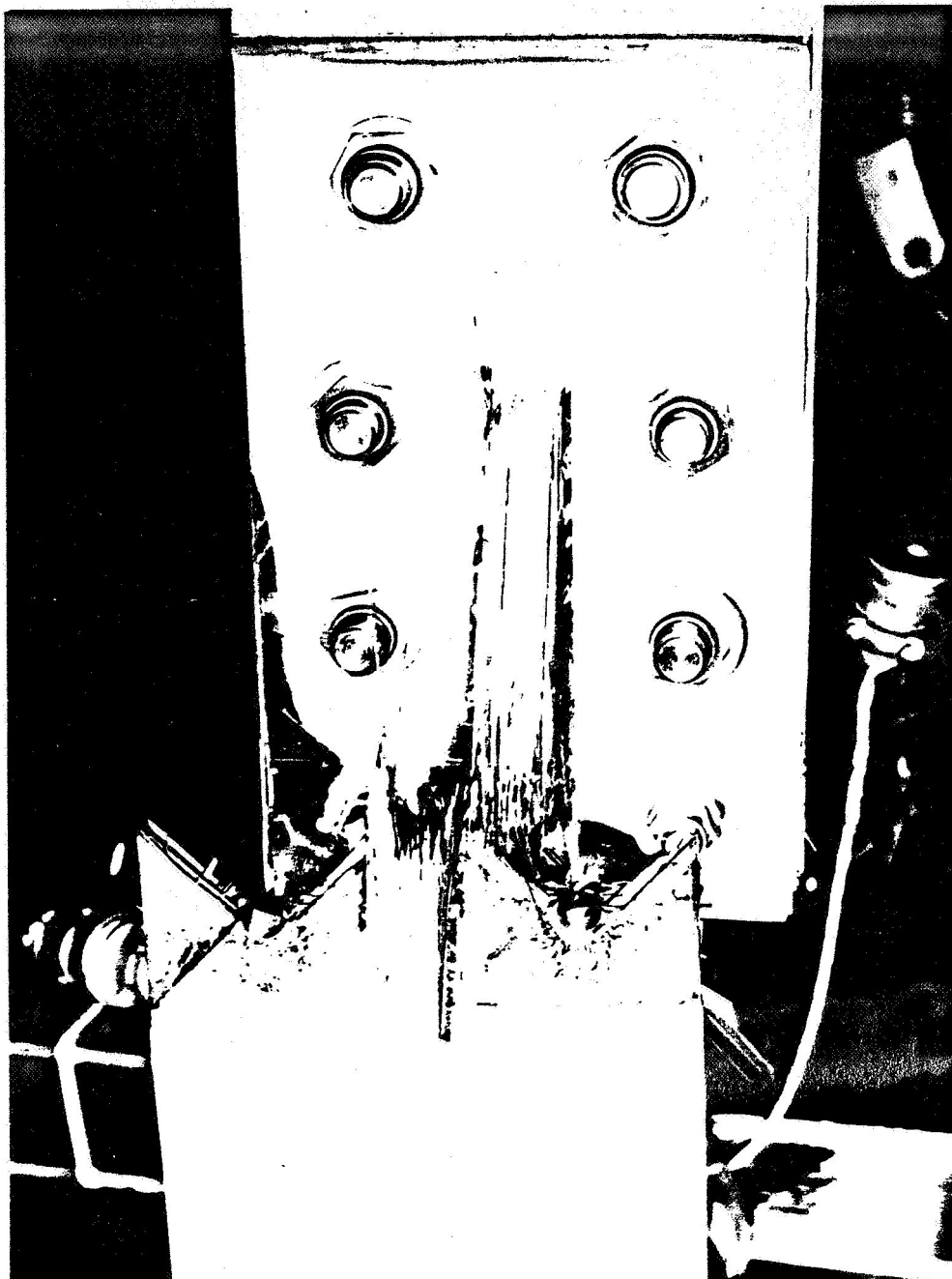
The bolted joint failed in the analytically predicted location at an ultimate load of 197,200 pounds, or at a running load intensity of 34,300 pounds per inch. This corresponds to an average gross-section stress level of about 50,000 psi in the basic section, prior to the thickness buildup outside the joint. The failure mode was a net-section tension failure which occurred through the first (outermost) row of fasteners at a high-bypass, low-bearing load combination, followed by a tension failure through the minimum section of the stringer blade. Figures 18 through 23 show the specimen failure viewed from several different angles.

ORIGINAL PAGE IS
OF POOR QUALITY



FIGURE 18 STRINGER TRANSITION TEST - FAILED SPECIMEN

ORIGINAL PAGE IS
OF POOR QUALITY



ORIGINAL PAGE IS
OF POOR QUALITY

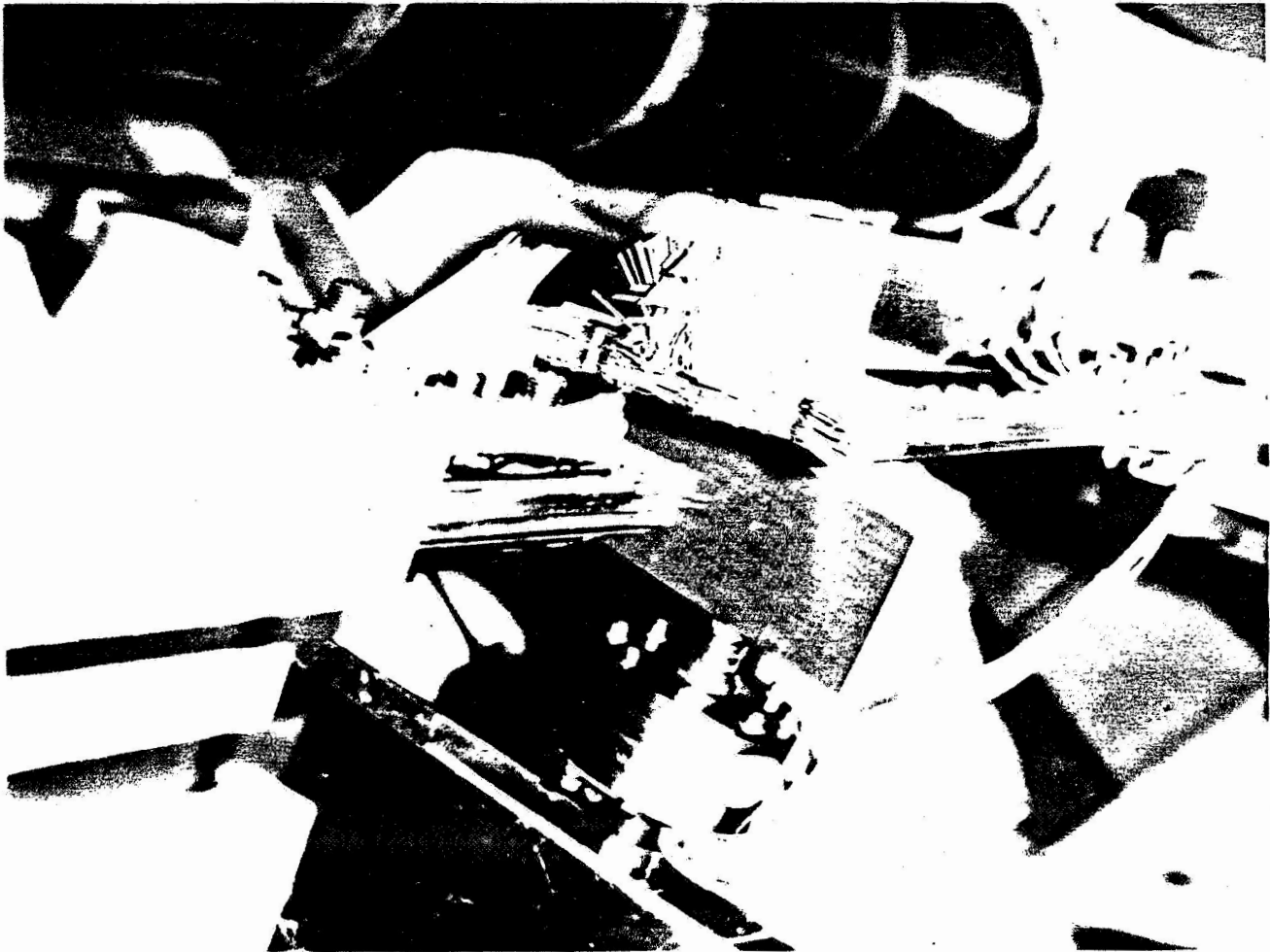
FIGURE 19 STRINGER TRANSITION TEST - FAILED SPECIMEN



FIGURE 20 STRINGER TRANSITION TEST - FAILED SPECIMEN

ORIGINAL PAGE IS
OF POOR QUALITY

ORIGINAL PAGE IS
OF POOR QUALITY



ORIGINAL PAGE IS
OF POOR QUALITY

FIGURE 21 STRINGER TRANSITION TEST - FAILED SPECIMEN



FIGURE 22 STRINGER TRANSITION TEST - FAILED SPECIMEN

ORIGINAL PAGE IS
OF POOR QUALITY

ORIGINAL PAGE IS
OF POOR QUALITY

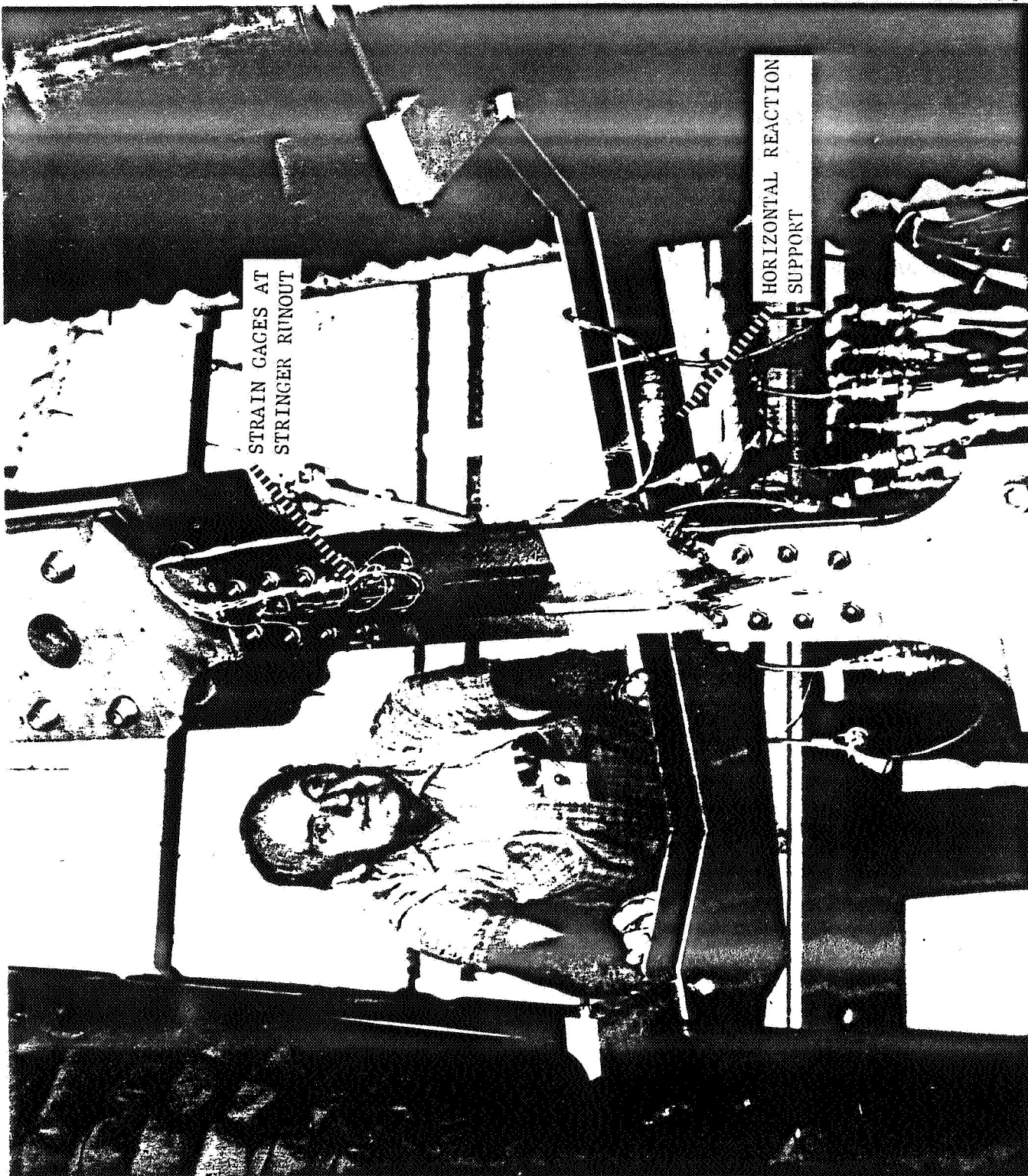


FIGURE 23 STRINGER TRANSITION TEST - FAILED SPECIMEN

The analytically predicted strength of 183,700 pounds was roughly 7 percent below the tested value. A detailed discussion of the analytical approach and resulting correlation will be presented in the contract Final Report.

Strain readings taken throughout the test are presented numerically and graphically in Appendix A. The data indicates a strain level in the skin prior to the buildup of 5,891 microstrain, which corresponds to an average strain in the skin at the bolted joint of roughly 4,700 microstrain. The predicted value of 5,945 microstrain at the same location shows excellent correlation between analysis and test results. The actual strain readings taken immediately outside the joint at gage number 6 indicate a somewhat lower value, but this result is attributable to the changing cross-section and inherent variations in the stress distributions. All strain gage results were plotted in pairs versus applied load with the exception of gage number 13, which apparently broke a wire or lost sufficient contact at a point between 100,000 and 120,000 pounds of applied load. (Appendix A contains a plot of the gage 13 readings during the continuous ramp from 100,000 to 120,000 pounds of applied load, illustrating the point at which gage effectiveness was lost.) Gage number 13 was placed on the edge of the stringer blade at the tip of the transition. By extrapolating the readings taken up to 100,000 pounds of applied load, the strain level at the tip of the blade (at failure of the joint) would apparently have reached 8,000 to 9,000 microstrain. The erratic readings of gage 12 are also suspect. Continuous plots of gage 12 output during the failure ramp are contained in Appendix A, showing the erratic response. Strain readings from all other gage locations behaved generally as expected.

The purpose of the photo-elastic survey was to provide a qualitative assessment of specimen stress/strain distributions. It is possible to obtain quite accurate stress measurements by this technique through the use of a polariscope, whereby the photo-elastic fringe orders can be precisely measured (to within 0.01 fringe orders). However, such a level of accuracy was not required for this test program since it was possible to mount strain gages directly to the external surfaces of the specimen at the opposite end.

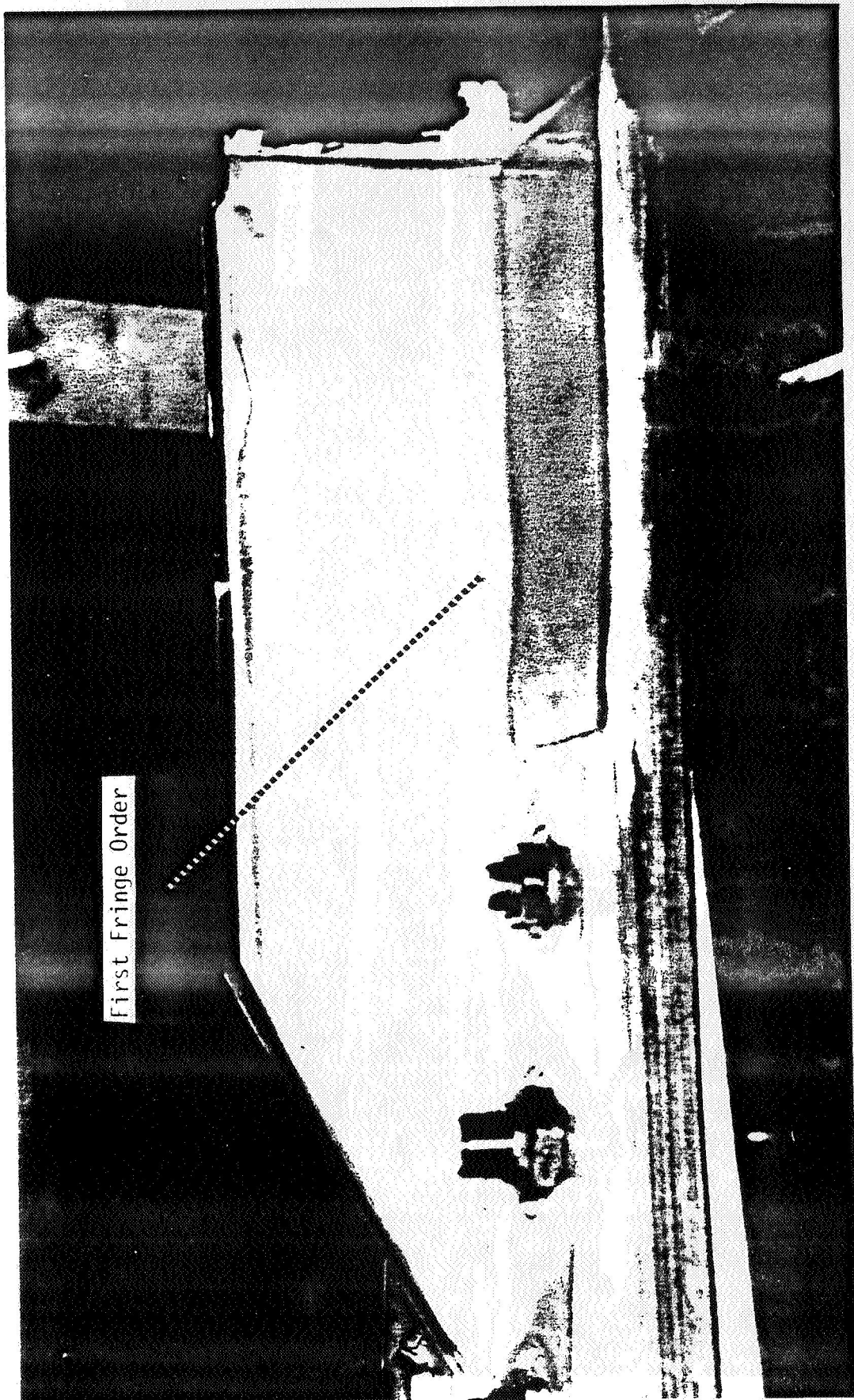
The first observations of the photo-elastic response were made prior to mounting the strain gages as described in Section 2.2 on instrumentation. Photographs taken during the static test to failure are presented in Figures 24 through 26 for the 40,000, 60,000, and 80,000 pound load levels. The actual fringe orders are more discernible with color reproductions of the photographs; the fringe orders of interest are identified on each figure. (Each fringe order corresponds to a stress variation of roughly 10,000 psi.) Figure 24 taken at the 40,000 pound load level shows minor variations in the stress levels throughout the stringer blade. A single fringe order is visible at the base of the blade, just outside the bolted joint. At the 60,000 pound load level the fringe orders have become more apparent as shown in Figure 25. The change in direction or "bend" in the first fringe order (now roughly at the center of the blade) results from the decrease in stress level due to the thickness buildup in the skin and stringer, combined with the presence of an additional load path through the fasteners into the splice members. This phenomenon is more apparent in Figure 26 taken at 80,000 pounds applied load which clearly reflects the higher stress levels and the rapid variations along the stringer blade. The stress distribution indicated by this photo suggests that a more shallow scarf angle in the blade would result in a more efficient section without adversely effecting the bolt load distributions. A more gradual scarf is desirable from the standpoint of relieving the stress concentration at the tip of the blade transition.

The photographs shown in Figures 27 through 28 show a view of the specimen looking down at the edge of the stringer blade and at the upper surface of the titanium splice. Two general observations can be made from these photographs. First, the stress concentration at the tip of the stringer transition is clearly visible in each figure. This point had been identified as a potentially critical location; it was unfortunate that the strain gage mounted on the opposite blade became ineffective during the test, as previously discussed. Second, the complex stress distributions that are visible on the surface of the titanium splice illustrates the difficulty in making strain gage measurements of joint members to determine bolt load

distributions. The effects of stress concentrations (due to the fastener holes and spotfacing) and hole shadowing (low stress regions between fasteners) make it extremely difficult to place a strain gage in a location that would provide a measurement that could be directly correlated with an average stress or load level.

ON FILE 1 10/15/67
STANDARD ROOM 30

ORIGINAL PAGE IS
OF POOR QUALITY



First Fringe Order

FIGURE 24 PHOTO-ELASTIC SURVEY - STRINGER BLADE
APPLIED LOAD = 40,000 POUNDS

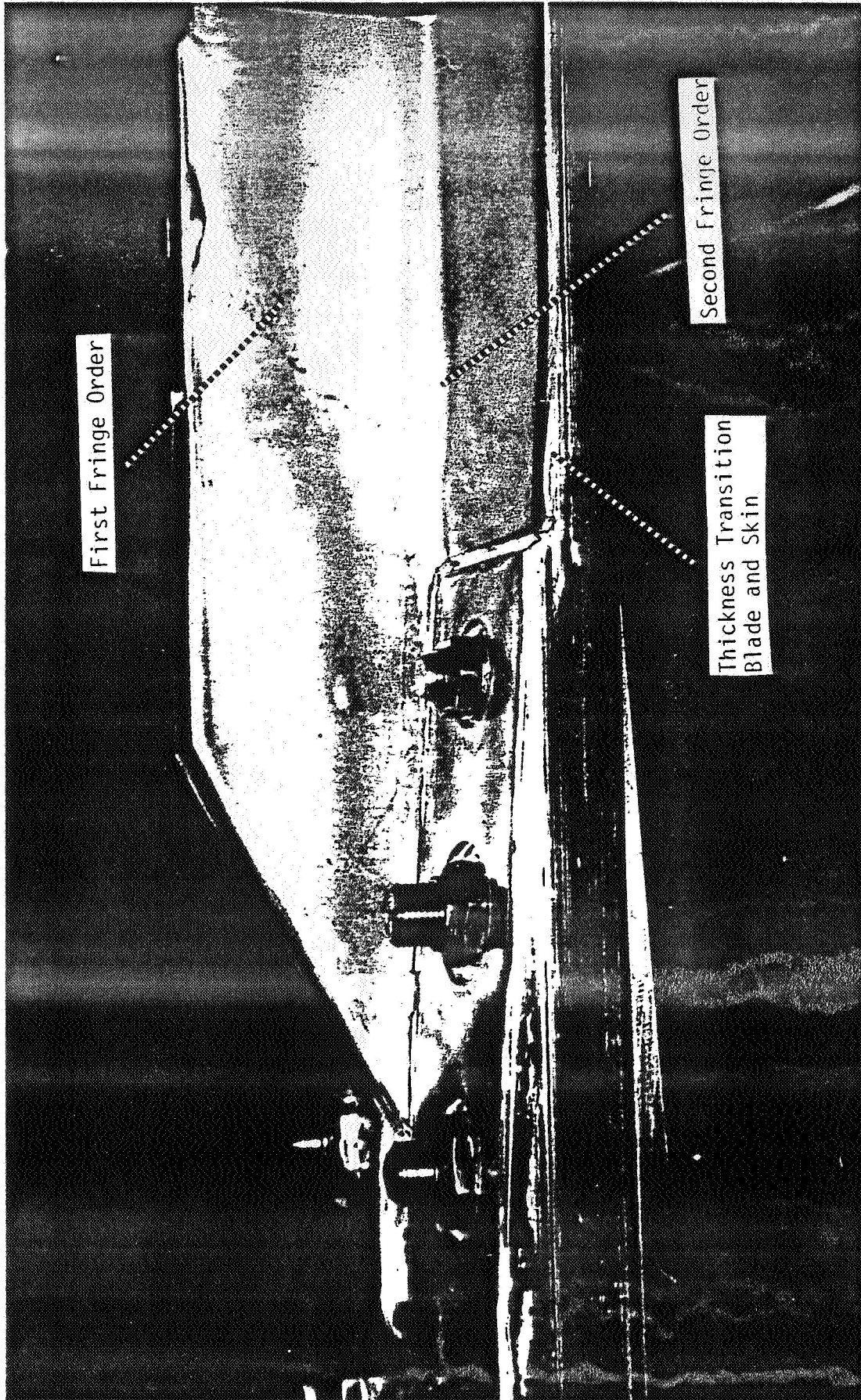


FIGURE 25 PHOTO-ELASTIC SURVEY - STRINGER BLADE
APPLIED LOAD = 60,000 POUNDS

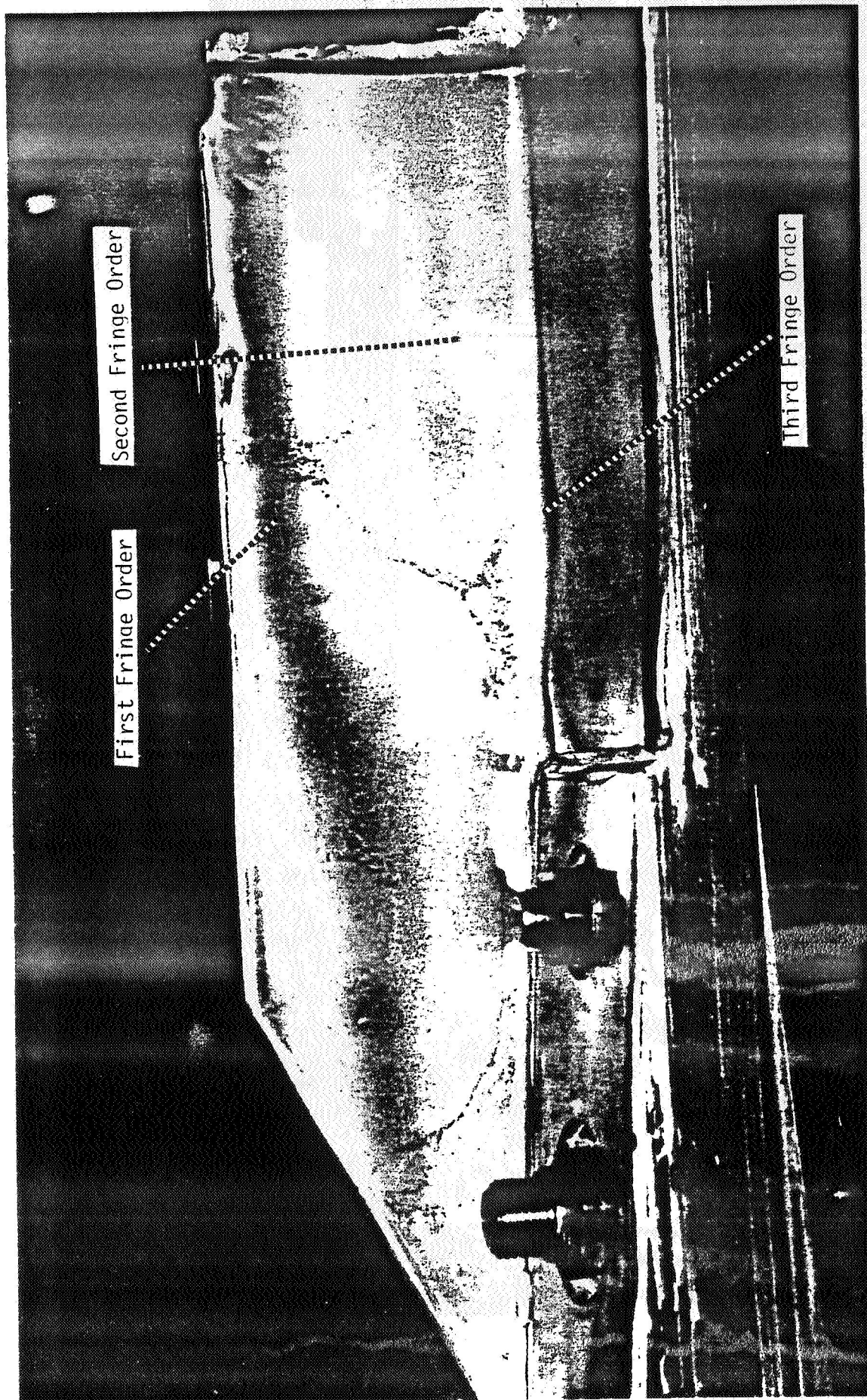


FIGURE 26 PHOTO-ELASTIC SURVEY - STRINGER BLADE
APPLIED LOAD = 80,000 POUNDS

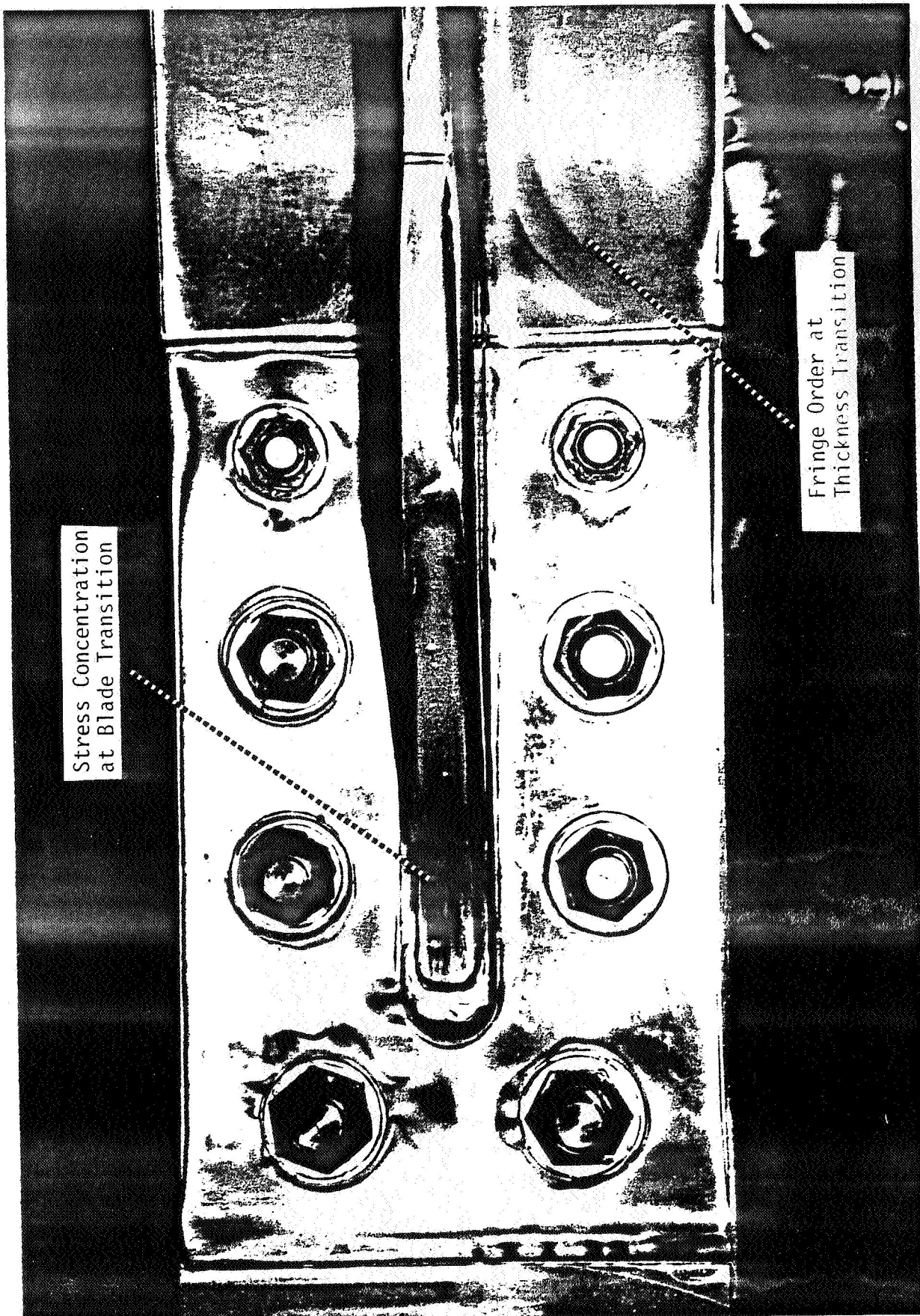


FIGURE 27 PHOTO-ELASTIC SURVEY - UPPER SPLICE
APPLIED LOAD = 40,000 POUNDS

ORIGINAL PAGE IS
OF POOR QUALITY

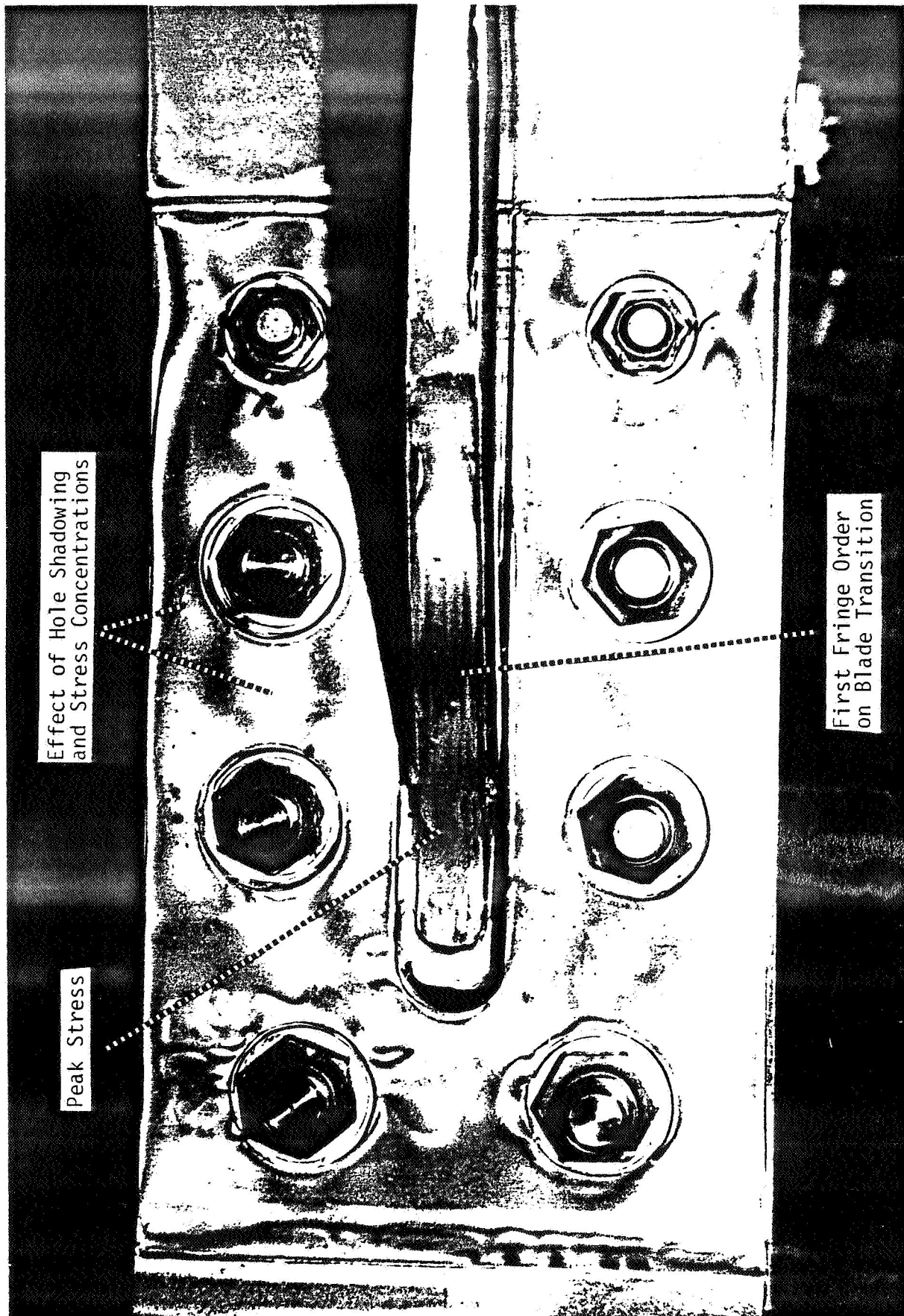


FIGURE 28 PHOTO-ELASTIC SURVEY - UPPER SPLICE
APPLIED LOAD = 80,000 POUNDS

SECTION 3.1

TECHNOLOGY DEMONSTRATION SUBCOMPONENT SPECIMENS

TEST ARTICLES

Two demonstration subcomponent specimens were fabricated and tested as representative sections of the upcoming technology demonstration article. These specimens were designed to provide some insight into the performance of the larger and more complex corner joint, and to develop a sufficient level of confidence in the selected analytical approach. Thus, the member thicknesses, fastener sizes, and overall geometry of the subcomponents were identical to the corresponding portions of the technology demonstration article.

Demonstration subcomponent specimen number 1 (hereafter referred to as subcomponent #1) represents the wing skin and spar cap portion of the side of fuselage splice at the lower rear spar. Figure 29 shows the technology demonstration article and illustrates that portion which is represented by subcomponent #1. This is the most complicated area of the demonstration article, where the spar cap and skin sections are spliced externally by a titanium splice, and internally by both a titanium "tee" splice and the aluminum corner fitting. Figures 30 and 31 show the pertinent specimen dimensions. The machined aluminum fitting was designed to approximate the effects of the aluminum corner fitting found in the actual corner joint.

Subcomponent #2 is representative of the spar cap and spar web portion of the corner joint. The composite laminates are spliced on the web side by a titanium splice plate and on the spar cap side by an aluminum "bath tub" fitting representing the vertical leg of the actual corner fitting. Subcomponent #2 was tested with a single column of fasteners, just as is found in the technology demonstration article. The specimen dimensions and geometry are shown in Figures 32 and 33.

For both specimens, the metallic splice members were machine tapered and spotfaced to accomodate the titanium fasteners. Load indicating bolts were used to attach the aluminum fittings in order to monitor the amount of load transferred through those members in each test. All composite laminates were of constant thickness with several field fasteners used to attach the two test laminates outside the joint area (typical of the actual structure). The laminates were widened or "dog-boned" at the specimen ends to accomodate the large diameter holes necessary for the pin-loaded attachments to the test machine. Aluminum doublers were bonded to the ends of each specimen for reinforcement at the point of load introduction. Each laminate was c-scanned prior to assembly showing acceptable results in all cases.

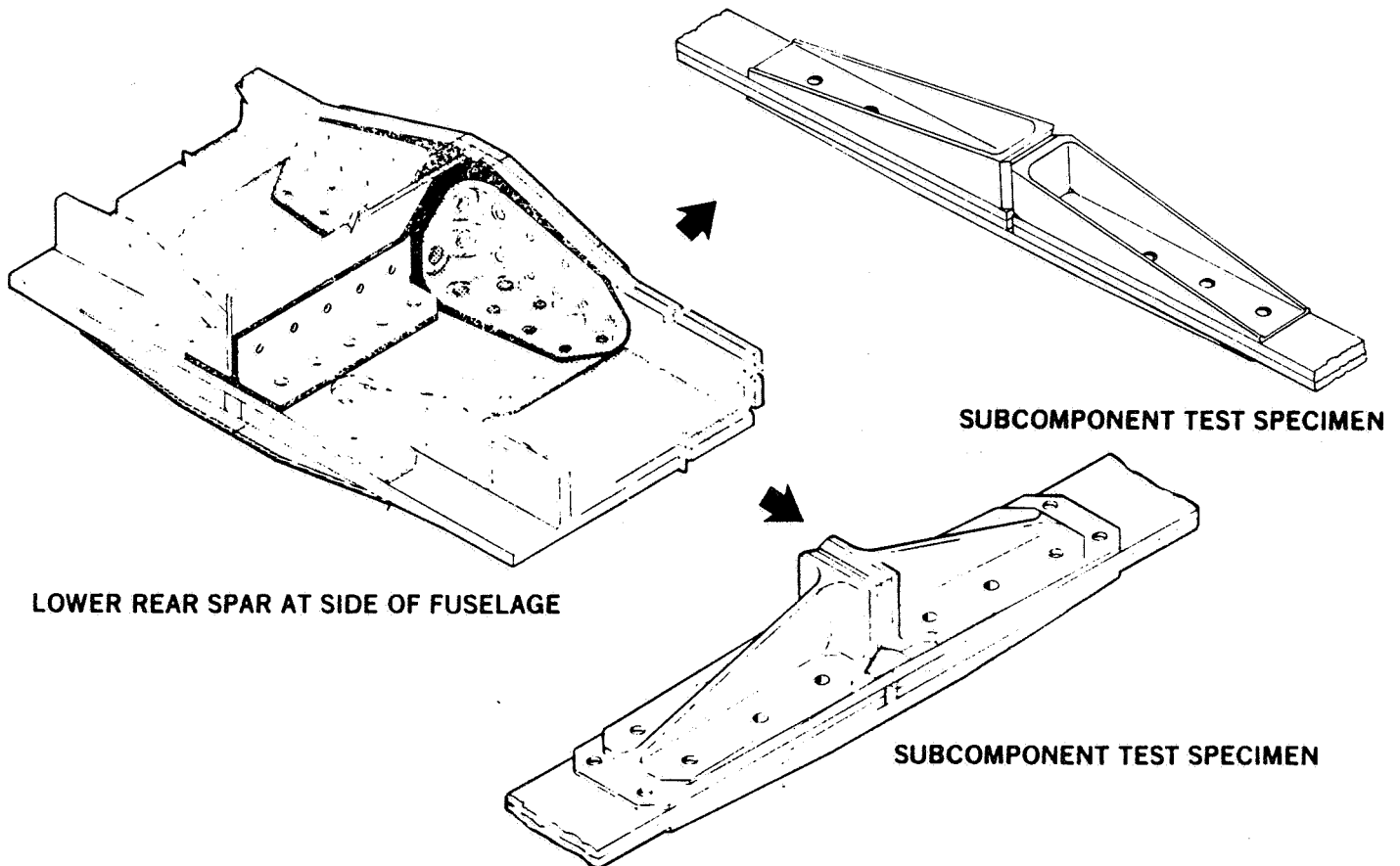


FIGURE 29 DEMONSTRATION SUBCOMPONENT CONCEPT

145 DIA 8 HOLES
265

.4995 DIA 4 HOLES
.5015

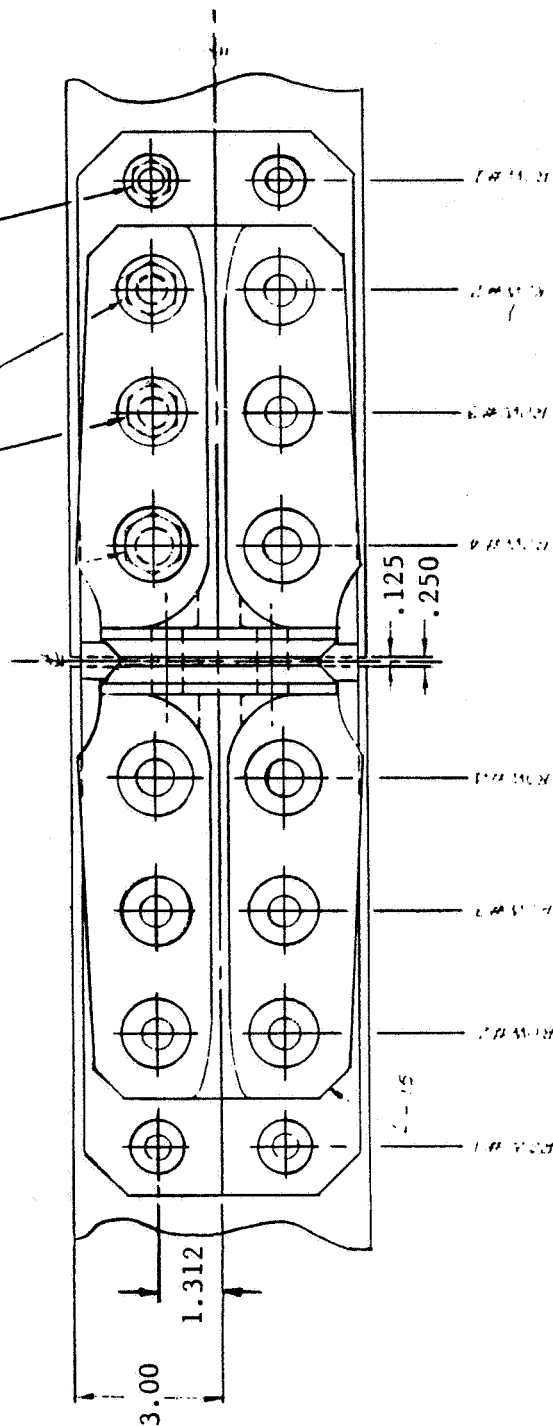


FIGURE 30 SUBCOMPONENT #1 - PLAN VIEW

ORIGINAL PAGE IS
OF POOR QUALITY

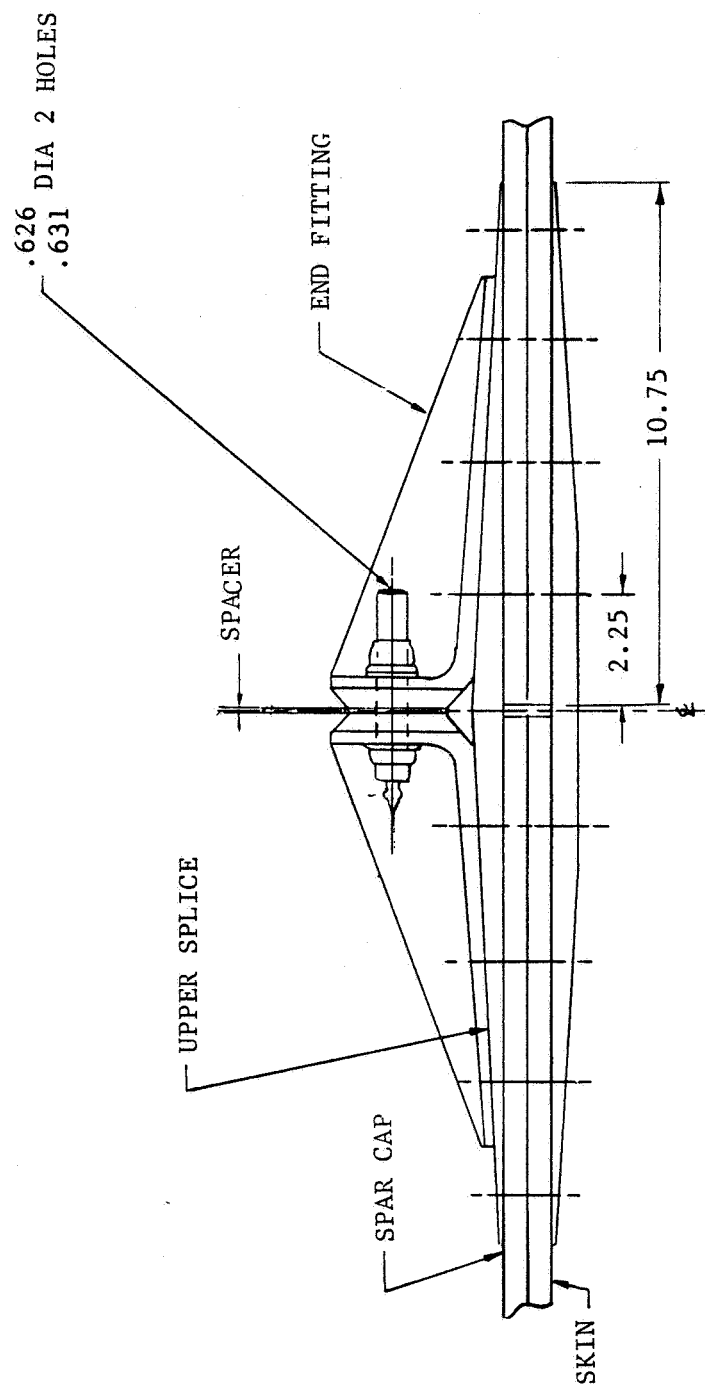


FIGURE 31 SUBCOMPONENT #1 - SIDEVIEW

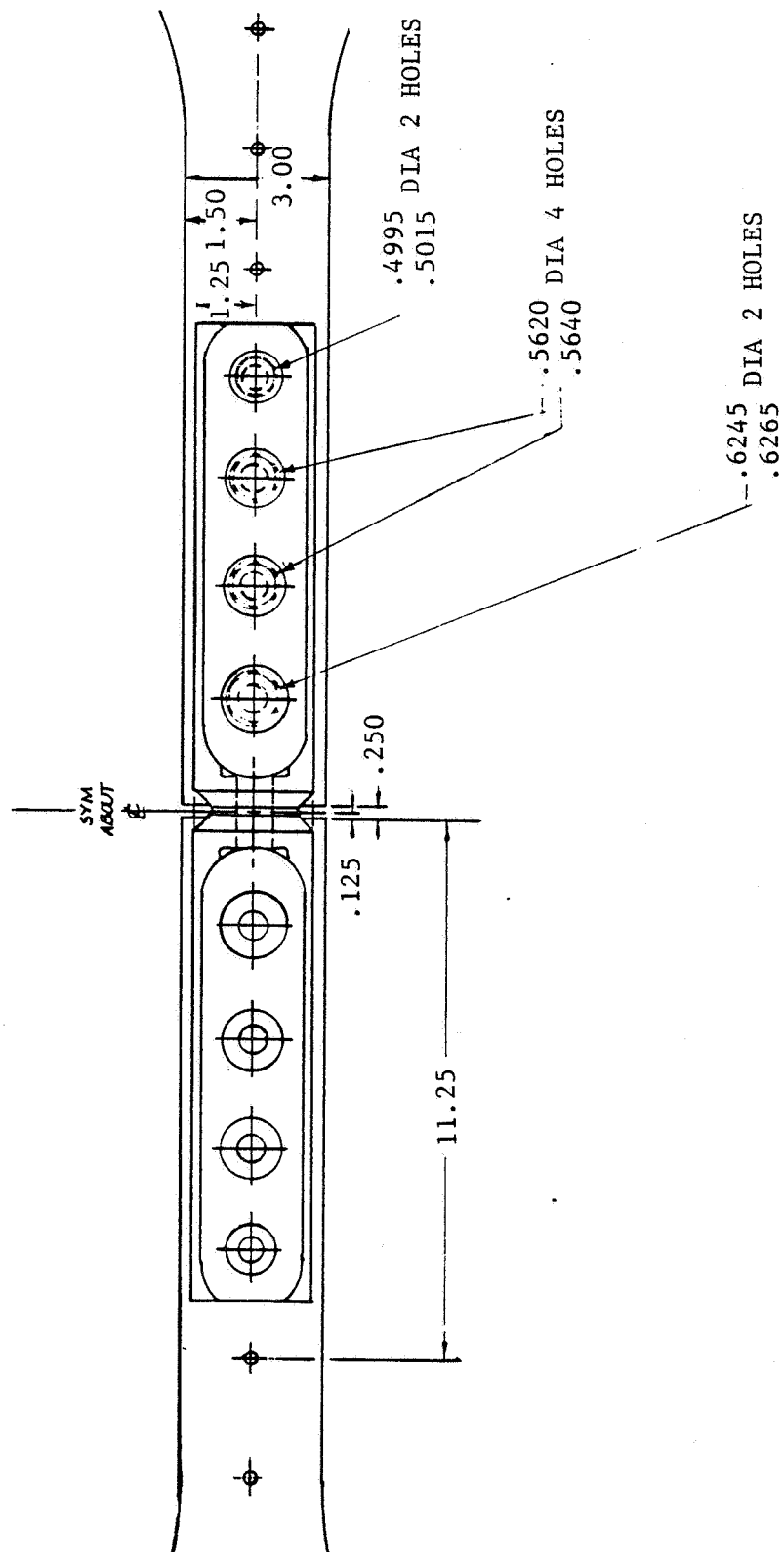


FIGURE 32 SUBCOMPONENT #2 - PLAN VIEW

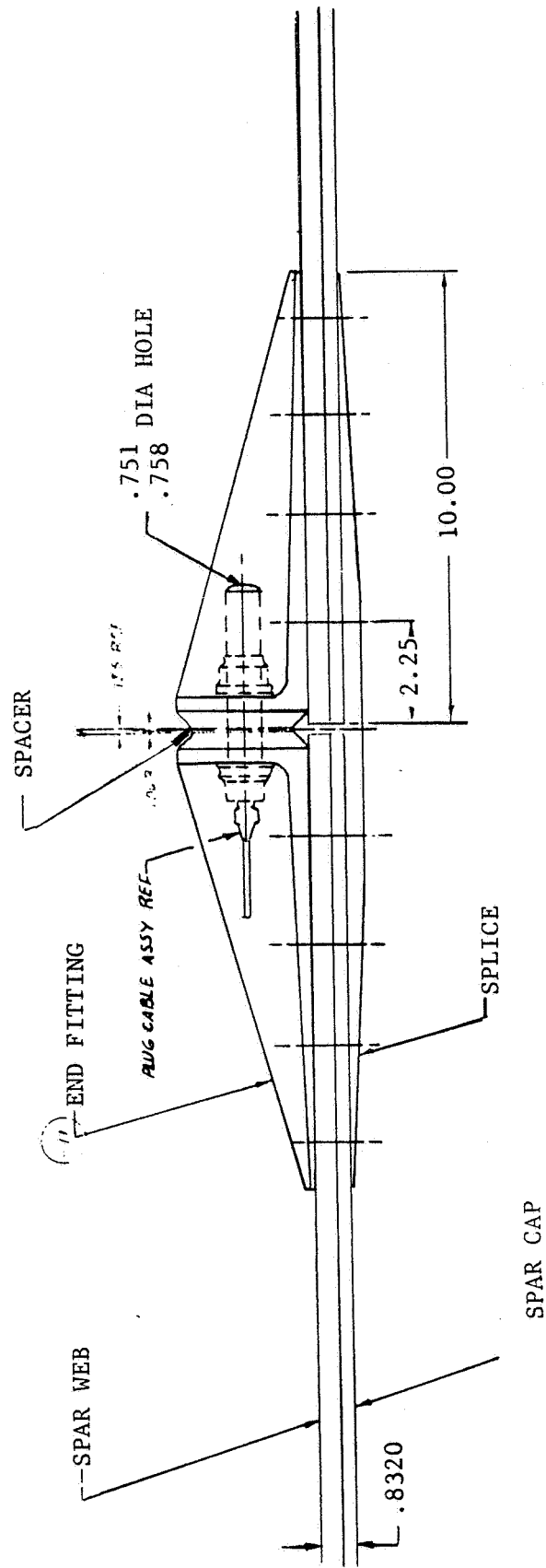


FIGURE 33 SUBCOMPONENT #2 - SIDE VIEW

SECTION 3.2

DEMONSTRATION SUBCOMPONENT SPECIMENS

INSTRUMENTATION

The instrumentation requirements for the two demonstration subcomponent specimens consisted of axial strain gages and load indicating bolts. Subcomponent #1 was equipped with 14 gages mounted in the locations shown in Figure 34. The gage locations were chosen to provide direct measurements of the load levels in each laminate and titanium splice. Several gages were also located along the bolted joint on the edge of each member to examine the load distributions between rows of fasteners. In addition to strain gages, two load indicating bolts were used to measure the amount of load transferred through the aluminum fittings. This approach was selected because of the relatively complex geometry of the fittings. The fitting design(s) did not afford a suitable location for mounting strain gages that would result in a true measurement of the total load transfer.

Subcomponent #2 was instrumented in the same manner as the previous specimen with 12 axial strain gages located as shown in Figure 35. A single load indicating bolt was used at the interface between aluminum fittings for load transfer measurement.

The strain gages were again type EA06-125-AC-350 and the same mounting procedures were used as described in Section 2.2 for the stringer transition specimen. The load indicating fasteners used for the two tests were model SDH-QB, manufactured by the Strainert Company. Subcomponent #1 was assembled with two 5/8-inch diameter bolts while subcomponent #2 used a single 3/4-inch diameter bolt. These fasteners are equipped with type EA-06-S1262-175 strain gages which measure the strain in the fastener under applied axial load. The fasteners were calibrated by the manufacturer prior to shipment, and the calibration data was provided in the form shown in Table 1. The same side restraint mechanism employed in the stringer transition test was used for the two subcomponents. A 10,000 pound capacity load cell was used to monitor the out-of-plane forces reacted by the side restraint.

ORIGINAL PAGE IS
OF POOR QUALITY

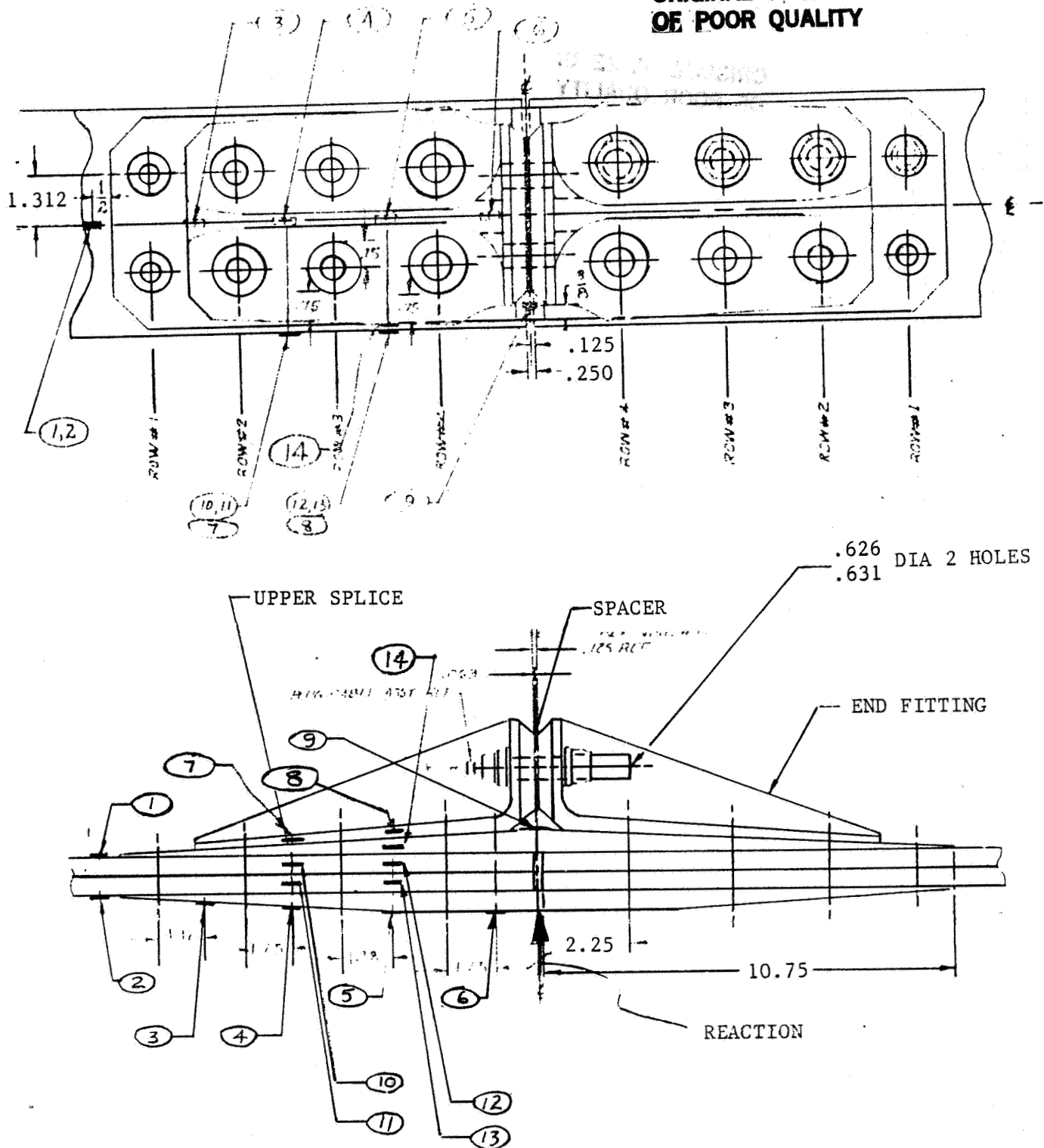
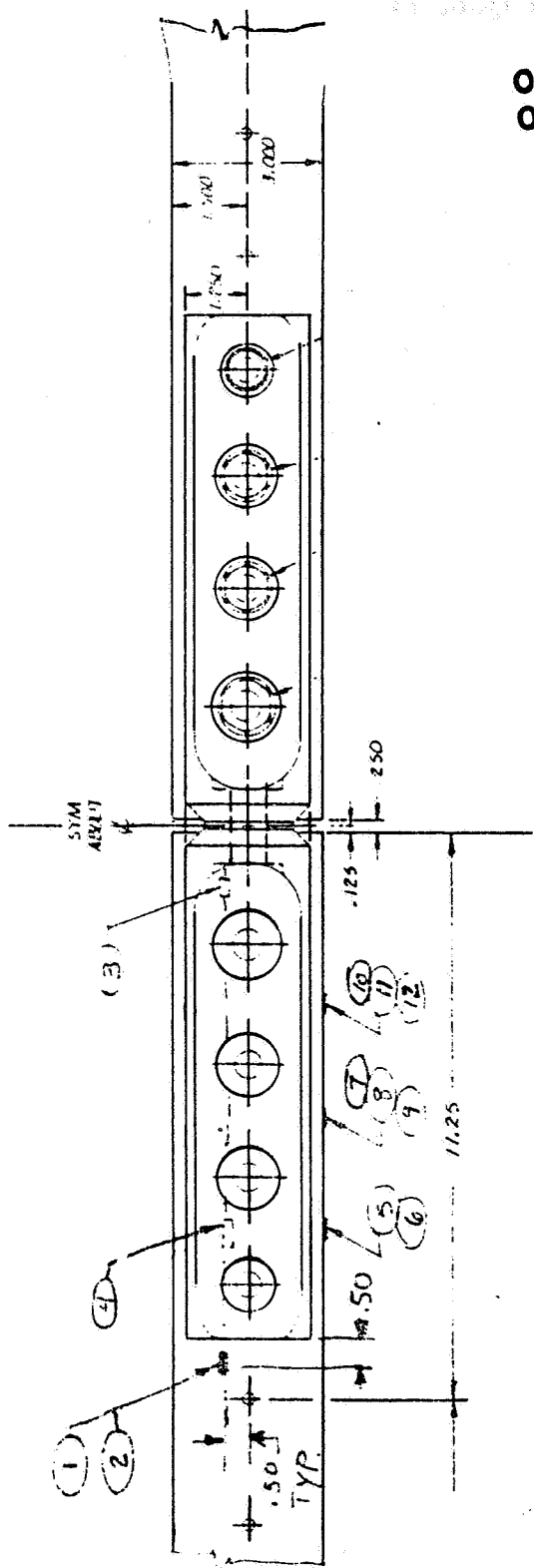


FIGURE 34 SUBCOMPONENT #1 - STRAIN GAGE LOCATIONS

ORIGINAL PAGE IS
OF POOR QUALITY



.751 DIA HOLE
.758

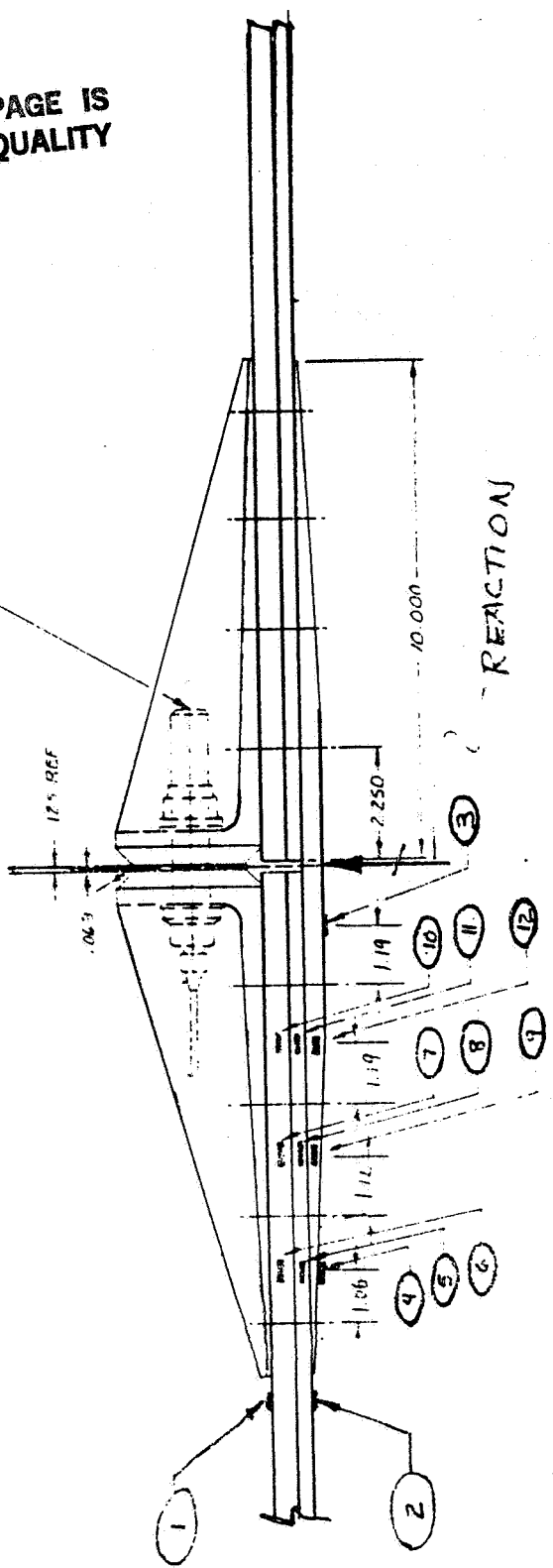


FIGURE 35 SUBCOMPONENT #2 - STRAIN GAGE LOCATIONS

TABLE I

STRAINERT
CALIBRATION DATA

Douglas Aircraft Long Beach, CA	Q-7098 Strainert Job No.
	Date: 2/20/84
Customer P.O. No. 4CY361229-9	Sign: CGH

Transducer:	12-pt. Cap Screw (SDH-QB) 5/8-18NF x 3-1/4 (350 Ω /300 $^{\circ}$ F) C To K So	
Gages: EA-06-S1262-175	Type: C (Viking VR7-4AG15)	
Service Temp.: 300 $^{\circ}$ F Max.	Ins. Res.: Over 10,000 megohms	
Calib. Temp.: 70 $^{\circ}$ F	S/N: Q7098-1	

Load LBS.	Straight Line Signal $\mu\epsilon$	Deviation, $\mu\epsilon$			Rep. $\mu\epsilon$
		Run 1	Run 2	Run 3	
0	0	0	0	0	0
5,000	635	-1	-1	-1	0
10,000	1,270	-3	-4	-4	1
15,000	1,905	-3	-3	-3	0
20,000	2,540	-1	0	0	1
25,000	3,175	3	3	3	0
20,000	2,540	0	0	0	0
15,000	1,905	-2	-2	-2	0
10,000	1,270	-2	-2	-2	0
5,000	635	-1	-1	-1	0
0	0	0	0	0	0
Hysteresis		1	2	2	

<u>Calibration Analysis:</u>					
Non-Linearity:	4	parts in	3,175	=	0.13%
Repetition					
Loading :	1	parts in	"	=	0.03%
Unloading:	0	parts in	-	=	--
Zero Load:	0	parts in	-	=	--
Max. Load:	0	parts in	-	=	--
End Point :	3	parts in	"	=	0.09%
Hysteresis :	2	parts in	"	=	0.06%

1. All $\mu\epsilon$ readings are with gage factor setting of 2.0.
2. To convert to mV/V, divide $\mu\epsilon$ values by 2000.

SECTION 3.3

DEMONSTRATION SUBCOMPONENT SPECIMENS

TEST SETUP

Both of the subcomponent specimens were tested in the 1,100,000 pound capacity Baldwin test machine. After instrumentation was completed, each specimen was attached to the test machine clevises at the end fittings through a pin loading arrangement. Figures 36 and 37 show subcomponents #1 and #2 mounted in the test machine. The presence of relatively large aluminum fittings on one side of the specimen resulted in a lack of symmetry which could have resulted in out-of-plane bending. Therefore, the same side restraint system (described in previous sections of this report) was used for the two subcomponent tests. Figures 38 through 40 show the side restraint system from several angles with the test specimen(s) in place.

ORIGINAL PAGE IS
OF POOR QUALITY

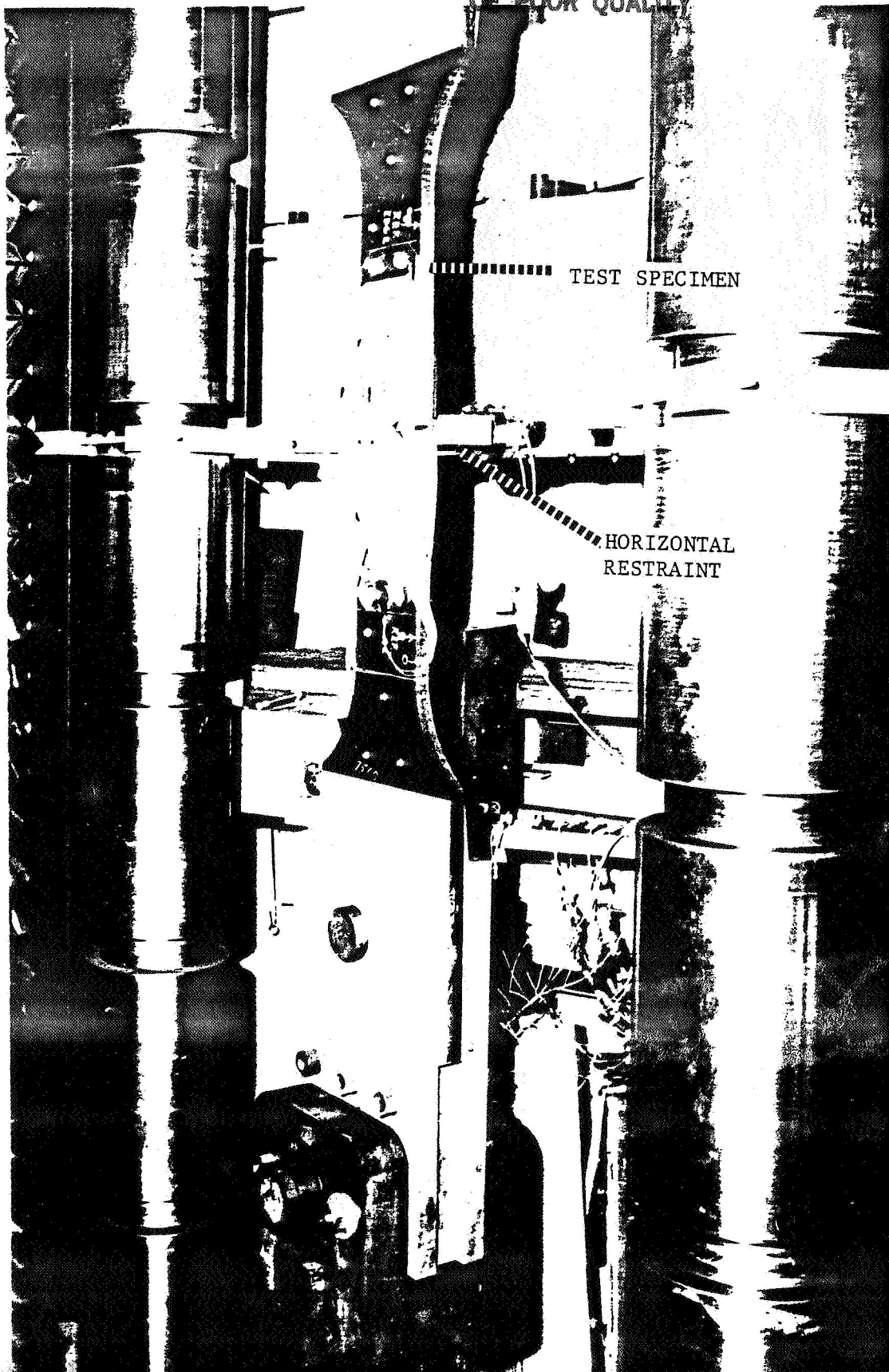
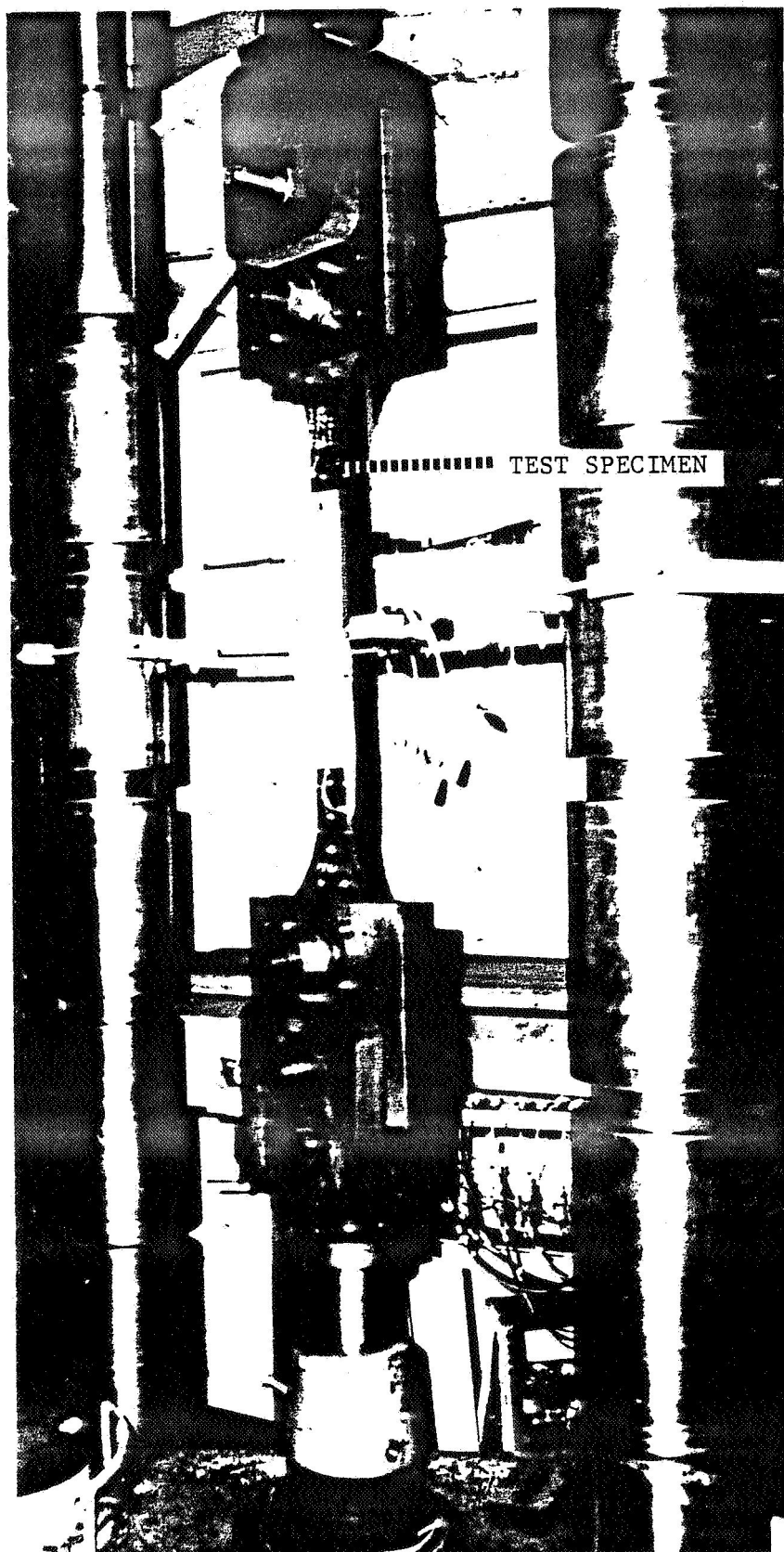


FIGURE 36 DEMONSTRATION SUBCOMPONENT #1



ORIGINAL PAGE IS
OF POOR QUALITY

FIGURE 37 DEMONSTRATION SUBCOMPONENT #2

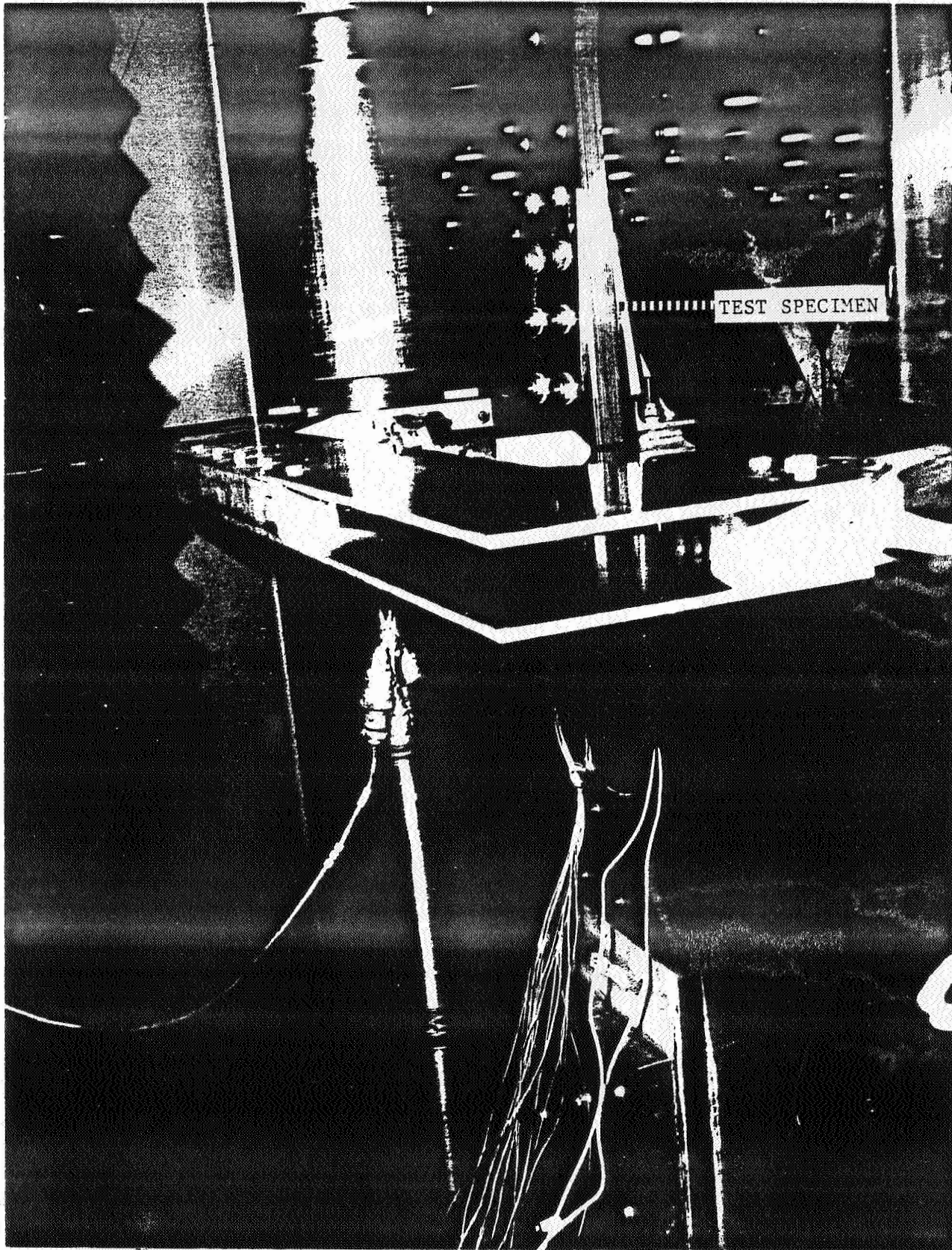


FIGURE 38 SIDE RESTRAINT SYSTEM - SUBCOMPONENT #1

ORIGINAL PAGE IS
OF POOR QUALITY

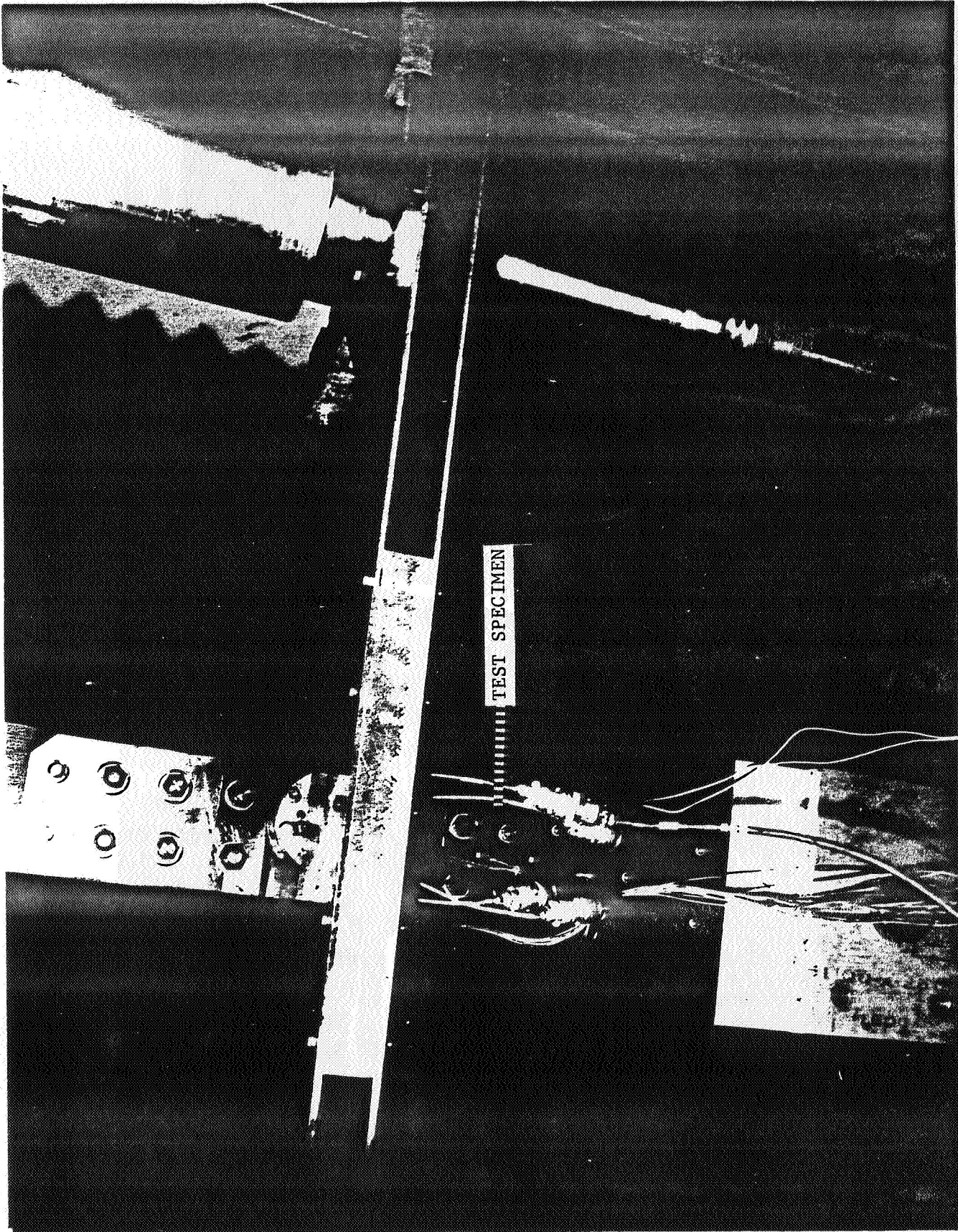


FIGURE 39 SIDE RESTRAINT SYSTEM - SUBCOMPONENT #1

ORIGINAL PAGE IS
OF POOR QUALITY

ORIGINAL PAGE IS
OF POOR QUALITY

ORIGINAL PAGE IS
OF POOR QUALITY

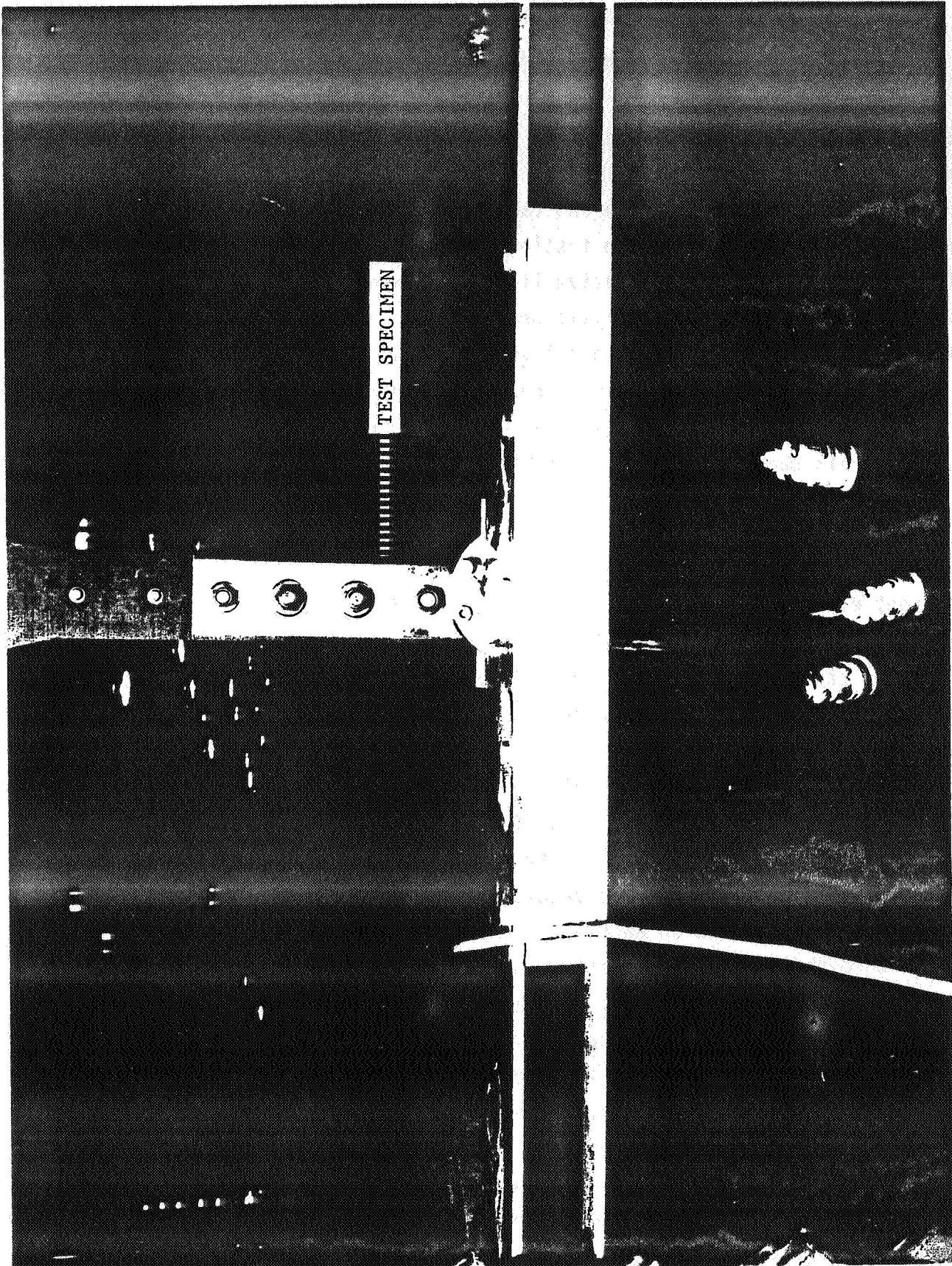


FIGURE 40 SIDE RESTRAINT SYSTEM - SUBCOMPONENT #2

SECTION 3.4

DEMONSTRATION SUBCOMPONENT SPECIMENS

TEST PROGRAM - PROCEDURES AND RESULTS

The demonstration subcomponent specimens were both tested to static failure under axial tension load. After installing each specimen in the test machine, the load application and data acquisition systems were checked for proper operation. The testing procedures were essentially the same for both tests. A representative limit load level was determined for each specimen on the basis of analysis predictions. For each test, the specimen was loaded to the limit load level, a visual inspection was conducted, and the applied load was increased at a continuous rate to static failure. Single data points were taken in increments of 20,000 pounds for strain gage, load indicating bolts, and load cell output, up to the limit load level. Strain and load output data were read continuously from limit load to failure.

Subcomponent #1 was loaded in axial tension to static failure at an ultimate load of 270,000 pounds. This corresponds to an average gross-section stress and strain of about 47,500 psi and 5,100 microstrain. The failure occurred in net-section tension through the first row of fasteners entering the joint as shown in Figures 41 and 42. This was precisely the predicted failure mode, and the 270,000 pound failure load was 4% above the analytically predicted strength. The strain gage, load bolt, and load cell data gathered throughout the test are presented graphically and numerically in Appendix B. The results of a linear analysis of joint behavior have been included on each plot. As expected, very little load was passed through the aluminum fitting, which sat above one of the titanium splices through which most of the load was transferred. The onset of nonlinearity in the specimen behavior is evident from the load-strain plots at roughly the 200,000 pound load level. (No evidence of damage or nonlinear effects were observed during the visual inspection at the 160,000 pound load level.) Note that while the analysis results plotted along with test data in Appendix B were derived from a linear solution, the final joint strength prediction shown in Table II was based on the results of a nonlinear solution.

The static test of Subcomponent #2 had similar results. Failure occurred at an applied load of 115,400 pounds, corresponding to a gross-section stress of 46,200 psi and strain level of 4,970 microstrain. The failure mode was again a net-section tension failure in the two composite members through the first row of bolts as shown in Figures 43 and 44. The failure load was approximately 28% above the original analysis prediction of 90,000 lb. However, a post-test examination of the analysis model revealed that the end constraints had not been properly represented, resulting in an overly conservative solution. The strain gage, load bolt, and load cell output are presented in graphic and tabular form in Appendix B.

The results of these tests provided the confidence level in both the design concepts and the analysis methodology to design and build the large technology demonstration specimen.

ORIGINAL PAGE IS
OF POOR QUALITY

ORIGINAL PAGE IS
OF POOR QUALITY

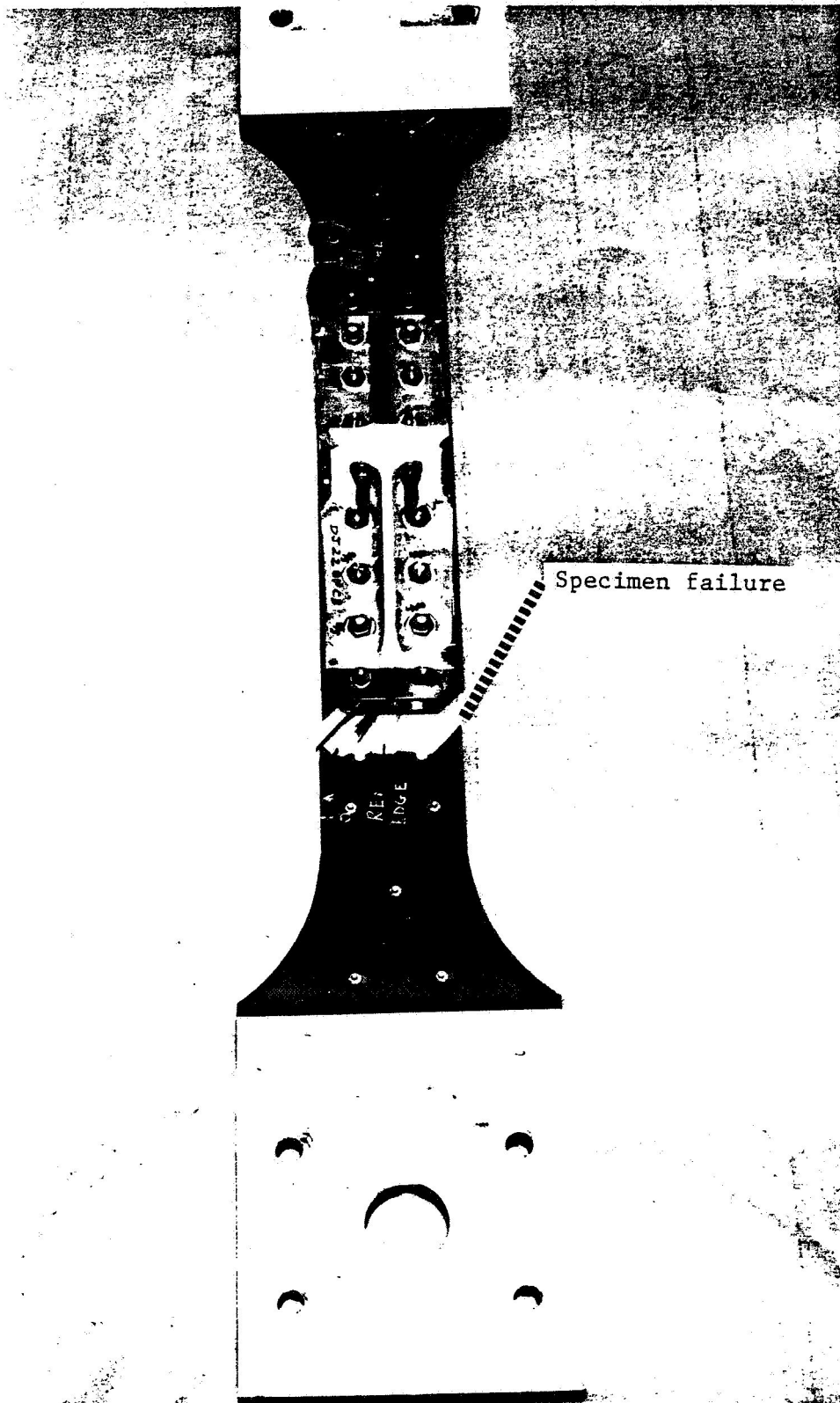
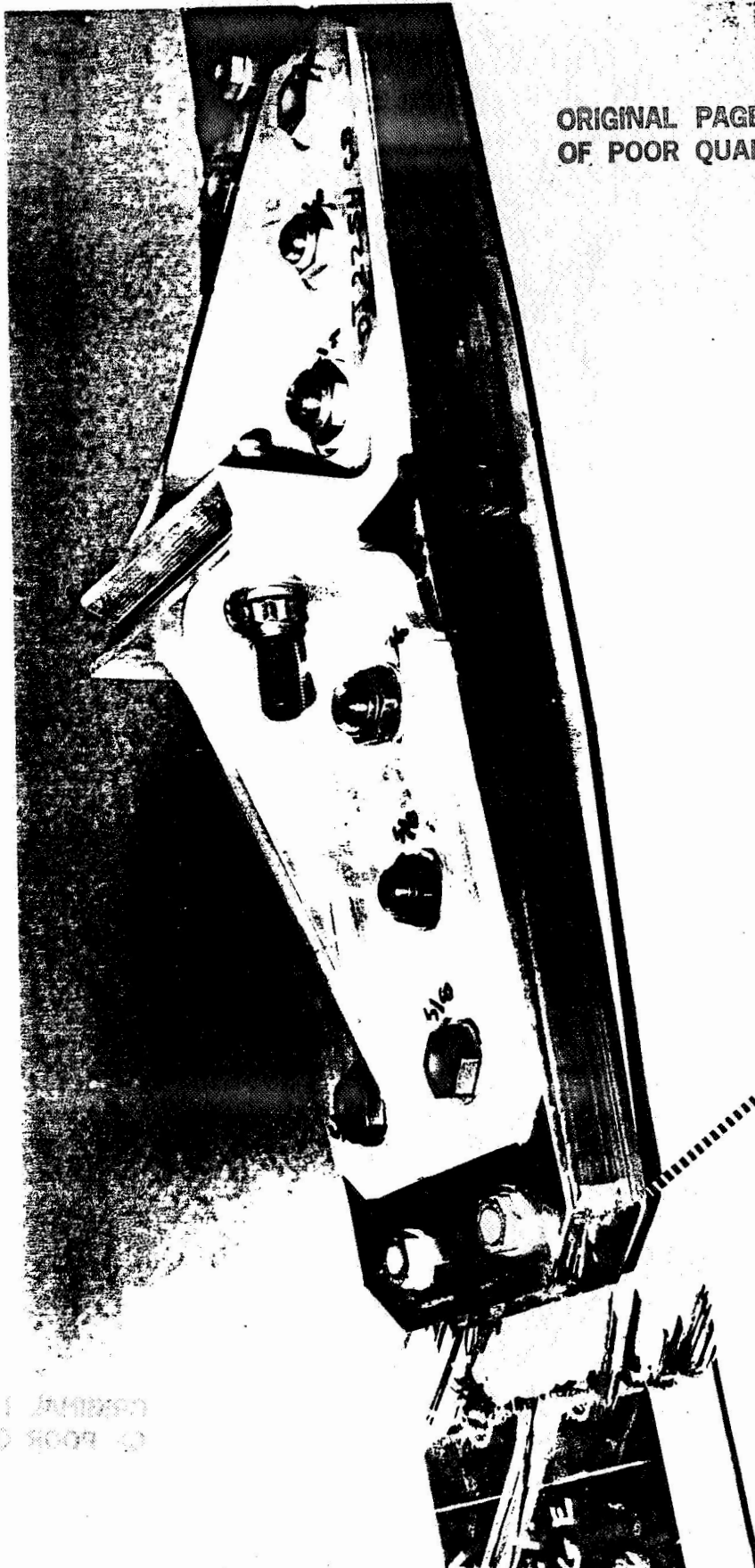


FIGURE 41 SUBCOMPONENT #1 - FAILED SPECIMEN

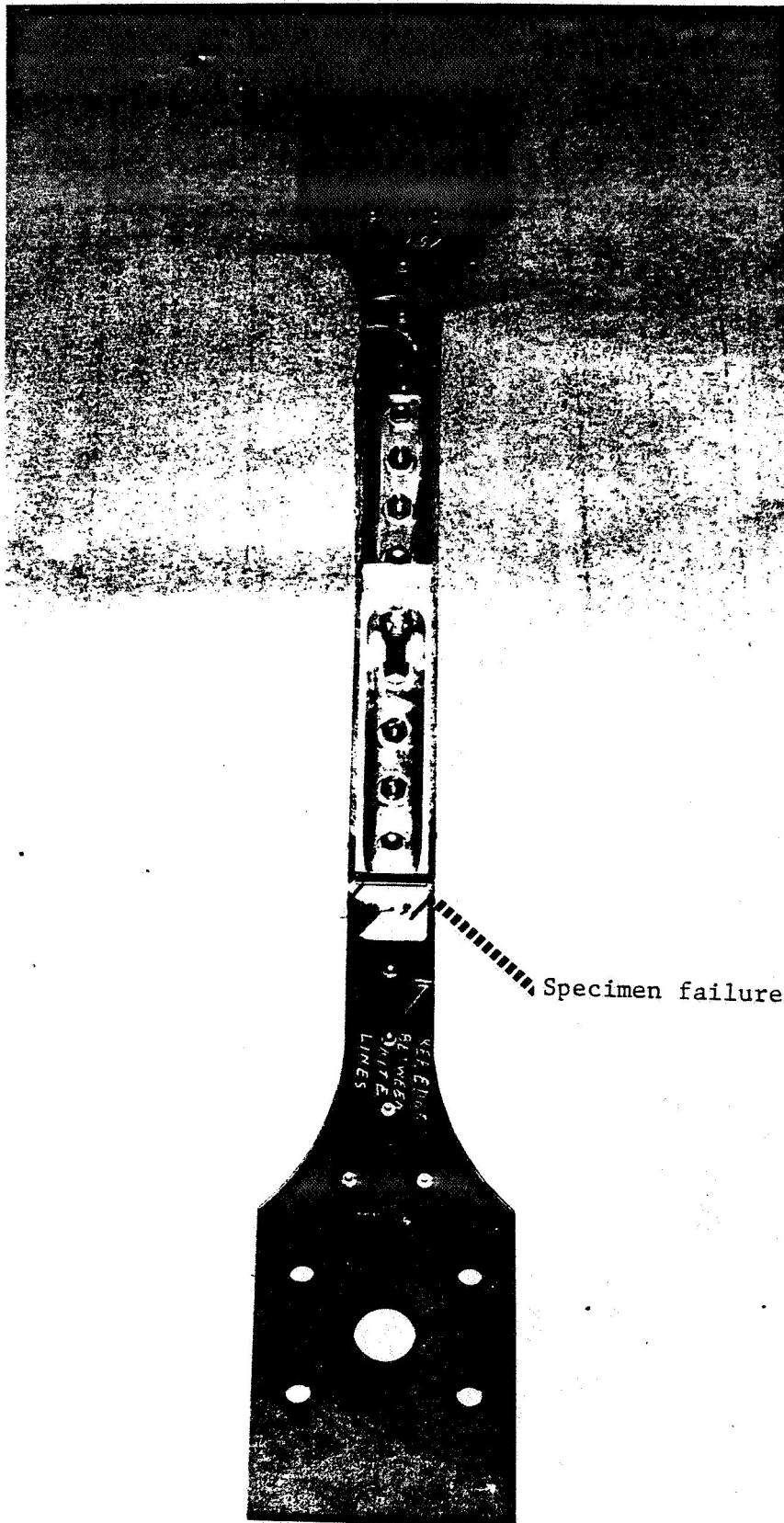
ORIGINAL PAGE IS
OF POOR QUALITY



ORIGINAL PAGE IS
OF POOR QUALITY

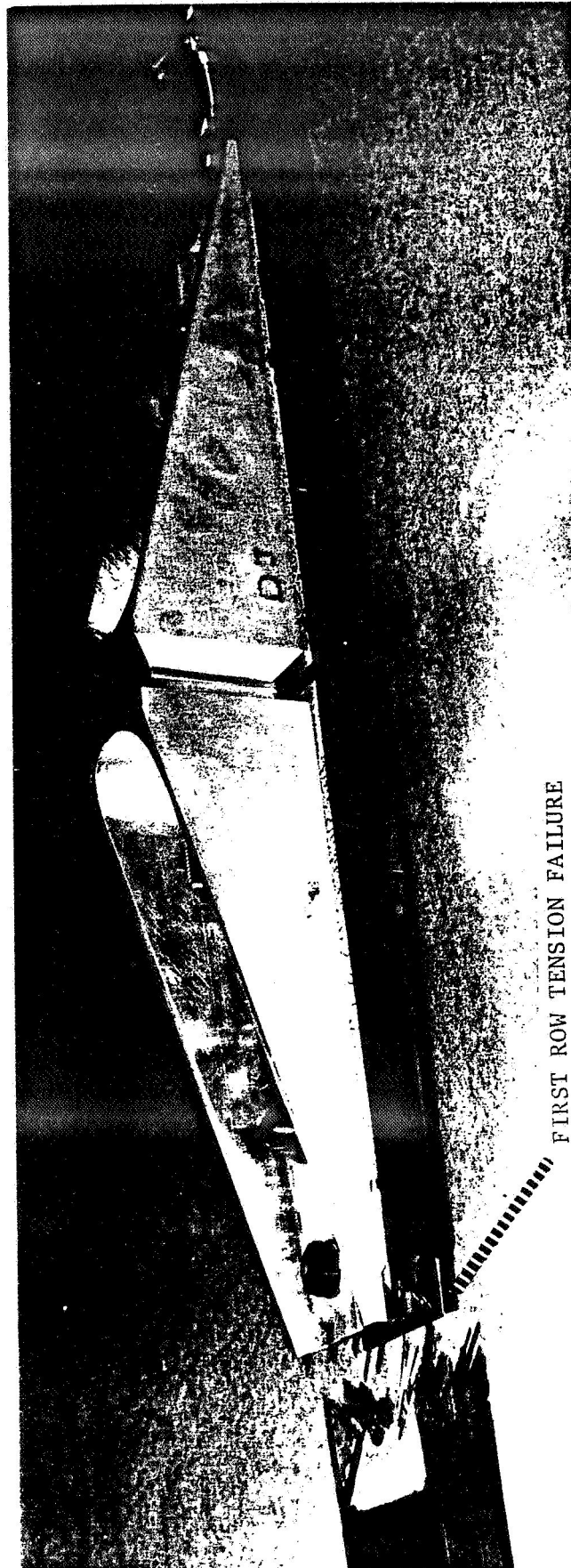
1st ROW TENSION FAILURE

FIGURE 42 SUBCOMPONENT #1 - FAILED SPECIMEN



ORIGINAL PAGE IS
OF POOR QUALITY

FIGURE 43 SUBCOMPONENT #2 - FAILED SPECIMEN



ORIGINAL PAGE IS
OF POOR QUALITY

FIRST ROW TENSION FAILURE

FIGURE 44 SUBCOMPONENT #2 - FAILED SPECIMEN

SECTION 4.1

TECHNOLOGY DEMONSTRATION TEST PROGRAM

TEST ARTICLE

The Phase II test program culminated in a static test of a large bolted joint representing the lower rear spar and wing splice at the side of fuselage attachment. The design concept shown in Figure 45 presented a challenging task from both an engineering and manufacturing standpoint. The composite joint members consisted of the wing skin, spar cap, and spar web members, while all the splices and fittings were made of titanium and aluminum, respectively. The titanium "tee" splice is representative of the side of the fuselage bulkhead. The wing skin, spar cap, and spar web members were fabricated with the same 10-mil tape material as previous specimens using the (37.5% 0°, 50% $\pm 45^\circ$, 12.5% 90°) fiber pattern. The lower wing cover panel structure away from the joint was designed to an ultimate strain level of roughly 5,250 microstrain, with a skin-stringer load intensity of 30,000 pounds-per-inch. In order to reduce the complexity of the test, the dihedral and sweep break that would be present in the actual baseline structure were eliminated.

Portions of the detailed assembly drawing are shown in Figures 46 and 48. The entire specimen including the end fittings was 100 inches in length between the centerlines of the pin loading attachments. The end fittings, made of 7075-T6 aluminum, were designed to a high margin of safety over the strength of the composite joint test section. The centerline of applied load from the fitting was adjusted in order to minimize the asymmetric effects induced by the shifting center of mass along the specimen length. Despite the effort to reduce these out-of-plane forces, provisions were made for side restraints to be attached at the specimen centerline as shown in Figure 48. For this test, the wing skin extended chordwise to a point even with the full design width of the spar cap, which is just in-board of the aft stringer.

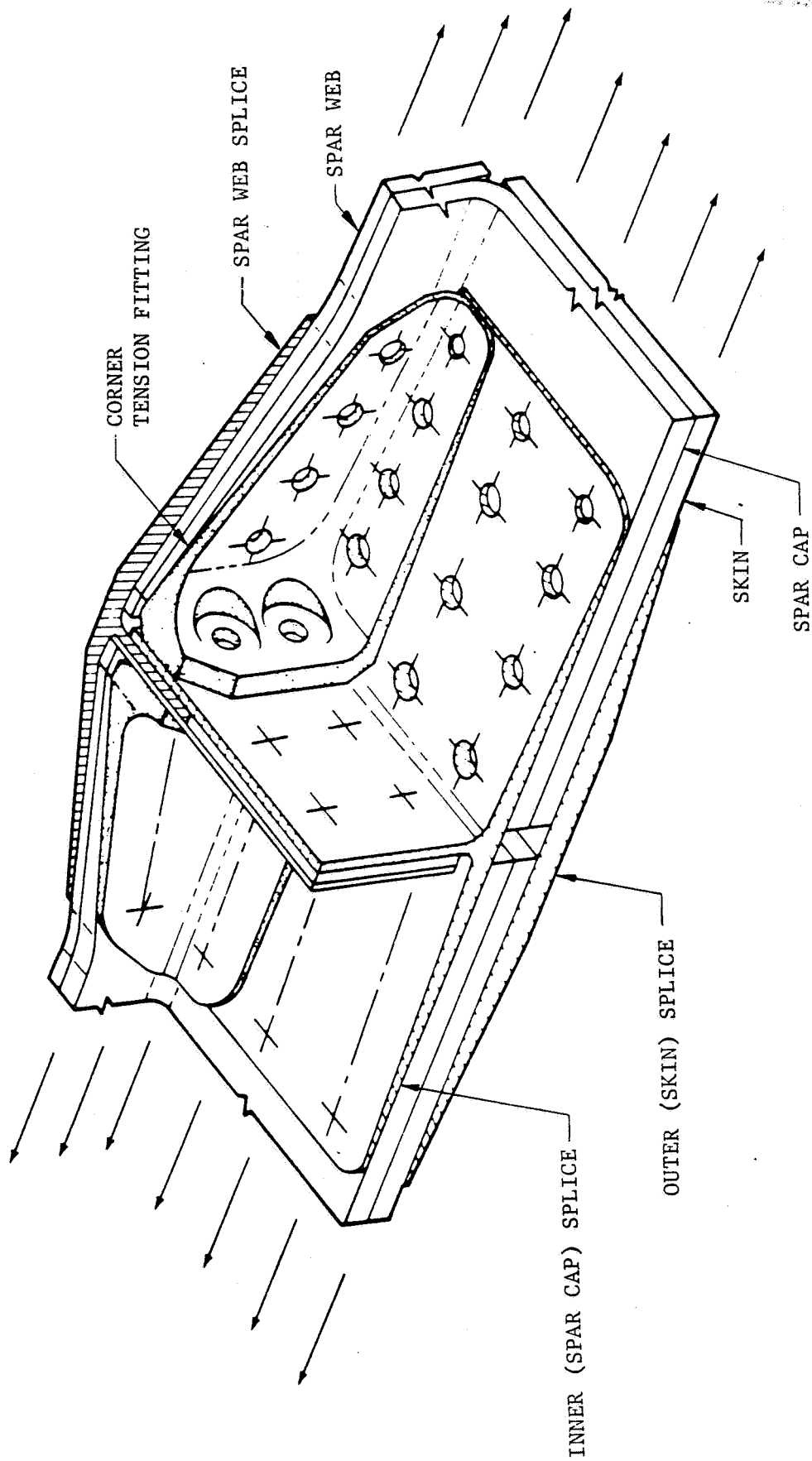


FIGURE 45 TECHNOLOGY DEMONSTRATION JOINT

ORIGINAL PAGE IS
OF POOR QUALITY

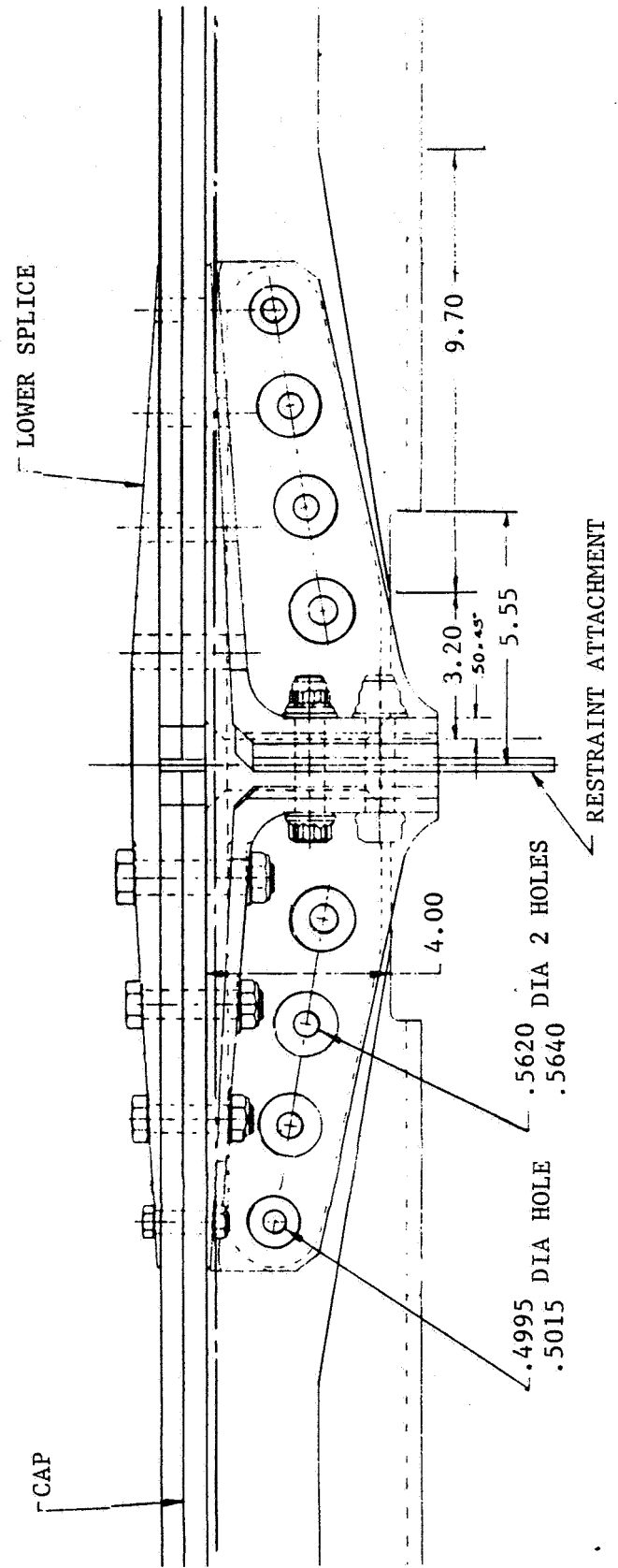
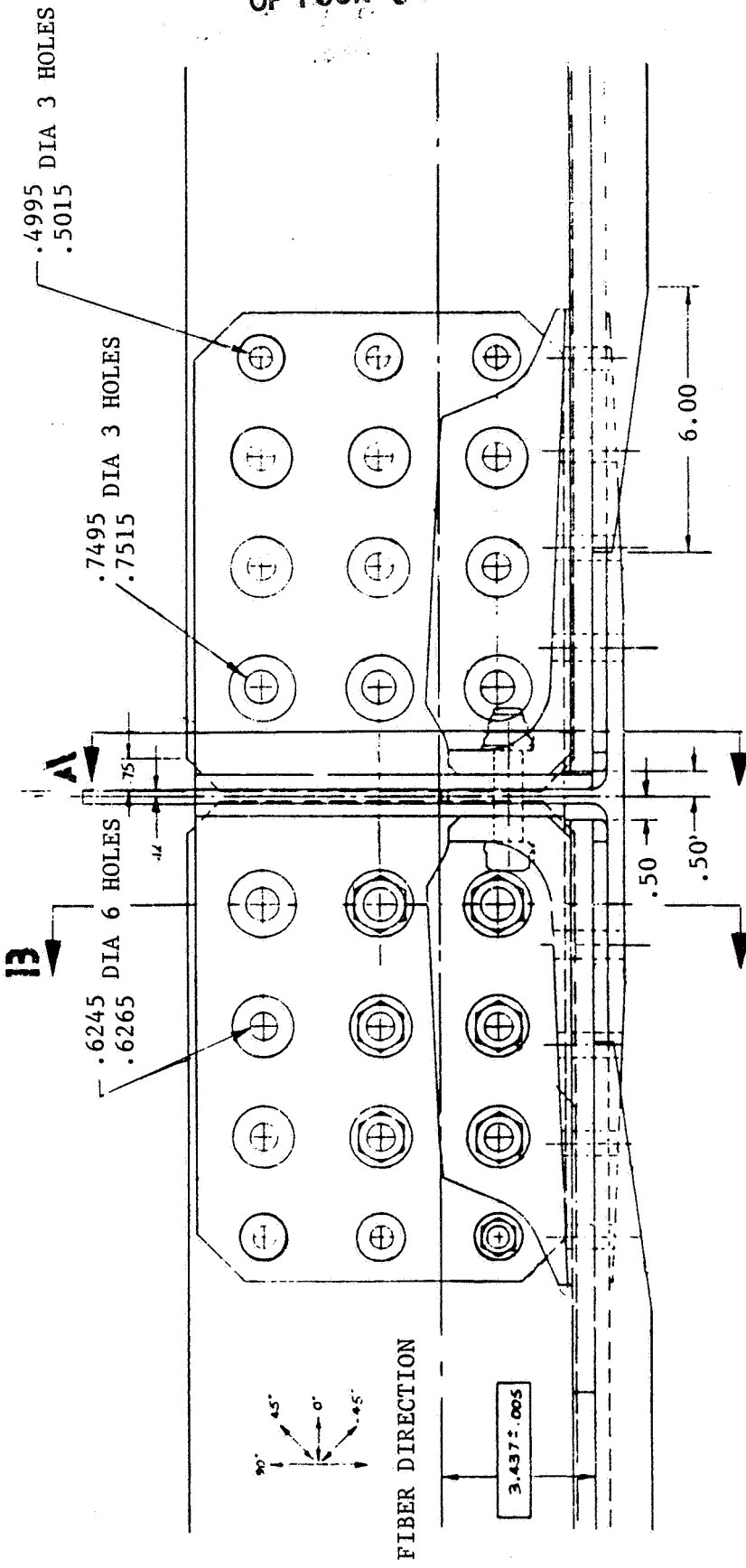
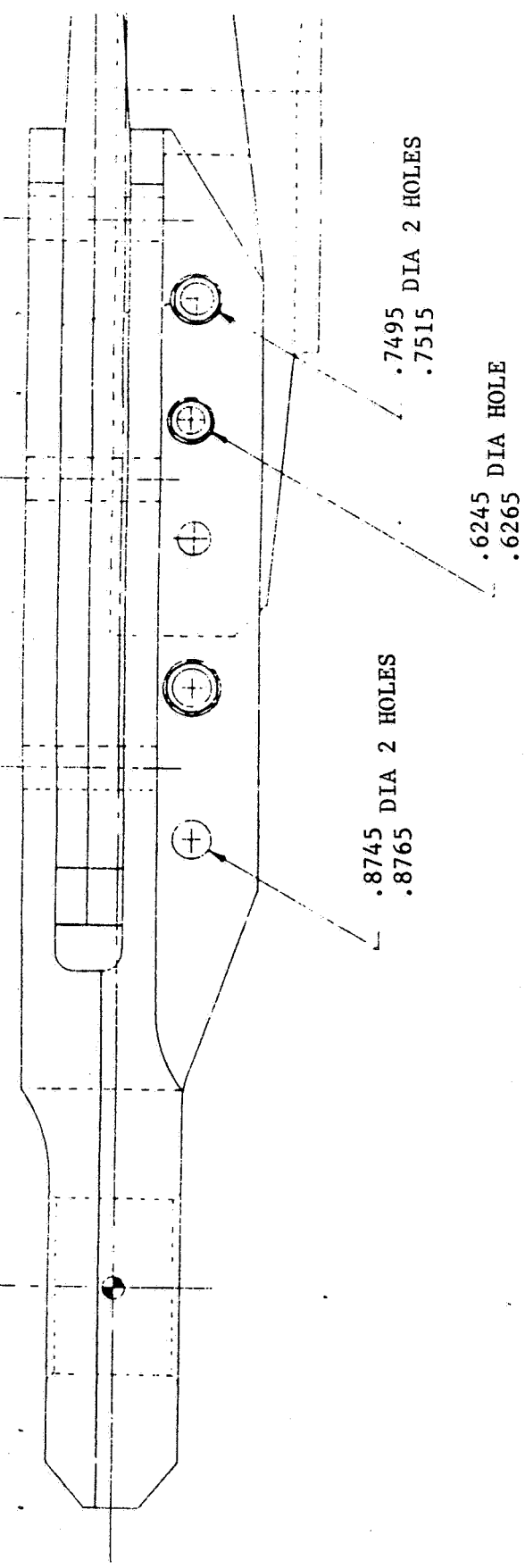


FIGURE 46 TECHNOLOGY DEMONSTRATION SPECIMEN ASSEMBLY

DE POOR QUALITY
ORIGINAL PAGE IS



ORIGINAL PAGE IS
OF POOR QUALITY

.9995 DIA 6 HOLES
1.0015

END FITTING ASSEMBLY

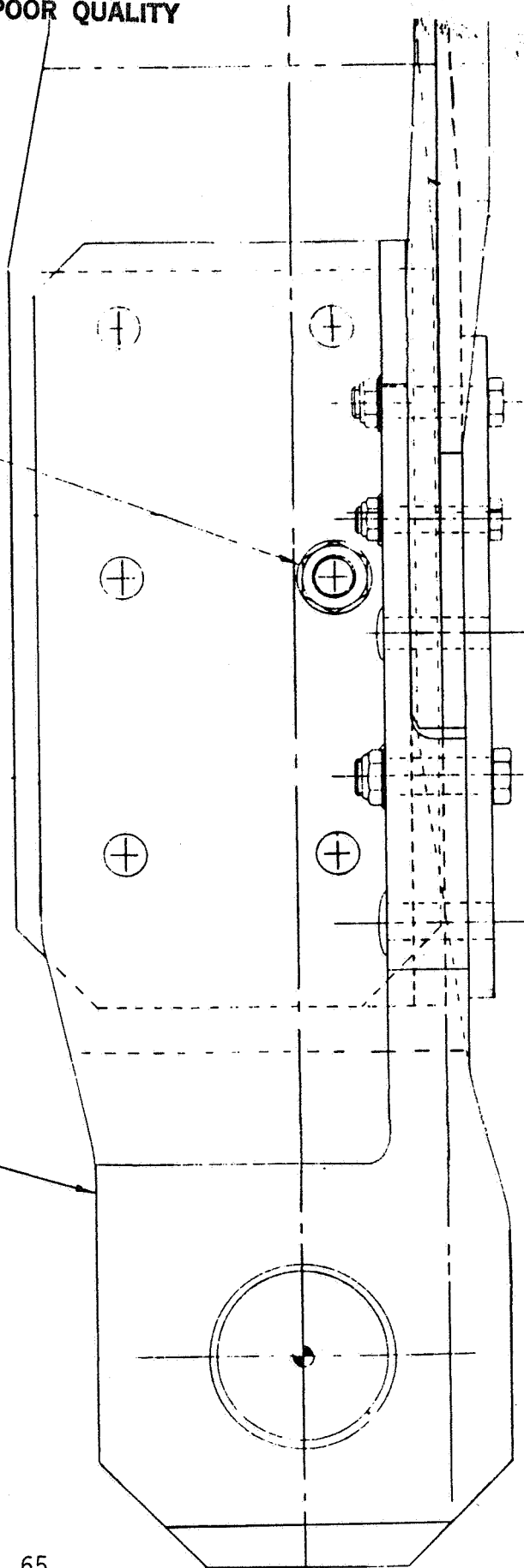
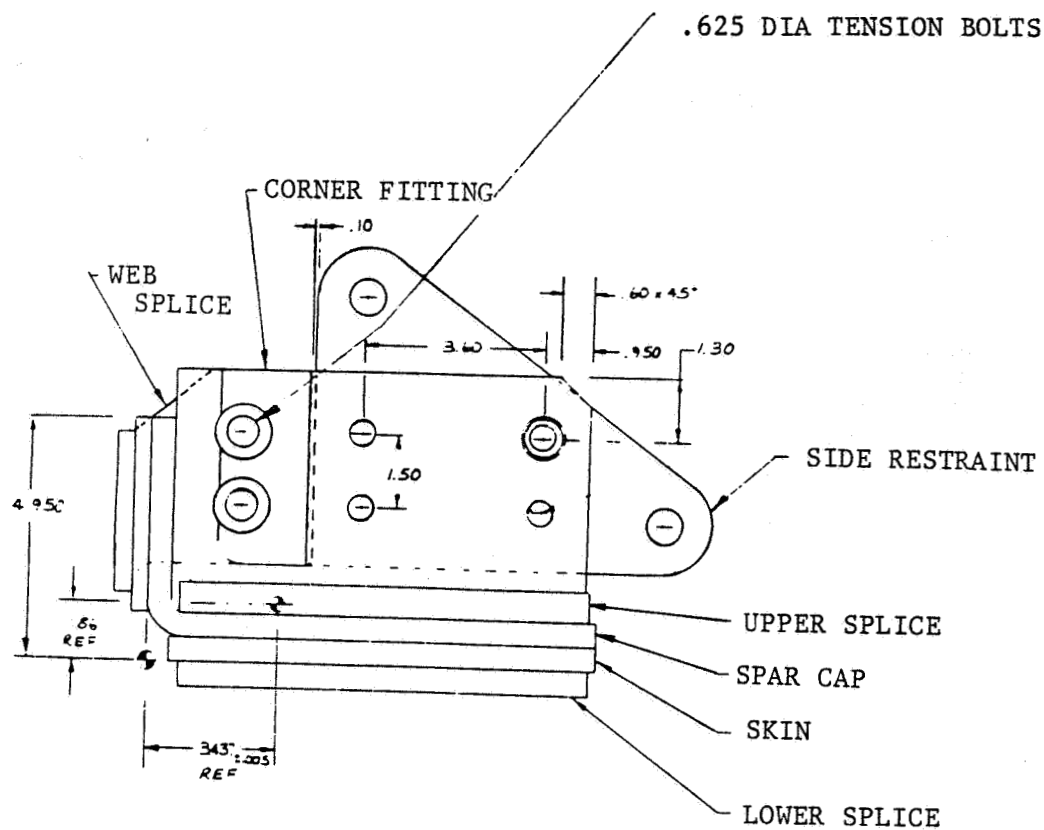
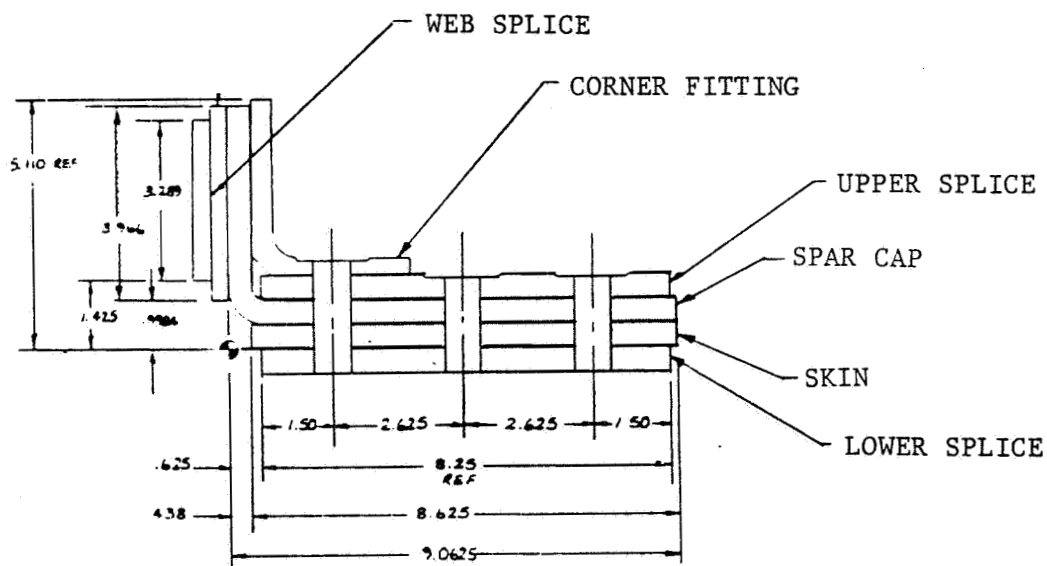


FIGURE 47 TECHNOLOGY DEMONSTRATION ARTICLE - END FITTINGS



SECTION **A-A**



SECTION **B-B**

ORIGINAL PAGE 15
OF POOR QUALITY

FIGURE 48 TECHNOLOGY DEMONSTRATION ARTICLE -
CROSS-SECTIONS

The specimen is shown at various stages of assembly in Figures 49 through 52. All of the composite joint members were flat plates, except for the spar cap members which were angle sections. The two spar cap members were fabricated on an aluminum male tool with the required thickness transitions machined into the tool surface. The spar cap member is shown in Figure 49 with the rest of the elements, trimmed to final dimensions with fastener holes drilled and ready for assembly. Figure 50 shows the specimen partially assembled. Titanium fasteners were used in all cases and tapered metallic surfaces were spotfaced to accommodate fastener seating. A closeup view of the bolted joint area is shown in Figure 52.

All test laminates were c-scanned prior to assembly. In all but one case, the c-scan results identified no anomalies. However, a c-scan of one of the spar cap members did show a region of questionable quality in the standing leg of the spar cap. The problem area appeared in the 0.50-inch thick section prior to the thickness buildup into the end fitting. Since the test was to be conducted under static tension loads only (no fatigue or load reversal), the decision was made to accept the part and complete the assembly. Field fasteners were added to the specimen prior to testing, representing the typical out-board attachments between the skin, spar, and web elements. Standard bolt torque values were used in all cases.



FIGURE 49 TECHNOLOGY DEMONSTRATION SPECIMEN ASSEMBLY

ORIGINAL PAGE IS
OF POOR QUALITY

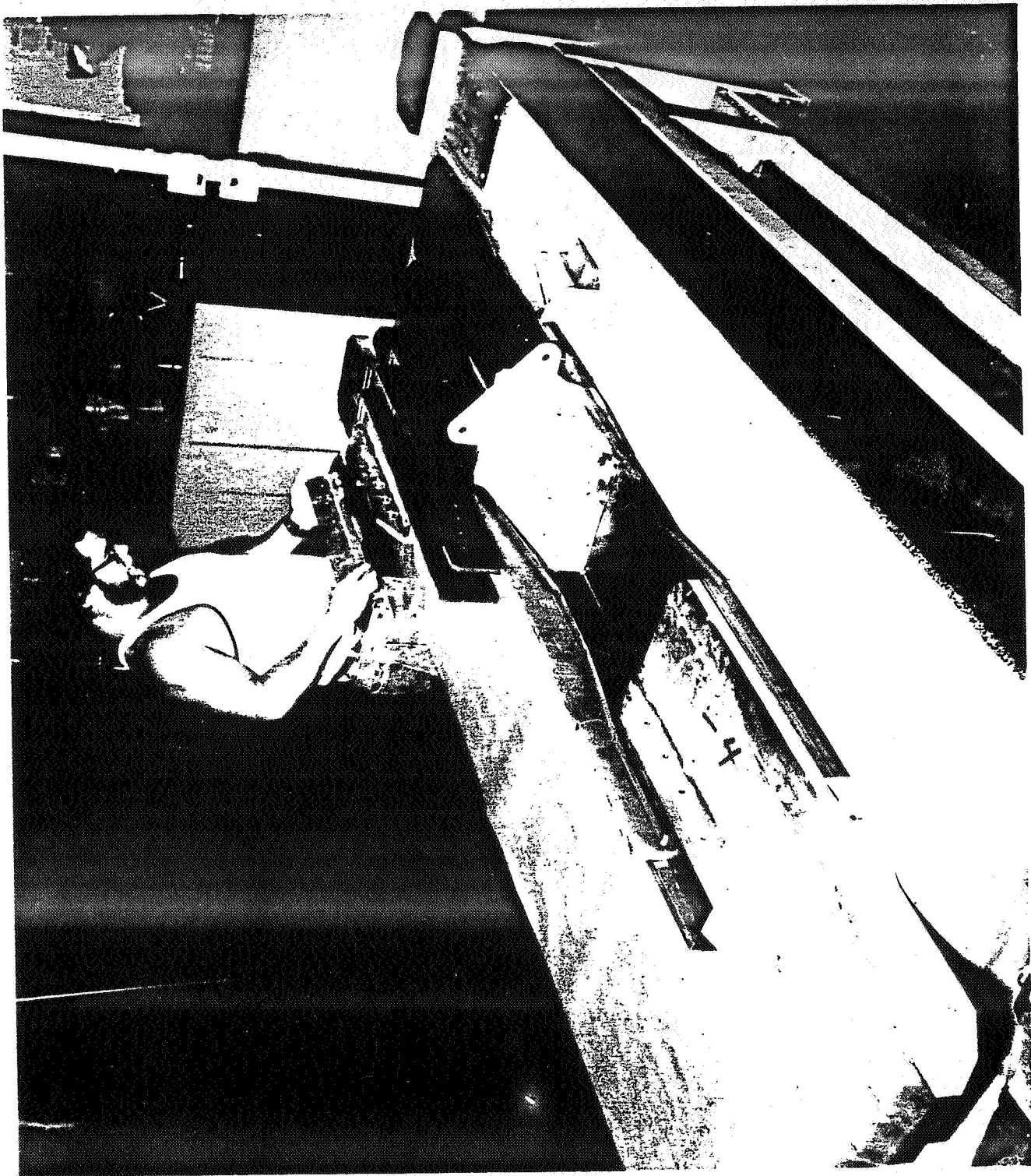


FIGURE 50 TECHNOLOGY DEMONSTRATION SPECIMEN ASSEMBLY

ORIGINAL PAGE IS
OF POOR QUALITY

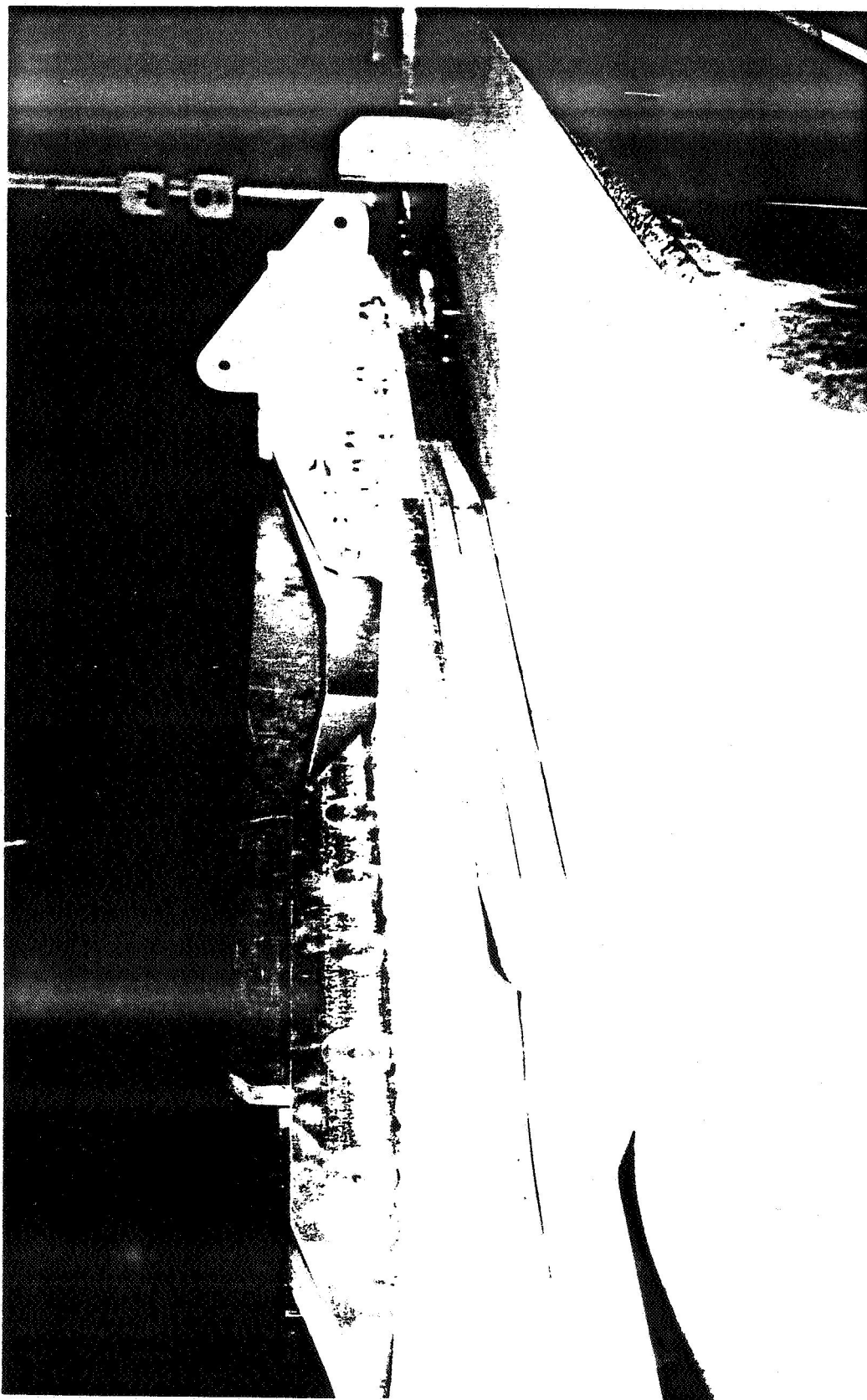


FIGURE 51 TECHNOLOGY DEMONSTRATION SPECIMEN ASSEMBLY

ORIGINAL PAGE IS
OF POOR QUALITY

ORIGINAL PAGE IS
OF POOR QUALITY

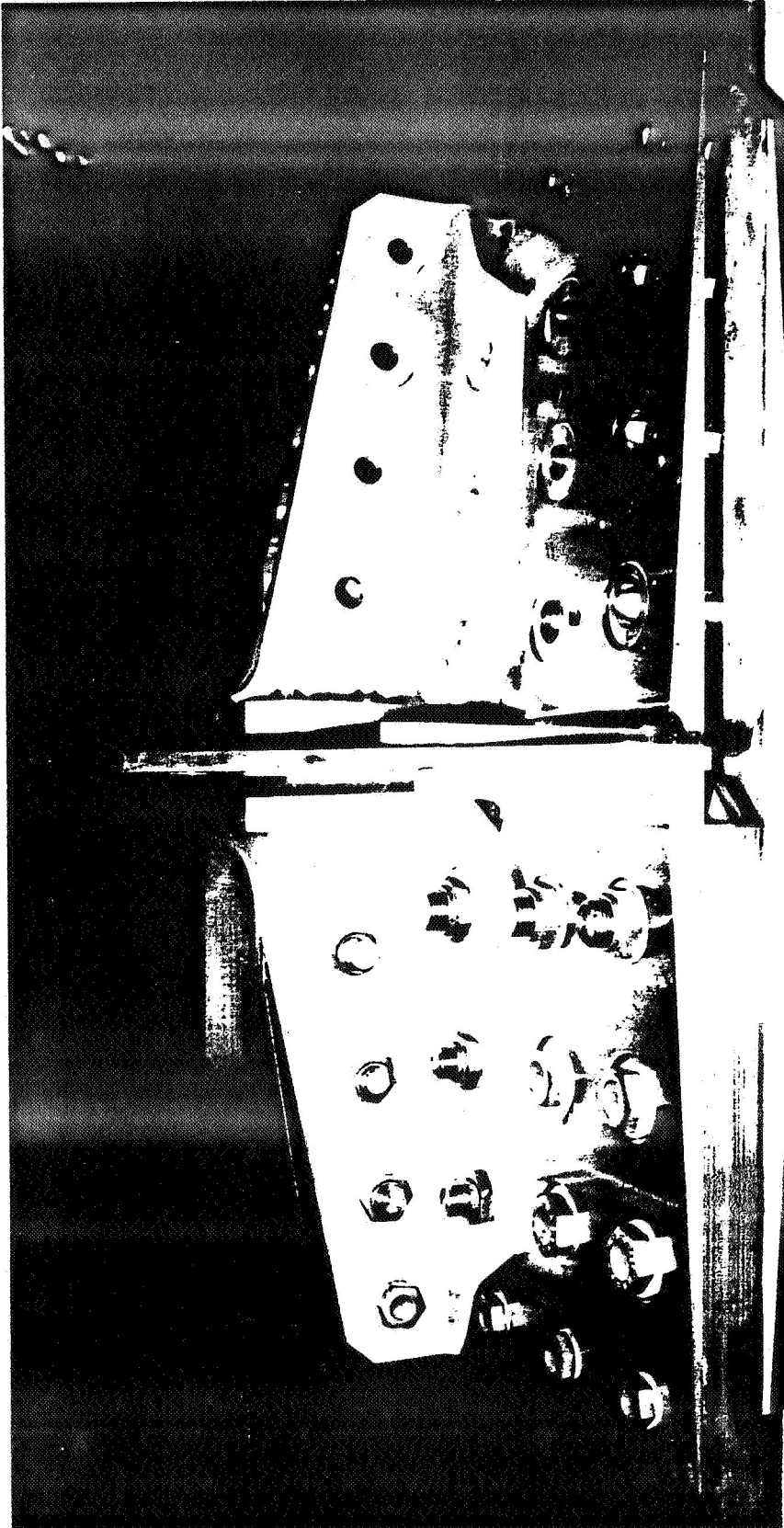


FIGURE 52 TECHNOLOGY DEMONSTRATION SPECIMEN -
TEST SECTION

SECTION 4.2
TECHNOLOGY DEMONSTRATION TEST
INSTRUMENTATION

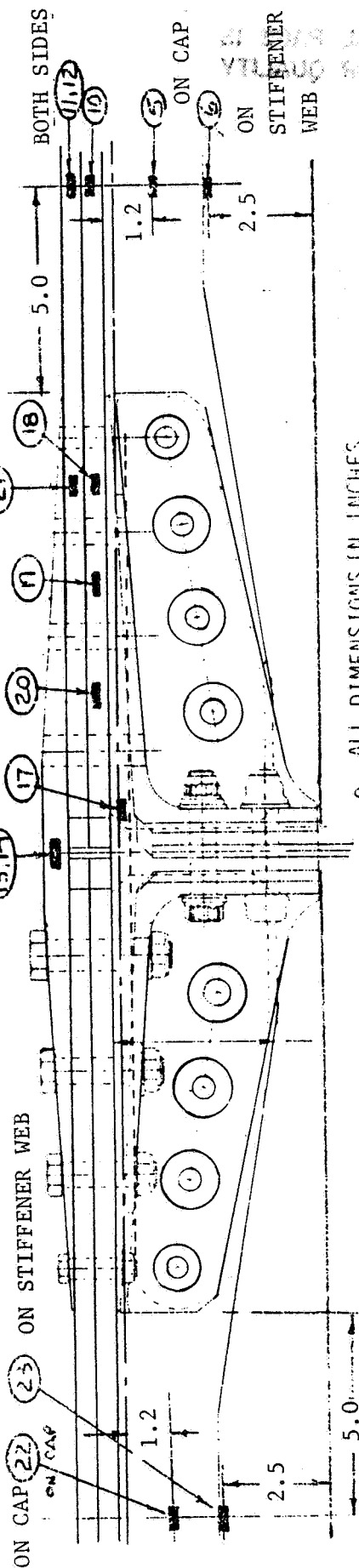
The technology demonstration article had 25 axial strain gages mounted to the specimen as shown in Figure 53 . Gage locations were selected to provide measurements of the amount of load distributed to each composite member and, where possible, to each splice member. Additional gages were placed along the bolted joint between rows of fasteners, at or near the critical locations as predicted by preliminary stress analysis. The strain gages were type EA-06-125AC-350. Surface preparation and methods for the attachment of gages to the specimen were the same as in previous tests. The side restraint at the specimen centerline was equipped with two 20,000 pound capacity load cells to monitor any out-of-plane forces induced by the applied tension loads.

The data acquisition system consisted of a Perkin Elmer computer which received the output from strain gages and side restraint load cells, and monitored the load applied by each of the two load actuators. The system was capable of single point or continuous read of strain gage and load cell output. A two channel strip chart recorder was used as a back-up to the digital system. Limit switches were included in the load control system to ensure that the intended load levels were not inadvertently exceeded.

The specimen is shown in Figures 54 through 57 with all strain gages attached and ready for test.

STRAIN GAGE LOCATIONS (25 TOTAL)

BOTH SIDES

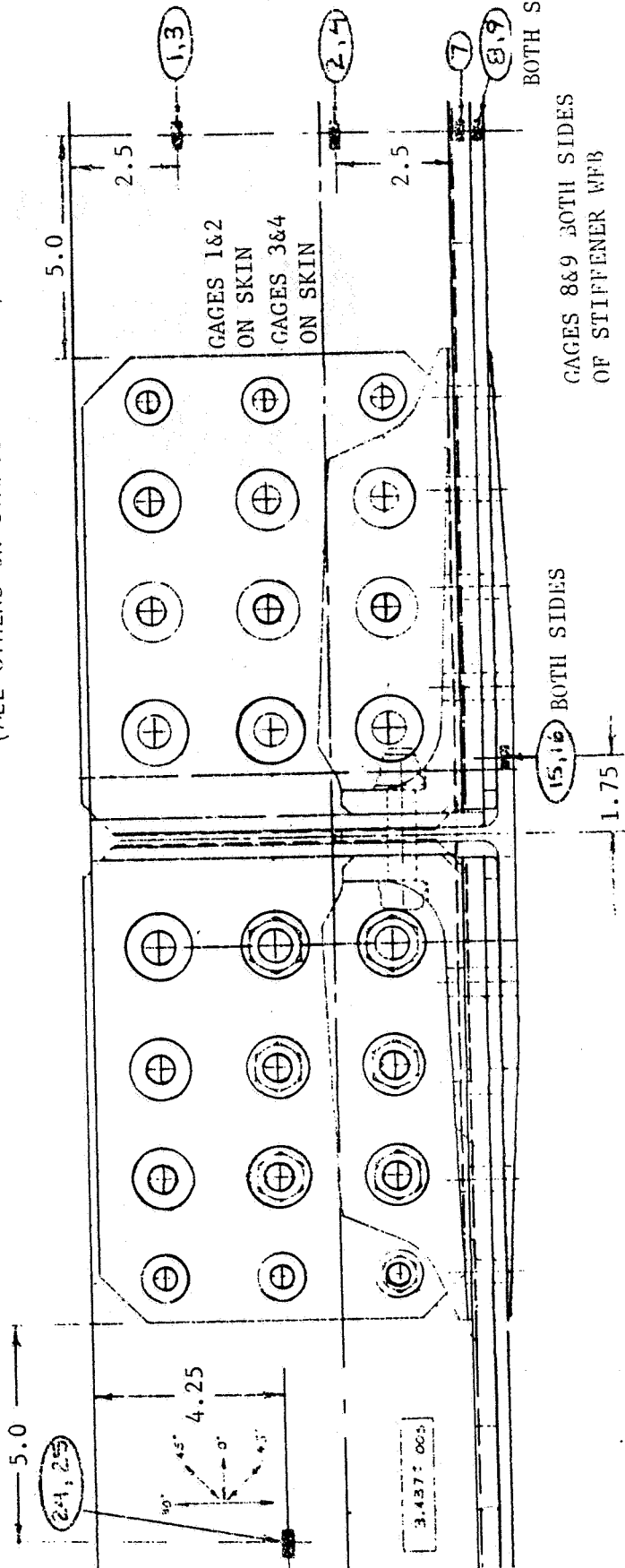


ALL DIMENSIONS IN INCHES

- GAGES CENTERED ON SPECIMEN EDGE
- GAGES 18-21 CENTERED BETWEEN FASTENER ROWS
- GAGES 13-17 ARE MOUNTED ON TITANIUM (ALL OTHERS ON COMPOSITE PARTS)

GAGE 24 ON SKIN
GAGE 25 ON CAP

ORIGINAL PAGE IS
OF POOR QUALITY



BOTH SIDES

GAGES 8&9 BOTH SIDES
OF STIFFENER WEB

BOTH SIDES

1.75

FIGURE 53 TECHNOLOGY DEMONSTRATION ARTICLE - STRAIN GAGE LOCATIONS

ORIGINAL PAGE IS
OF POOR QUALITY

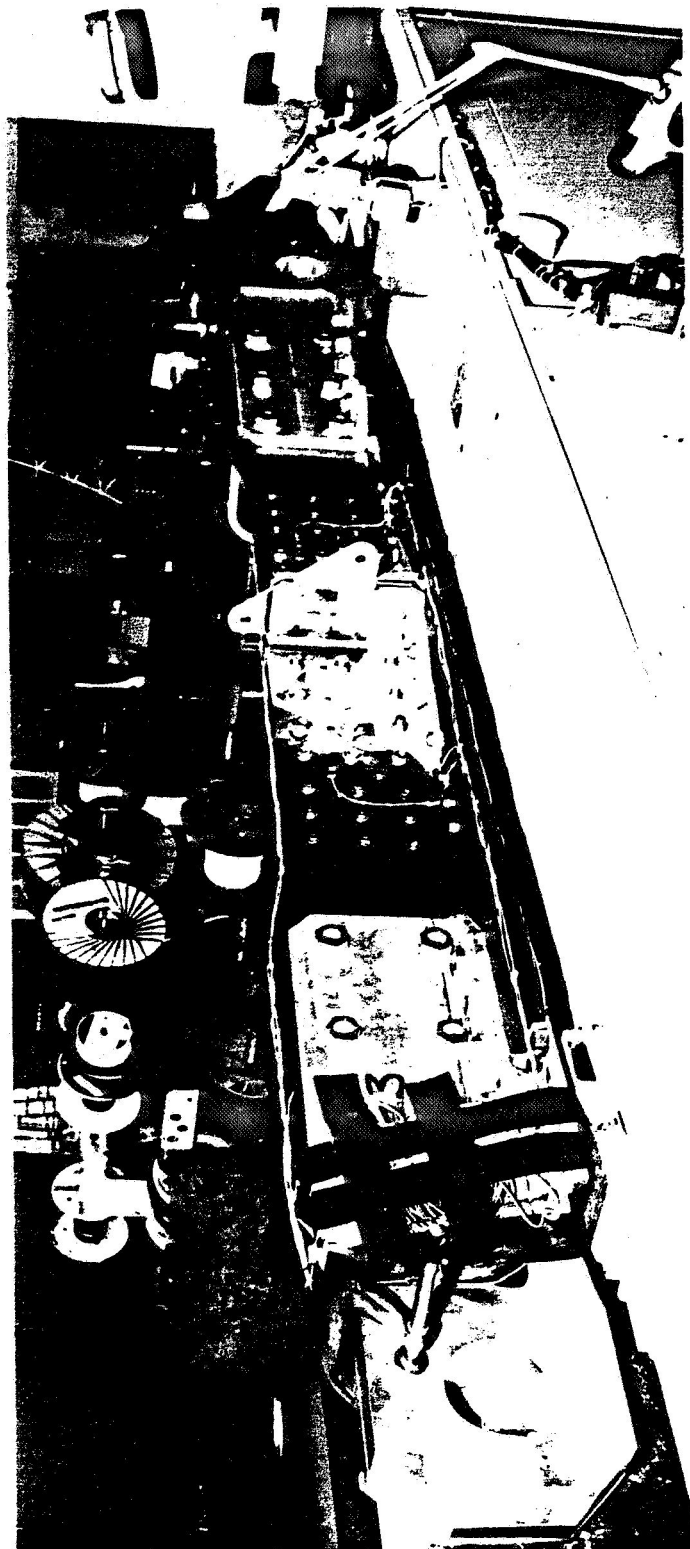


FIGURE 54 TEST ARTICLE AFTER INSTRUMENTATION - SPAR CAP SIDE

ORIGINAL PAGE IS
OF POOR QUALITY

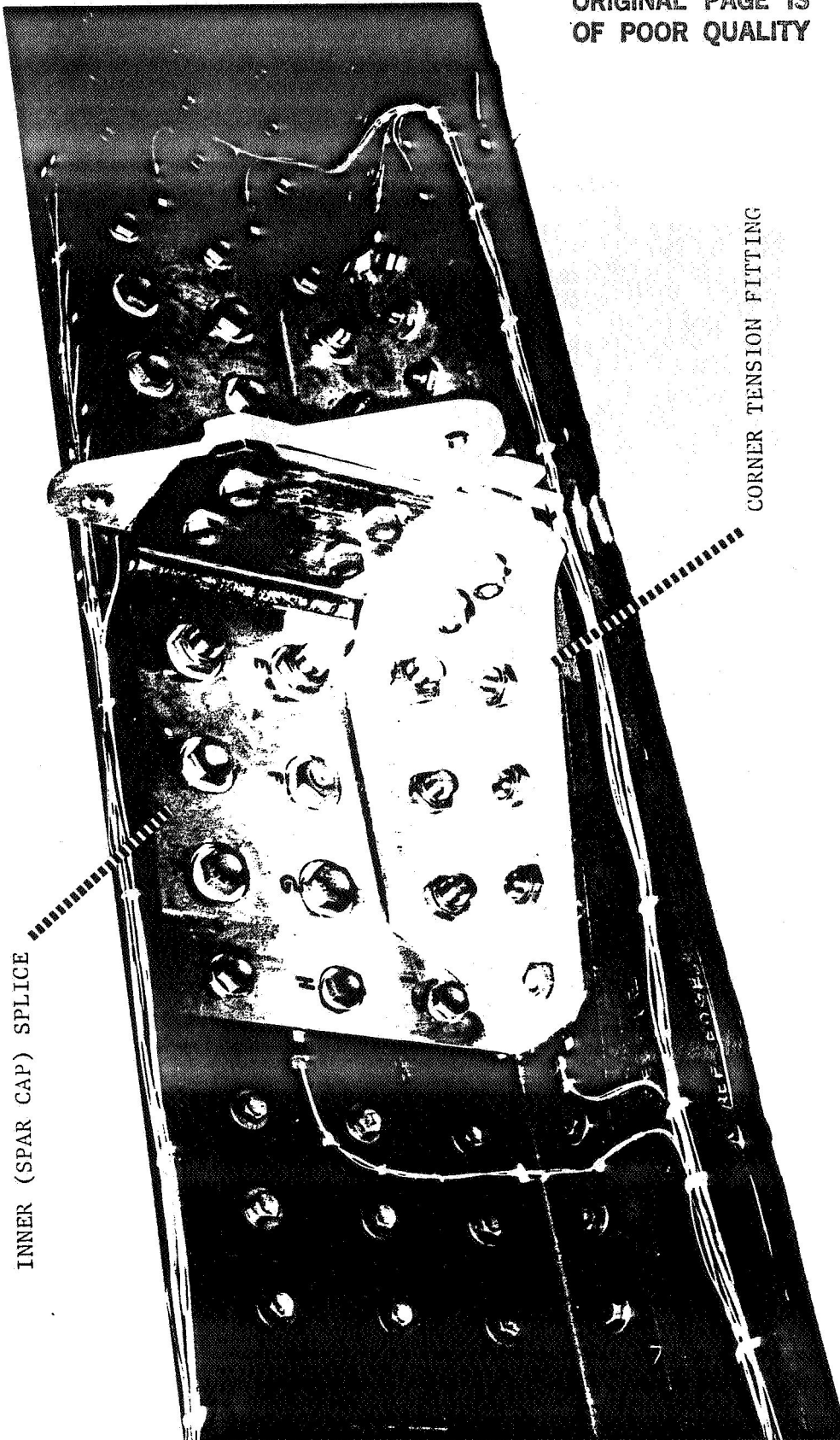


FIGURE 55 TEST ARTICLE AFTER INSTRUMENTATION - SPAR CAP SIDE

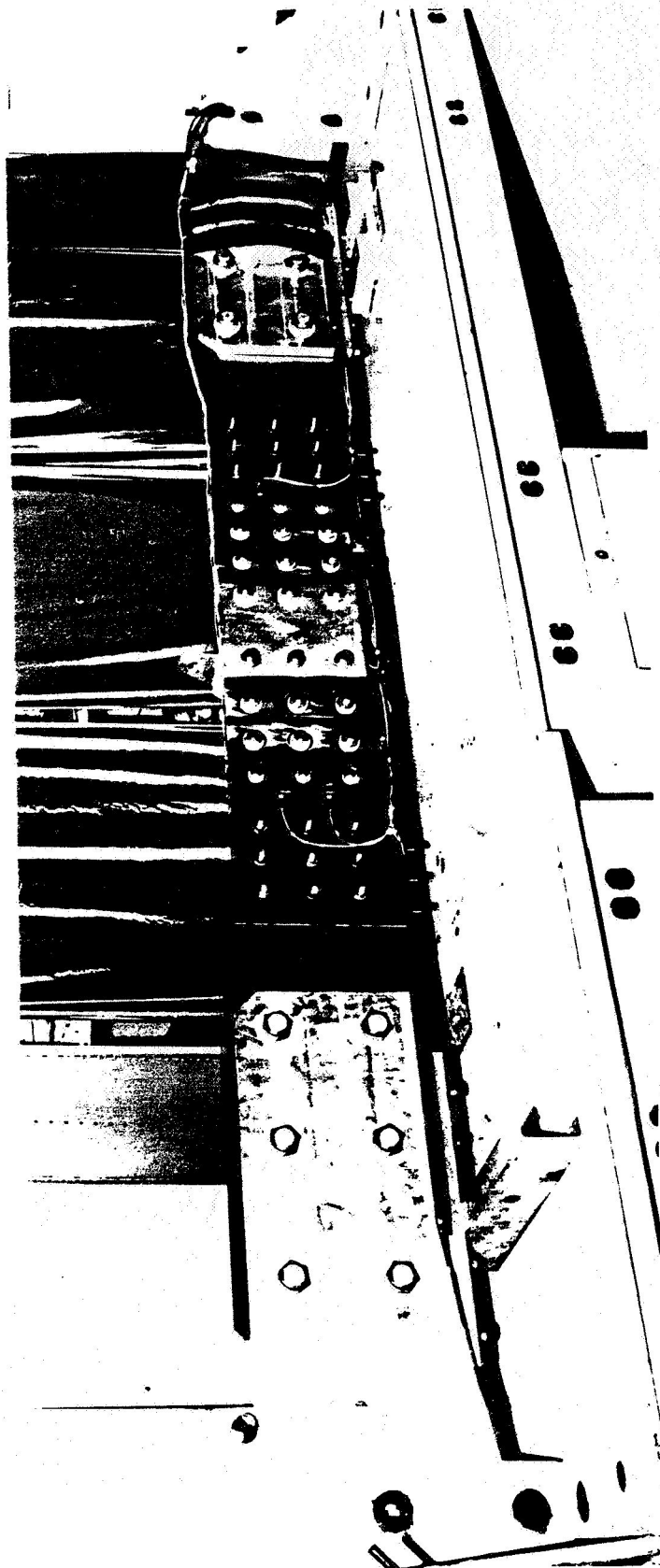


FIGURE 56 TEST ARTICLE AFTER INSTRUMENTATION - SKIN SIDE

ORIGINAL PAGE IS
OF POOR QUALITY

ORIGINAL PAGE IS
OF POOR QUALITY

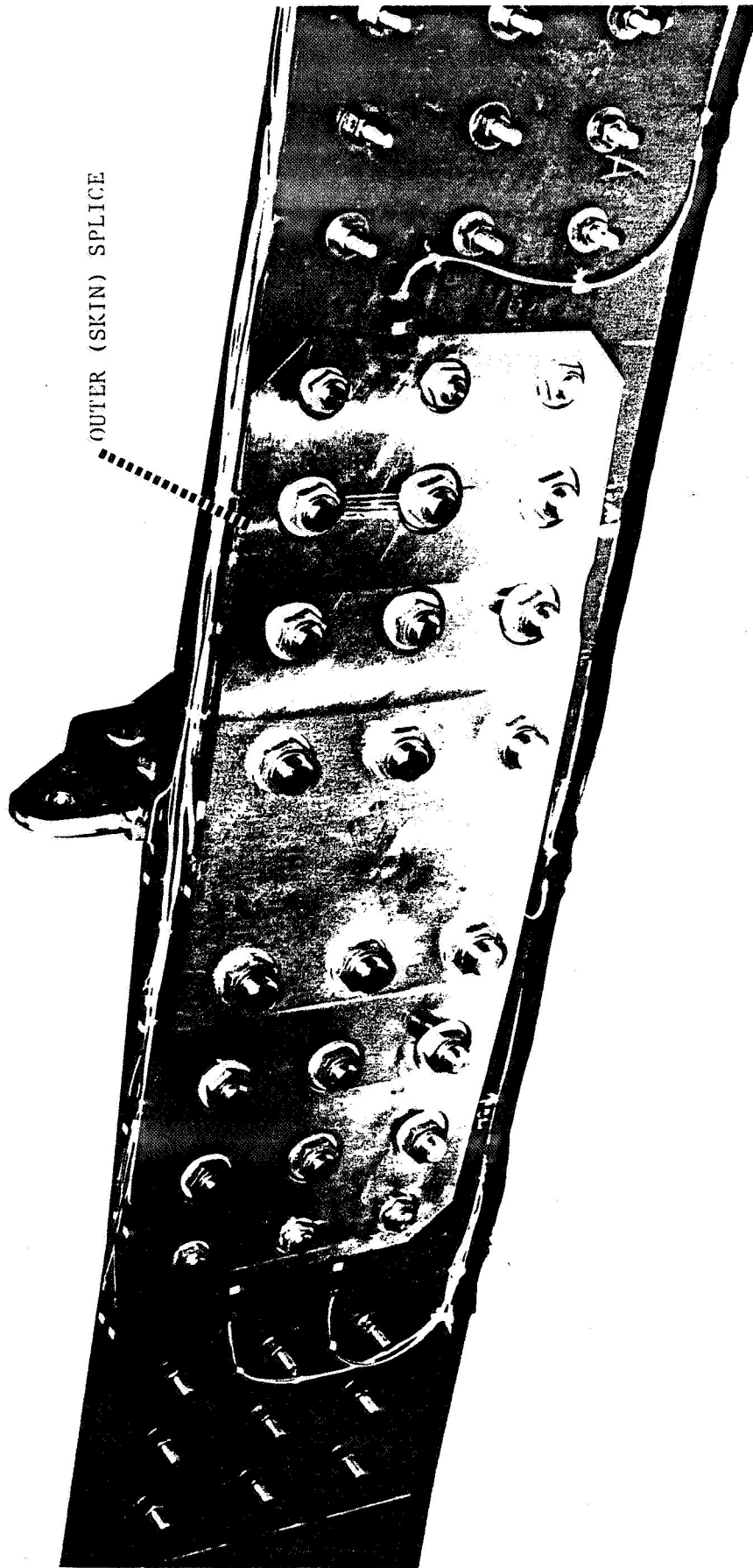


FIGURE 57 TEST ARTICLE AFTER INSTRUMENTATION - SKIN SIDE

SECTION 4.3
TECHNOLOGY DEMONSTRATION TEST
TEST SETUP

The static tension test of the technology demonstration article was conducted in a 2,500,000 pound capacity test tower, shown in Figures 58 and 59. Two 500,000 pound capacity load cells were used to apply the test loads (Figure 60). After completing the instrumentation procedures, the specimen was mounted in the test machine with large diameter steel pins attaching to a clevis arrangement which branched out to the two load actuators as shown in Figure 61. The same attachment system was used at the opposite end of the specimen (Figure 62). After properly positioning the specimen in the test fixture, the side restraints were attached to the aluminum loading plate at the specimen centerline. One of the side restraint load cells is shown prior to attachment to the specimen in Figure 63 .

ORIGINAL PAGE IS
OF POOR QUALITY

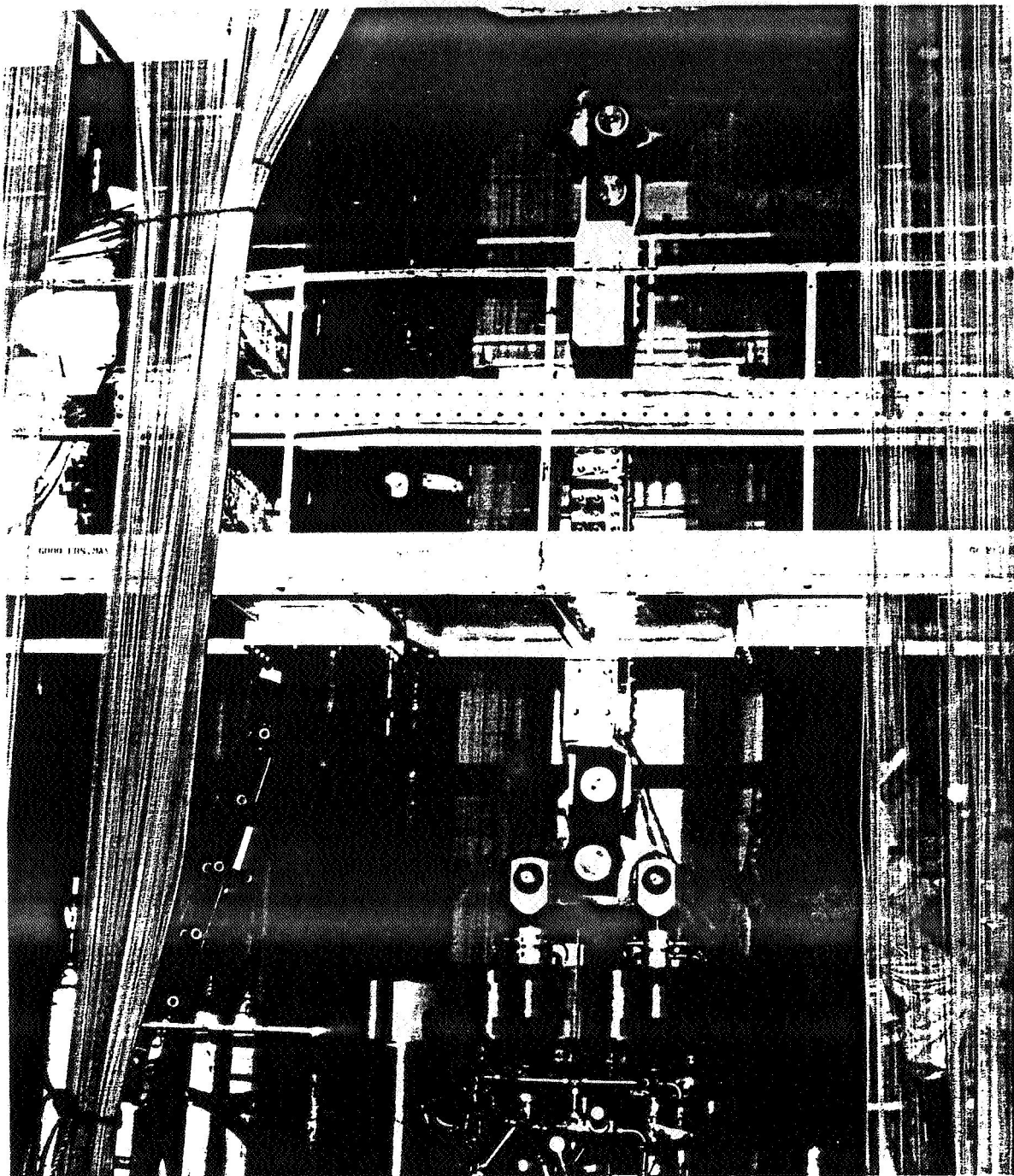


FIGURE 58 TECHNOLOGY DEMONSTRATION TEST SETUP

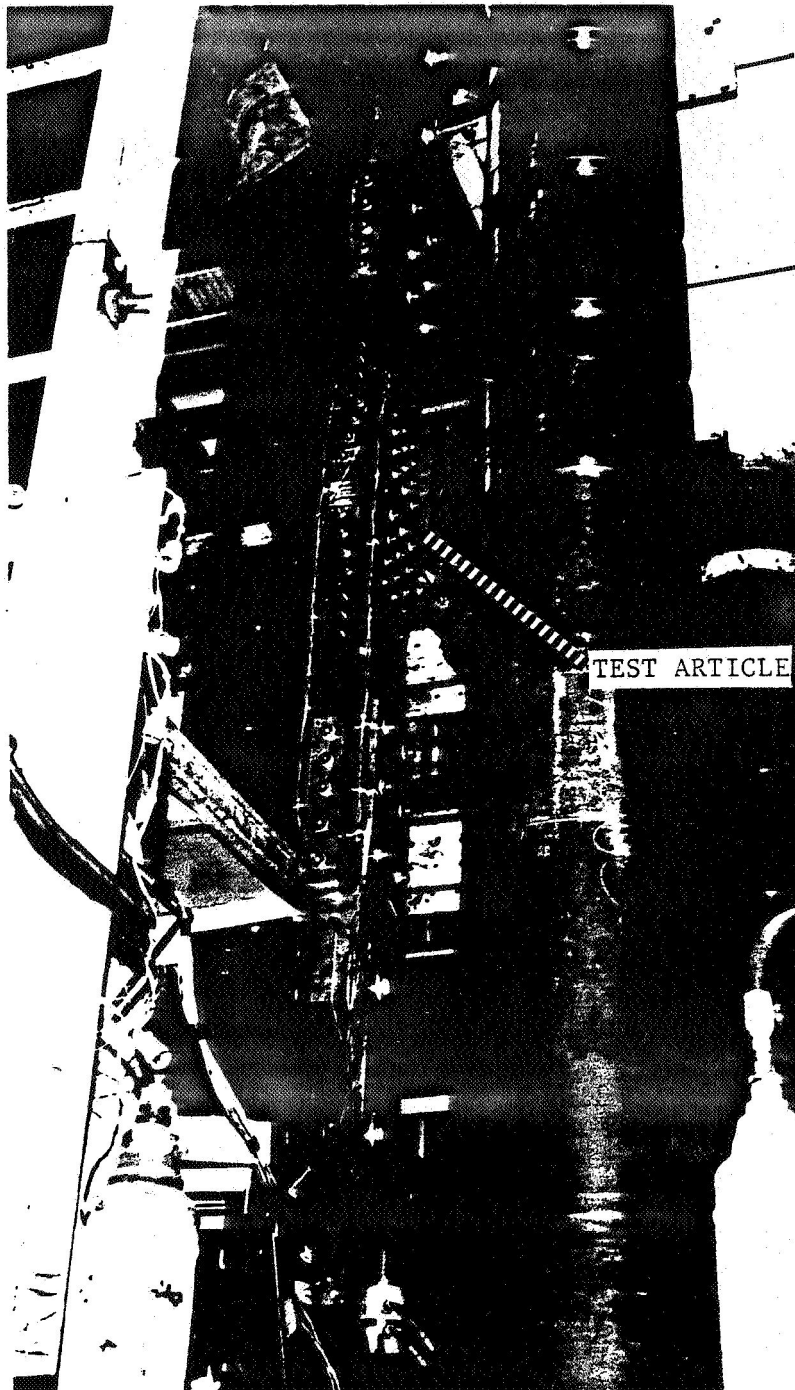


FIGURE 59 TECHNOLOGY DEMONSTRATION TEST SETUP

ORIGINAL PAGE IS
OF POOR QUALITY

41 8009 JAXBRO ORIGINAL PAGE IS
STANDARD PAGE 90 OF POOR QUALITY

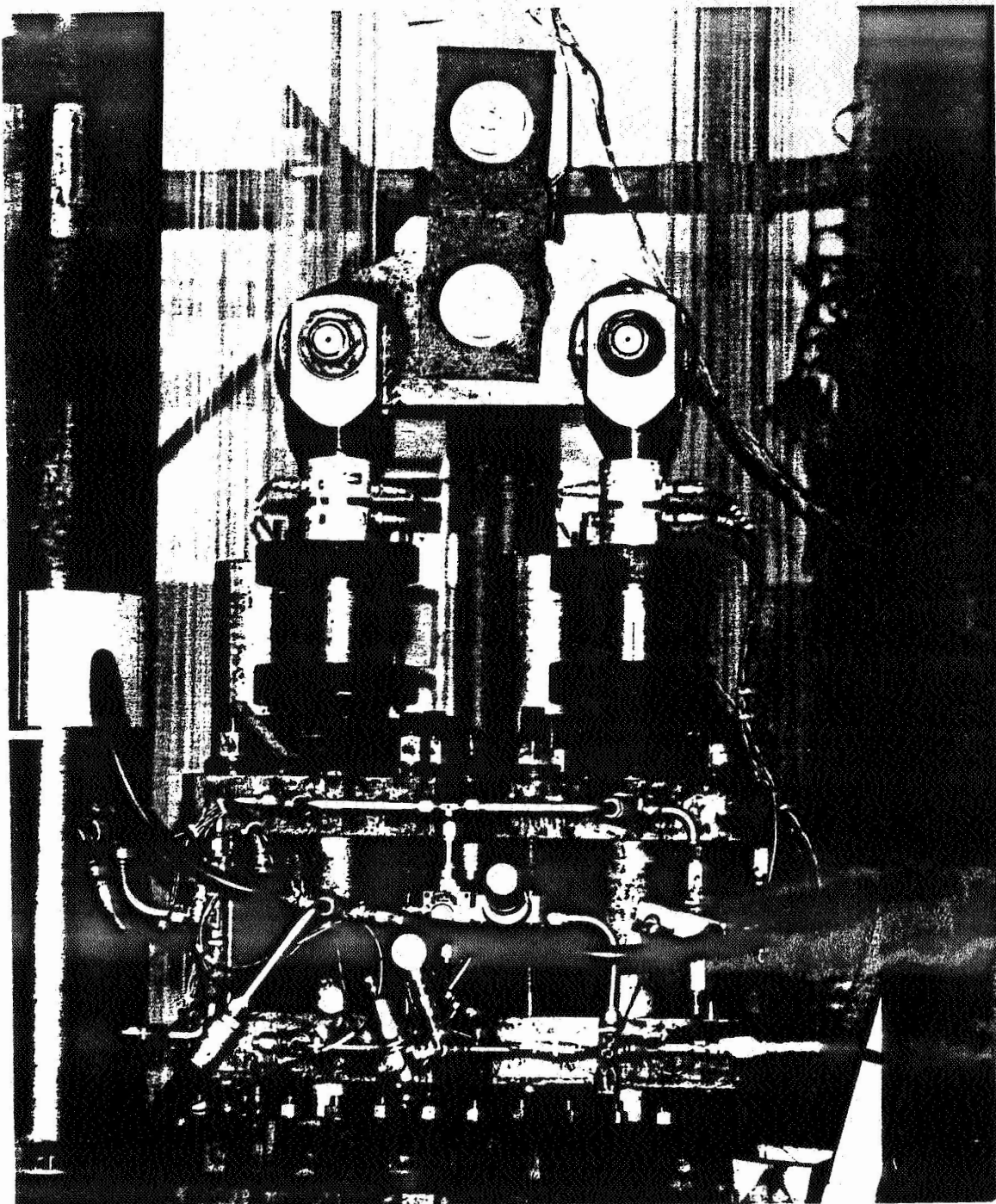


FIGURE 60 TECHNOLOGY DEMONSTRATION TEST - LOAD ACTUATORS

ORIGINAL PAGE IS
OF POOR QUALITY

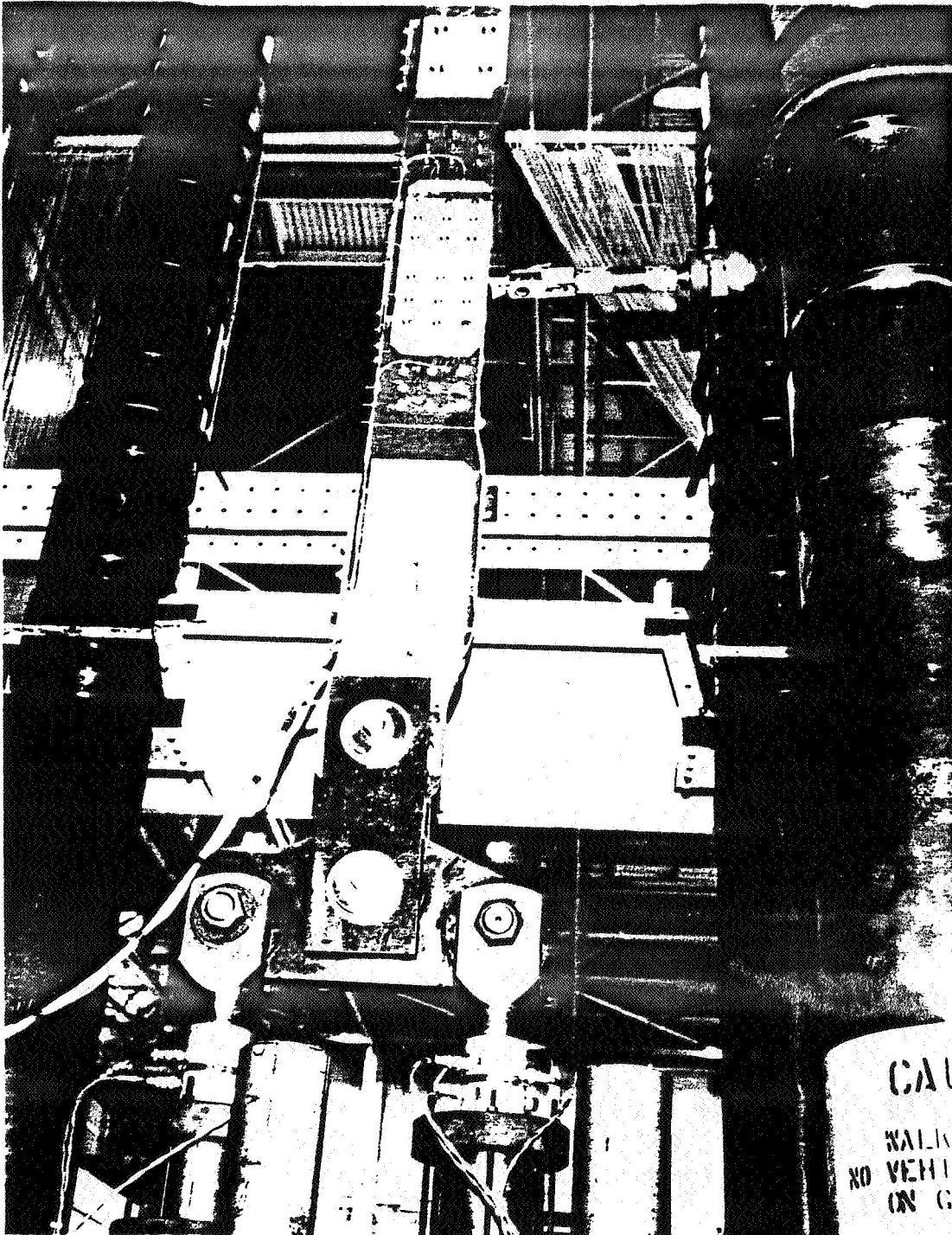


FIGURE 61 TECHNOLOGY DEMONSTRATION - LOWER END FITTING

ORIGINAL PAGE IS
OF POOR QUALITY

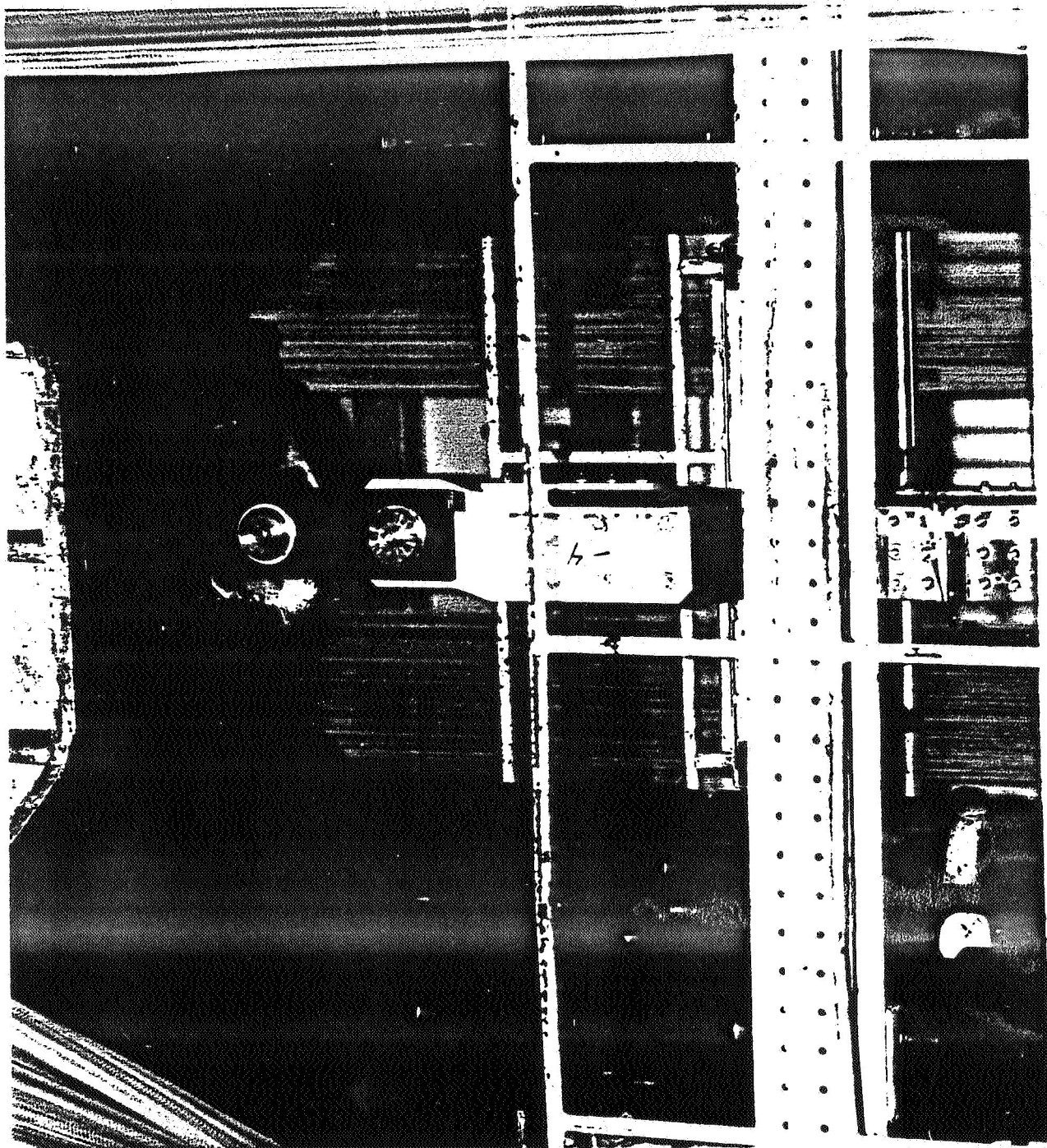
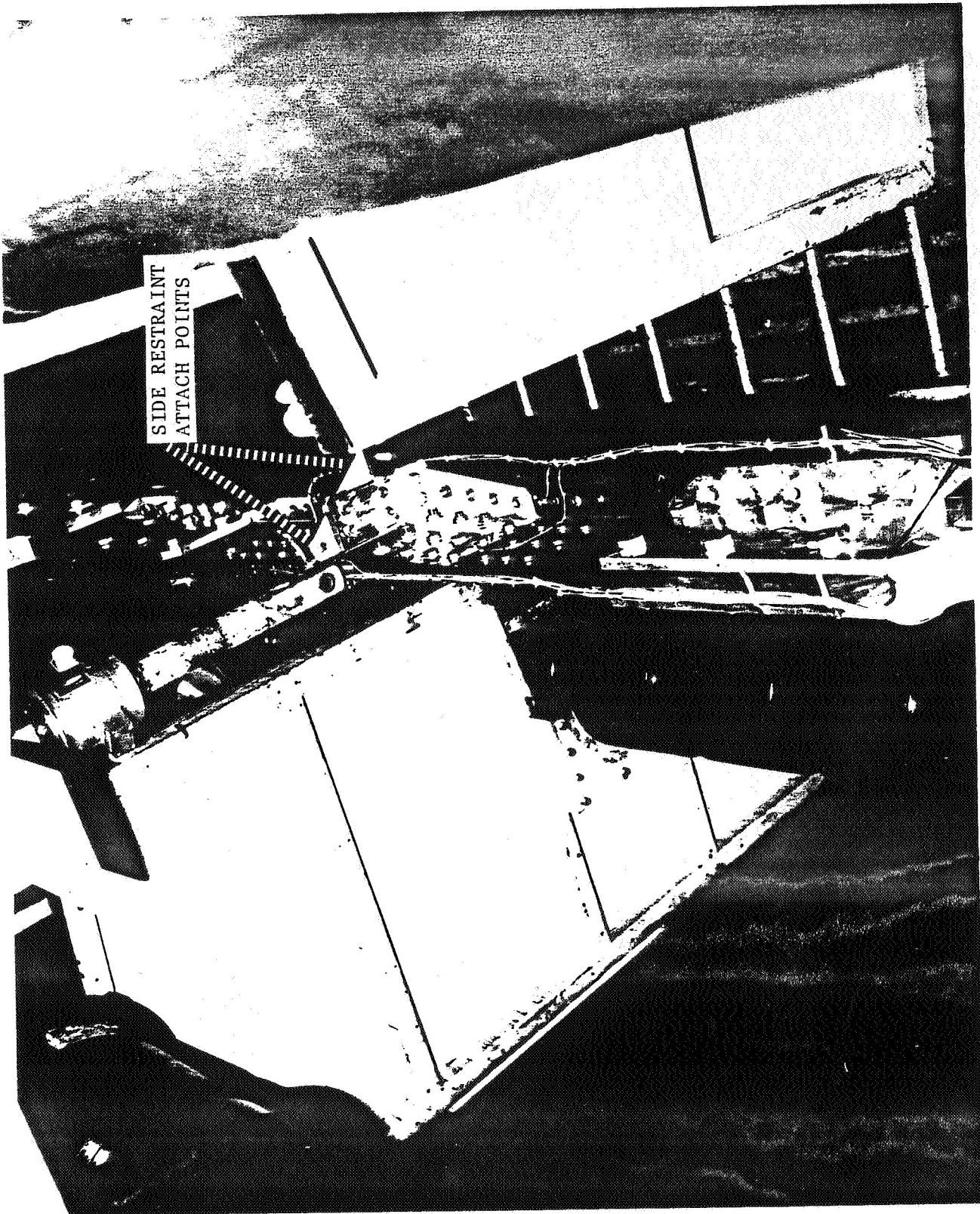


FIGURE 62 TECHNOLOGY DEMONSTRATION - UPPER END FITTING

ORIGINAL PAGE IS
OF POOR QUALITY



SECTION 4.4

TECHNOLOGY DEMONSTRATION TEST

TEST PROGRAM - PROCEDURES AND RESULTS

The technology demonstration test was a static tension test to failure. The general procedures consisted of a "limit load" test, return to zero load, visual inspection, and static test to failure. After completing a check of the load application and data acquisition system, the testing began with the limit load test. The specimen was loaded to 300,000 pounds of applied load. The loading was applied in increments of 25,000 pounds with strain gage and load cell data points taken at each increment. The specimen load was then returned to zero and a visual inspection of the specimen was conducted. The inspection revealed no flaws or damage to the specimen. A review of the strain data to the 300,000 pound level did not show any nonlinearities in the specimen behavior. Plots of the strain gage data for this initial run are presented in Appendix C, along with the corresponding analysis predictions. The static test to failure then began with load applied in 25,000 pound increments (as in the first run) to the 300,000 pound load level. The specimen was then loaded continuously to failure, with continuous recording of strain gage data throughout.

Failure of the specimen occurred at an applied tension load of 488,000 pounds, roughly 92 percent of the predicted test section strength (based on equal load sharing between skin and cap members). However, the failure was located in the end fitting area, away from the joint test section, as shown in Figures 64 and 65. A closeup view of the failure shown in Figure 66 shows that the spar cap member was actually delaminated starting at buildup in thickness on the inner surface of the cap to the first row of fasteners in the end fitting, where a net-section failure occurred in the reduced thickness of the spar cap member. The skin and web members failed through the first row of field fasteners. Although it is not possible to verify the actual cause of failure, it appears that the failure was in fact, initiated by the delamination of the spar cap member. (It was this laminate, as previously discussed, which showed questionable c-scan results in the vicinity of the delamination.) It appears that once this delamination extended to the first row of fasteners in the end fitting,

ORIGINAL PAGE IS
OF POOR QUALITY

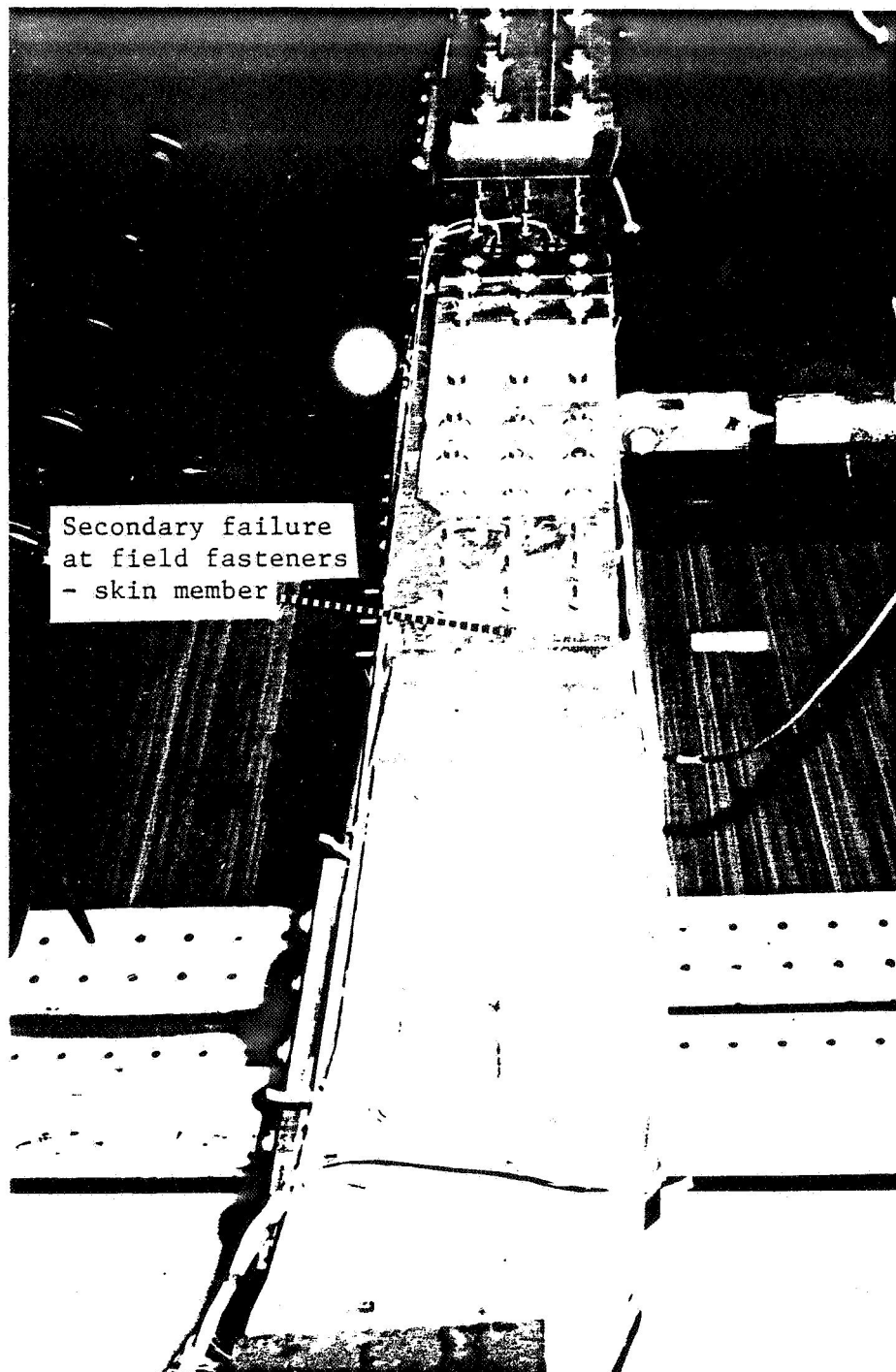


FIGURE 64 TECHNOLOGY DEMONSTRATION TEST #1 - END FITTING FAILURE

ORIGINAL PAGE IS
OF POOR QUALITY

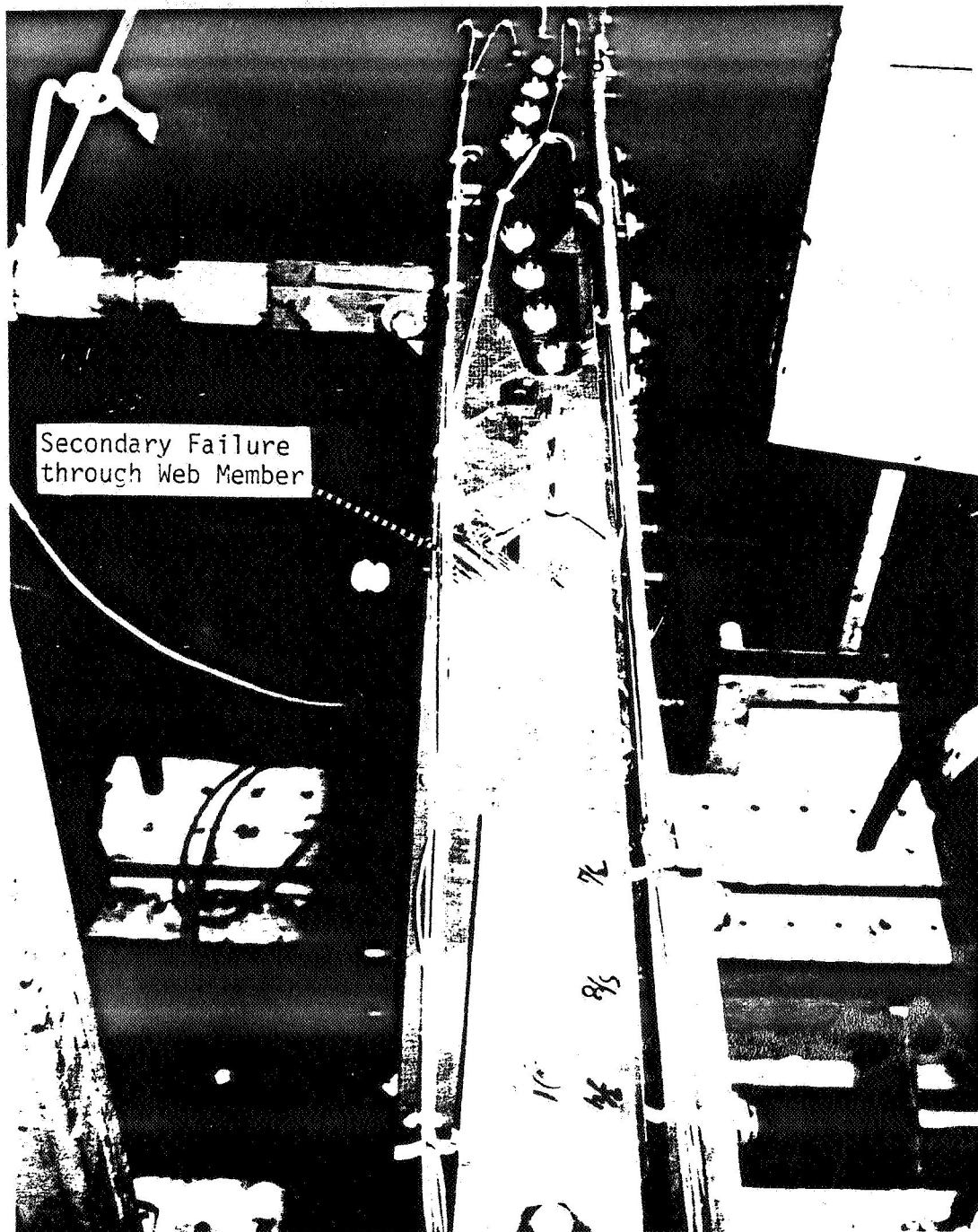


FIGURE 65 TECHNOLOGY DEMONSTRATION TEST #1 - END FITTING FAILURE

ORIGINAL PAGE IS
OF POOR QUALITY

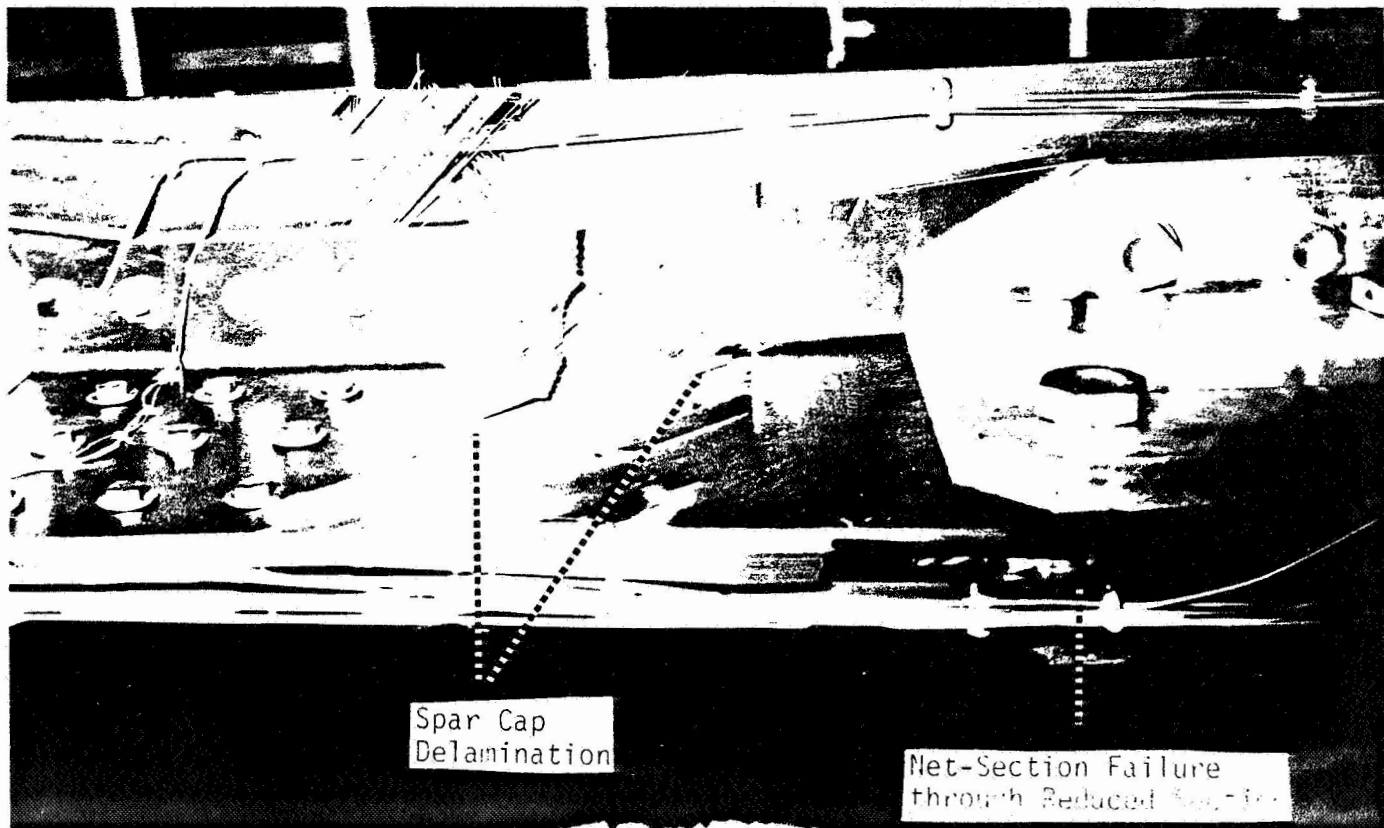


FIGURE 66 TECHNOLOGY DEMONSTRATION TEST #1 - END FITTING FAILURE

the effective thickness at the net-section was reduced by one-third to the 0.50 inch thickness of the basic cap section. A net-section tension failure then occurred in the cap member. This was followed by the net-tension failure in the skin and web members at the first row of field fasteners. This failure sequence seems logical, since after failure of the spar cap member, all of the applied loads would have to be carried by the skin and web members. The first row of field fasteners thus became the first row of bolts through which load was being transferred (back into the spar), forcing the final net-tension failure to occur. A graphic representation of the failure is shown in Figure 67 .

The technology demonstration test article was fully disassembled and visually inspected. The appearance of the broken joint members substantiated the initial observations and conclusions regarding the cause and mode of failure. C-scan results of the unfailed portions of the joint show that irreversible damage had occurred in the critical joint locations. This indicates that the specimen was close to failing in the test section when the premature end fitting failure took place. The c-scan results in Figure 68 correspond well with the results of c-scans performed on the unfailed side of several Phase I subcomponent joints, which had essentially reached their ultimate load capacity, but had failed in the opposite (mirror image) side of the specimen (Reference 1).

Strain gage data for the static test to failure are presented in Appendix C. Strain level predictions based on a linear analysis of the joint behavior are plotted along with the test results. As with previous tests, two gage readings are plotted on each page. The readings are plotted in numerical order and are not necessarily related.

After reviewing the possible program options, the decision was made to refurbish the failed specimen and conduct another static test. This effort was conducted under Douglas development funds. The following section of this report describes the Douglas sponsored effort, from the fabrication of replacement parts to the results of a second static test.

ORIGINAL PAGE IS
OF POOR QUALITY

84 JUN 22 1997

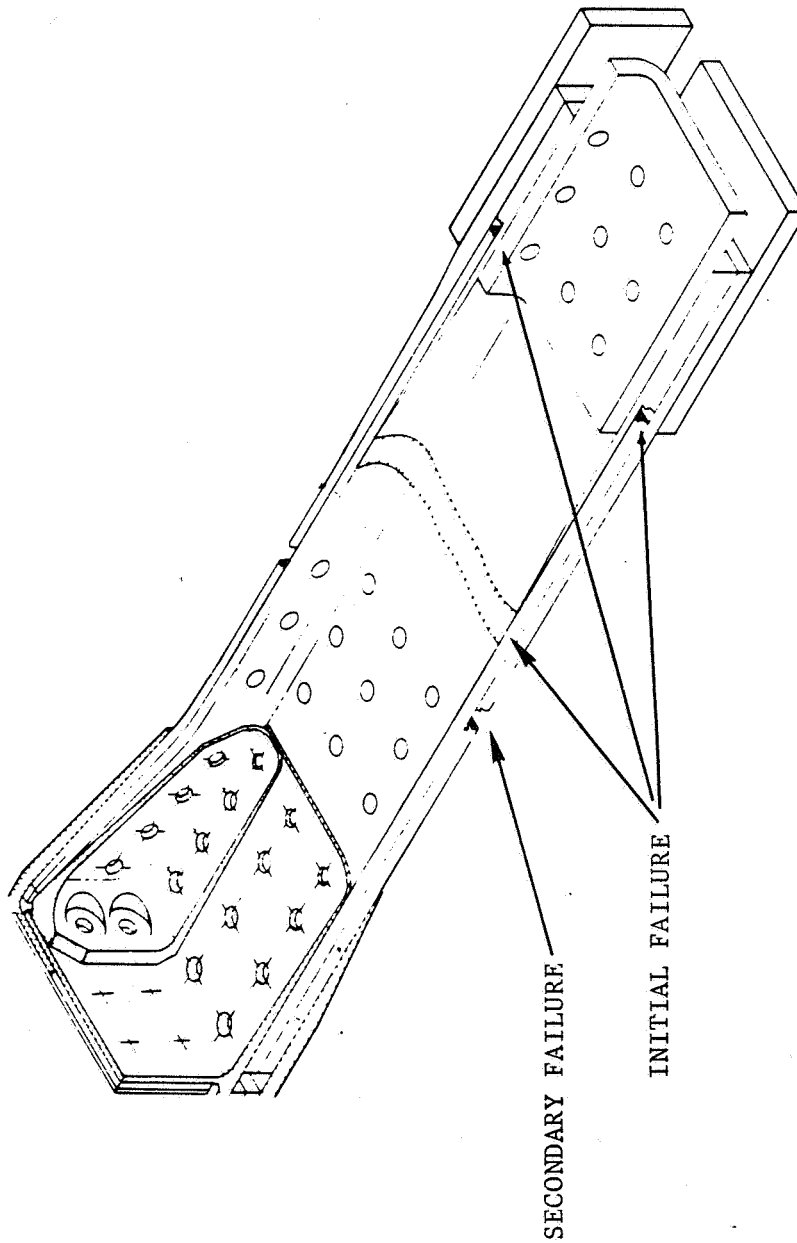


FIGURE 67 END FAILURE REPRESENTATION

FIRST CRIT
(BEAR)

ORIGINAL PAGE IS
OF POOR QUALITY

DIRECTION
OF
LOAD

FIGURE 68 C-SCAN RESULTS SPAR CAP MEMBER

SECTION
TECHNOLOGY DEMONSTRATION ARTICLE
SPECIMEN REBUILD AND TEST

In an effort to achieve the initial objectives of the technology demonstration program, a Douglas sponsored effort was initiated to rebuild the test article and conduct another static test. The goal was to fail the specimen at the critical location in the test section, without suffering a premature failure at some other location. Since it was determined that the prior specimen failure was the result of a poor quality laminate, the decision was made to replace the broken parts with "dummy" joint members and re-test the specimen.

After visual inspections and NDI of the unfailed parts were completed, the specimen was re-assembled from one end fitting to the joint centerline. Two aluminum plates were designed and fabricated to replace the three composite joint members from the failed side of the specimen. One aluminum plate replaced the wing skin and spar cap members, while the other replaced the upper leg of the spar cap angle section and the attached web member. The aluminum parts were machined to the exact thicknesses of the original composite parts, both in the joint test section and end fitting areas. This facilitated the specimen re-assembly by ensuring proper fit and alignment between members. The re-assembly was completed with no shimming required.

The aluminum plates were made of 7075-T6 material. Since the Young's modulus value for this alloy is within about 10% of the value for composite laminates used in the specimen, it was determined that the resulting stiffness imbalance would be minimal and have virtually no effect on the joint load distributions. The 7075-T6 material was of sufficient ultimate tension strength to ensure that the failure would occur in the composite joint members. The specimen is shown with a view of the aluminum replacement section of the joint from several angles in Figures 69 through 71 . The overall test setup is shown in Figure 72 .

ORIGINAL PAGE IS
OF POOR QUALITY

ORIGINAL PAGE IS
OF POOR QUALITY

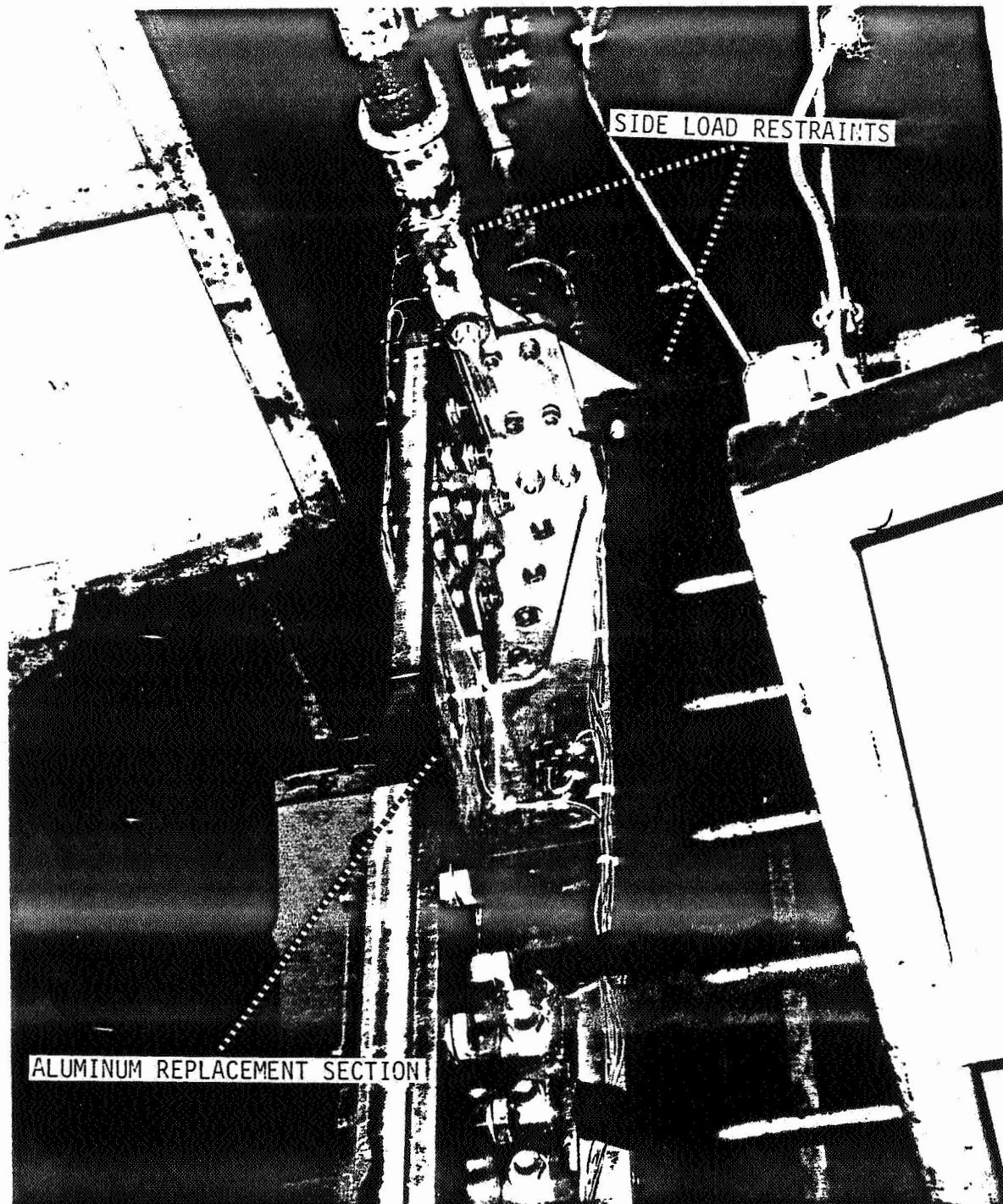


FIGURE 69 JOINT RE-TEST WITH ALUMINUM REPLACEMENT PART

ORIGINAL PAGE IS
OF POOR QUALITY

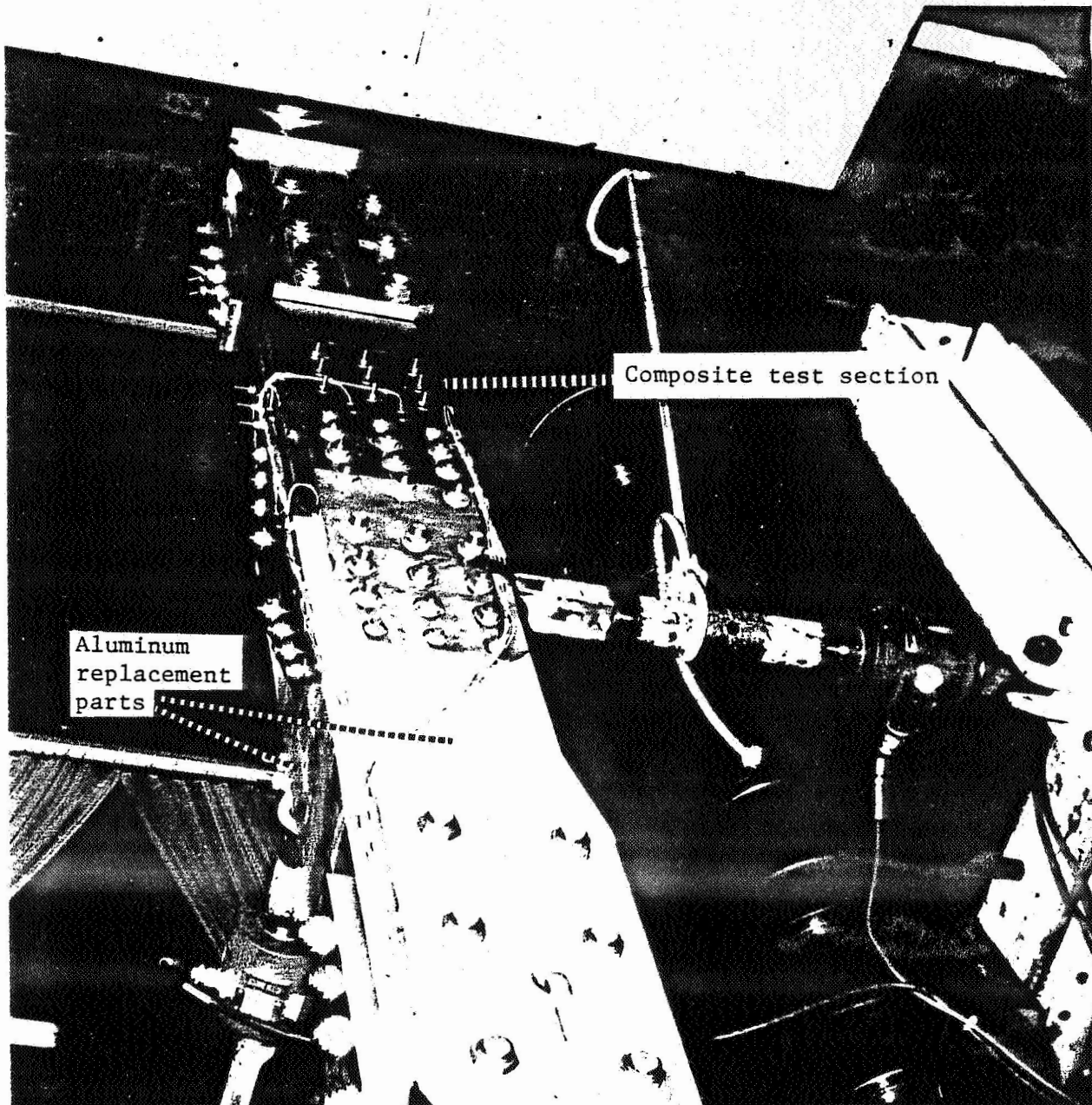


FIGURE 70 JOINT RE-TEST WITH ALUMINUM REPLACEMENT PART

ORIGINAL PAGE IS
OF POOR QUALITY

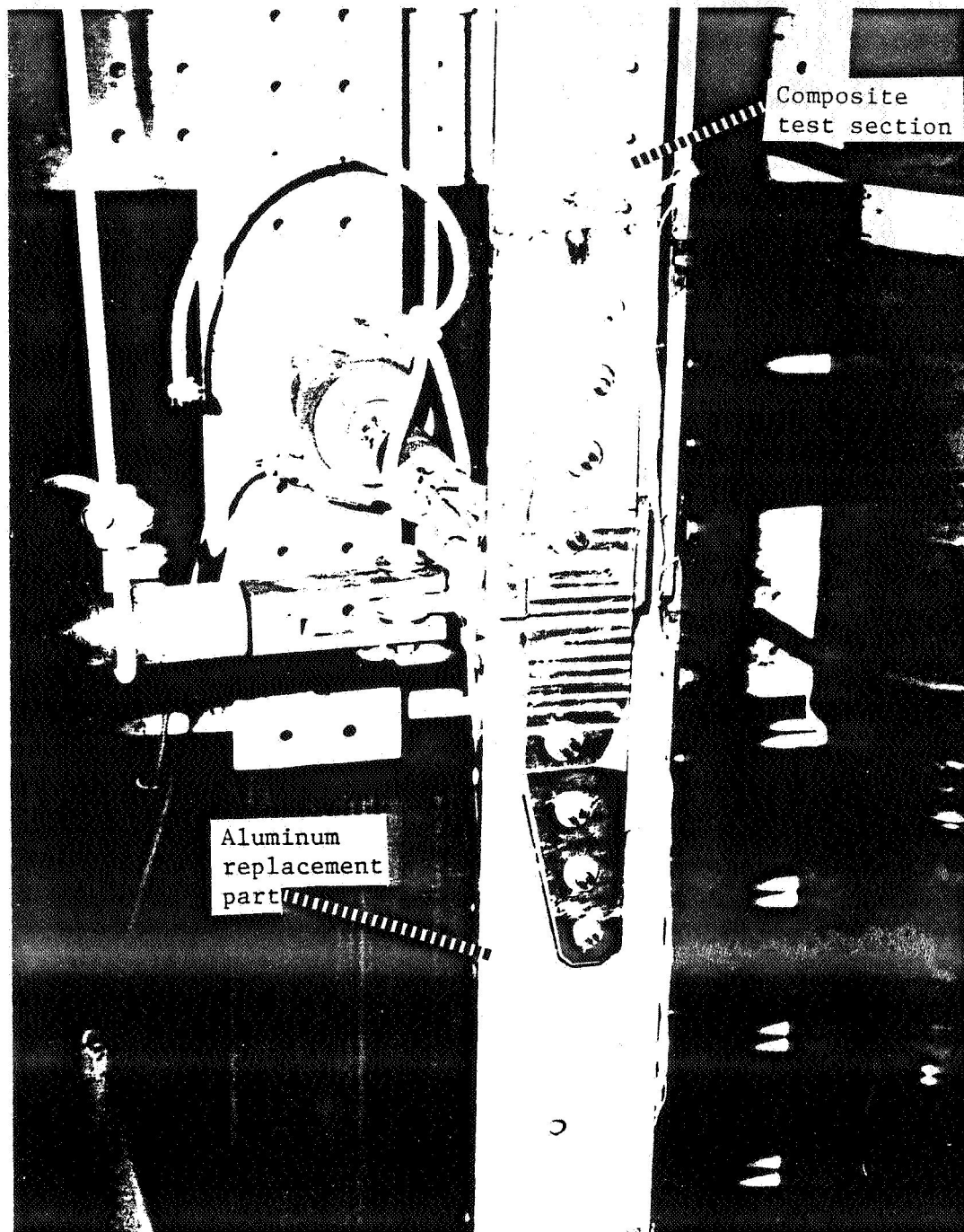


FIGURE 71 JOINT RE-TEST WITH ALUMINUM REPLACEMENT PART

ORIGINAL PAGE IS
OF POOR QUALITY

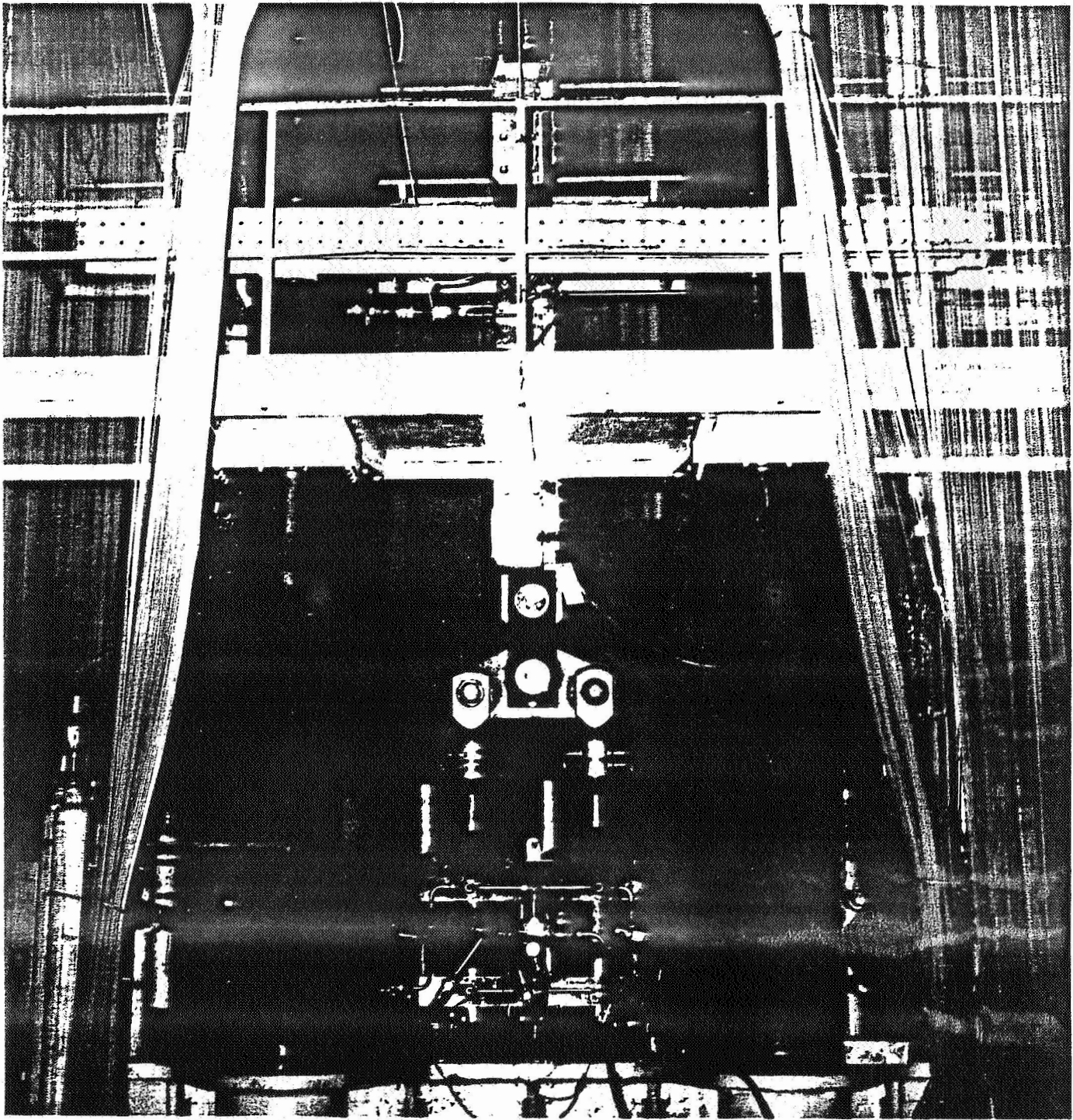


FIGURE 72 JOINT RE-TEST SETUP

Strain gage locations were identical to the previous test except for those gages which had been mounted on the failed composite members. One strain gage was placed on each aluminum replacement part to monitor the respective load levels. The locations of gages 1 through 21 were unchanged and were mounted as shown in Figure 53. Gages 22 and 23 were relocated on the aluminum web and skin members, respectively. The test specimen is shown in Figure 73 with the strain gages attached to the composite joint members. The same side restraint system was also used, as shown in Figure 74. The data acquisition system and test procedures were essentially the same. The only significant change was that the specimen was loaded directly to failure with no return to zero load at any point throughout the test. Strain readings were again taken at 25,000 pound increments up to 300,000 pounds applied load, followed by continuous read to failure.

After reinstalling the specimen in the test fixture, the second static test was conducted with excellent results. The specimen failed at an applied load of 484,420 pounds with both the failure load and location showing good correlation with analytical predictions. The failure load of 484,420 pounds corresponds to a far-field stress level of around 46,500 psi. The maximum strain in the composite laminates at failure was slightly above 5000 microstrain, which occurred in the spar cap member. The failure was a net-section tension failure through the first (outermost) row of fasteners in the joint test section as shown in Figure 75. The wing skin, spar cap, and spar web members all failed through this location. Figures 76 through 78 show several views of the failed specimen, still in the test machine. In general, the failure was a very clean break, particularly through the skin and cap members where there was very little evidence of delamination.

The failure load for the second test was nearly equal to that of the initial test, which resulted in the premature end fitting failure. The failure load for the second test (actually slightly lower than the first test) is attributable to the difference in stress (or strain) levels

between the composite skin and spar cap members; particularly as compared to the analysis solutions. It was recognized at the outset of the analysis effort that a precise representation of the test specimen including the effects of the actual test machine fixturing would be a difficult task. While the finite element solution for the demonstration joint analysis did indicate that the composite spar and skin members were carrying very nearly the same load, the actual test measurements showed that the spar cap member was working to (roughly) a 10 percent higher strain level than the skin member. This phenomenon is a probable cause for the joint failure occurring at a lower applied load than had been analytically predicted. This also indicates that the test section was very close to failure during the initial test.

Strain gage readings for the second static test are plotted against applied load and presented in Appendix C. The darker, slightly scattered portions of the plots indicate that continuous read of strain gages was underway.

ORIGINAL PAGE IS
OF POOR QUALITY

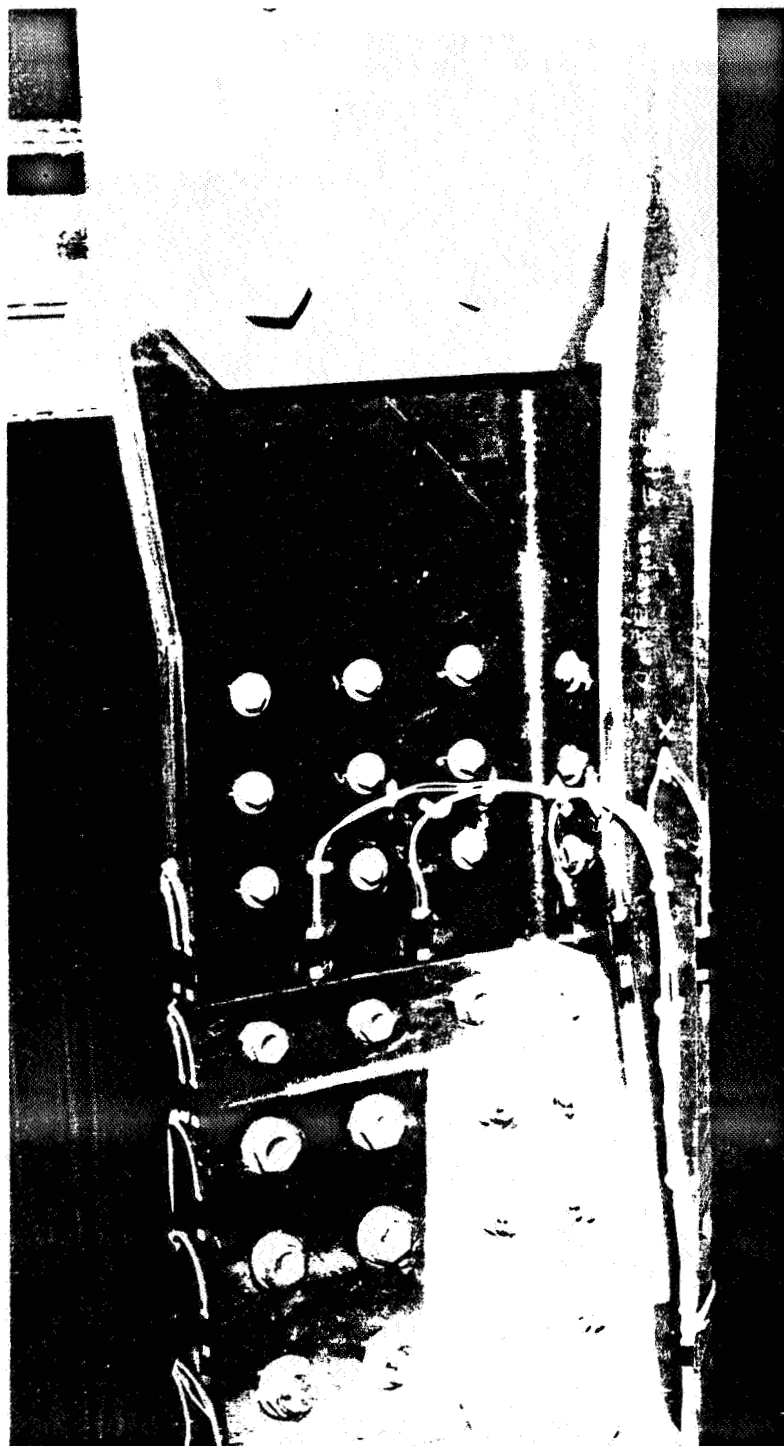


FIGURE 73 DEMONSTRATION JOINT TEST SECTION

ORIGINAL PAGE IS
OF POOR QUALITY

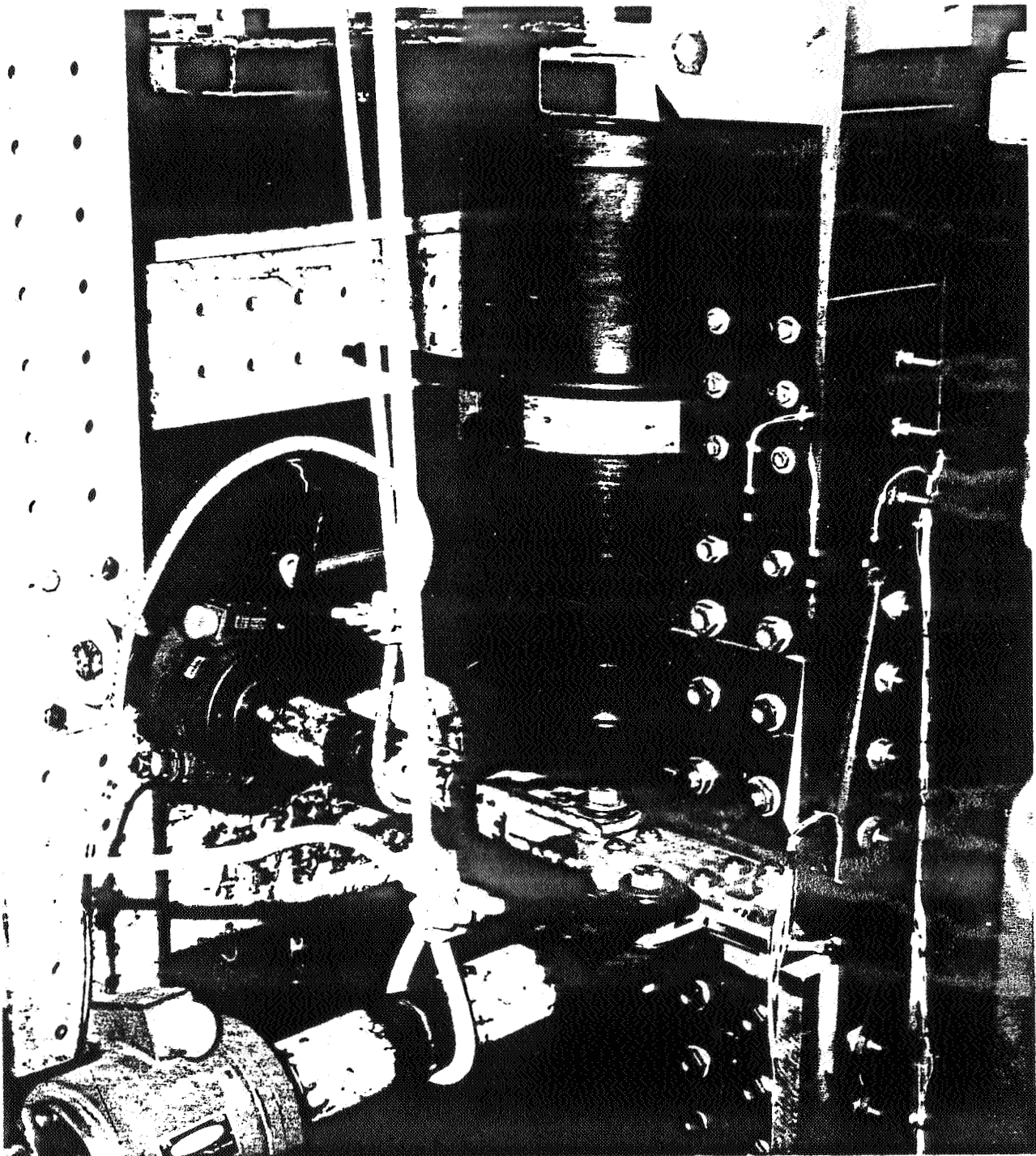


FIGURE 74 DEMONSTRATION SIDE RESTRAINT SYSTEM

ORIGINAL PAGE IS
OF POOR QUALITY

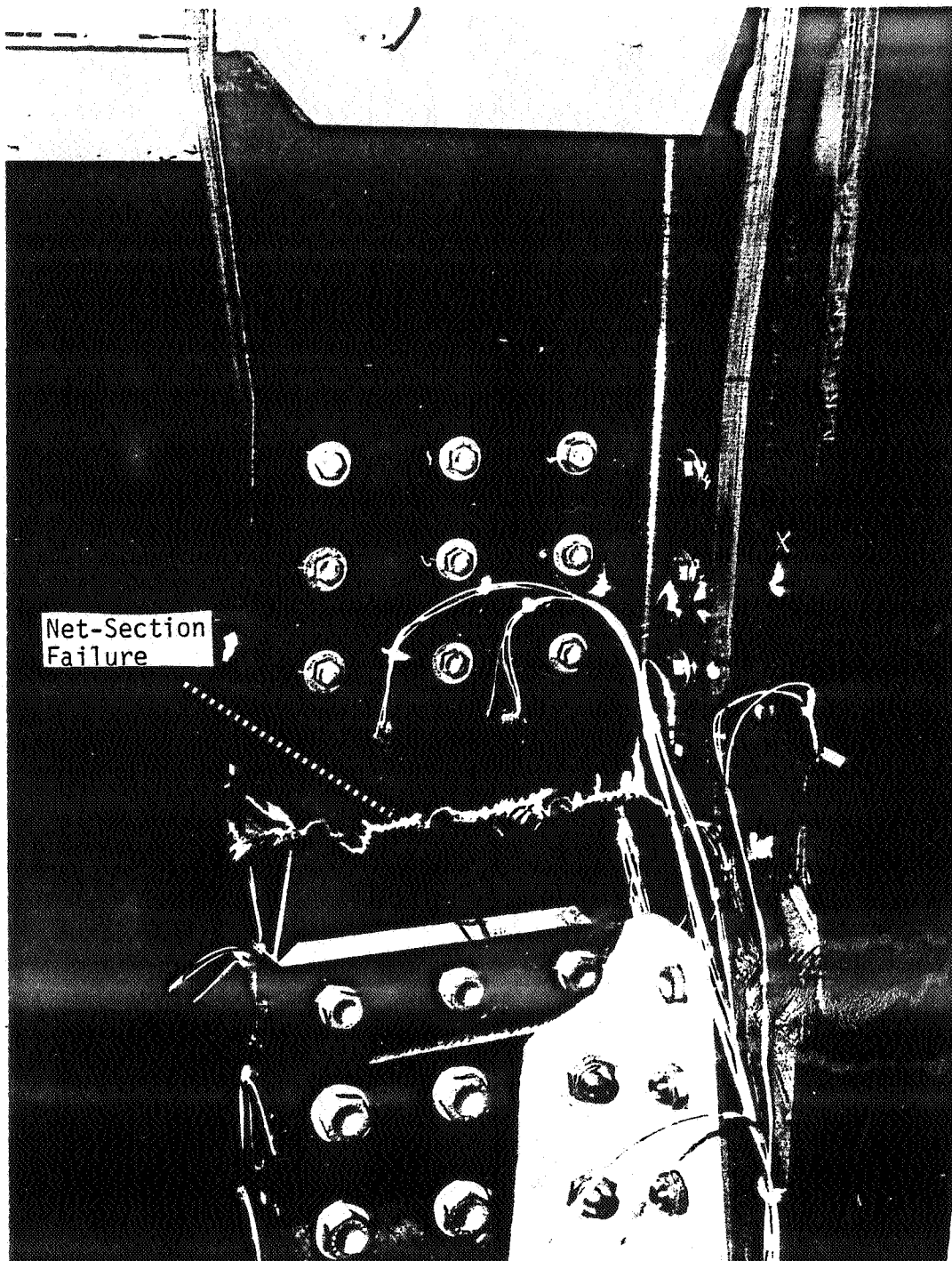


FIGURE 75 TECHNOLOGY DEMONSTRATION - TEST SECTION FAILURE

ORIGINAL PAGE IS
OF POOR QUALITY

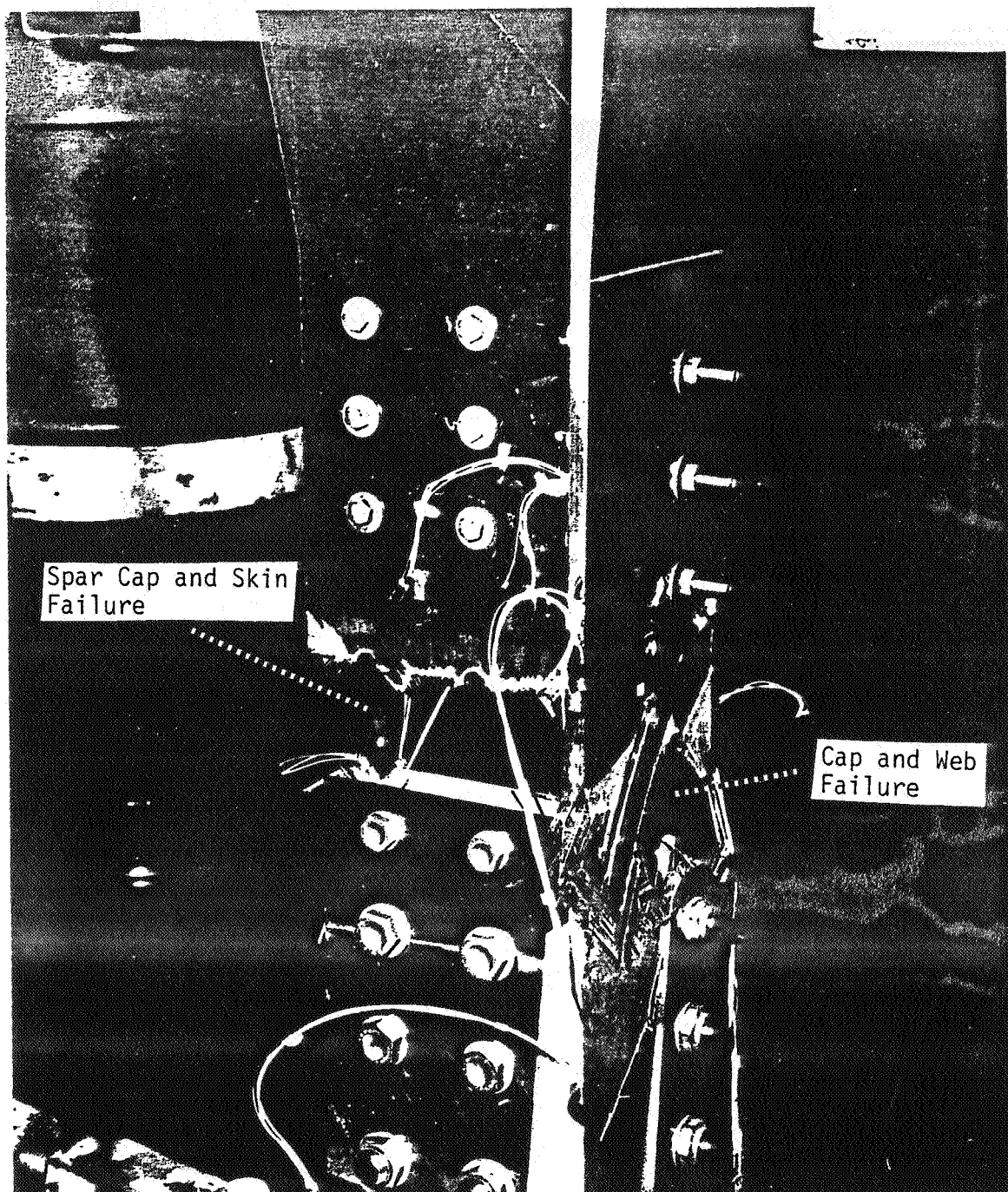


FIGURE 76 TECHNOLOGY DEMONSTRATION - TEST SECTION FAILURE

21 3049 104
YTJAUQ 8002

ORIGINAL PAGE IS
OF POOR QUALITY

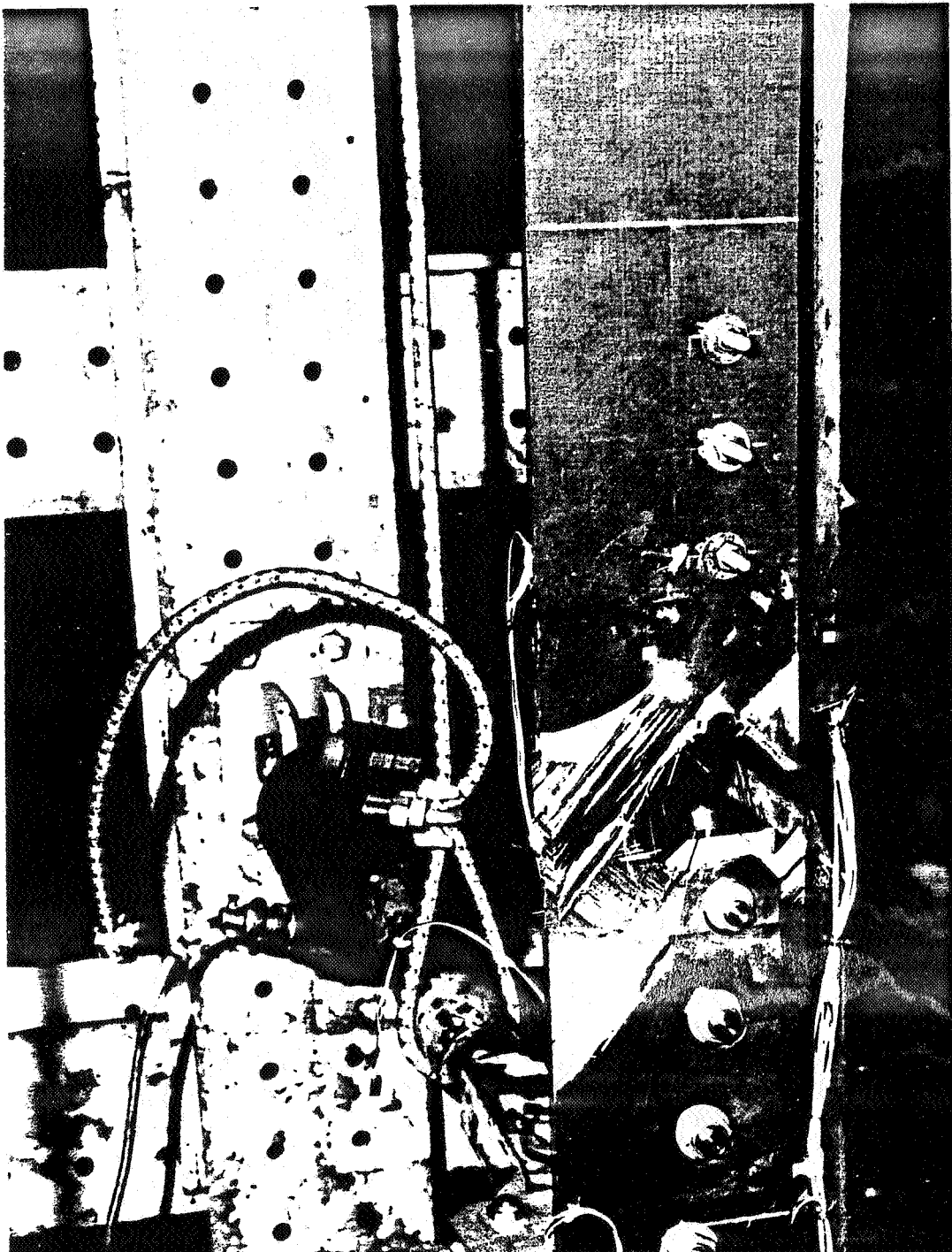


FIGURE 77 TECHNOLOGY DEMONSTRATION - TEST SECTION FAILURE

ORIGINAL PAGE IS
OF POOR QUALITY

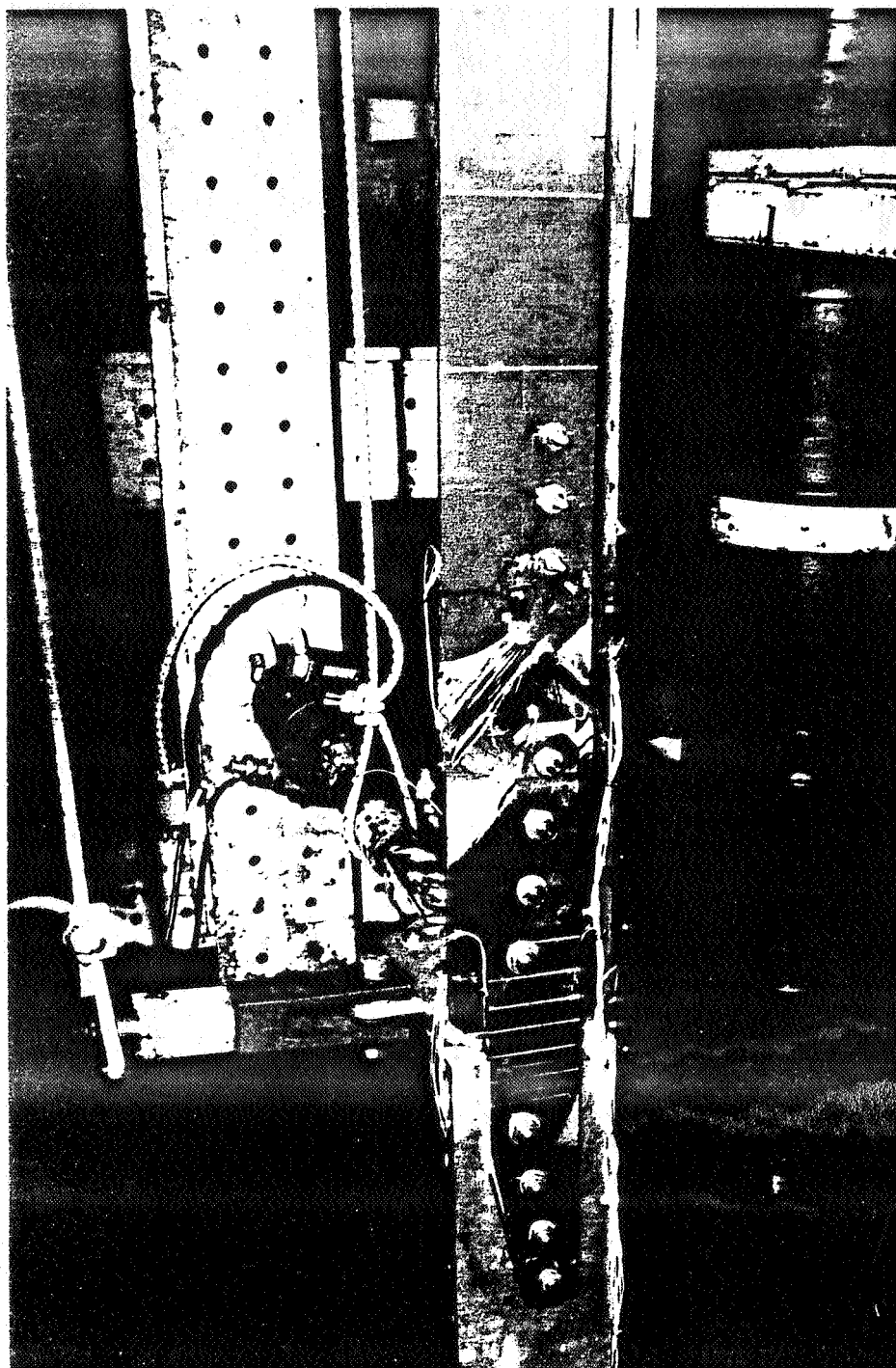


FIGURE 78 TECHNOLOGY DEMONSTRATION - TEST SECTION FAILURE

SECTION

CONCLUSIONS

The tests conducted under the Phase II program have demonstrated the ability to design and fabricate bolted joints in large composite wing structures which meet the design requirements of a large commercial transport aircraft. Gross-section stress levels of 45,000 to 50,000 psi. and corresponding strain levels on the order of 4,700 to 5,000 microstrain were achieved along with good correlation between analysis and test results. The results of the test program are summarized in Table II.

The stringer transition joint specimen was successful in providing an efficient means of load transfer with a minimum of design complexity. The results of the photo-elastic survey seem to indicate that a more gradual scarf angle for the stringer blade would be beneficial. Nevertheless, the tested configuration for the stringer runout demonstrated the level of structural integrity required to equal that of the bolted joint structure. This concept avoids the need for a bolted splice through the stringer blade itself, greatly simplifying fabrication and assembly requirements.

The results of the demonstration subcomponent tests provided the necessary level of confidence in the analysis methodology developed throughout the program. The principle of designing to a high bypass/low bearing load combination at the first row of fasteners for maximum efficiency in a multirow joint was demonstrated in each case.

The testing of the technology demonstration article successfully concluded the test program and demonstrated the ability to design and fabricate a large composite bolted joint representative of the load levels and complexity found in transport wing structure. While the second static test was successful, the premature end fitting failure suffered during the first run restates the need for reliable flaw/damage assessment techniques and suitable acceptance criteria.

The stress and strain levels achieved during this program were near the highest attainable for the material system and fiber patterns used. The benefits and improved performance afforded by some of the new high stress/high strain fibers and tougher resin systems will translate directly into higher strengths for bolted composite joints.

All of the joints tested during Phase II of the program were loaded in static tension. The ability to attain similar joint strengths in compression was demonstrated during the Phase I effort, although the failure modes and associated analysis methods required for compression joints warrant further development. In any case, the use of metallic splice members eliminates the potential for the typical compression failure modes suffered by composite laminates which are not fully clamped up in double shear. In addition, the presence of out-of-plane forces in complex joint structure such as the technology demonstration article suggests that metal materials are a logical choice for splice members. For a large transport wing, the splicing members account for a small percentage of the total wing weight, so that the use of metals in this application has a minimal effect on the overall weight savings attainable through the use of advanced composite materials.

TABLE II

PHASE II TEST PROGRAM

TECHNOLOGY DEMONSTRATION TEST RESULTS

TEST SPECIMEN	FAILURE, LOAD (LB)	PREDICTED STRENGTH (LB)	GROSS-SECTION STRESS AT FAILURE (PSI)	GROSS-SECTION STRAIN AT FAILURE (MICROSTRAIN)	PREDICTED STRAIN LEVEL AT FAILURE (MICROSTRAIN)	FAILURE MODE
STRINGER TRANSITION	197,200	183,700	50,000*	5,891 4,700 **	5,945 4,800	Net-Section Tension
SUBCOMPONENT #1	270,000	260,000	47,500	5,100	4,920	Net-Section Tension
SUBCOMPONENT #2	115,400	90,000 ***	46,200	4,970	3,900 ***	Net-Section Tension
TECHNOLOGY DEMONSTRATION ARTICLE Test No. 1	488,000	531,000	43,700 (skin) 45,600 (spar)	4,700 (skin) 4,900 (spar)	5,100 (Skin) 5,300 (Spar)	End Fitting
TECHNOLOGY DEMONSTRATION ARTICLE Test No. 2	484,400	531,000 ****	42,800 (skin) 46,500 (spar)	4,600 (skin) 5,000 (spar)	5,100 (Skin) 5,330 (Spar)	Net-Section Tension

- * Average stress in basic section prior to thickness buildup
- ** Calculated strain level at bolted joint after thickness buildup
- *** Refer to discussion - page 57
- **** Refer to discussion - pages 96 and 97

SECTION
REFERENCES

1. Bunin, B.L., "Critical Joints in Large Composite Primary Aircraft Structures, Volume III - Ancillary Test Results, NASA-CR-172588, June 1985
2. Bunin, B.L., "Critical Composite Joint Subcomponents - Analysis and Test Results," NASA CR 3711, September 1983.
3. Nelson, W.D., Bunin, B.L., and Hart-Smith, L. J., "Critical Joints in Large Composite Aircraft Structure," NASA CR 3710, August 1983.

APPENDIX A

STRINGER TRANSITION TEST DATA

SG# - Strain Gage Number

LR# - Load Restraint Number

15 Strain Gages

1 Load Restraint

Strain Gage Locations shown on pages 17 - 19.

CRITICAL JOINT TEST
STRESS SURVEY & LOAD TO FAILURE

APPLIED LOAD	LR1 (LBS)	SG1 (UIN/IN)	SG2 (UIN/IN)	SG3 (UIN/IN)	SG4 (UIN/IN)	SG5 (UIN/IN)
0	5.381	0.000	0.000	1.592	0.000	0.000
10000	-21.523	20.061	193.738	292.971	0.000	130.585
20000	-59.187	130.773	426.224	608.233	43.675	290.180
30000	-118.374	232.486	658.710	918.718	87.350	444.956
40000	-188.323	334.100	881.500	1214.873	135.878	584.887
50000	-252.891	450.441	1109.152	1520.582	194.112	749.655
60000	-317.459	566.684	1341.638	1816.737	242.639	904.422
70000	-382.026	692.614	1574.123	2127.222	296.020	1064.026
80000	-457.356	818.544	1796.922	2400.048	359.106	1213.957
90000	-521.923	949.318	2024.565	2695.649	412.487	1368.724
100000	-591.872	1075.247	2247.364	2987.028	470.721	1523.402
120000	-731.769	1341.638	2707.402	3584.115	587.187	1842.609
160000	-995.421	1835.670	3618.062	4759.183	771.593	2466.605
170000	-1043.847	1951.913	3850.548	5079.221	791.005	2631.046
180000	-1108.415	2043.939	4078.191	5361.046	805.563	2795.486
190000	-1162.221	2116.591	4296.146	5661.978	776.446	2964.763
197200	-1184.505	2145.651	4455.980	5891.260	708.507	3080.838

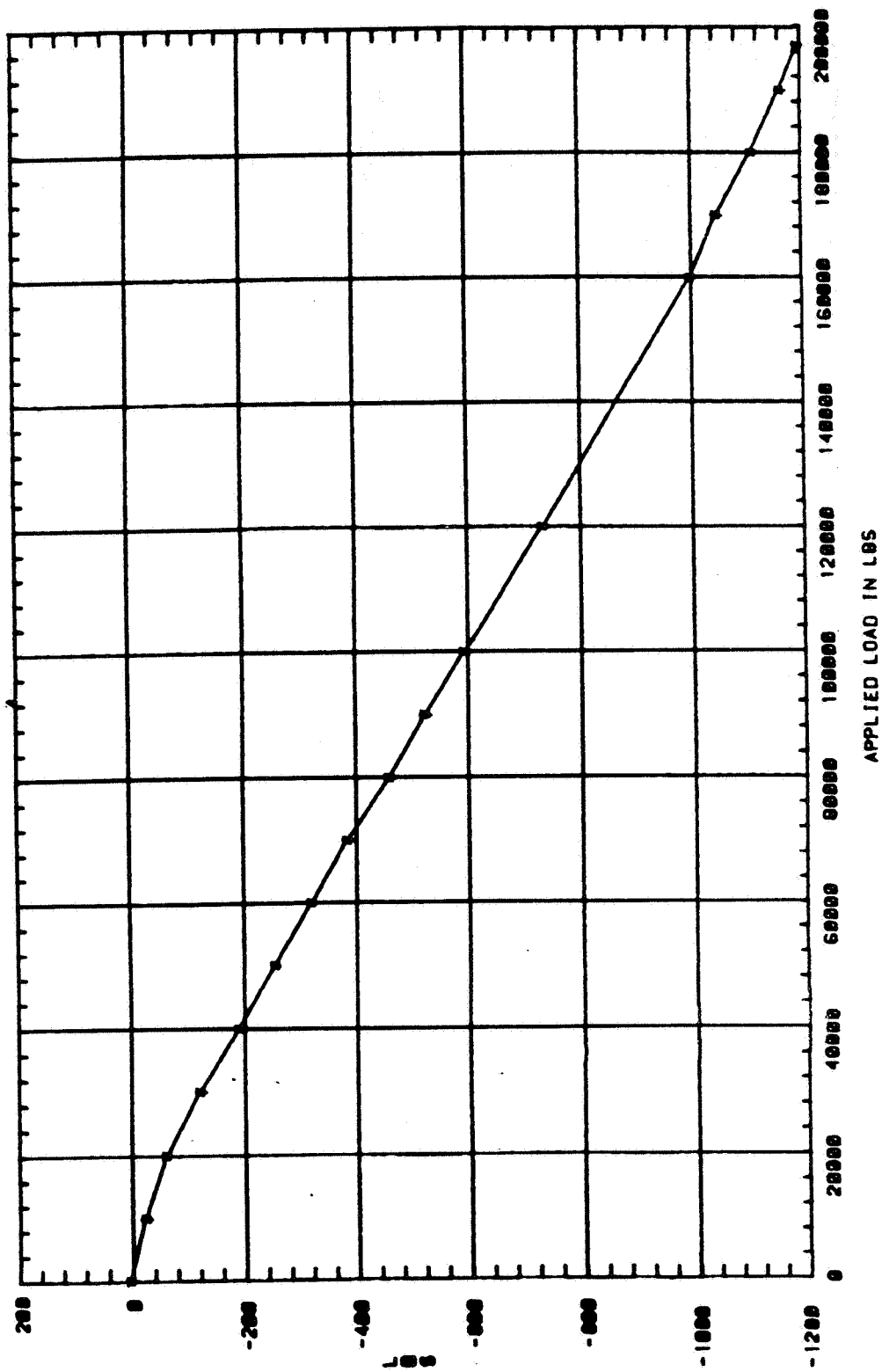
CRITICAL JOINT TEST
STRESS SURVEY & LOAD TO FAILURE

APPLIED LOAD	SC6 (UIN/IN)	SC7 (UIN/IN)	SC8 (UIN/IN)	SC9 (UIN/IN)	SC10 (UIN/IN)	SC11 (UIN/IN)
0	-3.180	4.830	0.000	0.000	4.834	6.363
10000	192.382	33.807	116.467	81.945	82.181	92.264
20000	407.023	111.079	281.462	173.530	169.196	154.304
30000	612.124	193.181	431.808	332.599	309.386	254.522
40000	821.995	255.965	577.482	491.669	459.245	359.512
50000	1027.096	342.896	732.771	641.098	594.602	450.186
60000	1222.658	415.339	878.355	766.425	720.290	540.859
70000	1437.299	492.612	1043.350	901.393	855.646	626.761
80000	1628.091	560.225	1179.228	1017.080	957.164	698.345
90000	1814.113	637.497	1339.370	1123.126	1058.681	774.702
100000	2023.984	709.940	1484.953	1224.352	1150.530	836.741
120000	2410.338	845.167	1780.974	1397.882	1295.555	936.959
160000	3178.275	1028.689	2339.044	1764.223	1561.434	1089.673
170000	3397.686	1038.348	2489.481	1855.809	1600.107	1103.989
180000	3617.097	1009.371	2562.273	1937.753	1672.619	1113.534
190000	3841.277	922.439	2644.770	2034.159	1749.966	1127.851
197200	4022.529	777.554	2664.181	2087.182	1798.308	1094.445

CRITICAL JOINT TEST
STRESS SURVEY & LOAD TO FAILURE

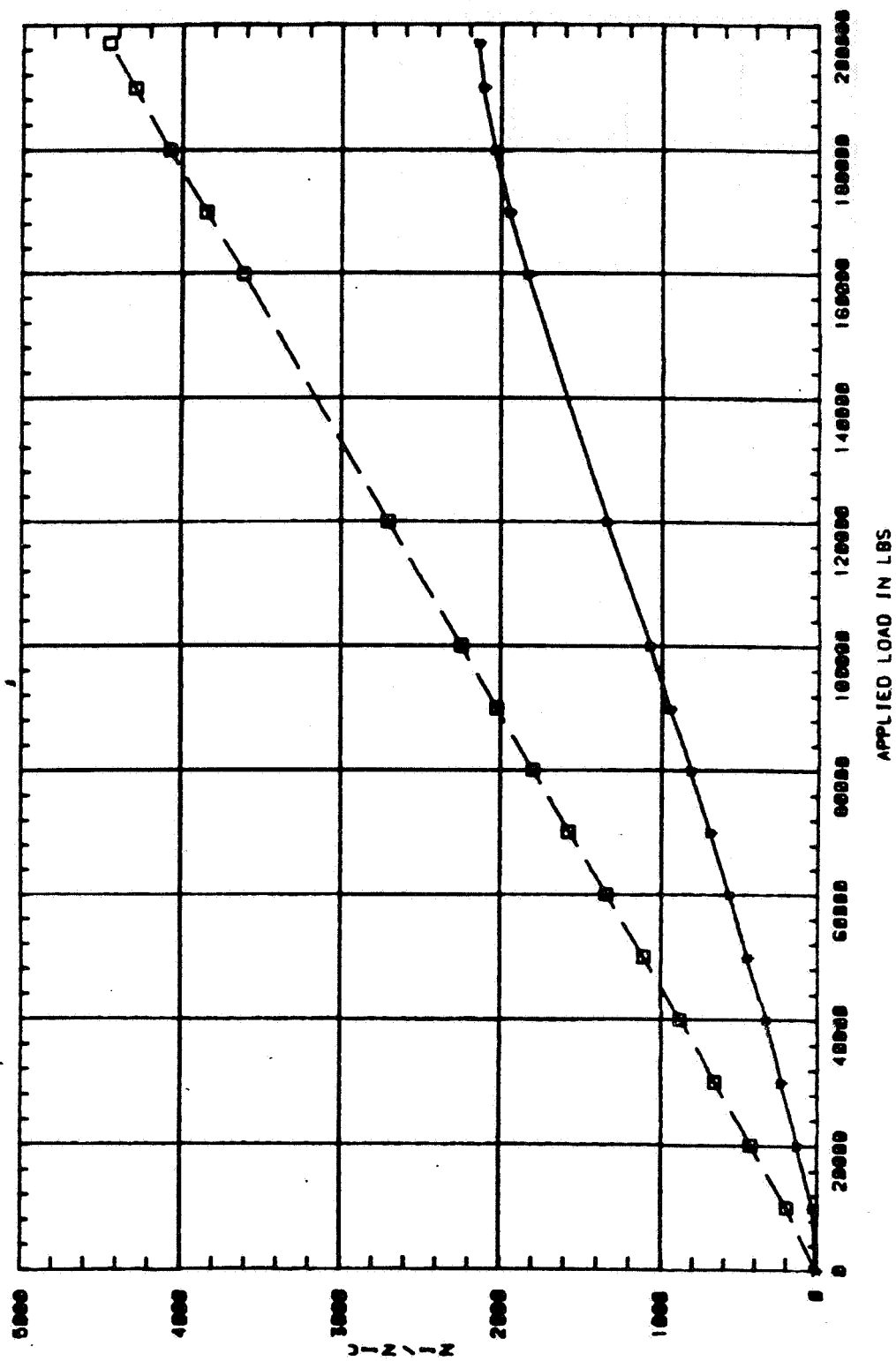
APPLIED LOAD	SC12 (UIN/IN)	SC13 (UIN/IN)	SC14 (UIN/IN)	SC15 (UIN/IN)
0	1.624	4.770	3.174	0.000
10000	103.927	257.569	41.259	42.785
20000	269.560	648.692	69.823	66.555
30000	454.670	1092.284	103.147	109.340
40000	610.569	1402.321	136.471	123.602
50000	761.588	1750.516	174.556	147.372
60000	912.606	2093.941	222.163	171.141
70000	532.624	2623.389	269.769	199.665
80000	737.230	3047.901	312.615	228.188
90000	961.322	3710.903	360.221	256.712
100000	1204.900	4407.293	407.827	294.743
120000	1570.267	9654.071	583.971	366.052
160000	1487.450	9654.071	764.874	527.686
170000	1277.973	9654.071	807.720	565.717
180000	513.138	9654.071	845.805	608.502
100000	362.119	9654.071	874.369	656.042
107200	167.257	9654.071	898.172	694.073

CRITICAL JOINT TEST (BLDG 3)
STRESS SURVEY & LOAD TO FAILURE
DATE: 28 JUN 84
LR1 VS APPLIED LOAD

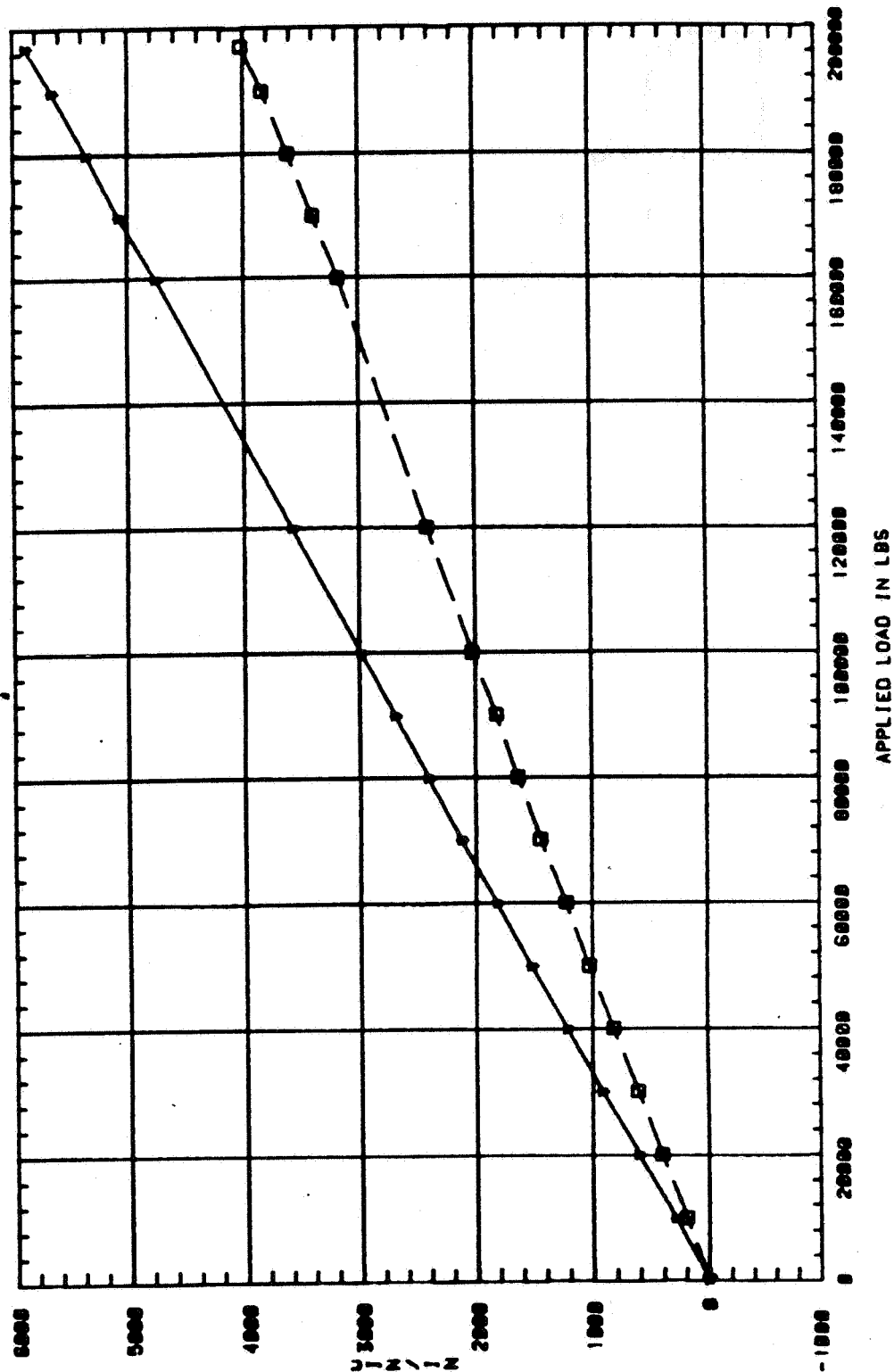


ORIGINAL PAGE IS
OF POOR QUALITY

CRITICAL JOINT TEST (BLOC 3)
STRESS SURVEY & LOAD TO FAILURE
DATE: 26 JUN 84
SC119) SC210) vs APPLIED LOAD



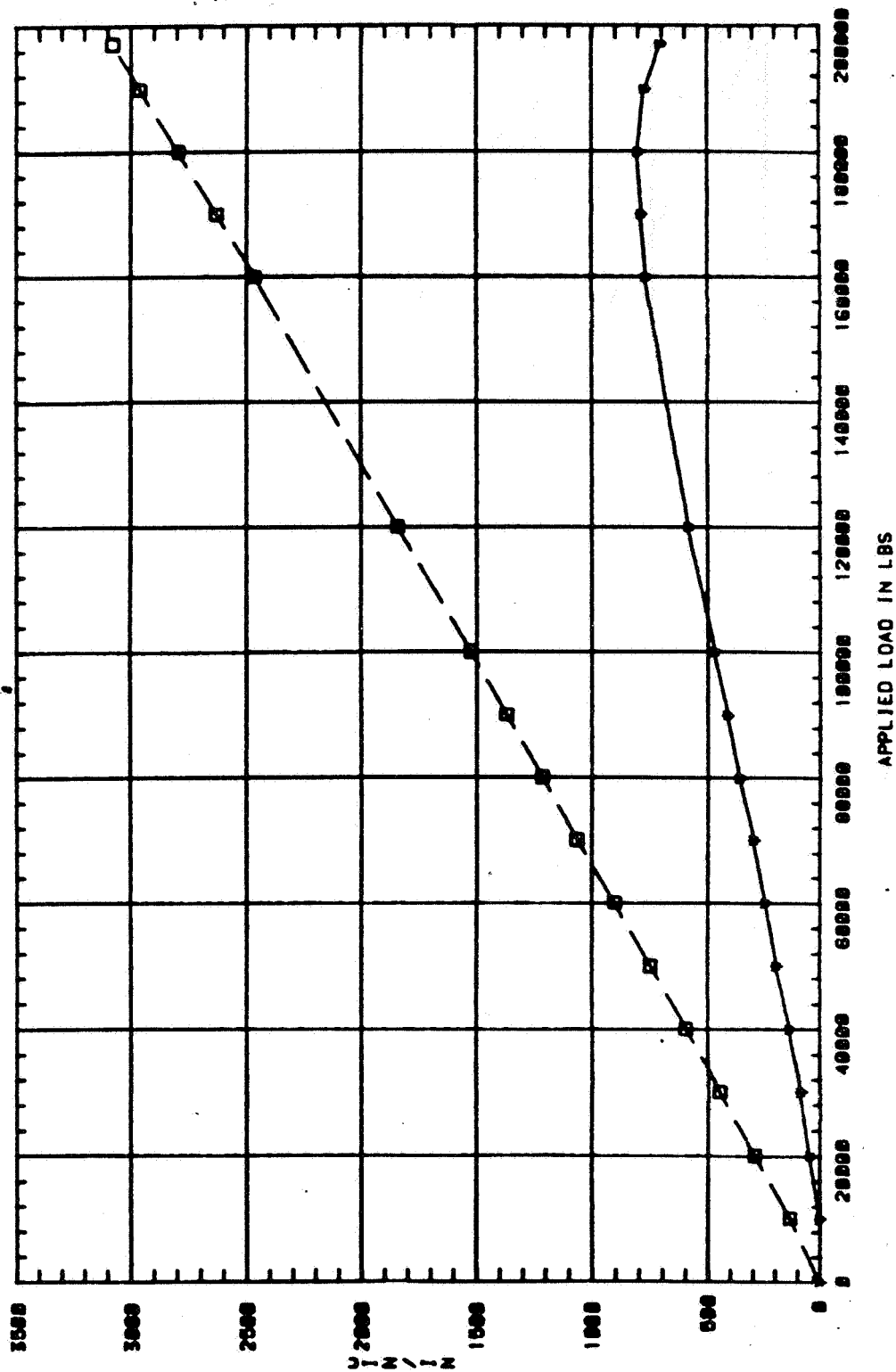
CRITICAL JOINT TEST (BLOG 3)
STRESS SURVEY & LOAD TO FAILURE
DATE: 26 Jun 84
SC318 SC6(D) vs APPLIED LOAD



CRITICAL JOINT TEST (BLOC 3)
STRESS SURVEY & LOAD TO FAILURE

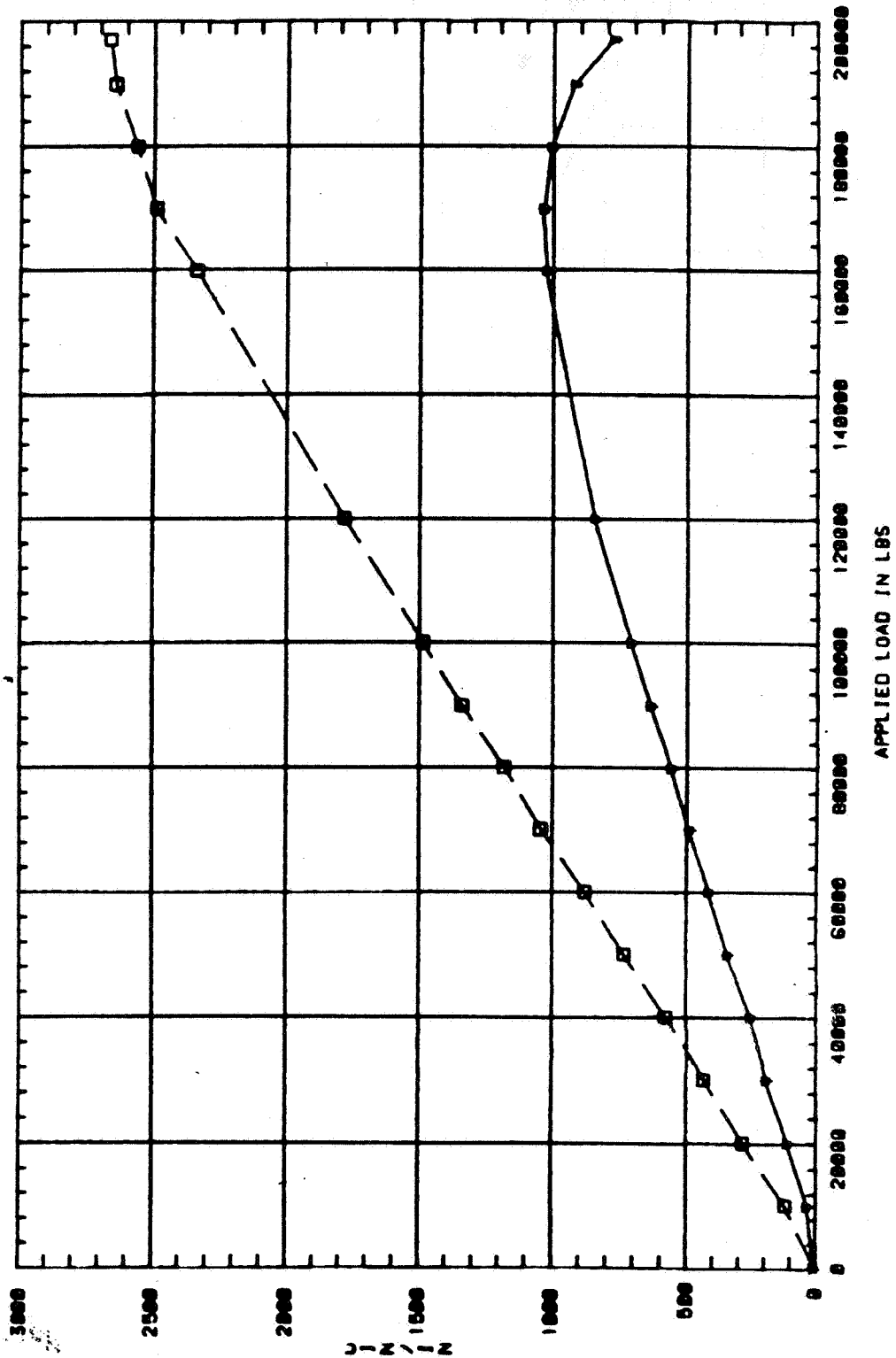
DATE: 28 JUN 84

SC4 (x) SC5 (□) vs APPLIED LOAD

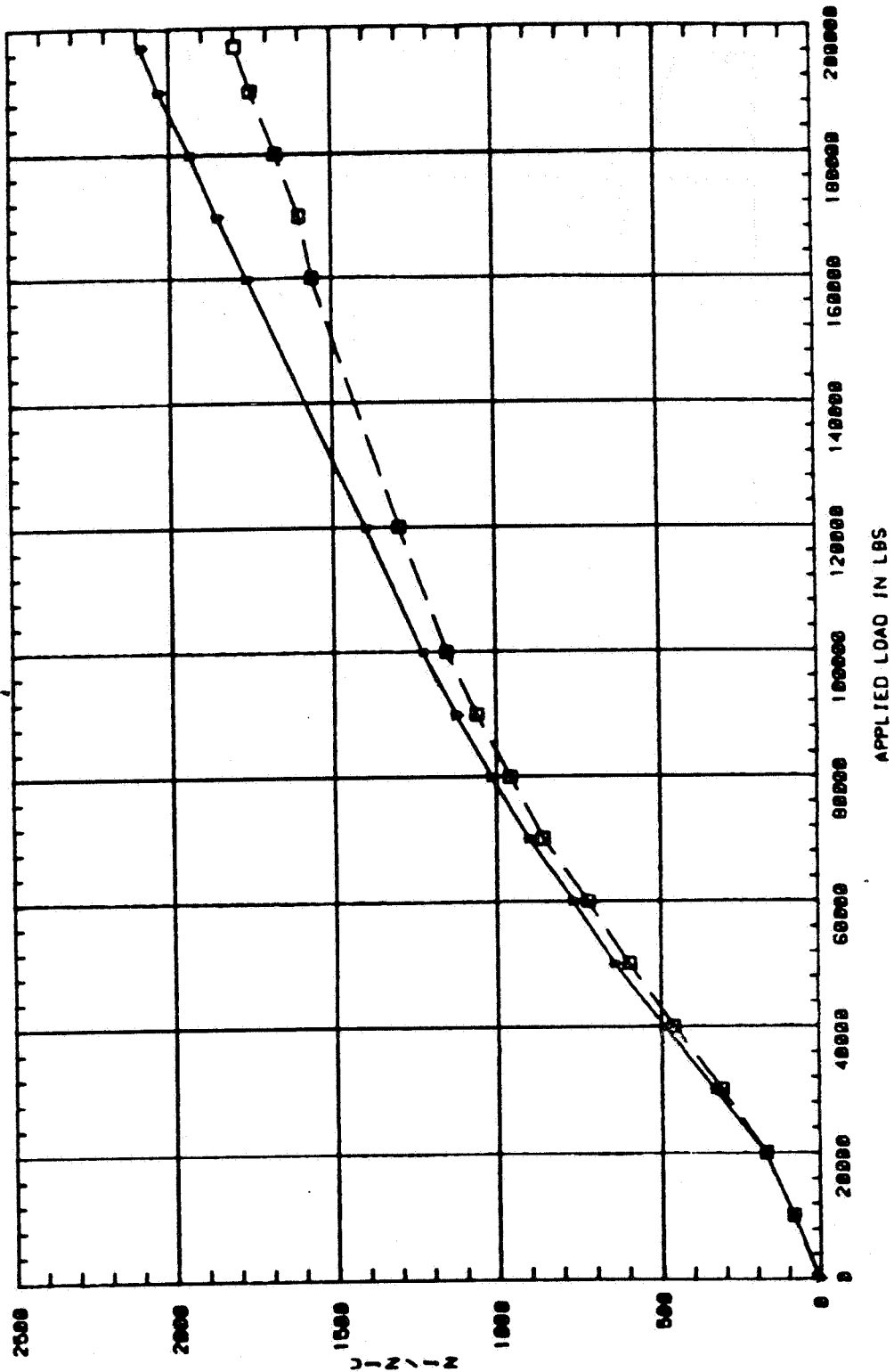


CRITICAL JOINT TEST (BLOG 3)
STRESS SURVEY & LOAD TO FAILURE

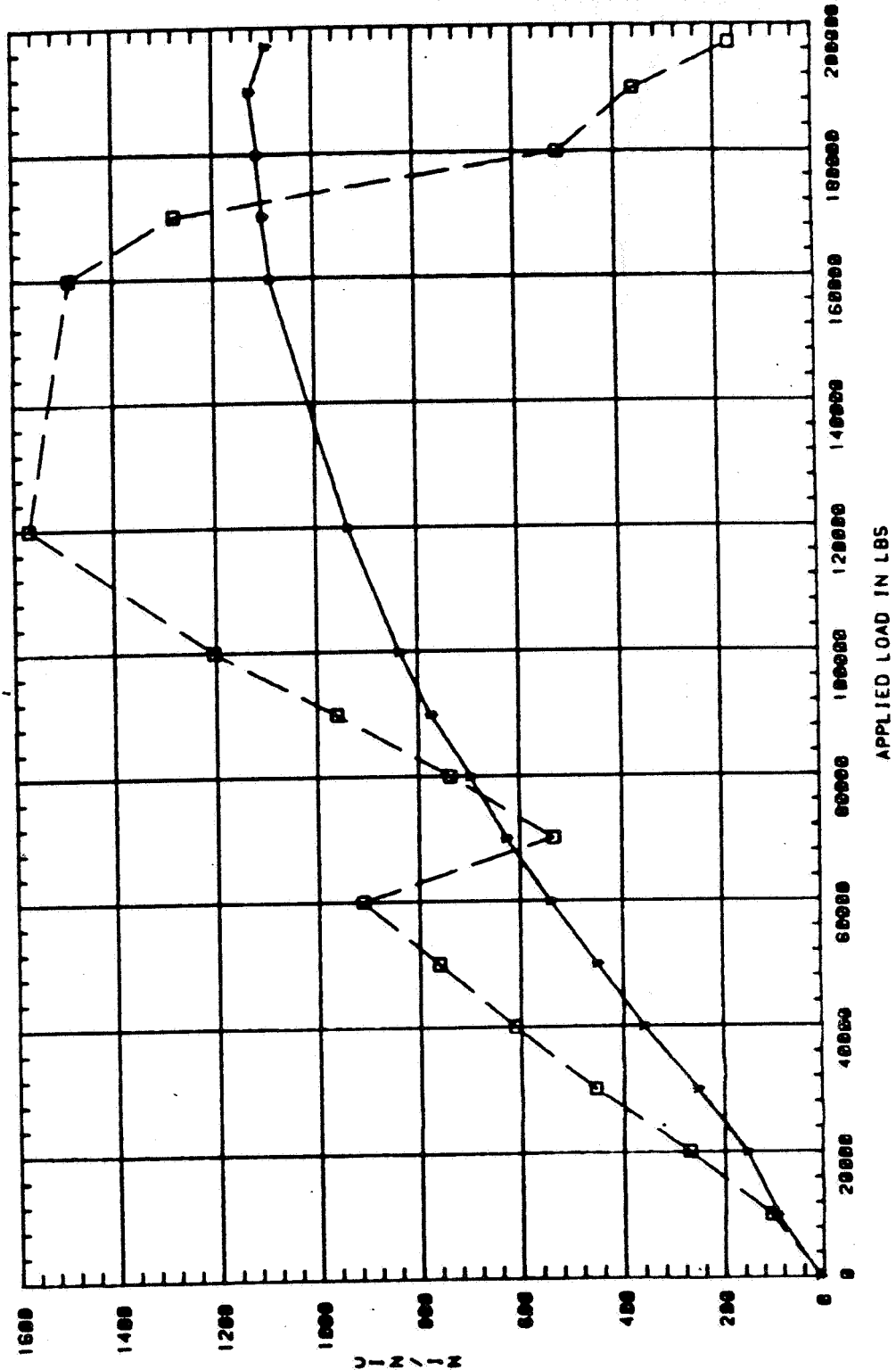
DATE: 26 JUN 84
SC7(*) SC8(□) vs APPLIED LOAD



CRITICAL JOINT TEST (BLOC 3)
STRESS SURVEY & LOAD TO FAILURE
DATE: 26 JUN 84
SC0101 SC10101 vs APPLIED LOAD

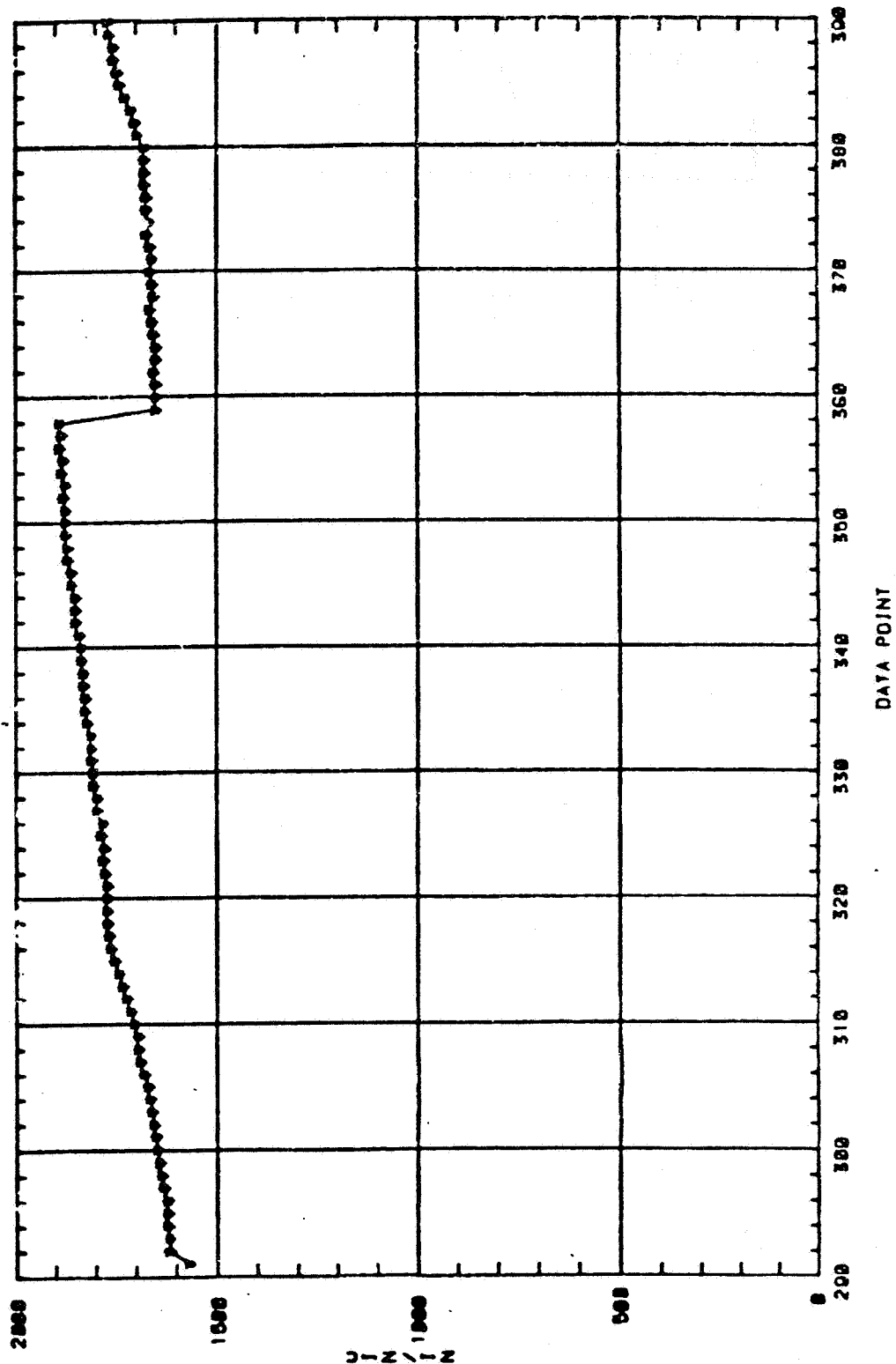


CRITICAL JOINT TEST (BLOC 3)
STRESS SURVEY & LOAD TO FAILURE
DATE: 26 JUN 84
SG11(+) SG12(□) vs APPLIED LOAD



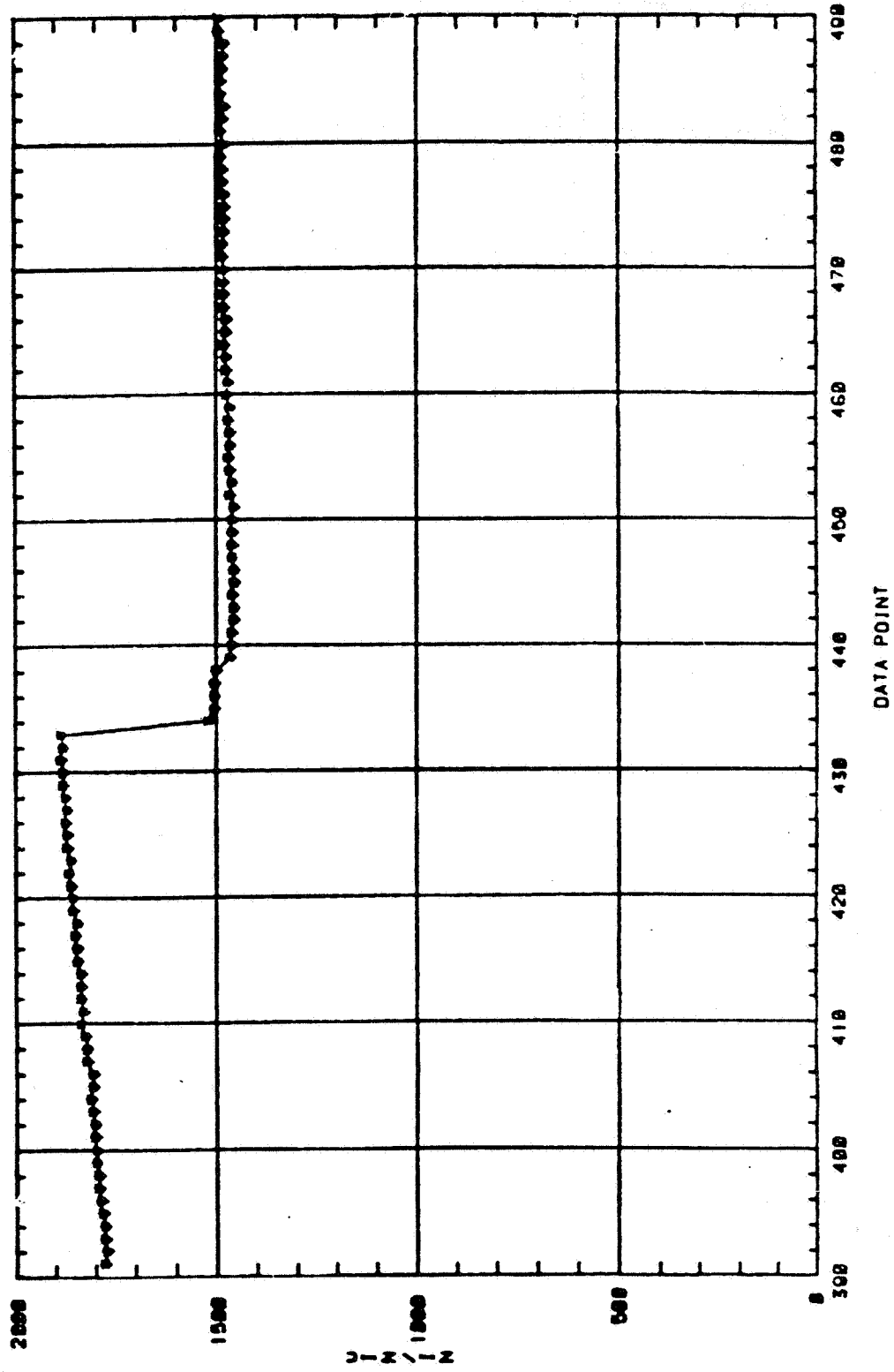
CRITICAL JOINT TEST (BLDG 3)
STRESS SURVEY & LOAD TO
FAILURE

DATE: 26 JUN 84
SG12 vs DATA POINT NUMBER



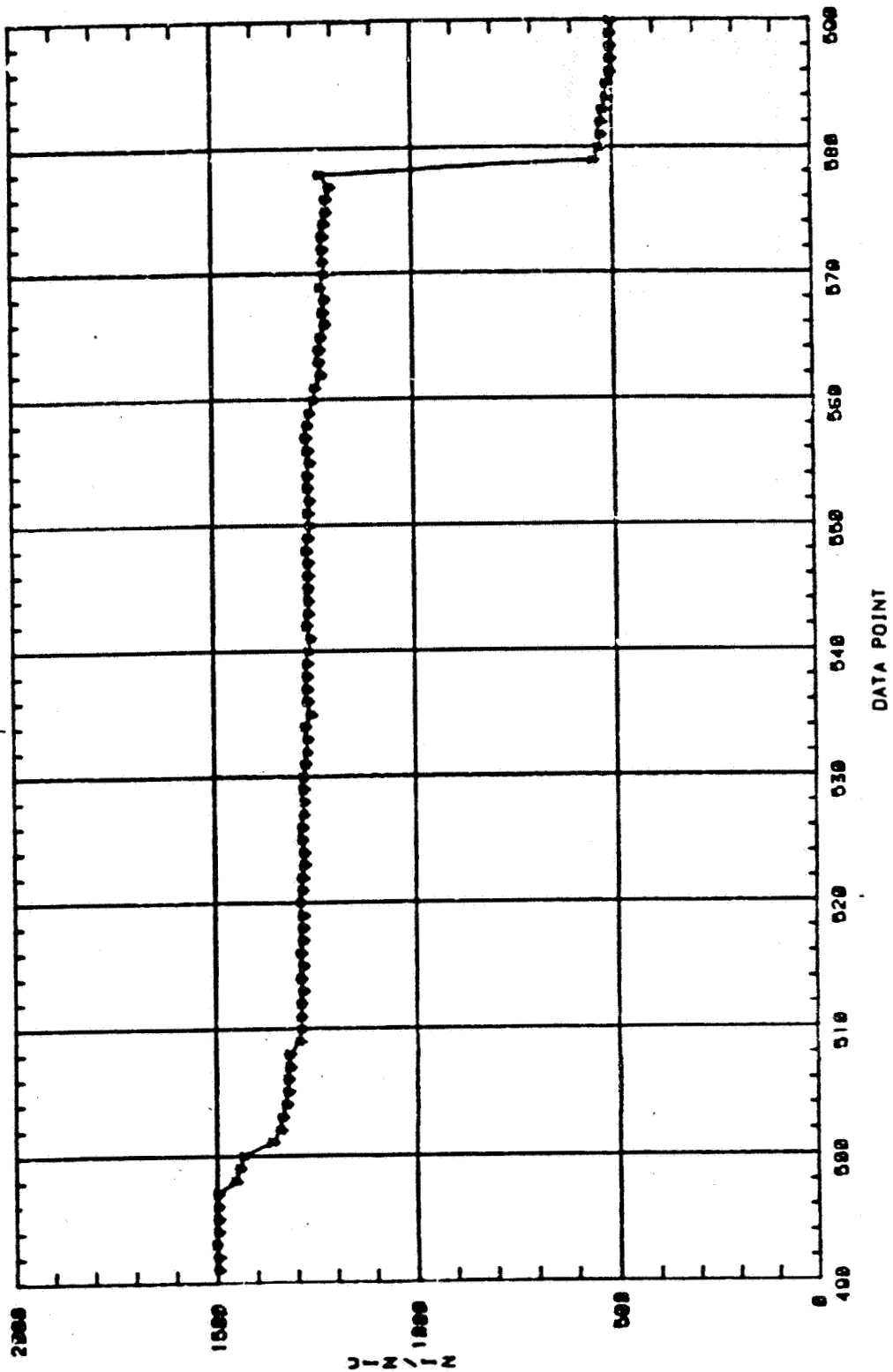
CRITICAL JOINT TEST (BLDG 3)
 STRESS SURVEY & LOAD TO FAILURE

DATE: 26 JUN 84
 SG12 vs DATA POINT NUMBER



CRITICAL JOINT TEST (BLDG 3)
STRESS SURVEY & LOAD TO FAILURE

DATE: 26 JUN 84
SG12 vs DATA POINT NUMBER



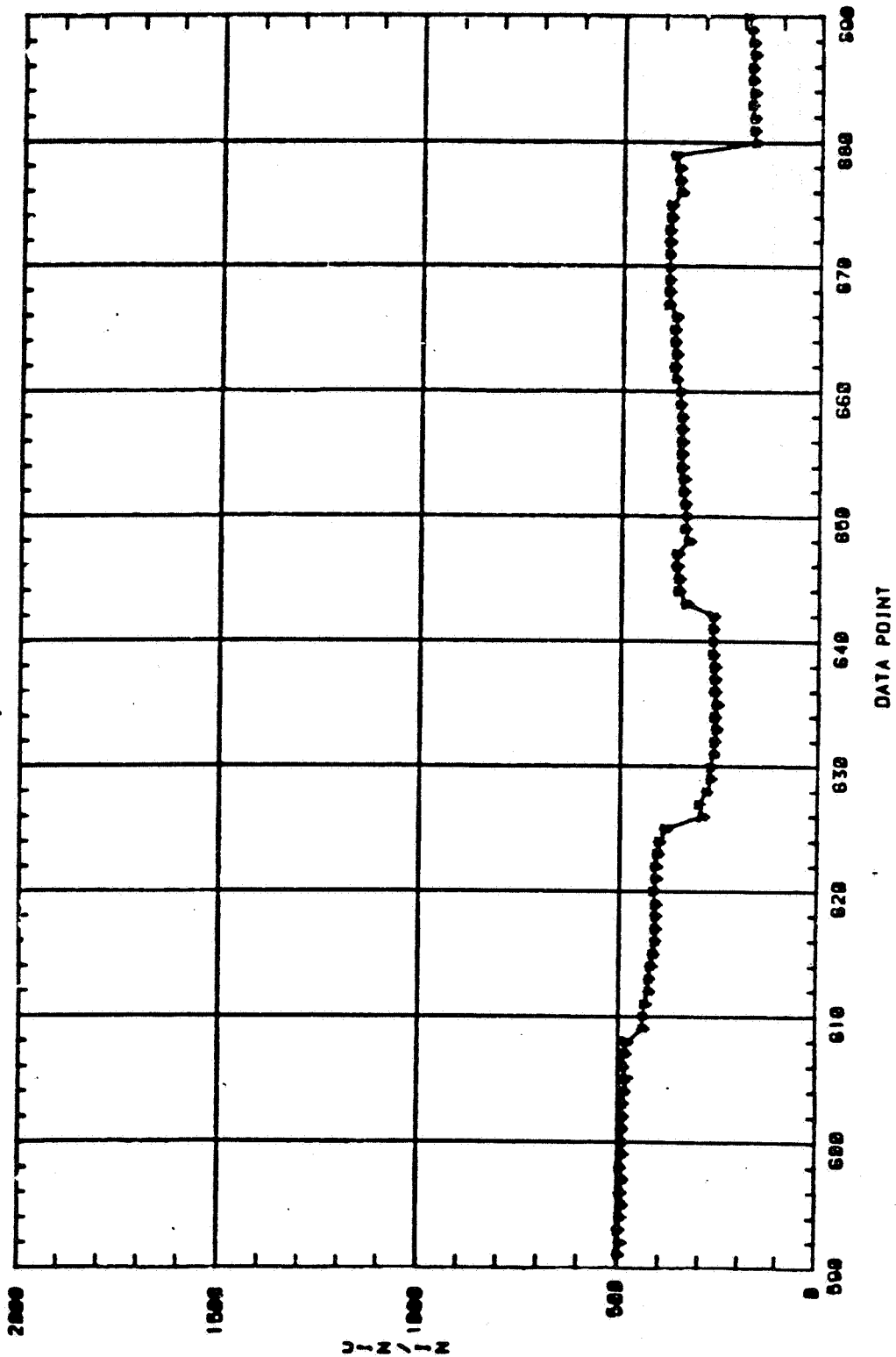
Fixed Scale

Frame 3 of 4

SG12 During Failure Ramp

ORIGINAL PAGE IS
OF POOR QUALITY

CRITICAL JOINT TEST (BLOC 3)
STRESS SURVEY & LOAD TO FAILURE
DATE: 26 JUN 84
SG12 vs DATA POINT NUMBER



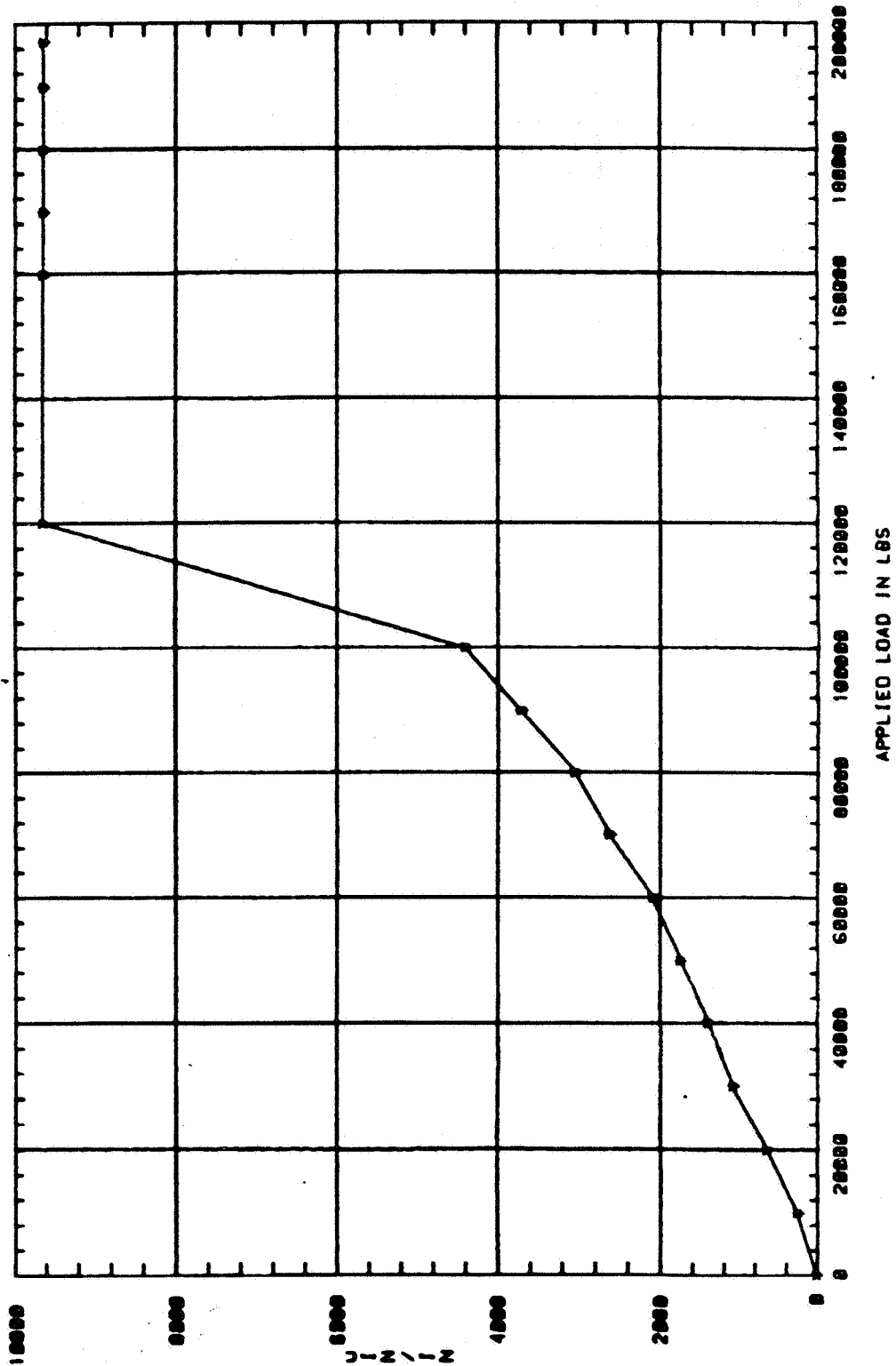
SG12 During Failure Ramp

Frame 4 of 4

Fixed Scale

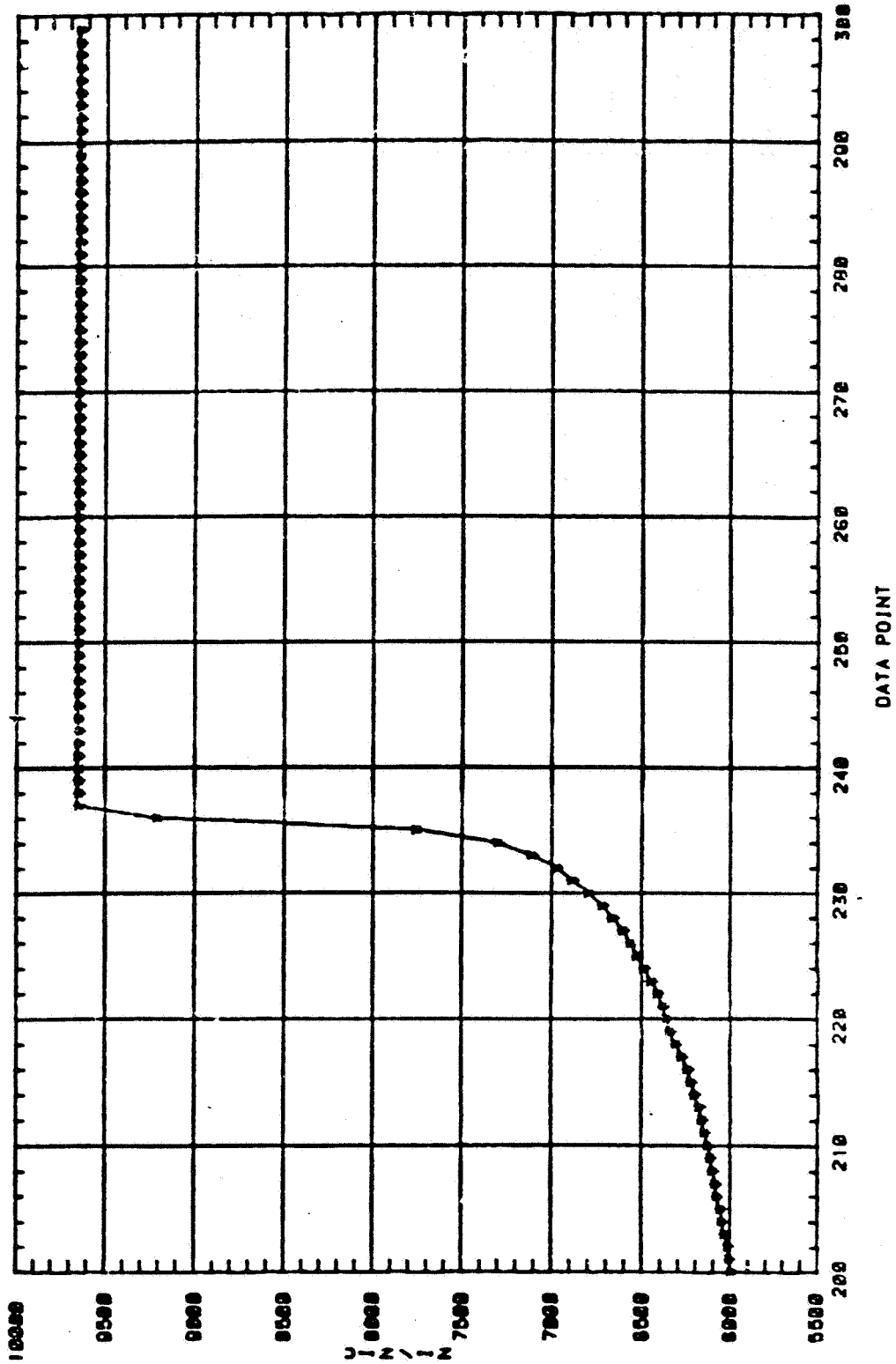
CRITICAL JOINT TEST (BLDG 3)
STRESS SURVEY & LOAD TO FAILURE

DATE: 26 JUN 84
SC13 VS APPLIED LOAD



CRITICAL JOINT TEST (BLDG 3)
STRESS SURVEY & LOAD TO FAILURE

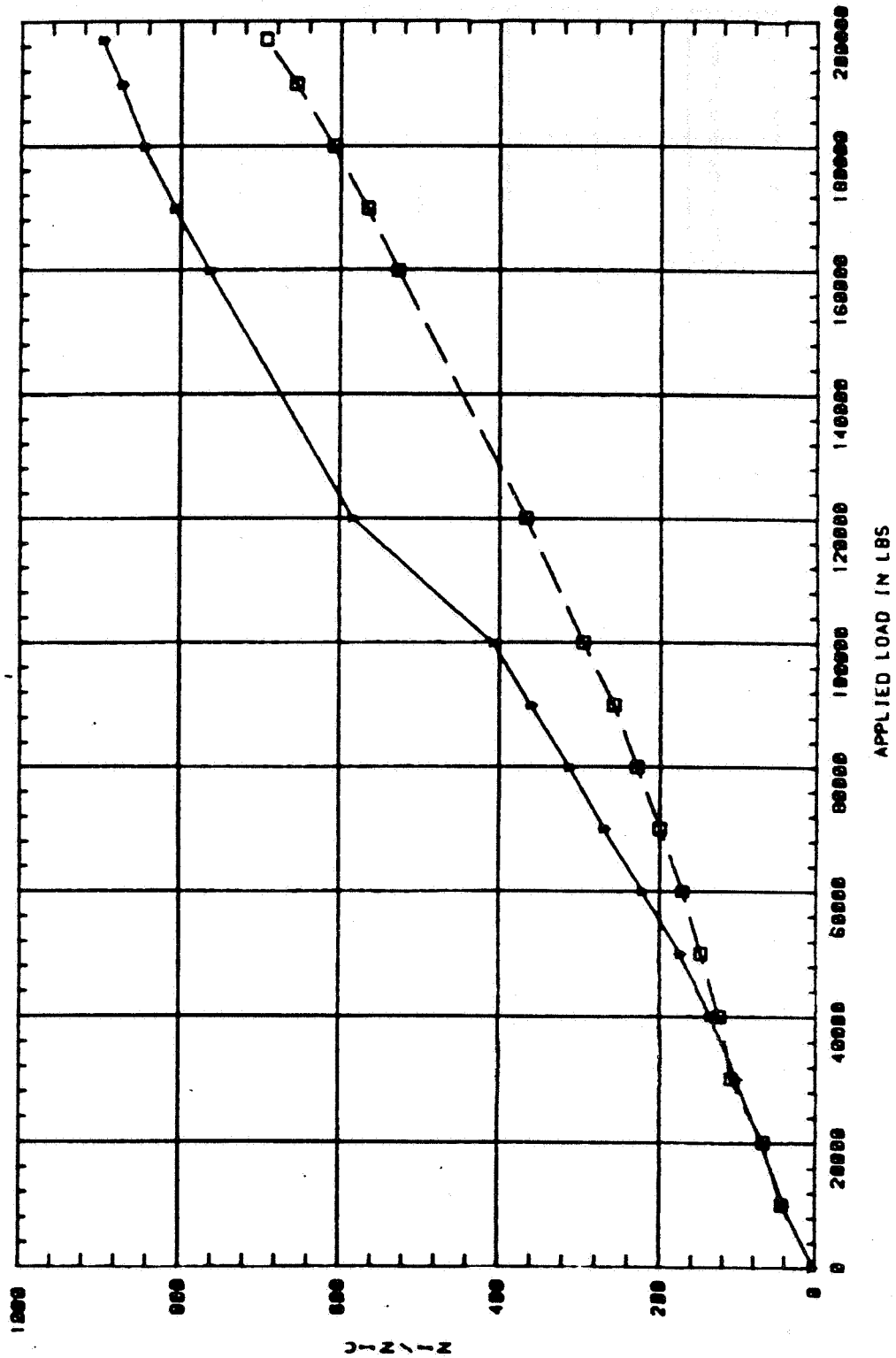
DATE: 26 JUN 84
SG13 vs DATA POINT NUMBER



Failure of SG13 During Continuous Ramp from 100,000 to 120,000 lbs.

The 9658 in/in Reading is Full Scale on the Data System

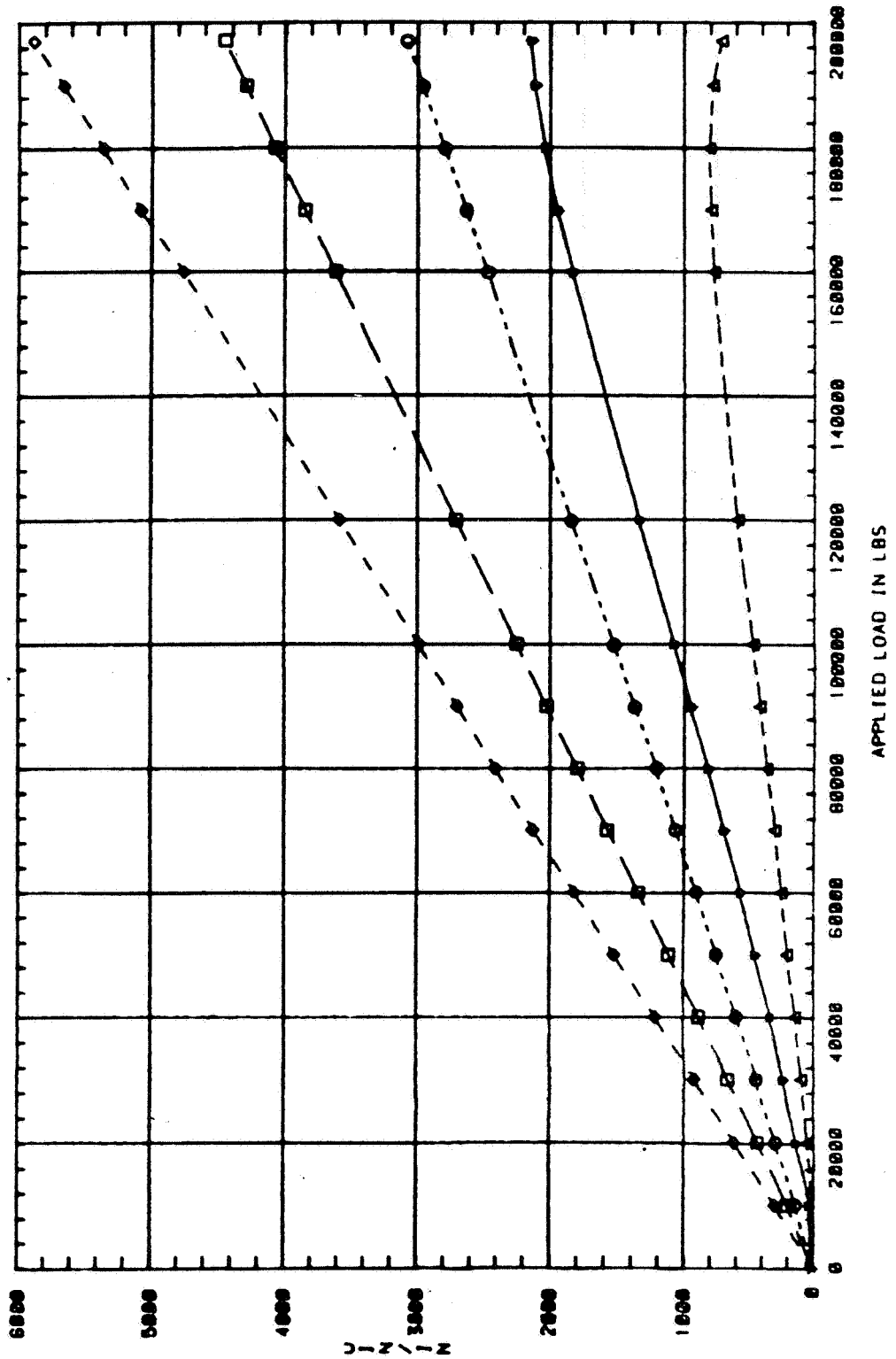
CRITICAL JOINT TEST (BLDG 3)
 STRESS SURVEY & LOAD TO FAILURE
 DATE: 26 Jun 84
 SC14(8) SC15(1) vs APPLIED LOAD



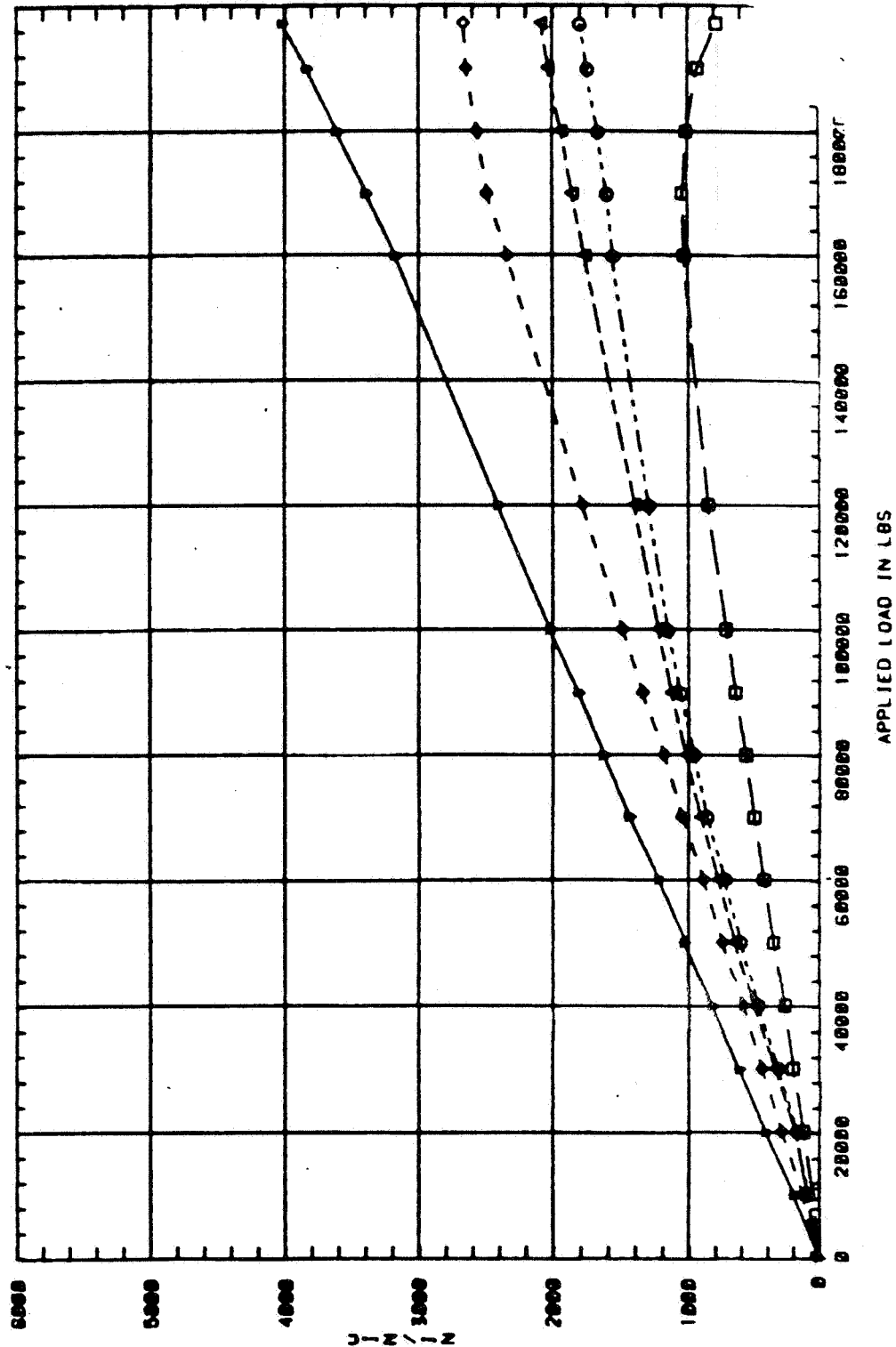
21 JUL 84 08:00
YOUNG 5000

ORIGINAL PAGE IS
OF POOR QUALITY

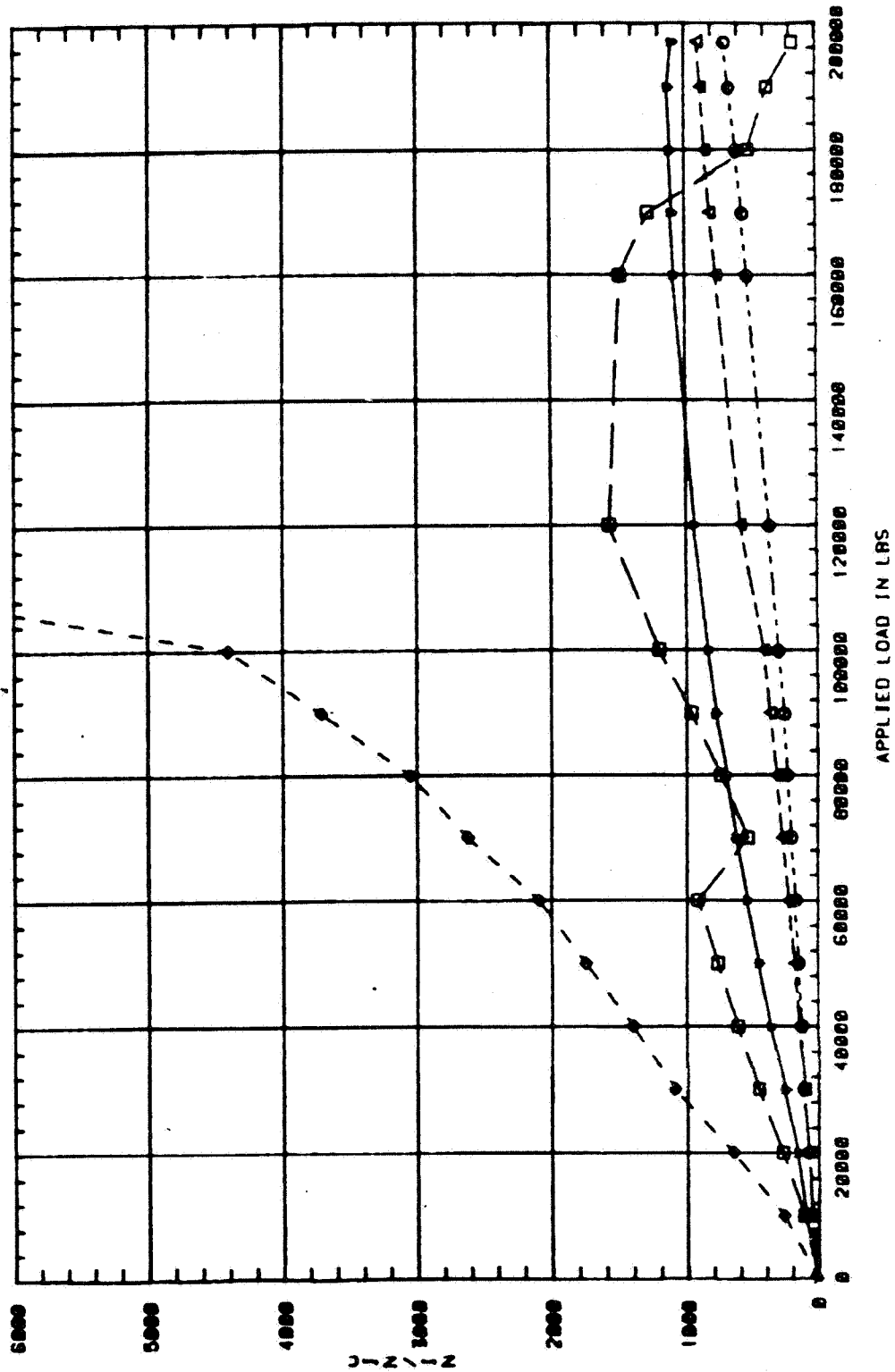
CRITICAL JOINT TEST (BLDC 3)
STRESS SURVEY & LOAD TO FAILURE
DATE: 26 JUN 84
SC1(7) SC2(D) SC3(O) SC4(D) SC5(O) vs APPLIED LOAD



CRITICAL JOINT TEST (BLOG 3)
STRESS SURVEY & LOAD TO FAILURE
DATE 26 Jun 84
SC6(□) SC7(□) SC8(○) SC9(△) SC10(○) vs APPLIED LOAD



CRITICAL JOINT TEST (BLOC 3)
STRESS SURVEY & LOAD TO FAILURE
DATE: 26 JUN 84
SG11(●) SG12(□) SG13(○) SG14(△) SG15(○) vs APPLIED LOAD



APPENDIX B

Demonstration Subcomponent Test Data

Subcomponent #1 - Page B2
(ZJ117560)

Subcomponent #2 - Page B17
(ZJ117561)

Subcomponent #1 Test Data
(Dwg. No. ZJ117560)

SG # - Strain Gage Number
LB # - Load Bolt Number
(Strain Indicating Fasteners)

14 Strain Gages

2 Load Bolts

Strain Gage locations shown on Page 47 .

Plots labeled with digits (strain gage numbers)
Indicate analysis results.

Subcomponent #1
(DWG. No. ZJ117560)

CRITICAL JOINT TEST (BLDG 3)
STRESS SURVEY & LOAD TO FAILURE

APPLIED LOAD	TEST RUN # 9						DATE: 17-JUL-84					
	SG1 (UIN/IN)	SG2 (UIN/IN)	SG3 (UIN/IN)	SG4 (UIN/IN)	SG5 (UIN/IN)	SG6 (UIN/IN)						
0	61.647	-38.898	-126.478	-71.623	-8.065	6.492						
20000	631.074	102.106	-29.187	74.878	185.492	230.478						
40000	996.011	486.221	126.478	250.680	417.759	508.024						
60000	1370.812	870.336	301.602	455.781	650.027	785.571						
80000	1745.504	1235.001	491.320	670.650	872.617	1053.380						
100000	2125.21	1604.529	695.631	895.285	1090.368	1311.449						
120000	2490.219	1964.337	899.942	1110.153	1303.280	1564.650						
140000	2855.246	2319.274	1104.253	1310.371	1501.676	1822.720						
160000	3210.519	2674.215	1308.564	1510.509	1704.910	2000.790						
172000	3439.273	2893.016	1435.373	1627.702	1821.311	2231.735						
180000	3609.615	3053.468	1527.469	1705.924	1917.822	2358.337						
190000	3794.557	3233.370	1615.031	1793.825	2014.600	2480.068						
200000	3979.499	3432.720	1697.729	1881.725	2116.218	2616.407						
210000	4183.909	3627.209	1780.426	1974.509	2227.513	2757.615						
220000	4393.185	3724.453	1819.342	2018.460	2285.580	2845.261						
230000	4582.994	3923.803	1902.040	2096.594	2392.036	2981.600						
240000	4704.667	4166.914	1984.737	2174.728	2479.136	3103.331						
250000	4923.677	4385.713	2057.706	2247.978	2575.914	3229.931						
260000	5132.953	4619.099	2120.945	2326.112	2677.531	3356.532						
270000	5361.698	4813.588	2203.642	2309.363	2774.310	3478.263						

21 3044 110000
YT11AUG 8000 10

ORIGINAL PAGE IS
OF POOR QUALITY

Subcomponent #1
(DWG. No. ZJ117560)

CRITICAL JOINT TEST (BLDG 3)
STRESS SURVEY & LOAD TO FAILURE

TEST RUN # 9

DATE: 17-JUL-84

APPLIED LOAD	SG7 (μ IN/IN)	SG8 (μ IN/IN)	SG9 (μ IN/IN)	SG10 (μ IN/IN)	SG11 (μ IN/IN)	SG12 (μ IN/IN)
0	-37.170	-19.430	-38.786	68.202	0.000	34.101
20000	50.098	72.863	67.875	360.498	0.000	151.019
40000	103.428	131.153	159.991	594.334	0.000	263.066
60000	176.151	179.729	256.955	828.171	0.000	399.471
80000	239.178	223.446	353.919	1091.237	0.000	545.618
100000	297.357	272.022	455.731	1364.046	0.000	701.509
120000	360.383	320.597	538.151	1622.240	0.000	852.529
140000	423.410	354.600	625.418	1875.563	0.000	998.676
160000	476.740	393.460	717.534	2138.629	0.000	1154.567
170000	515.526	417.748	770.865	2299.391	0.000	1242.256
180000	544.615	442.035	819.347	2430.924	0.000	1320.201
190000	573.704	456.608	858.132	2572.201	0.000	1407.890
200000	597.945	480.896	906.614	2742.706	0.000	1495.579
210000	627.034	505.183	959.044	2898.597	0.000	1578.396
220000	646.427	519.756	989.034	3054.488	0.000	1675.828
230000	665.820	548.901	1047.212	3239.609	0.000	1768.388
240000	675.516	553.759	1076.301	3371.142	0.000	1851.205
250000	704.606	582.904	1129.632	3595.235	0.000	1938.894
260000	733.695	612.049	1182.962	3799.842	0.000	2036.325
270000	772.481	636.337	1226.596	4004.449	0.000	2128.886

Subcomponent #1
(DWG. No. ZJ117560)

CRITICAL JOINT TEST (BLDG 3)
STRESS SURVEY & LOAD TO FAILURE

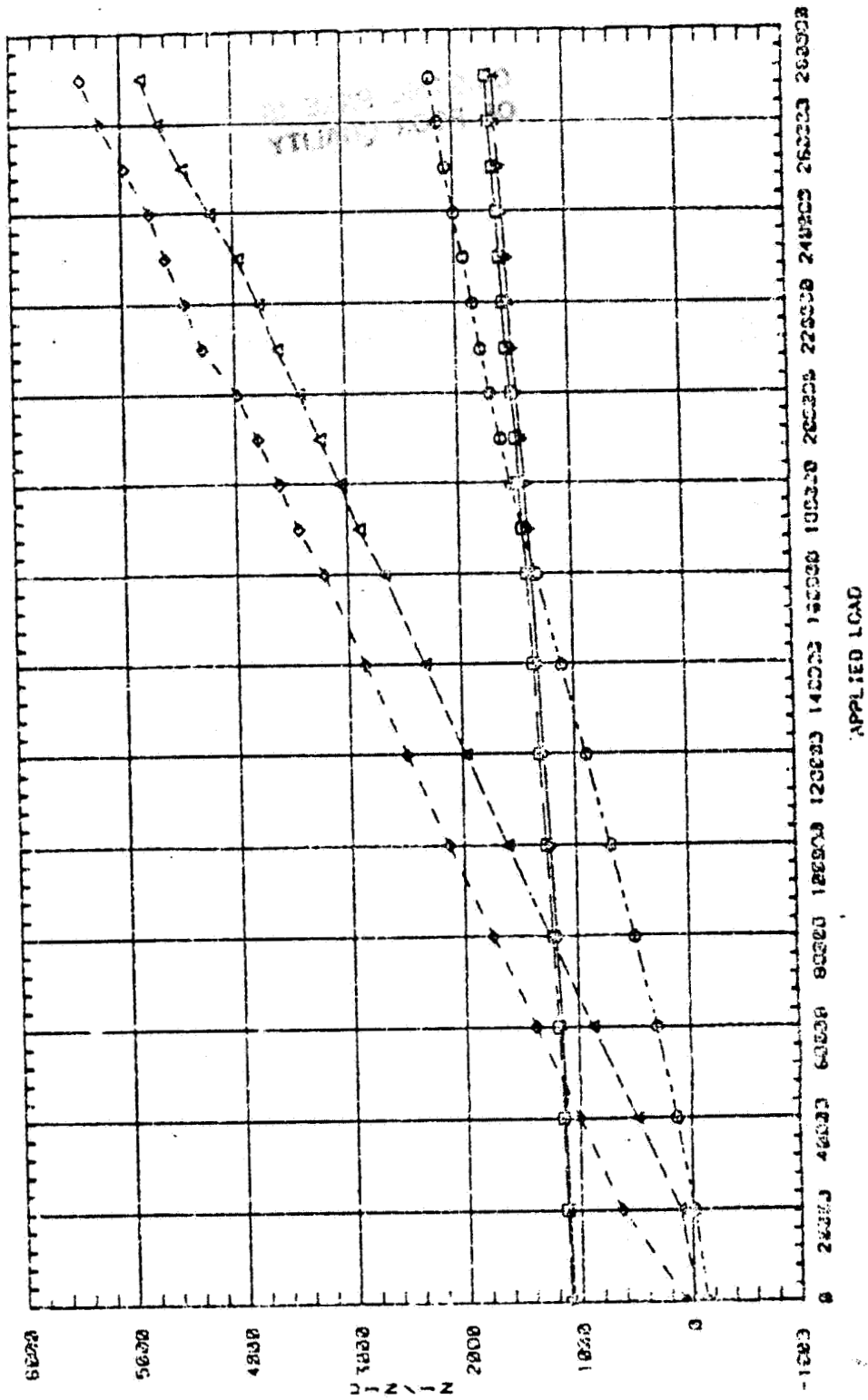
TEST RUN # 9			DATE: 17-JUL-84	
APPLIED LOAD	SG13 (UIN/IN)	SG14 (UIN/IN)	LB1 (LBS)	LB2 (LBS)
0	34.200	-9.701	8501.902	8699.883
20000	161.229	174.619	8659.832	8859.514
40000	268.715	358.939	8817.762	9059.052
60000	405.516	572.303	9015.174	9298.439
80000	556.974	790.637	9291.552	9617.761
100000	718.203	1013.761	9607.412	9976.930
120000	864.775	1217.484	9962.755	10376.007
140000	1016.232	1426.057	10278.615	10695.269
160000	1167.690	1624.929	10633.958	11054.438
170000	1260.519	1760.744	10870.853	11333.792
180000	1333.805	1852.904	11028.783	11533.331
190000	1421.748	1954.765	11265.678	11692.962
200000	1519.463	2056.626	11502.573	12012.224
210000	1592.749	2153.637	11739.468	12211.762
220000	1666.035	2250.647	11897.398	12411.301
230000	1758.864	2352.509	12134.293	12650.747
240000	1851.693	2439.818	12252.741	12810.378
250000	1949.407	2541.679	12410.671	13049.824
260000	2042.236	2643.541	12647.566	13249.363
270000	10005.981	9943.593	12805.496	13448.902

ORIGINAL PAGE IS
OF POOR QUALITY

Subcomponent #1
(DWG. No. ZJ117560)

CRITICAL JOINT TEST (BLDG 3)
STRESS SURVEY & LOAD TO FAILURE

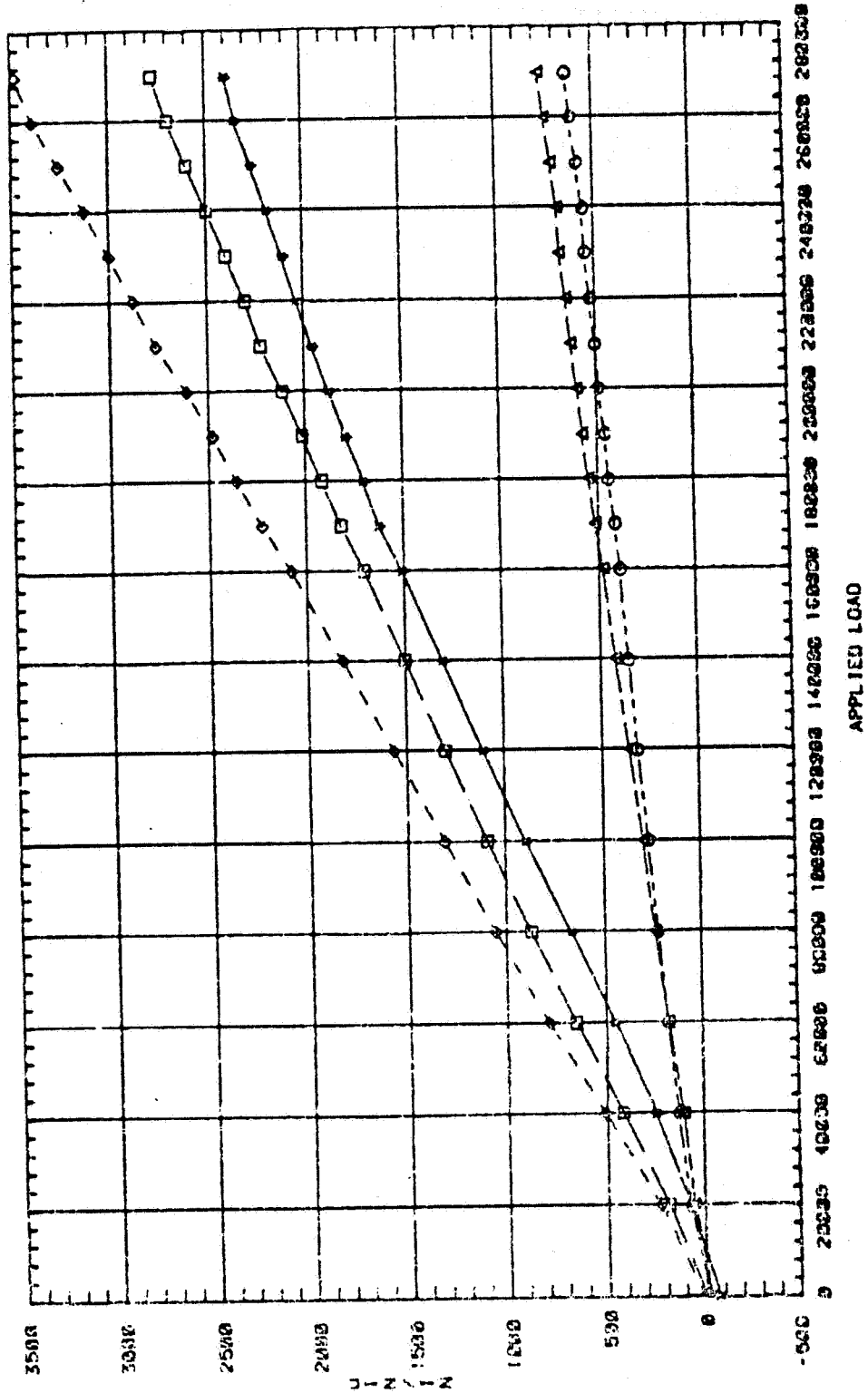
DATE: 17-JUL-84
LB117 (B21D) SC11(O) SC21(A) SC31(O) VS APPLIED LOAD



Subcomponent #1
(DWG. No. ZJ117560)

CRITICAL JOINT TEST (BLOC 3)
STRESS SURVEY & LOAD TO FAILURE

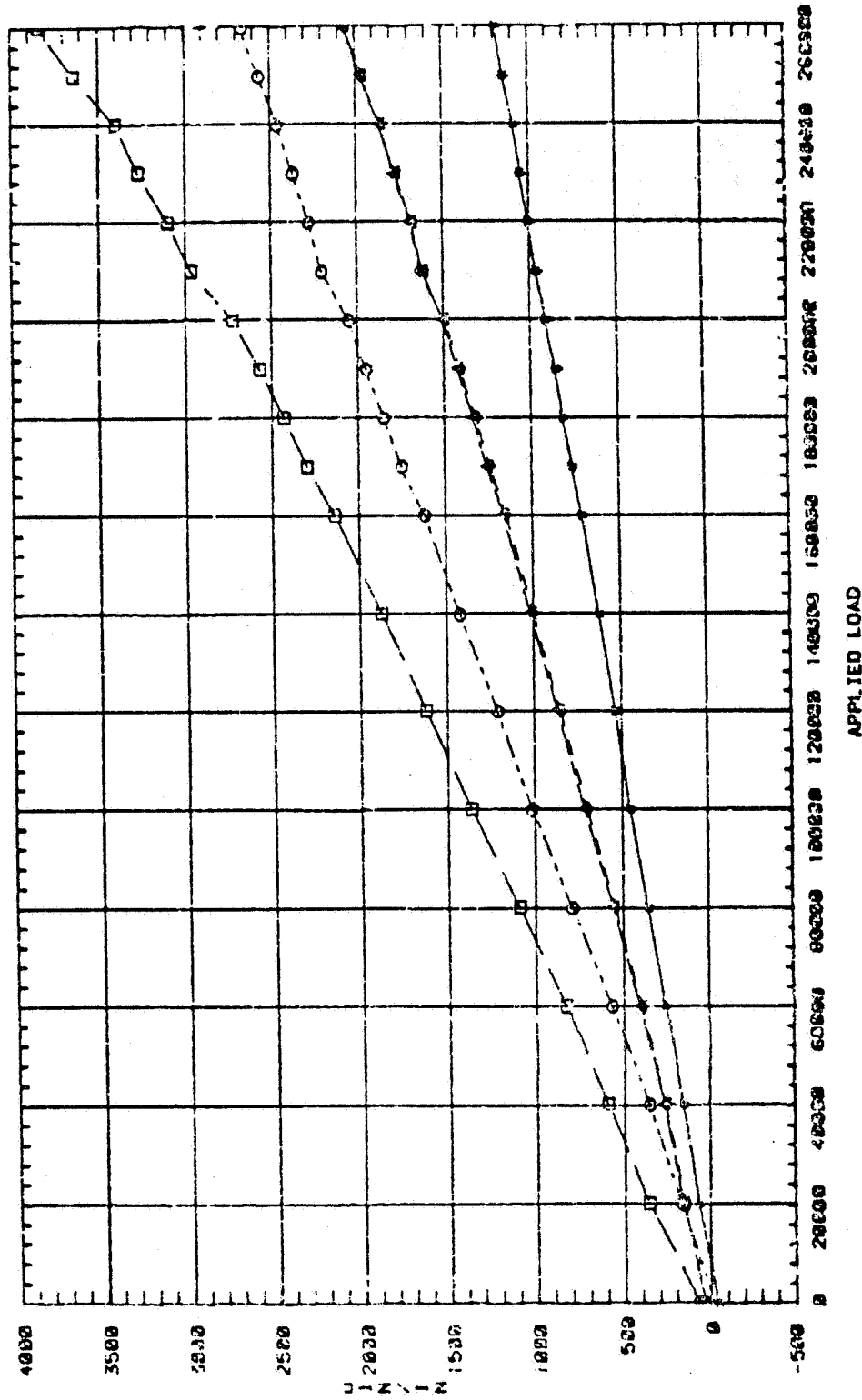
DATE: 17-JUL-84
SC4(8) SC5(17) SC6(17) SC7(17) SC8(17) vs APPLIED LOAD



Subcomponent #1
(DWG. No. ZJ117560)

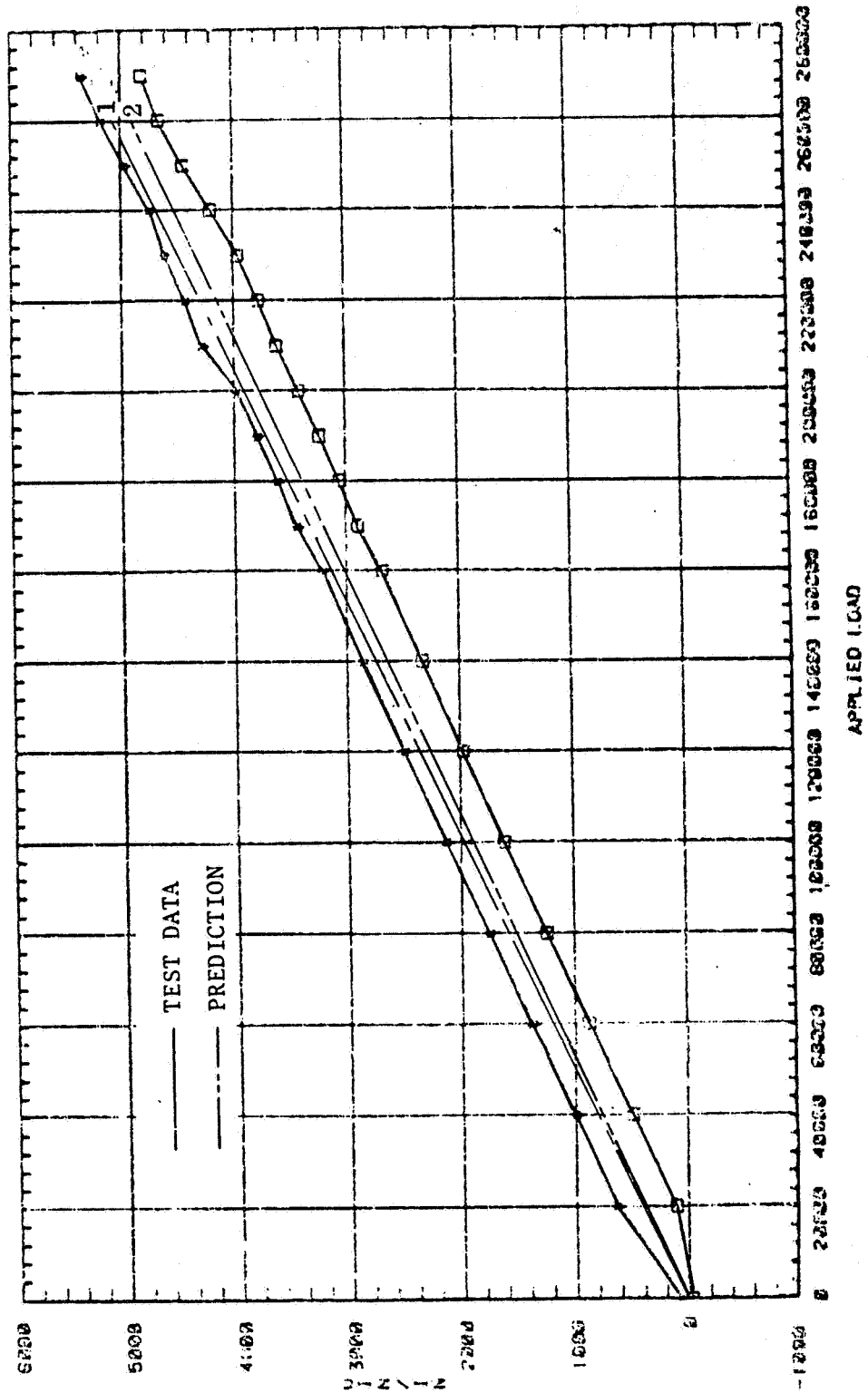
CRITICAL JOINT TEST IBLDC 31
STRESS SURVEY & LOAD TO FAILURE

DATE: 17-JUL-84
SG18(□) SG12(○) SG13(△) SG14(◇) vs APPLIED LOAD



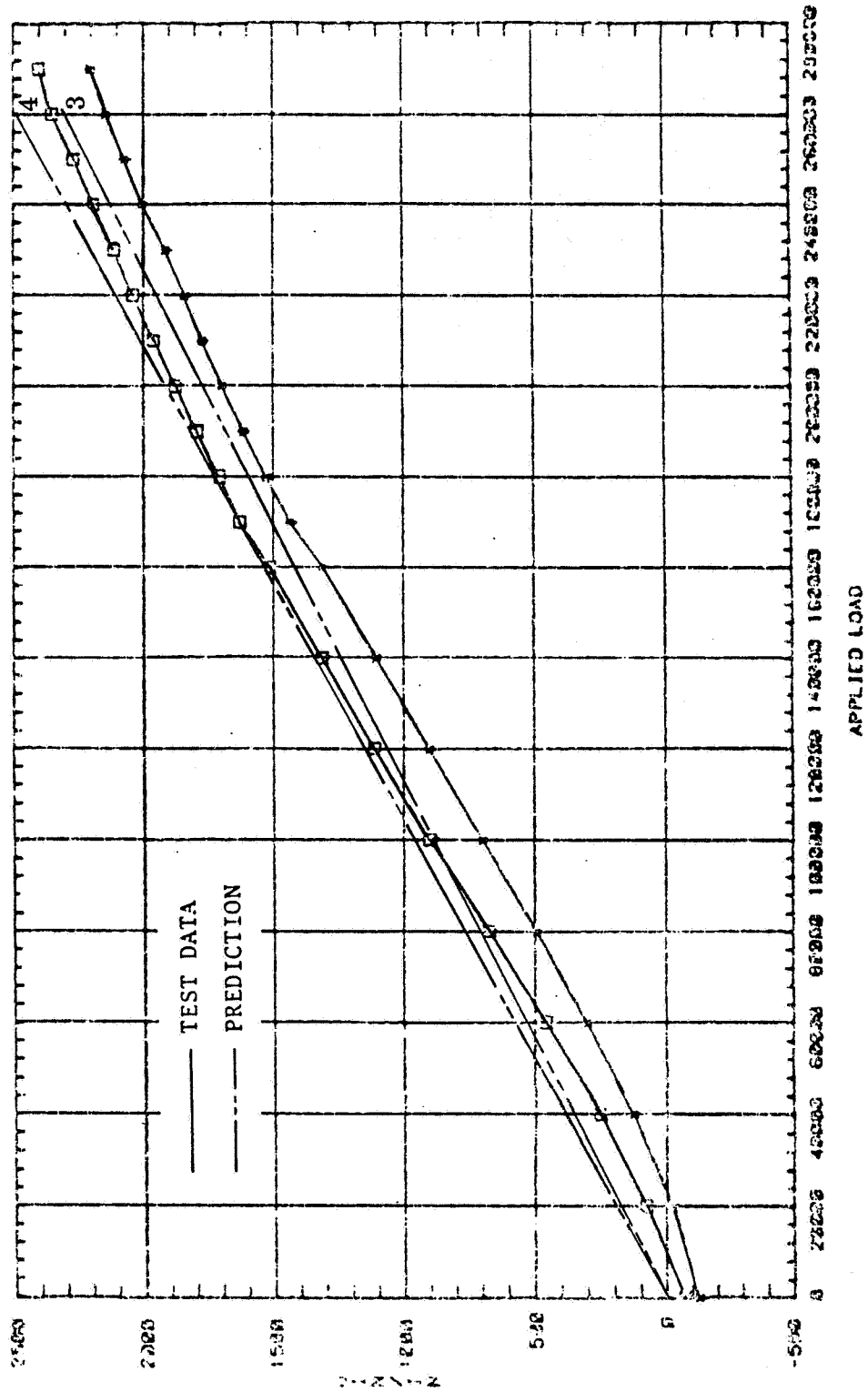
Subcomponent #1
(DWG. No. ZJ117560)

CRITICAL JOINT TEST (SLDC 3)
STRESS SURVEY & LOAD TO FAILURE
DATE: 17-JUL-84
SG11(7) SG2(10) vs APPLIED LOAD



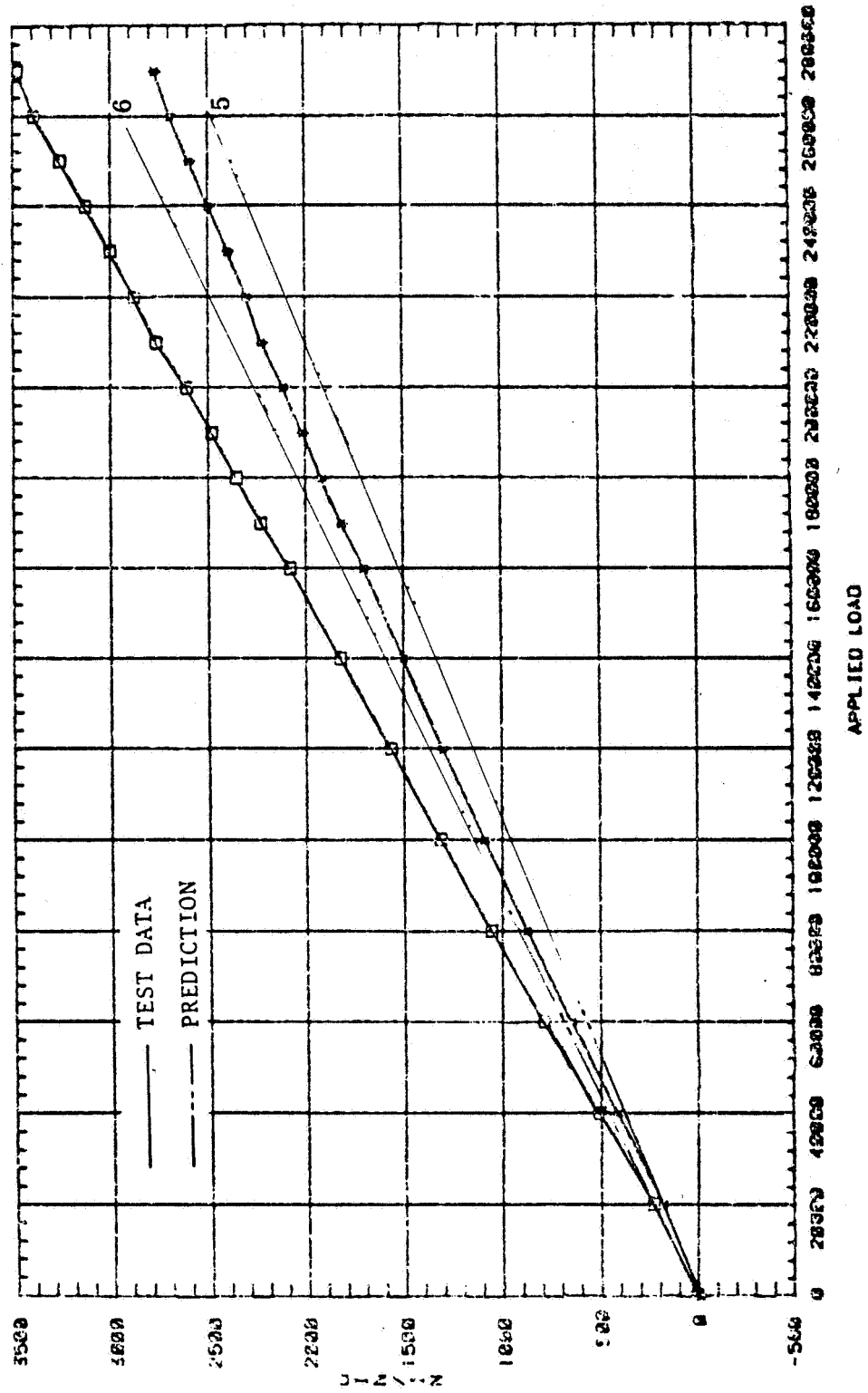
Subcomponent #1
(DWG. No. ZJ117560)

CRITICAL JOINT TEST (BLOS 3)
STRESS SURVEY & LOAD TO FAILURE
DATE: 17-JUL-84
SG3(7) SC1(1) vs APPLIED LOAD



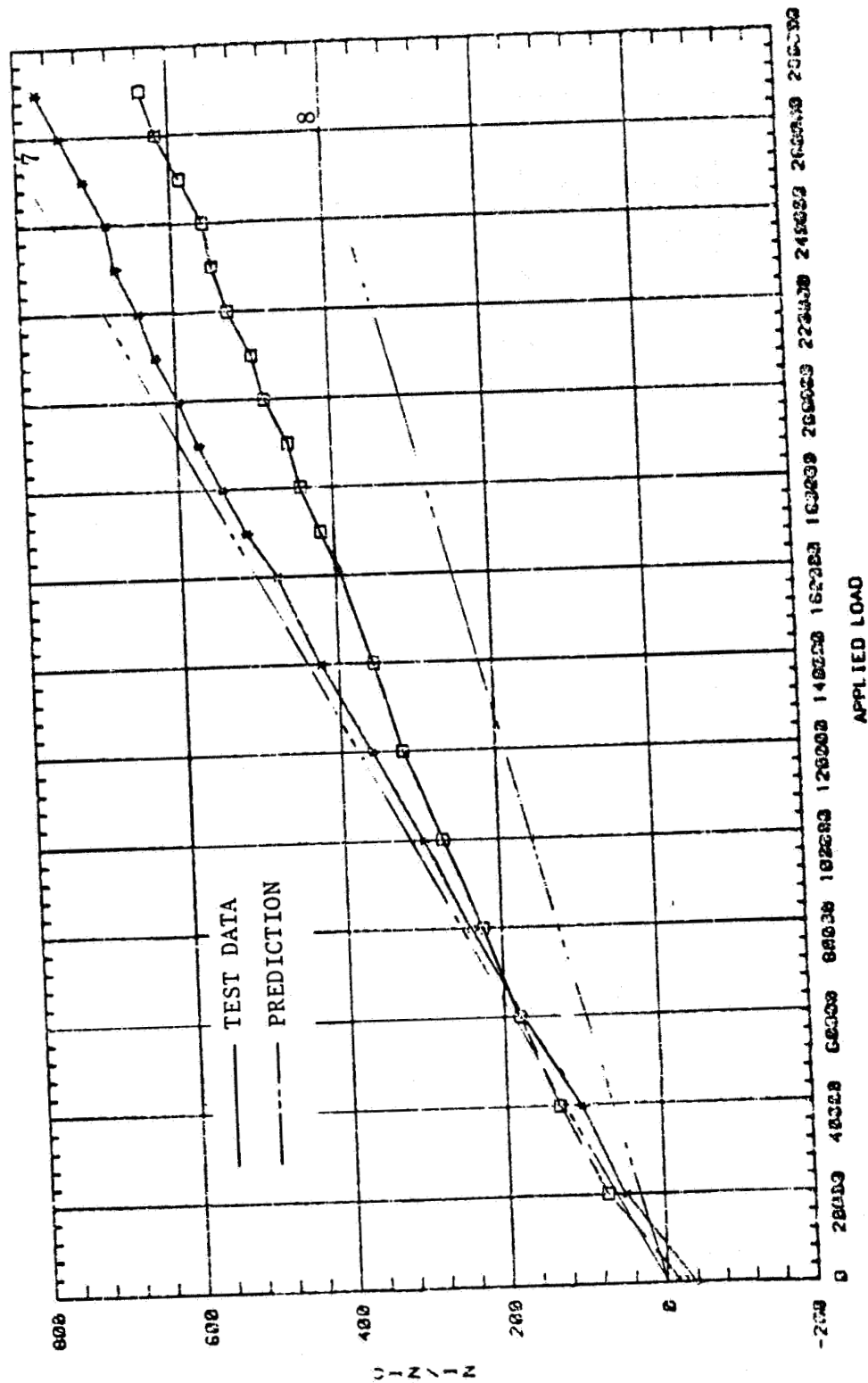
Subcomponent #1
(DWG. No. ZJ117560)

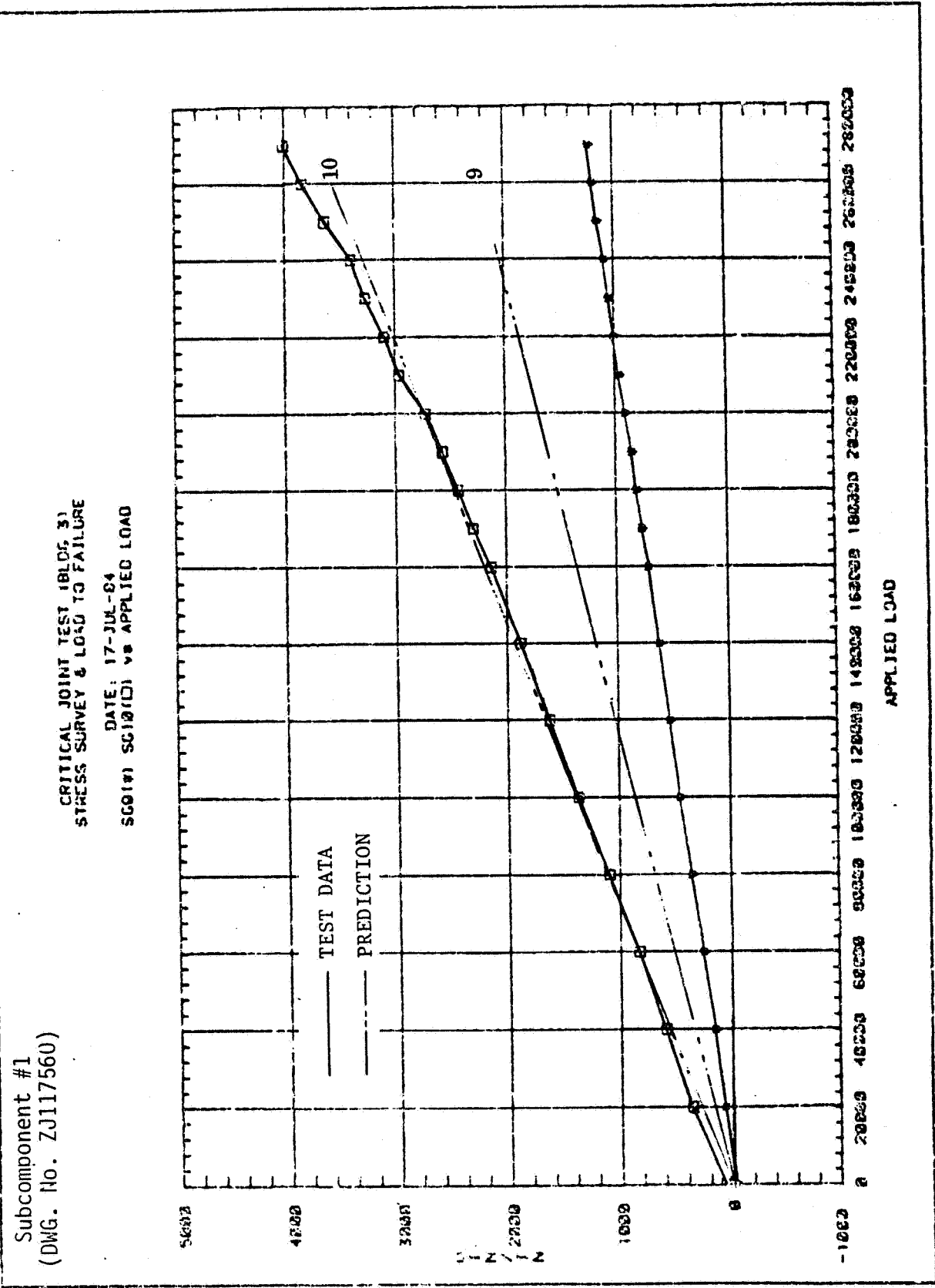
CRITICAL JOINT TEST (BLOC 3)
STRESS SURVEY & LOAD TO FAILURE
DATE: 17-JUL-84
SC5(4) SC6(3) vs APPLIED LOAD



Subcomponent #1
(DWG. No. ZJ117560)

CRITICAL JOINT TEST (BLOC. 3)
STRESS SURVEY & LOAD TO FAILURE
DATE: 17-JUL-84
SG7(8) SC8(1) vs APPLIED LOAD

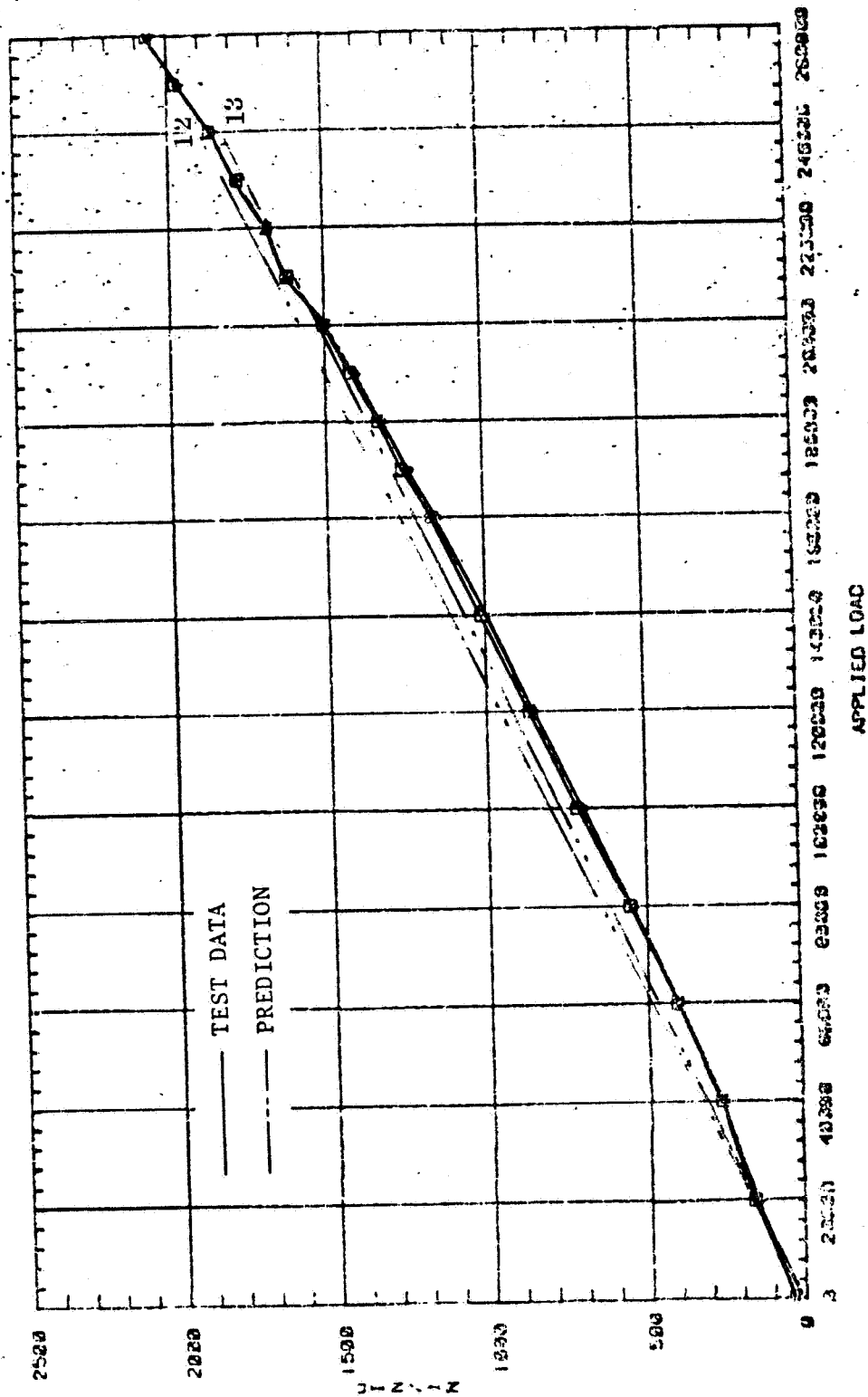




Subcomponent #1
(DWG. No. ZJ117560)

CRITICAL JOINT TEST (B.D.C. 3)
STRESS SURVEY & LOAD TO FAILURE

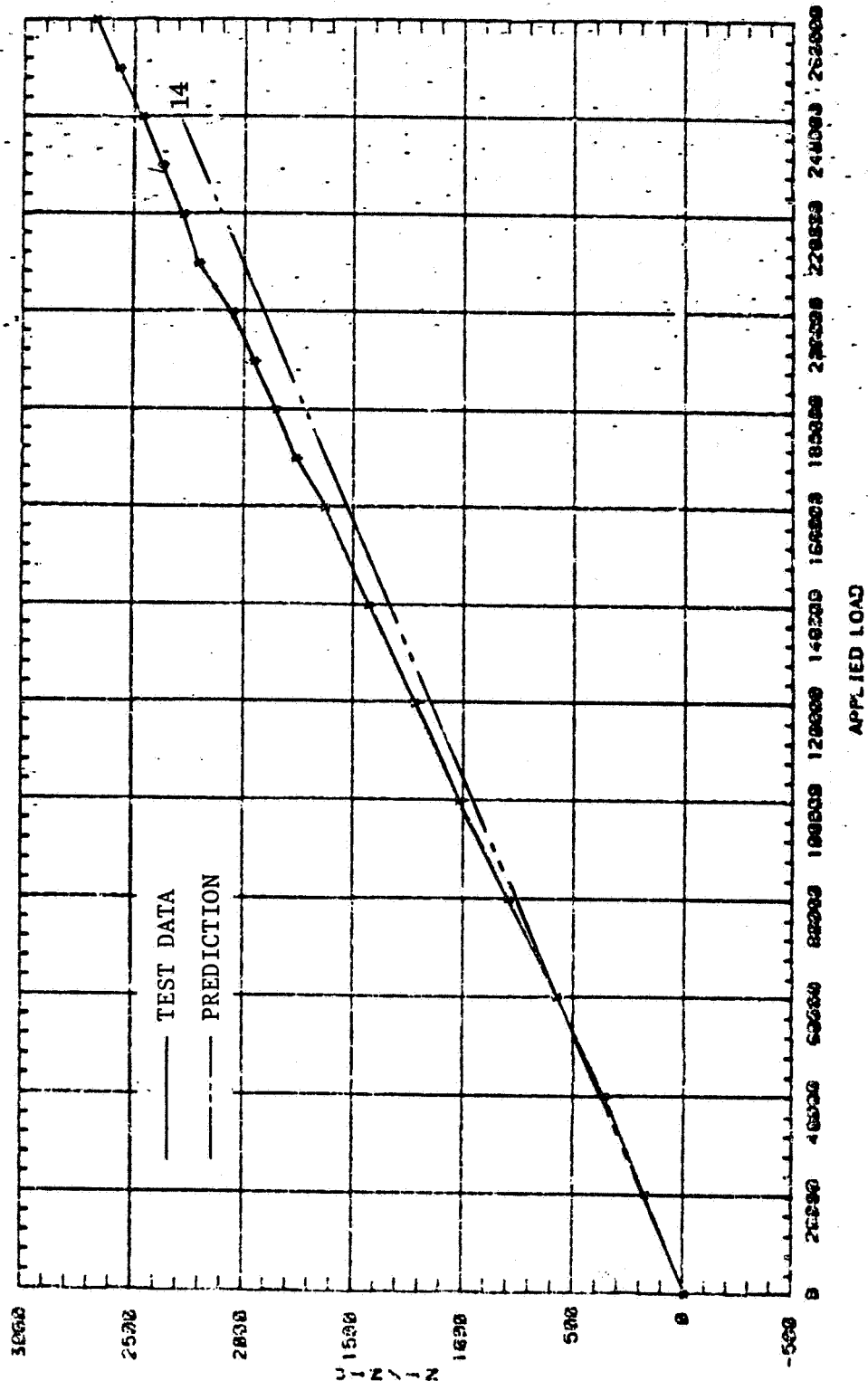
DATE: 17-JUL-64
SG12(7) SG13(10) vs APPLIED LOAD



Subcomponent #1
(DWG. No. ZJ117560)

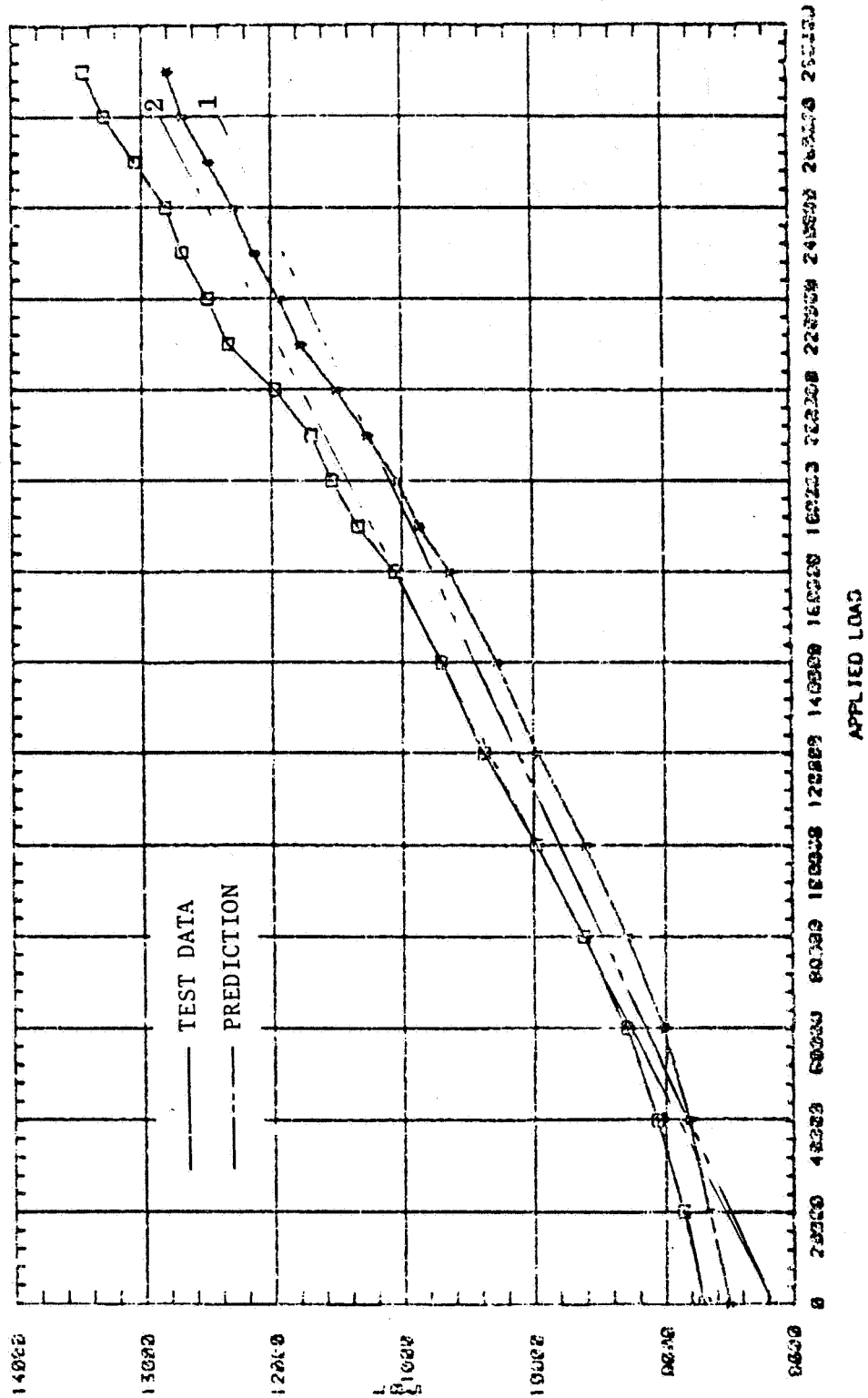
CRITICAL JOINT TEST (BLOC 3)
STRESS SURVEY & LOAD TO FAILURE

DATE: 17-JUL-84
SG14 vs APPLIED LOAD



Subcomponent #1
(DWG. No. ZJ117560)

CRITICAL JOINT TEST (RLDC 3)
STRESS SURVEY & LOAD TO FAILURE
DATE: 17-JUL-84
LB11#1 (B2101) VS APPLIED LOAD



Subcomponent #2 Test Data
(Dwg. No. ZJ117560)

SG # - Strain Gage Number
LB # - Load Bolt Number
LR # - Load Restraint Number

12 Strain Gages
1 Load Bolt
1 Load Restraint

Strain Gage locations shown on Page 48

ORIGINAL PAGE IS
OF POOR QUALITY

Subcomponent #2
(DWG. No. ZJ117561)

**CRITICAL JOINT TEST (BLDC 3)
STRESS SURVEY & LOAD TO FAILURE**

APPLIED LOAD	LR1 (LBS)	LB1 (UIN/IN)	SC1 (UIN/IN)	SC2 (UIN/IN)	SC3 (UIN/IN)	SC4 (UIN/IN)
0	19.758	348.405	196.488	-248.735	-151.765	-87.822
10000	19.758	534.332	688.518	153.068	322.700	170.853
20000	19.758	805.685	1053.888	626.621	754.032	281.029
30000	-7.185	1061.964	1467.973	1076.257	1199.741	352.883
40000	-98.792	1388.593	1911.288	1497.193	1655.036	391.625
50000	-195.789	1745.373	2335.116	1942.046	2110.331	424.737
60000	-292.785	2112.202	2739.459	2372.548	2560.833	472.640
70000	-335.894	2604.659	3041.497	2779.134	2953.824	525.333
80000	-459.834	2991.589	3440.968	3209.637	3404.326	635.509
90000	-578.385	3408.669	3825.824	3654.490	3873.999	726.524
100000	-729.268	3876.000	4132.734	4089.776	4334.086	831.910
110000	-863.985	4333.281	4366.570	4415.045	4717.492	865.442
115400	-982.536	4785.537	4507.846	4663.780	5033.802	884.603

ORIGINAL PAGE IS
OF POOR QUALITY

Subcomponent #2
(DWG. No. ZJ117561)

**CRITICAL JOINT TEST (BLDC 3)
STRESS SURVEY & LOAD TO FAILURE**

APPLIED LOAD	SG5 (UIN/IN)	SG6 (UIN/IN)	SG7 (UIN/IN)	SG8 (UIN/IN)	SG9 (UIN/IN)	SG10 (UIN/IN)
0	-84.628	-4.795	22.301	-28.659	-47.673	9.562
10000	332.125	489.078	323.364	272.259	343.248	157.775
20000	825.523	920.618	691.329	697.366	705.564	372.923
30000	1285.389	1352.157	987.613	1108.143	1067.881	592.852
40000	1716.513	1764.517	1283.896	1490.261	1415.896	784.095
50000	2152.428	2167.288	1604.074	1881.932	1763.911	980.119
60000	2573.971	2560.468	1914.694	2244.945	2097.624	1171.361
70000	2976.354	2910.495	2215.757	2579.298	2388.431	1338.699
80000	3383.527	3327.650	2545.492	2932.757	2726.911	1529.941
90000	3833.812	3778.369	2889.564	3314.876	3065.392	1735.527
100000	4408.645	4238.678	3271.865	3797.300	3394.337	1960.237
110000	4997.848	4660.628	3625.494	4208.077	3680.377	2146.699
115400	4715.222	5005.859	3964.787	4585.419	3923.511	2309.255

ORIGINAL PAGE IS
OF POOR QUALITY

**CRITICAL JOINT TEST (BLDG 3)
STRESS SURVEY & LOAD TO FAILURE**

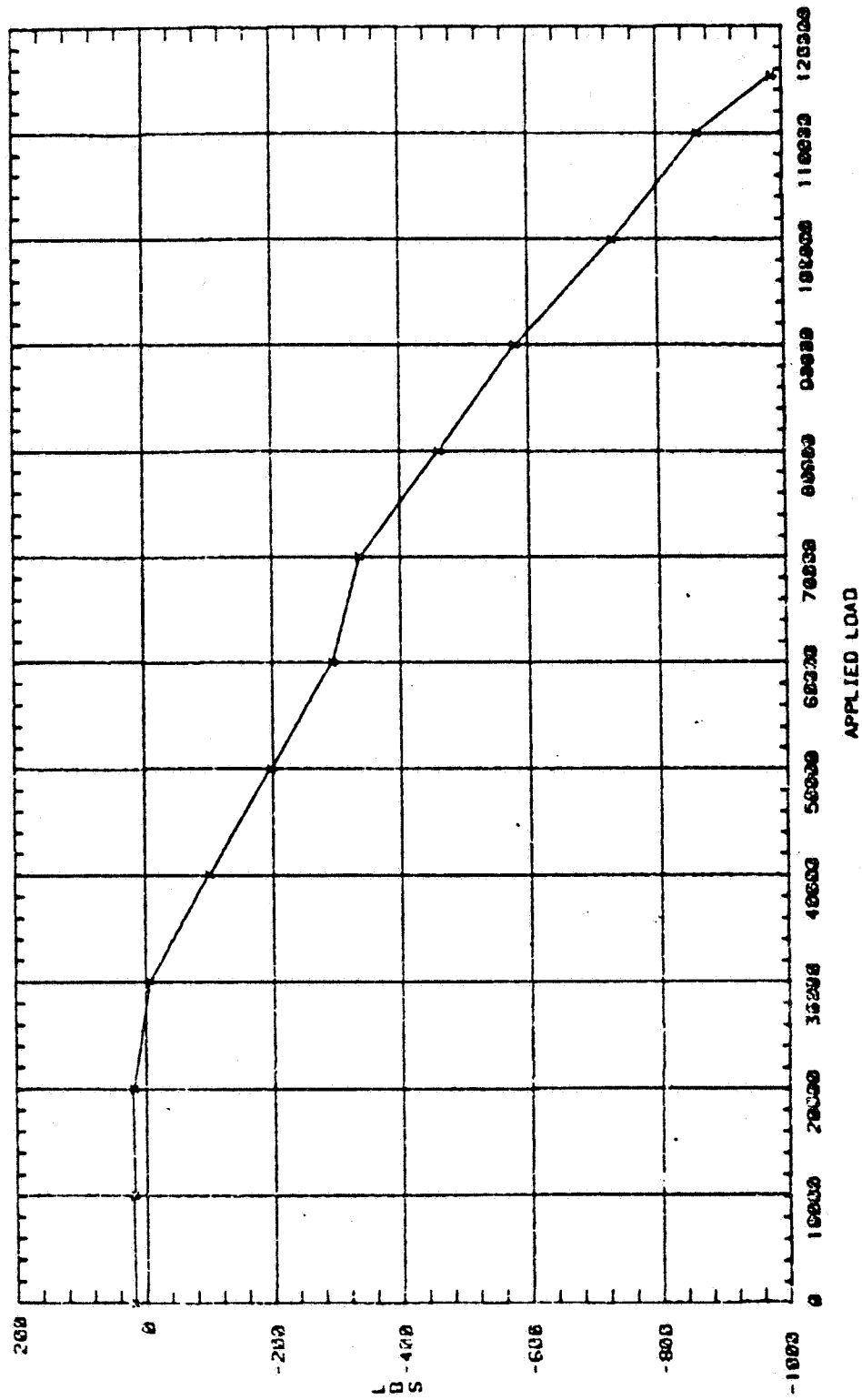
APPLIED LOAD	SG11 (UIN/IN)	SG12 (UIN/IN)
0	4.806	-7.995
10000	158.613	481.319
20000	447.001	917.863
30000	701.743	1349.611
40000	937.260	1762.170
50000	1163.163	2169.931
60000	1379.454	2563.301
70000	1576.519	2903.902
80000	1783.197	3335.650
90000	1999.488	3781.789
100000	2225.391	4242.320
110000	2388.811	4669.270
115400	2504.166	5009.871

BLDG 3
STRESS SURVEY

Subcomponent #2
(DWG. No. ZJ117561)

CRITICAL JOINT TEST (BLOC 3)
STRESS SURVEY & LOAD TO FAILURE

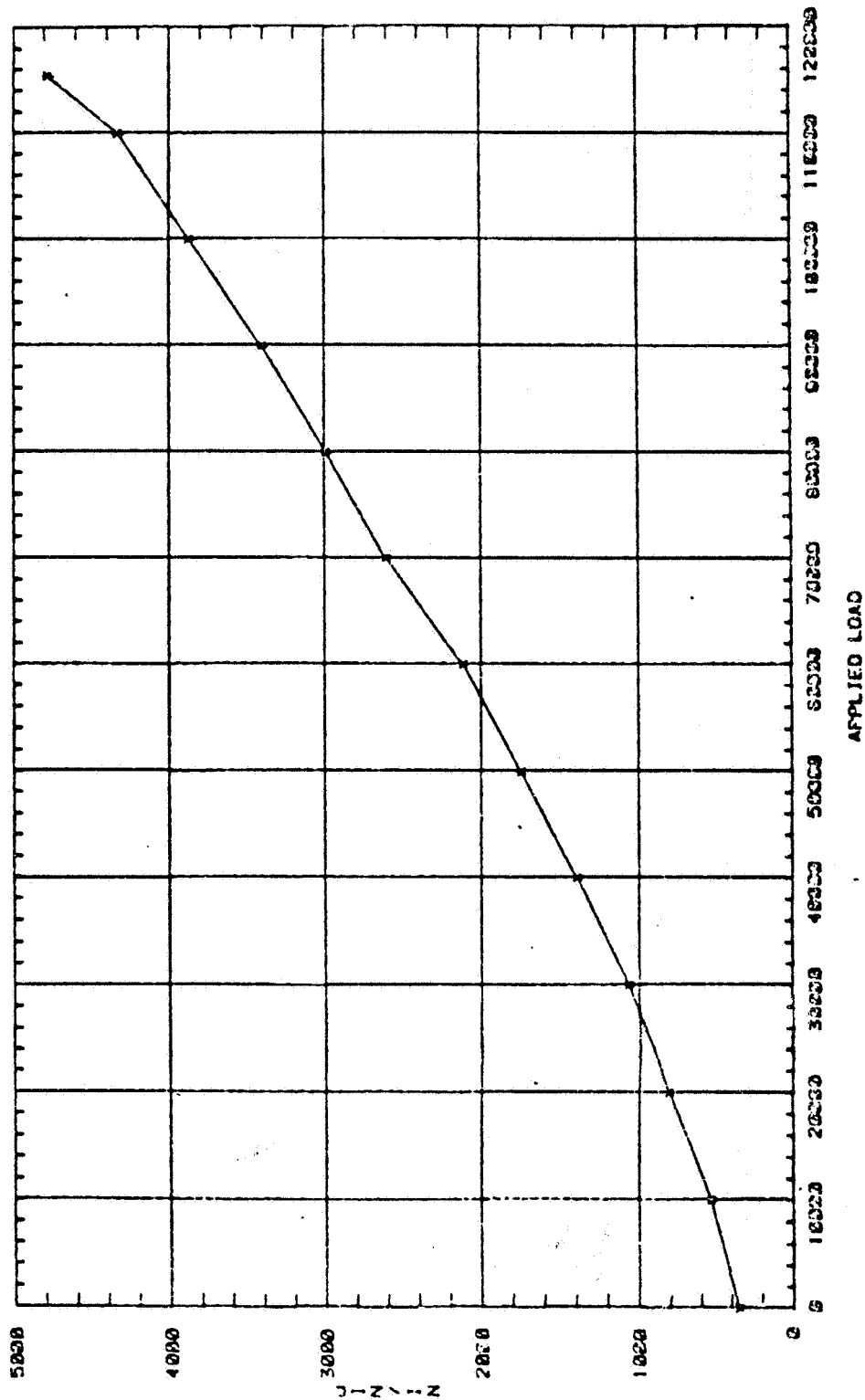
DATE: 18-JUL-84
LRI VS APPLIED LOAD



Subcomponent #2
(DWG. No. ZJ117561)

CRITICAL JOINT TEST (BLOC 3)
STRESS SURVEY & LOAD TO FAILURE

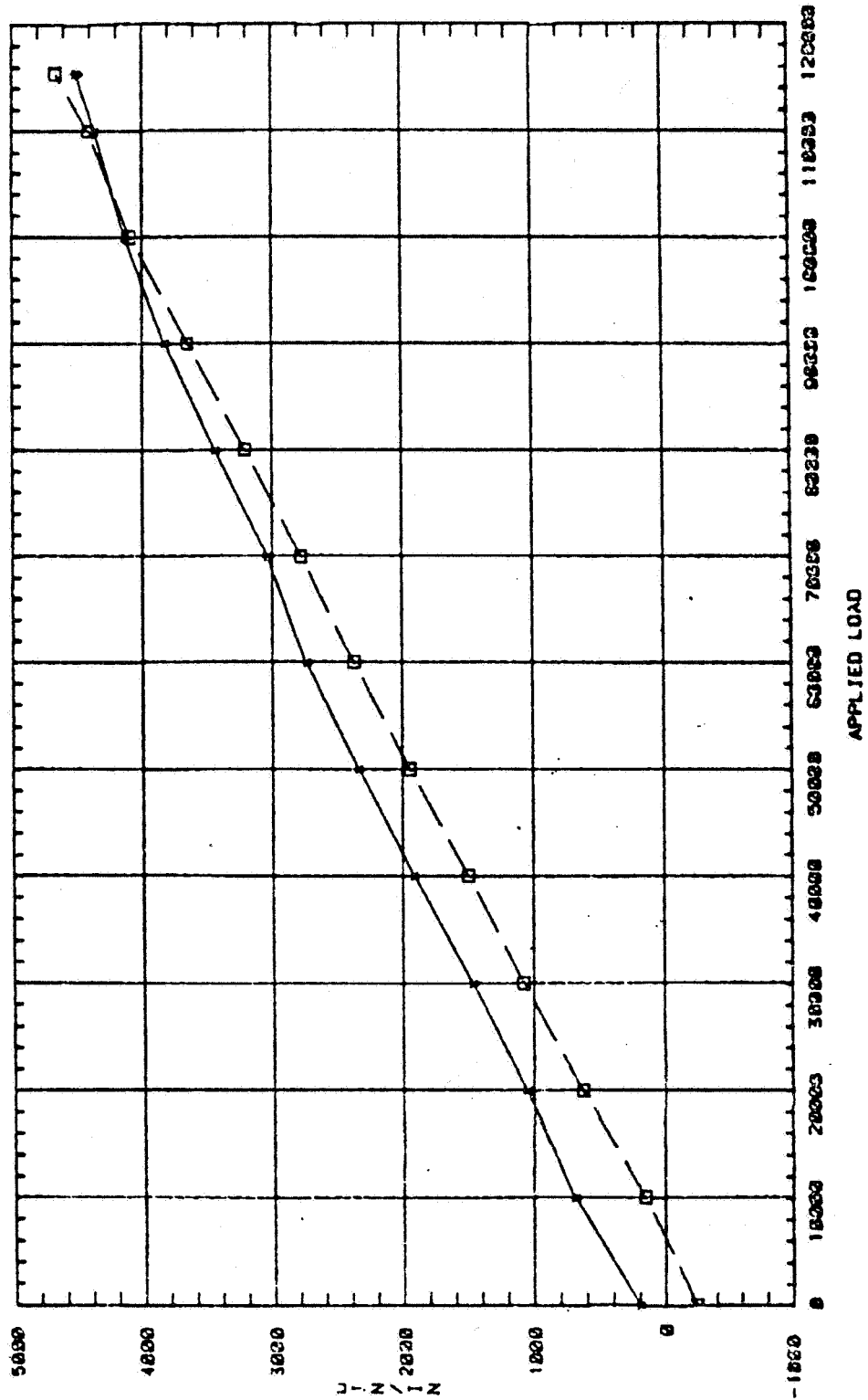
DATE: 10-JUL-84
LB1 vs APPLIED LOAD



Subcomponent #2
(DWG. No. ZJ117561)

CRITICAL JOINT TEST (BLOC 3)
STRESS SURVEY & LOAD TO FAILURE

DATE: 10-JUL-84
SG1 (S) SG2 (D) vs APPLIED LOAD

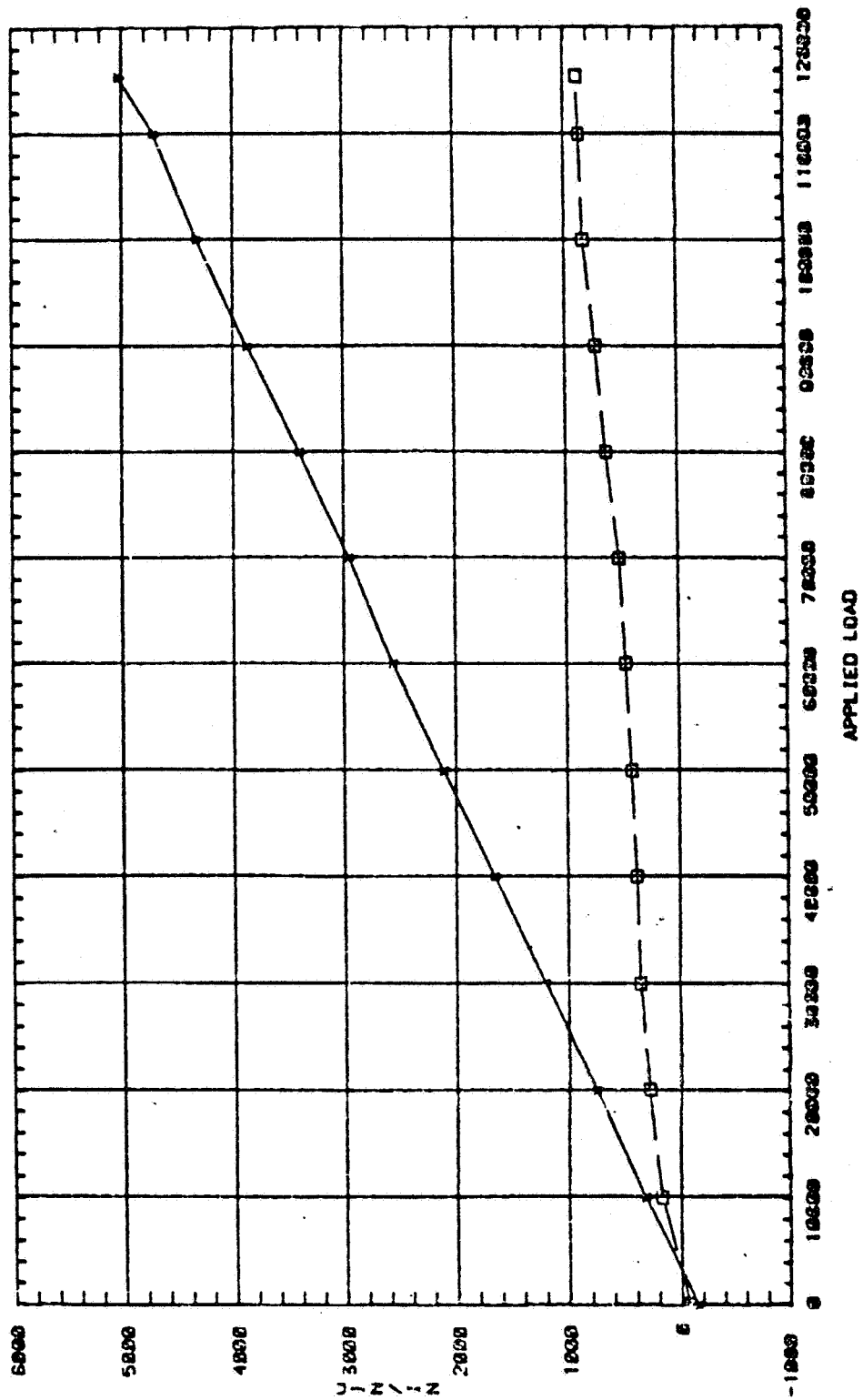


ORIGINAL PAGE IS
OF POOR QUALITY

Subcomponent #2
(DWG. No. ZJ117561)

CRITICAL JOINT TEST (BLDG 3)
STRESS SURVEY & LOAD TO FAILURE

DATE: 18-JUL-84
SC3(1) SC4(1) vs APPLIED LOAD



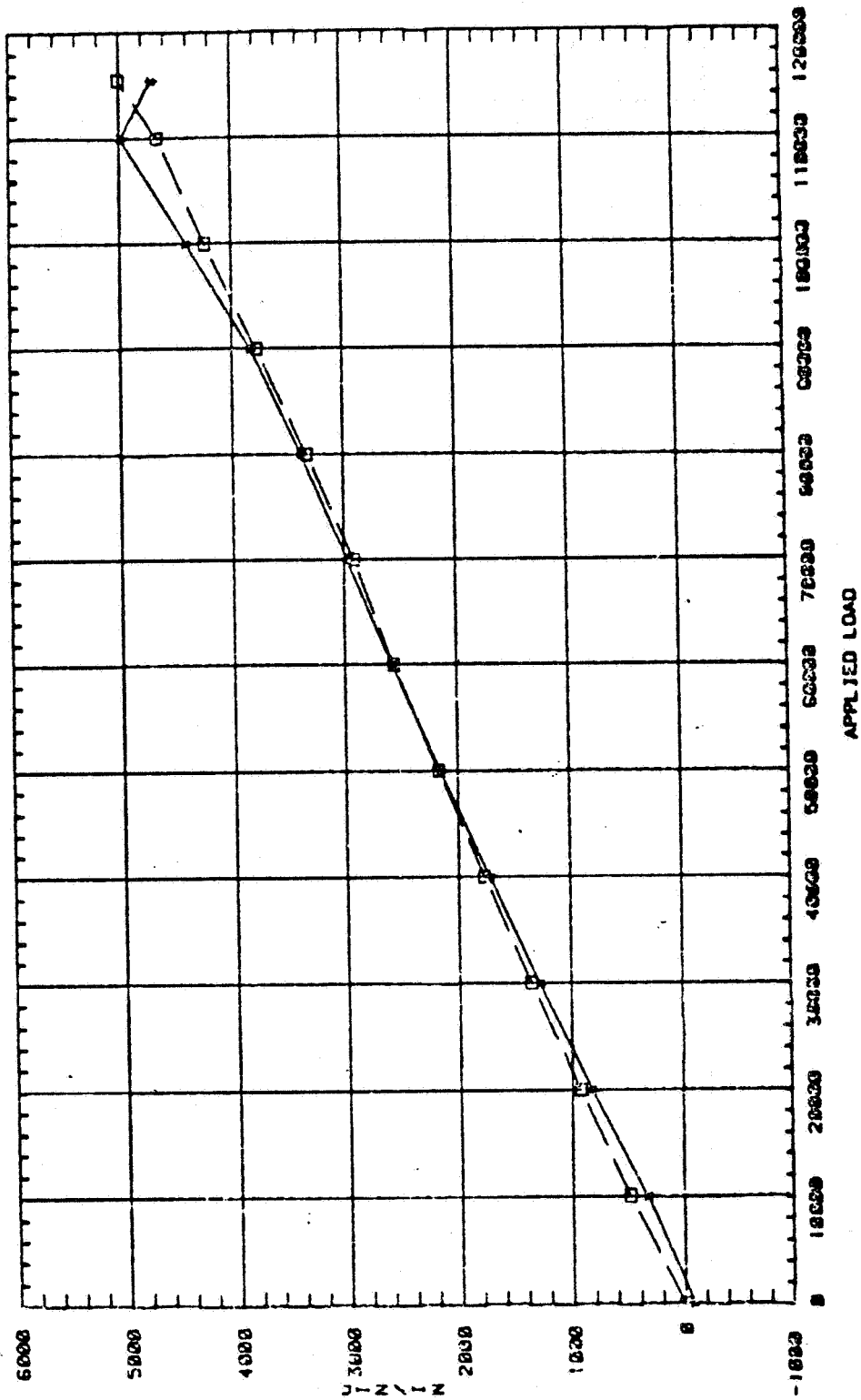
21 3045 2010000
ORIGINAL PAGE IS
OF POOR QUALITY

ORIGINAL PAGE IS
OF POOR QUALITY

Subcomponent #2
(DWG. No. ZJ117561)

CRITICAL JOINT TEST (BLOC 3)
STRESS SURVEY & LOAD TO FAILURE

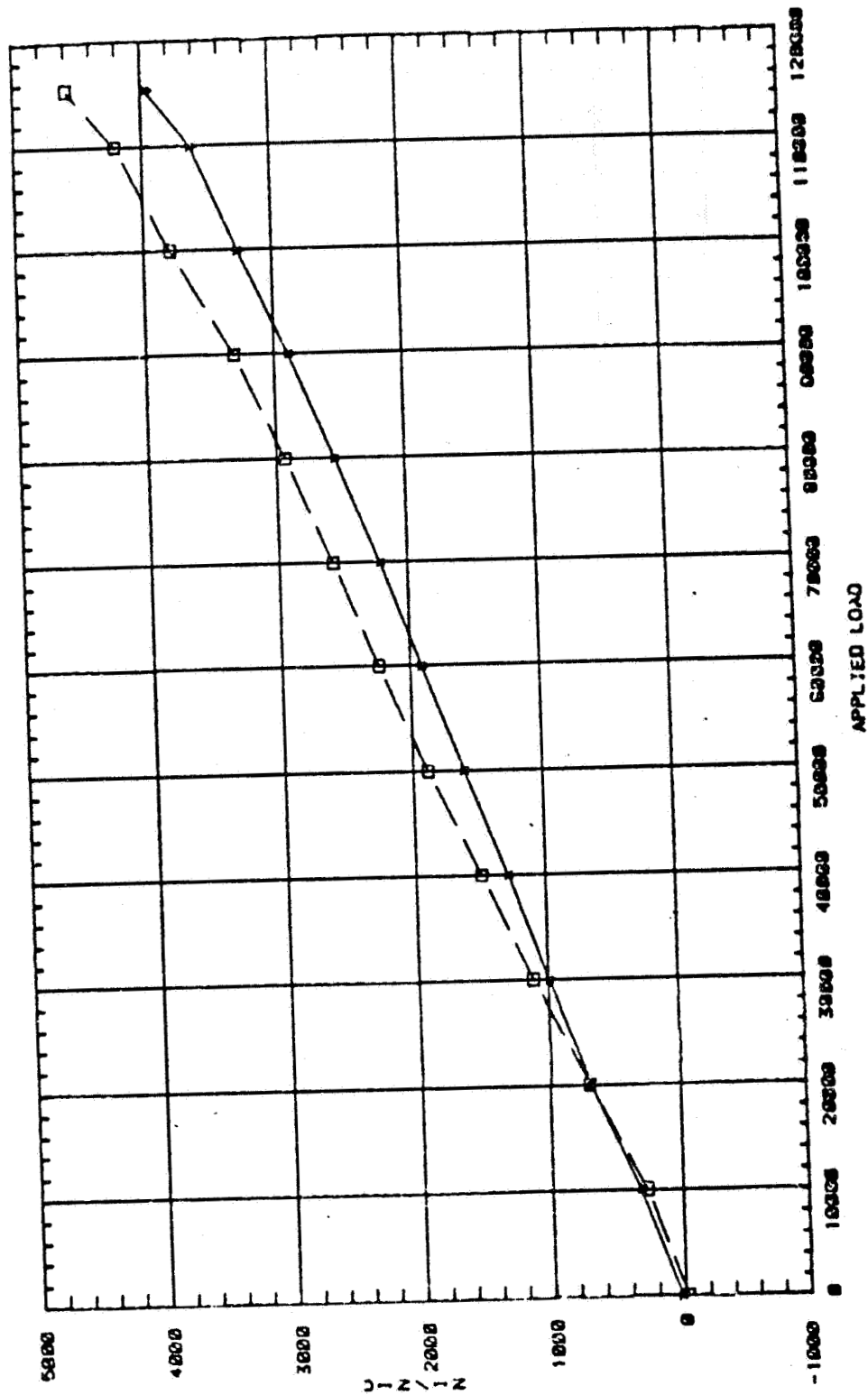
DATE: 10-JUL-84
SGS(7) SGS(□) vs APPLIED LOAD



ORIGINAL PAGE IS
OF POOR QUALITY

Subcomponent #2
(DWG. No. ZJ117561)

CRITICAL JOINT TEST (BLOC 31)
STRESS SURVEY & LOAD TO FAILURE
DATE: 10-JUL-84
SC7(†) SC8(□) VS APPLIED LOAD

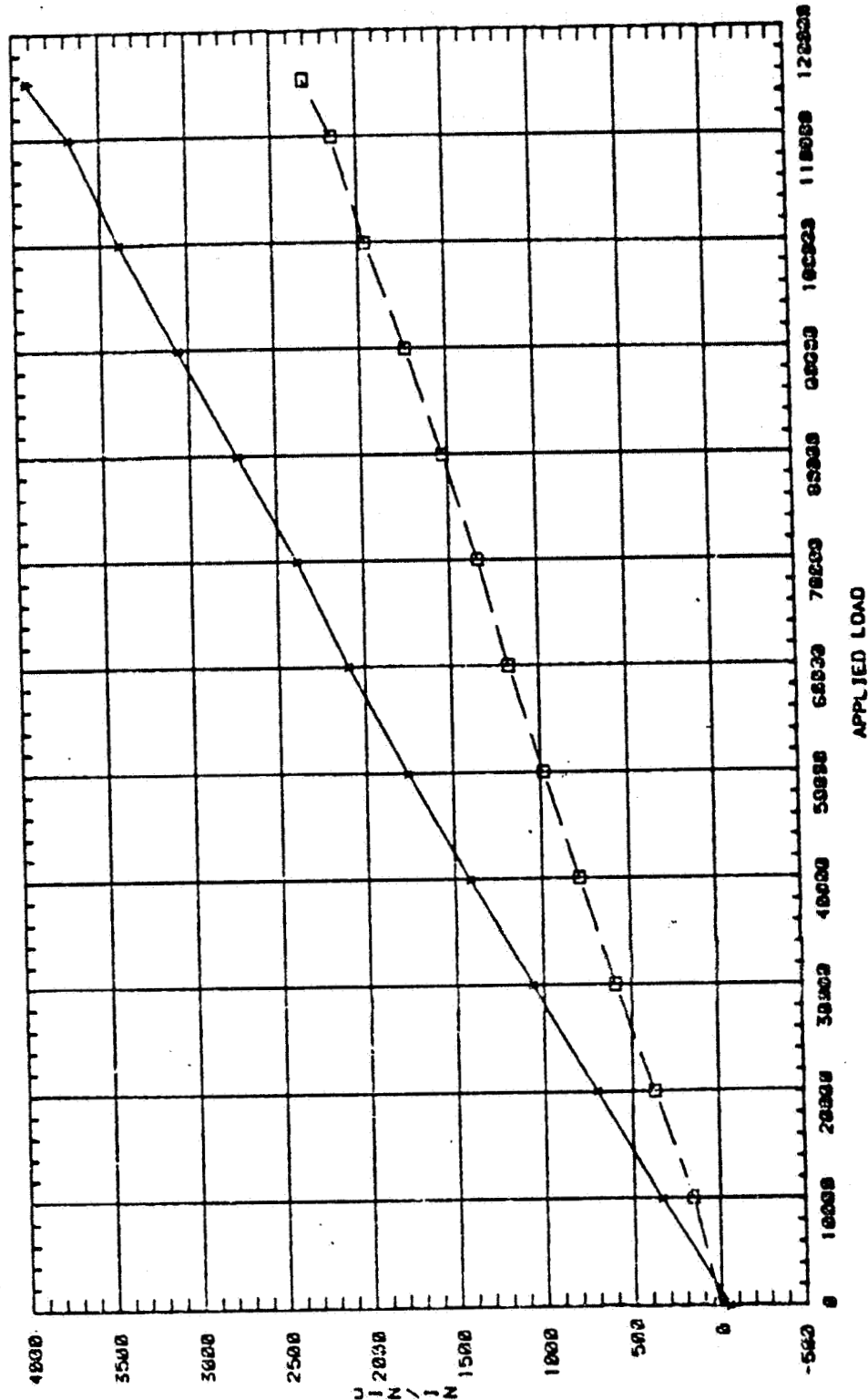


ORIGINAL PAGE IS
OF POOR QUALITY

Subcomponent #2
(DWG. NO. ZJ117561)

CRITICAL JOINT TEST (BLDG 3)
STRESS SURVEY & LOAD TO FAILURE

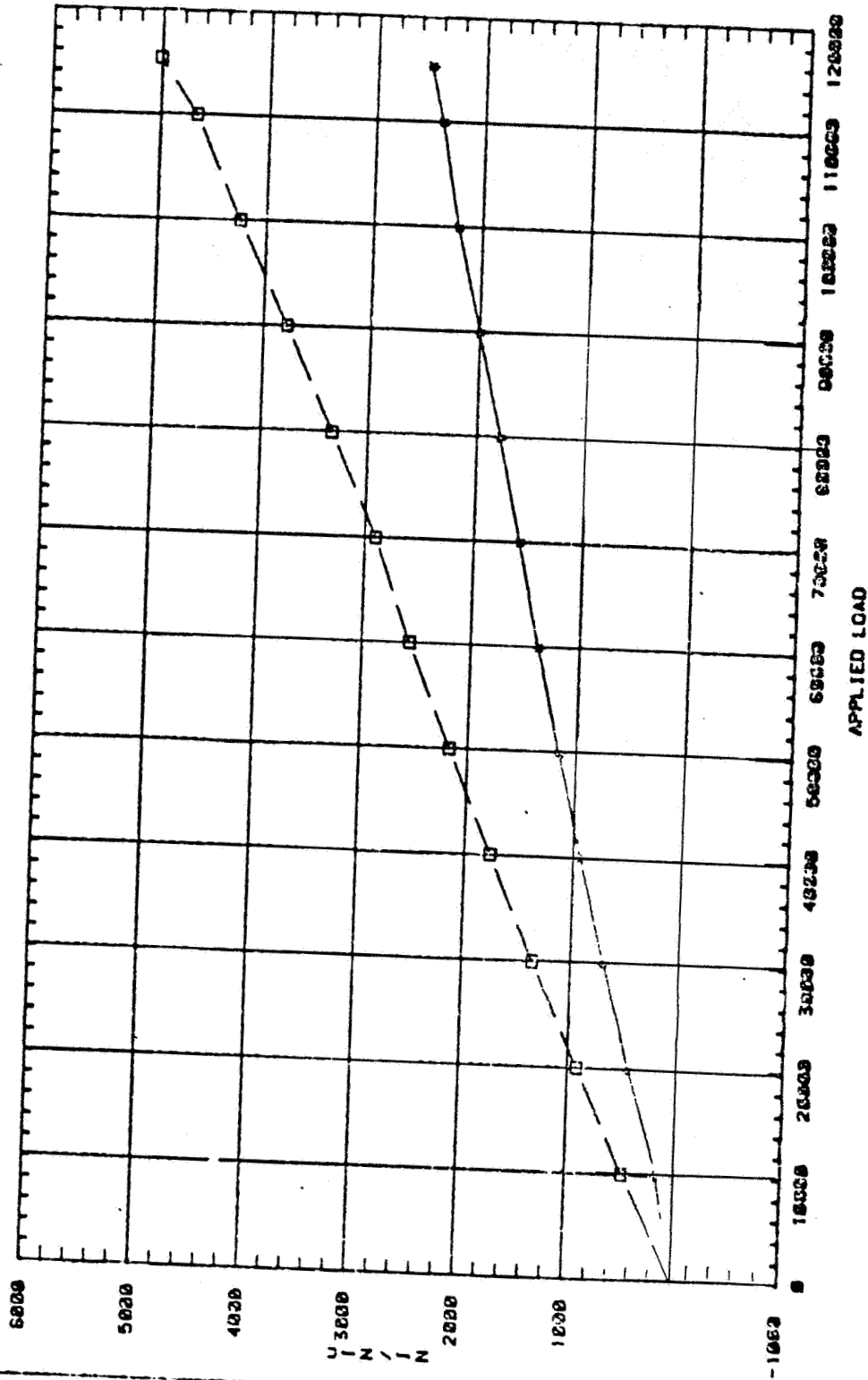
DATE: 18-JUL-84
SC01(1) SC18(1) vs APPLIED LOAD



ORIGINAL PAGE IS
OF POOR QUALITY

Subcomponent #2
(DWG. No. ZJ117561)

CRITICAL JOINT TEST (BLDG 3)
STRESS SURVEY & LOAD TO FAILURE
DATE, 18-JUL-84
SC111(7) SC121(1) vs APPLIED LOAD



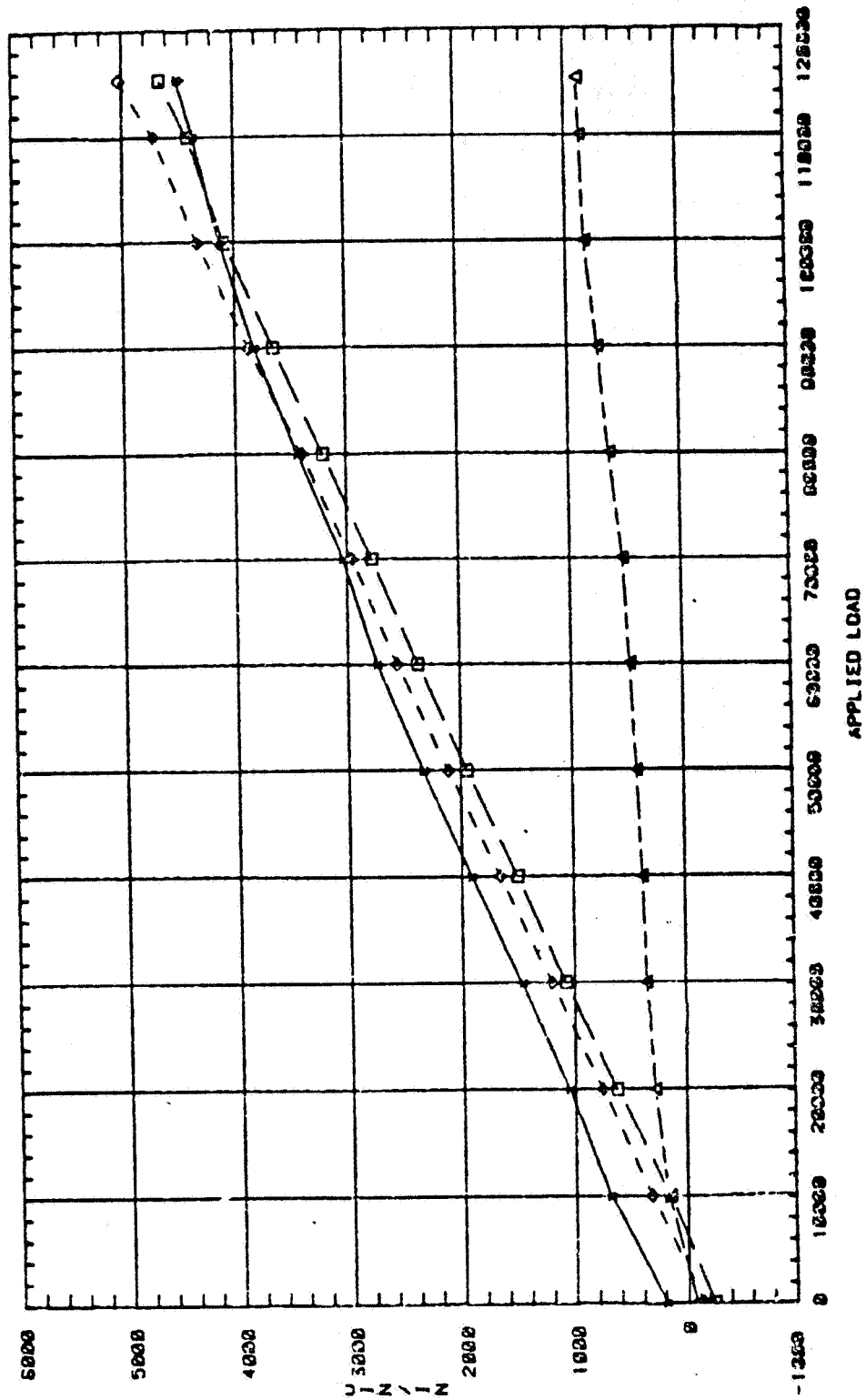
ORIGINAL PAGE IS
OF POOR QUALITY

ORIGINAL PAGE IS
OF POOR QUALITY

Subcomponent #1
(DWG. No. ZJ117561)

CRITICAL JOINT TEST (BLOC 3)
STRESS SURVEY & LOAD TO FAILURE

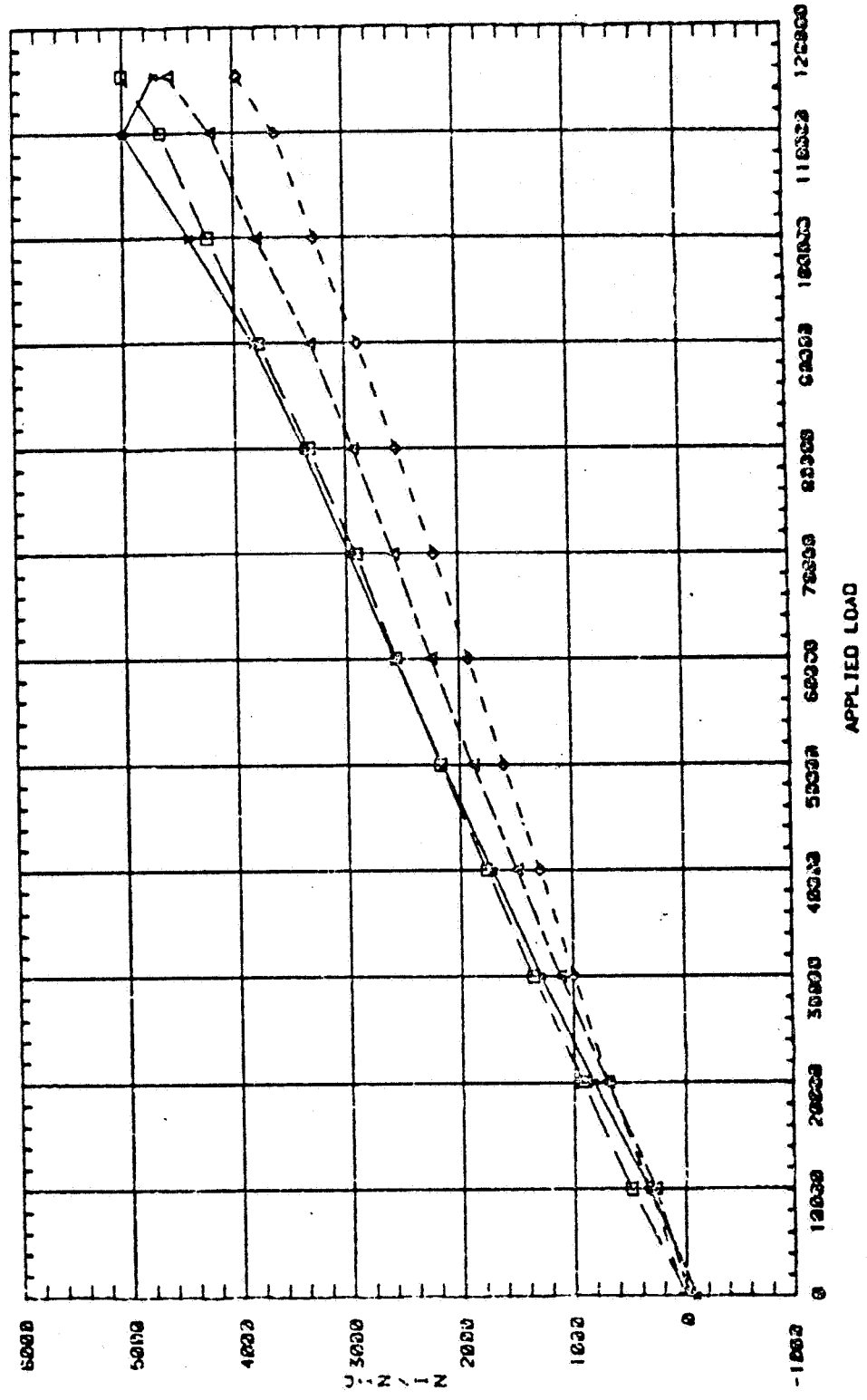
DATE: 10-JUL-84
SG1(*) SG2(O) SG3(O) SG4(O) vs APPLIED LOAD



Subcomponent #1
(DWG. No. ZJ117561)

CRITICAL JOINT TEST (RLDC 3)
STRESS SURVEY & LOAD TO FAILURE

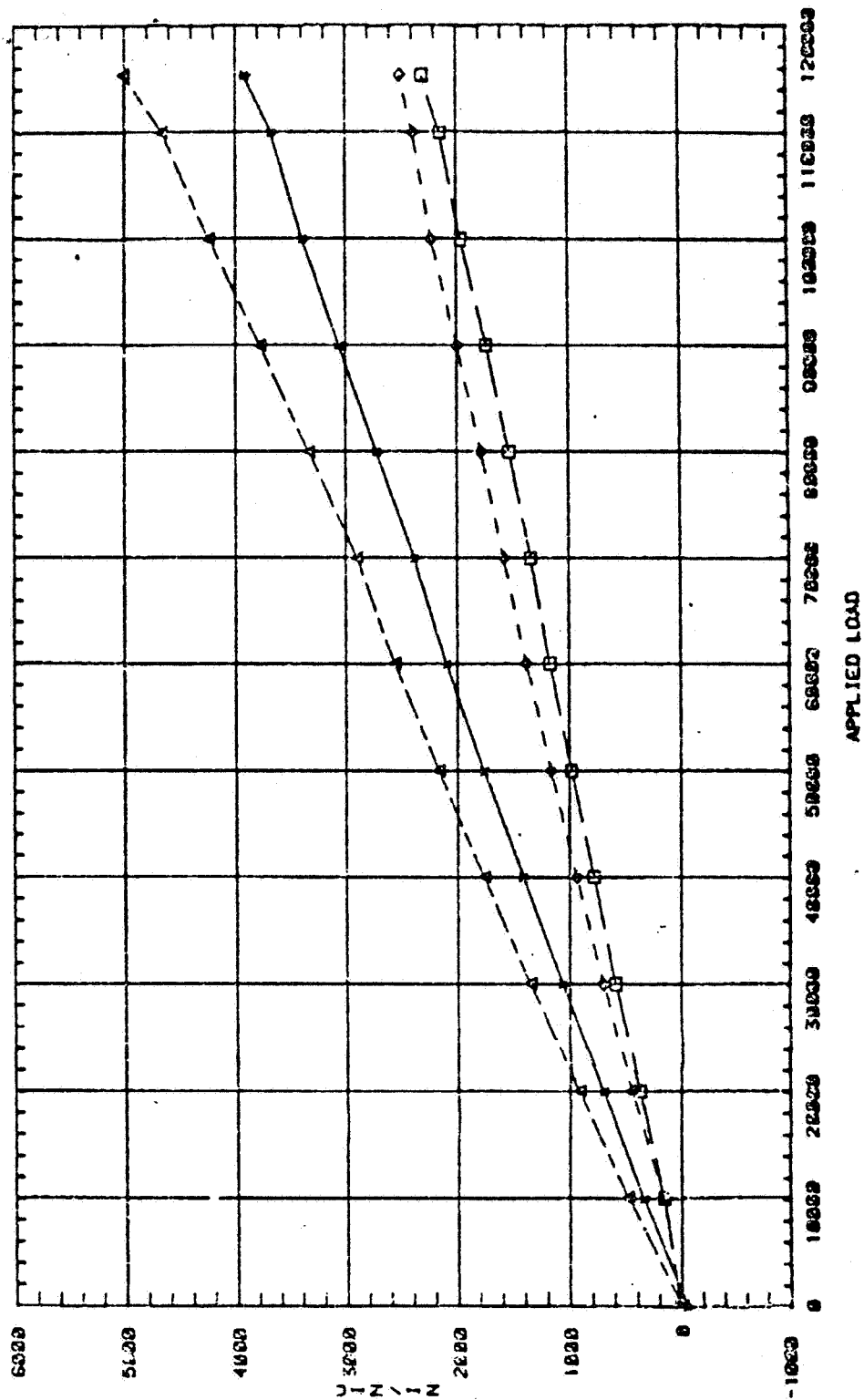
DATE: 10-JUL-84
SC5(+) SC6(□) SC7(◇) SC8(Δ) vs APPLIED LOAD



Subcomponent #2
(DWG. No. ZJ117561)

CRITICAL JOINT TEST (BLOC 3)
STRESS SURVEY & LOAD TO FAILURE

DATE: 18-JUL-84
SC0(2) SC10(D) SC11(O) SC12(Δ) vs APPLIED LOAD



APPENDIX C

Technology Demonstration Test Data

Static Test #1 (Limit Load) - Page C2

Static Test #1 (To Failure) - Page C18

Static Test #2 (To Failure) - Page C34

Technology Demonstration Article

Limit Load Test Data (Test #1) (with Analysis results)

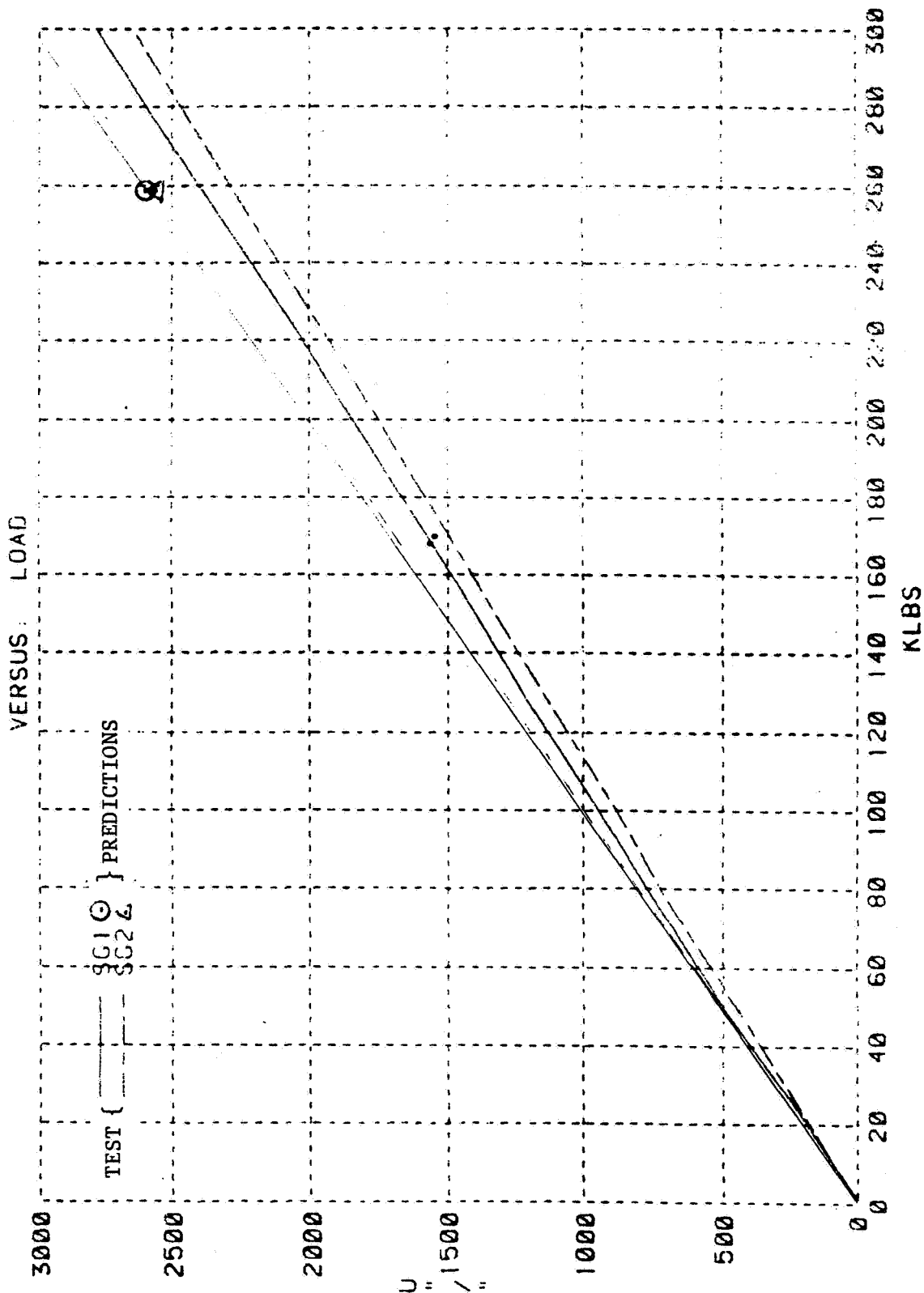
- SG # - Strain Gage Number
- LR # - Load Restraint Number
- DF1 - Machine Head Displacement
- ⊙ - Analysis Prediction (Linear Analysis)
- △ - Analysis Prediction (Linear Analysis)

25 Strain Gages

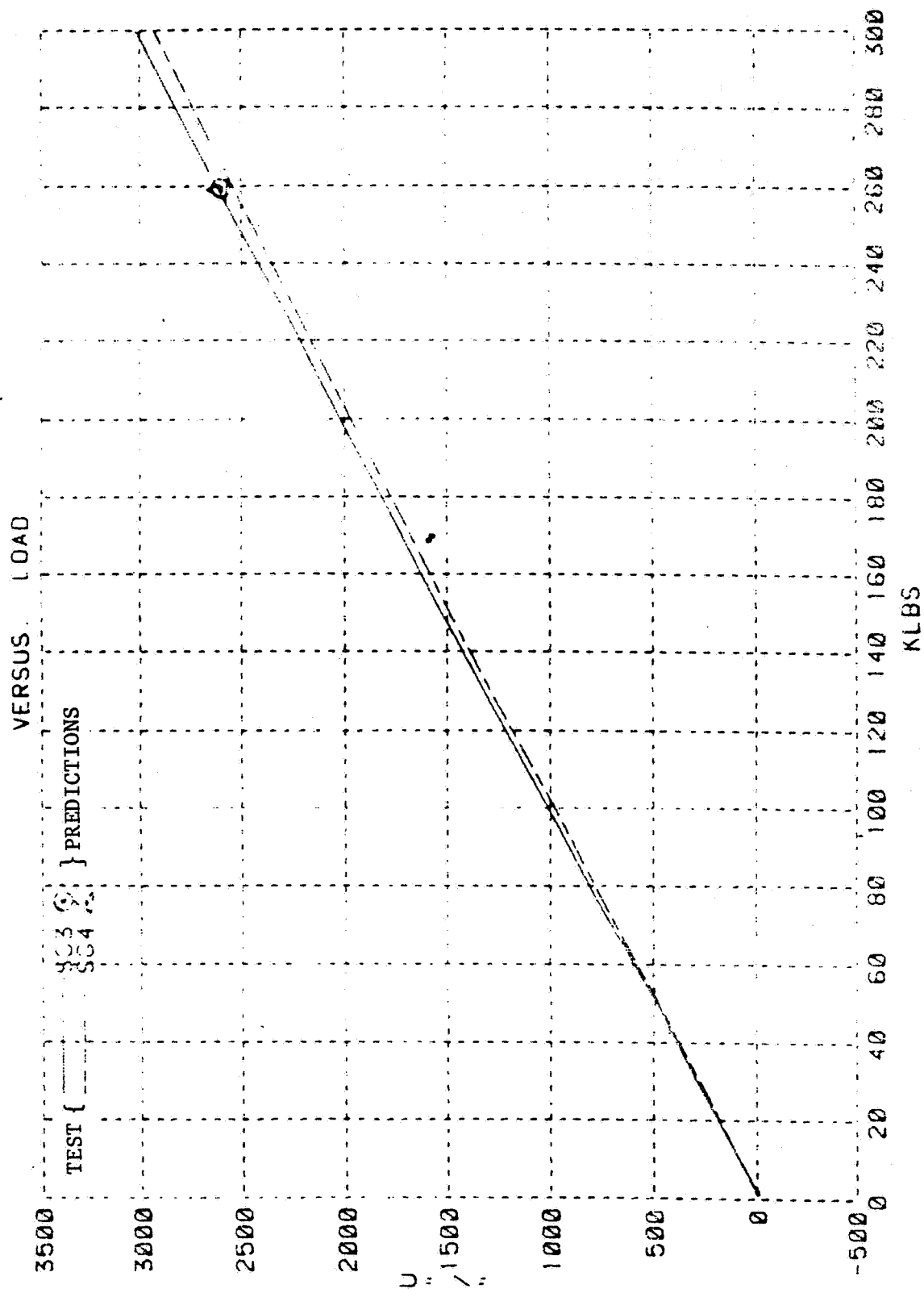
2 Load Restraints

ORIGINAL PAGE IS
OF POOR QUALITY

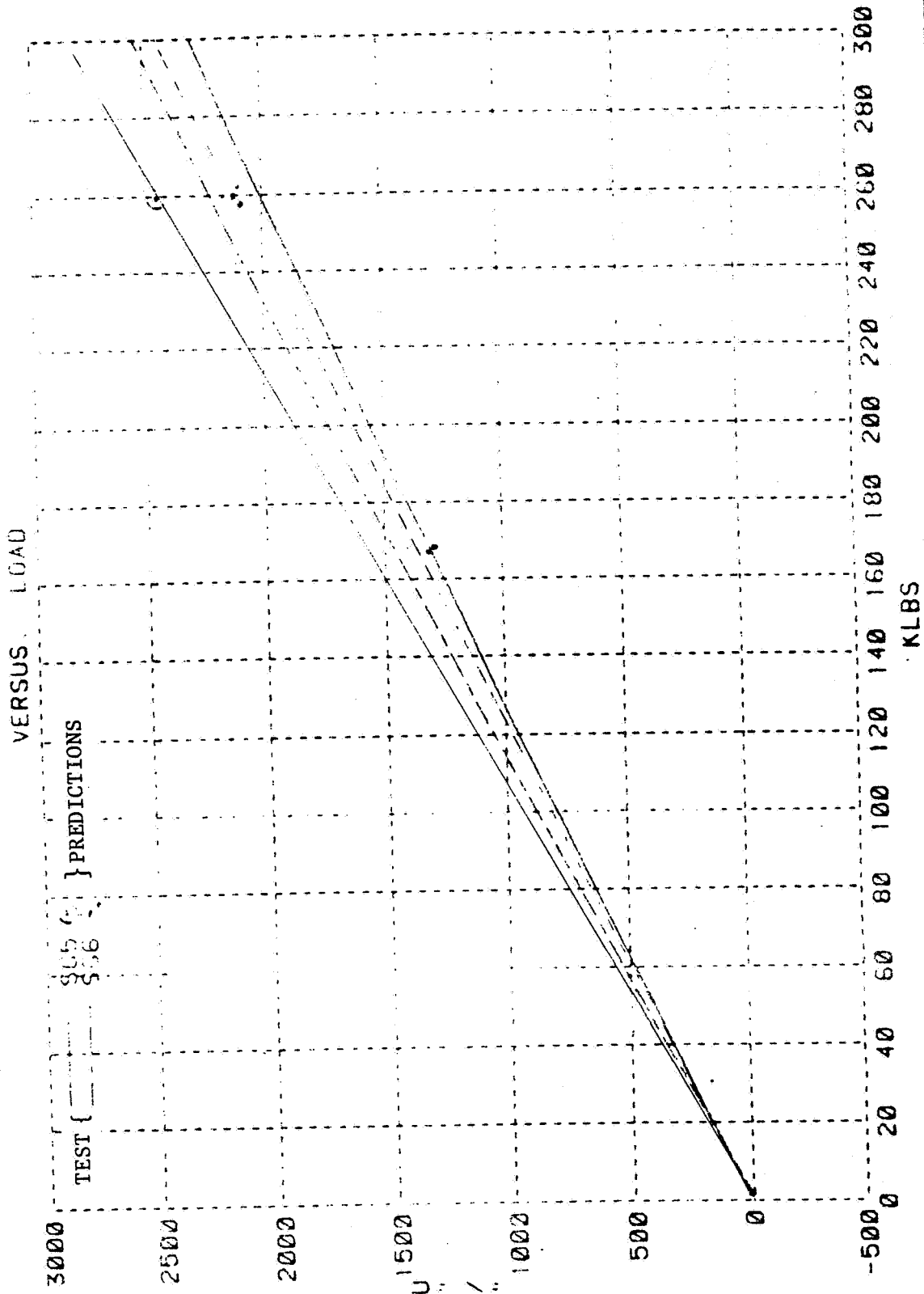
COMPOSITE CRITICAL JOINT DEMONSTRATION TEST
AUG 9, 1984 - BLOC 41 - LIMIT LOAD SURVEY



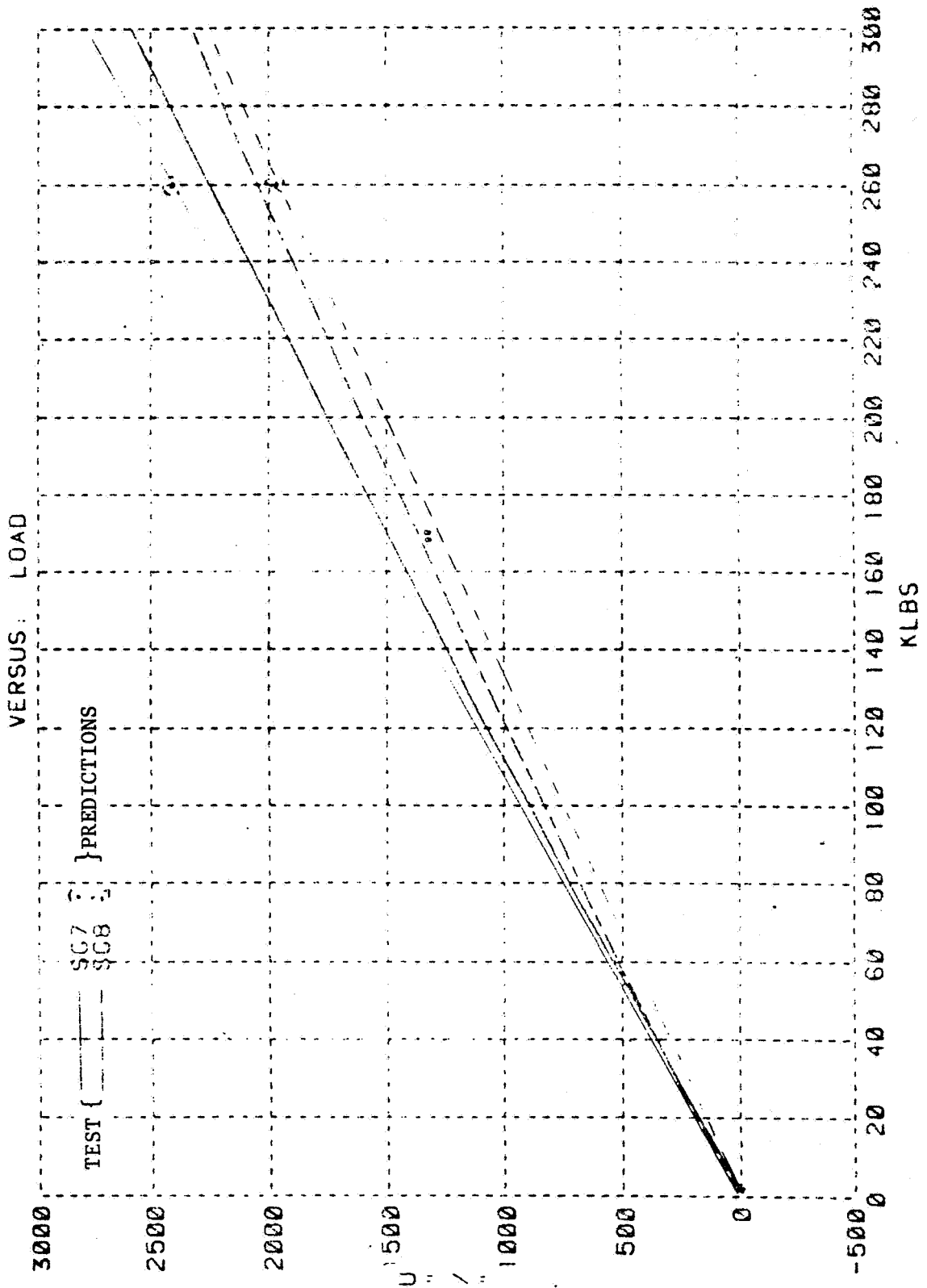
COMPOSITE CRITICAL JOINT DEMONSTRATION TEST
AUG 9, 1984 - BLDG 41 - LIM11 LOAD SURVEY



COMPOSITE CRITICAL JOINT DEMONSTRATION TEST
AUG 9, 1984 - BLDG 41 - LIMIT LOAD SURVEY

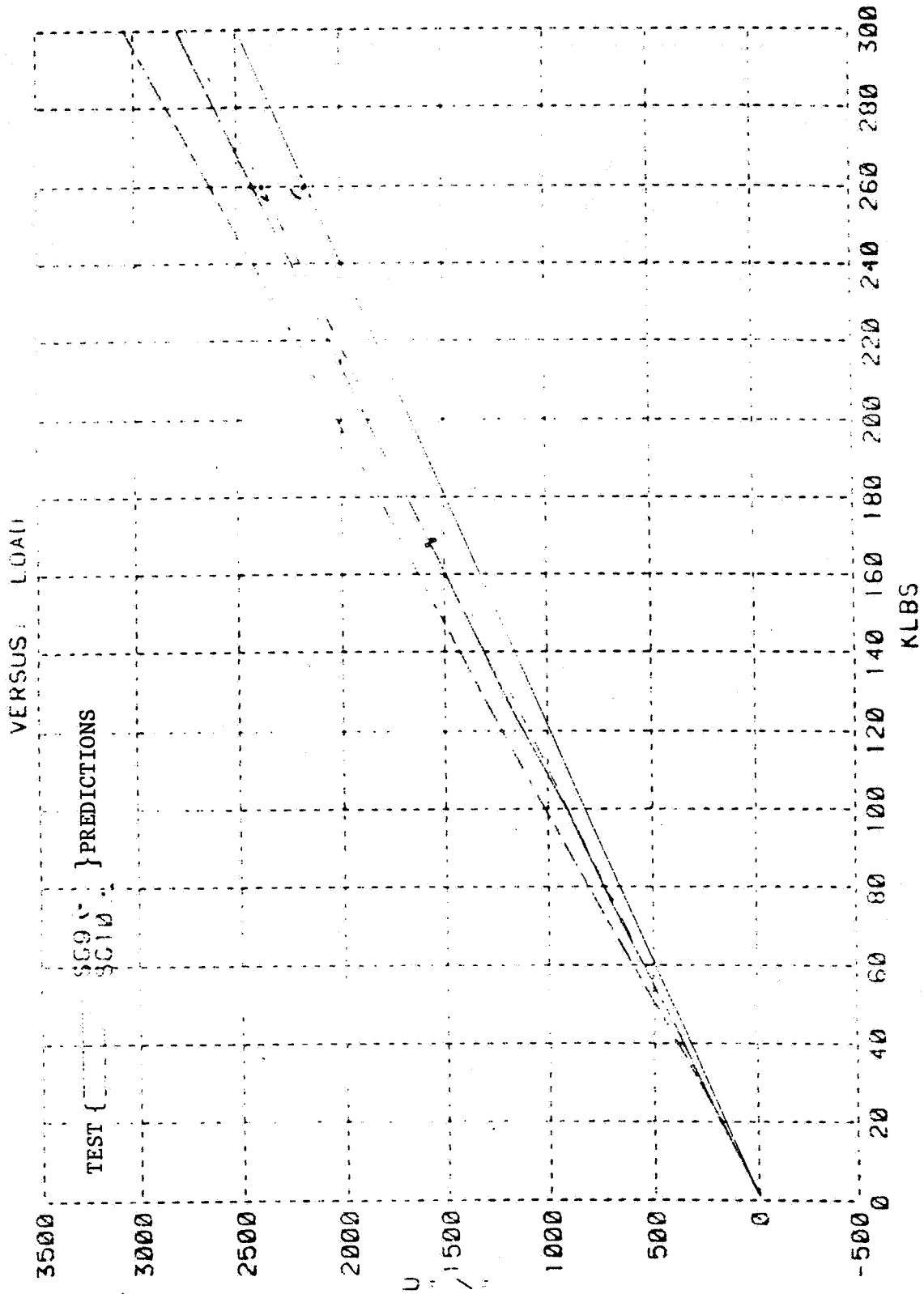


COMPOSITE CRITICAL JOINT DEMONSTRATION TEST
AUG 9, 1984 - BLDG 41 - LIMIT LOAD SURVEY

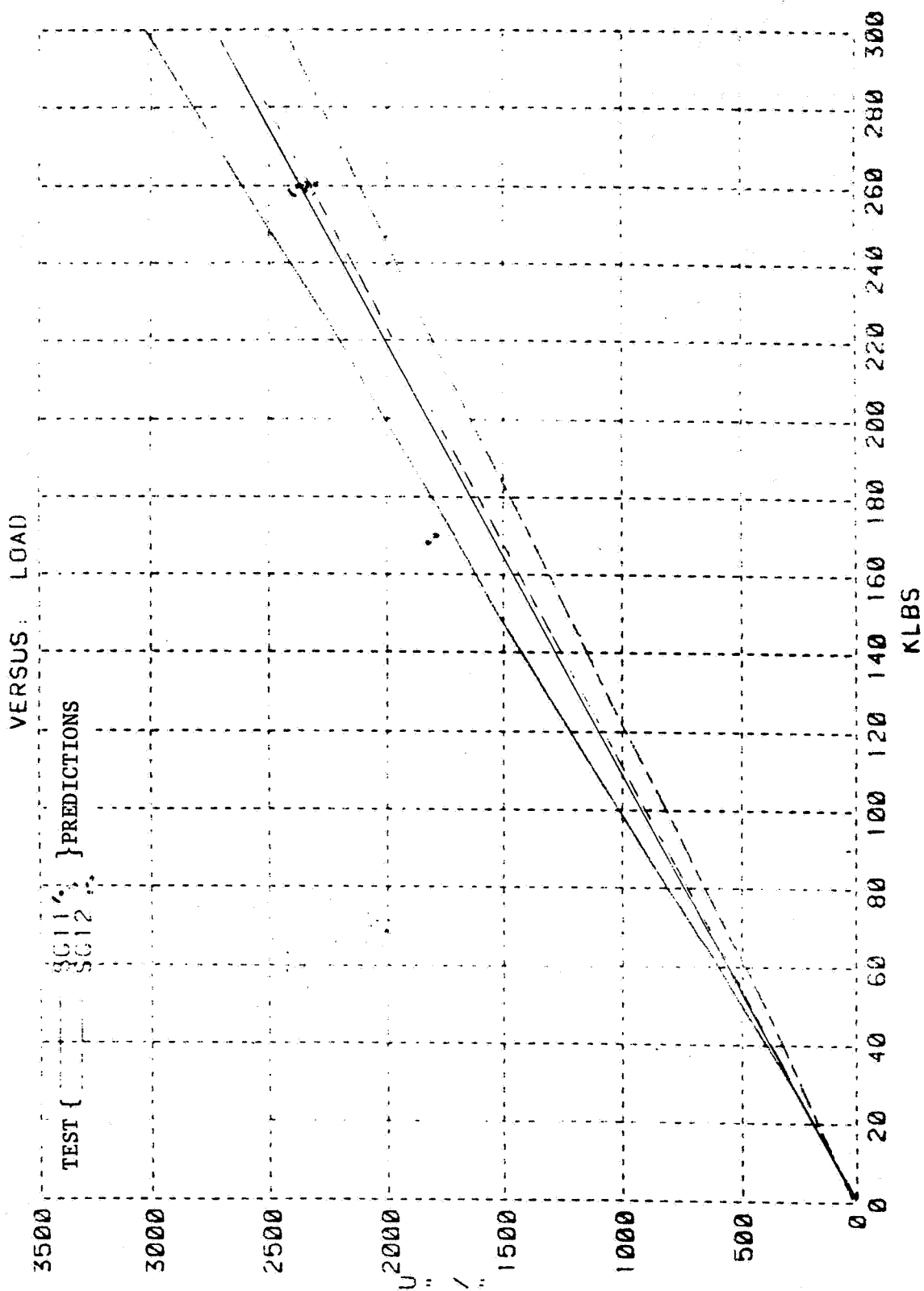


SI 3087 330
YTLAUG 2004

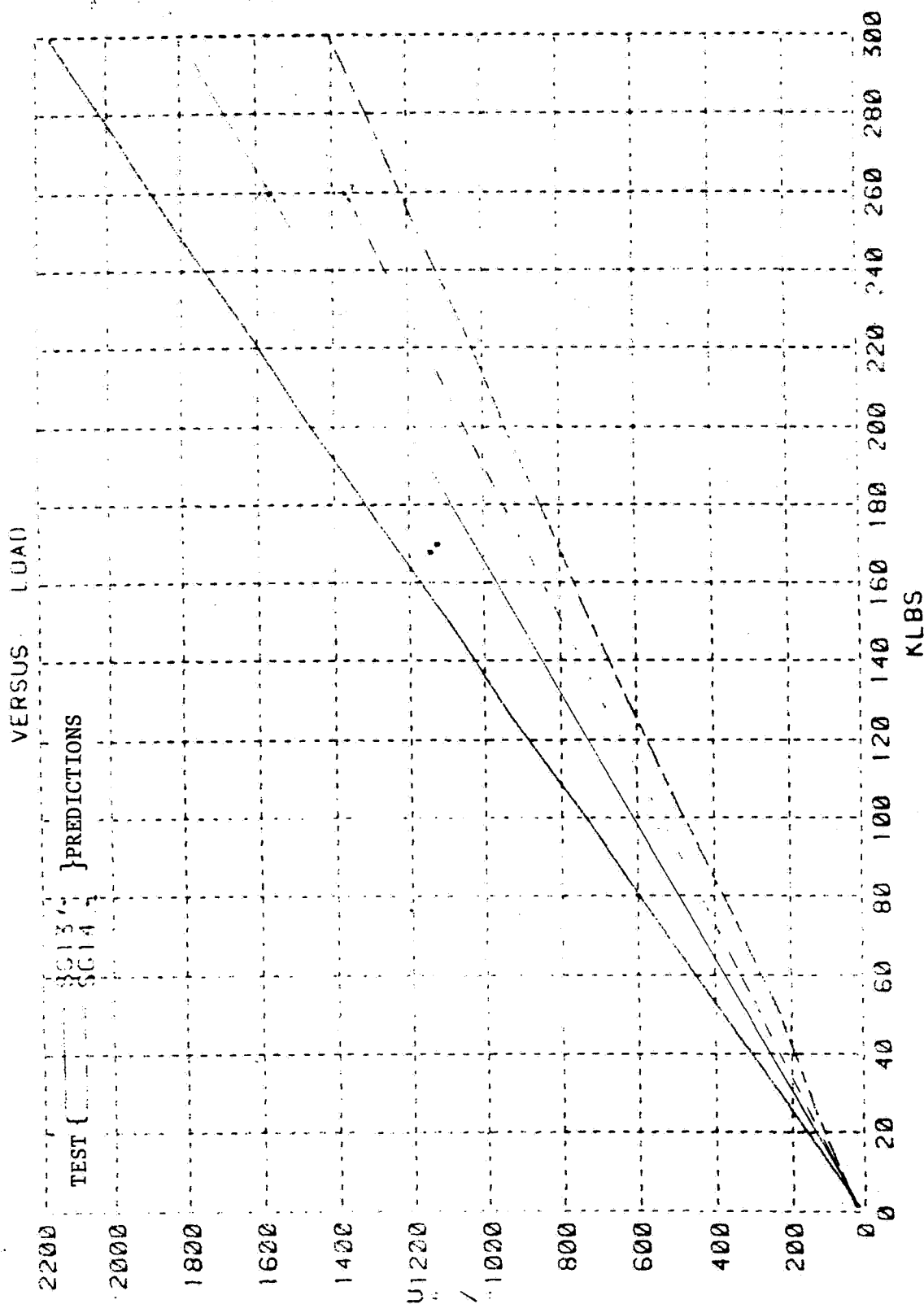
COMPOSITE CRITICAL JOINT DEMONSTRATION TEST
AUG 9 1984 - BLDG 41 - LIMIT LOAD SURVEY



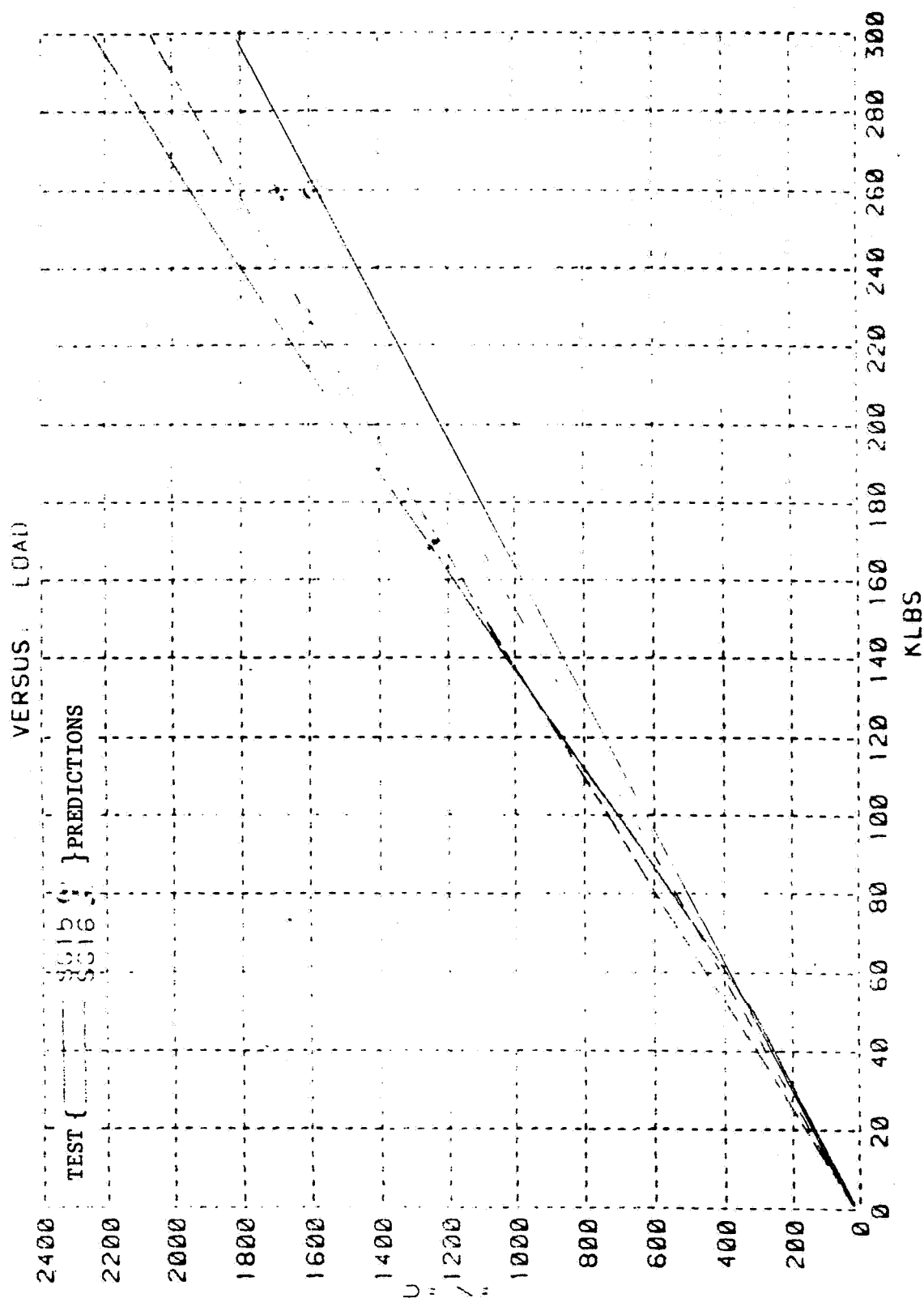
COMPOSITE CRITICAL JOINT DEMONSTRATION TEST
AUG 9, 1984 - BLOC 41 - LIMIT LOAD SURVEY



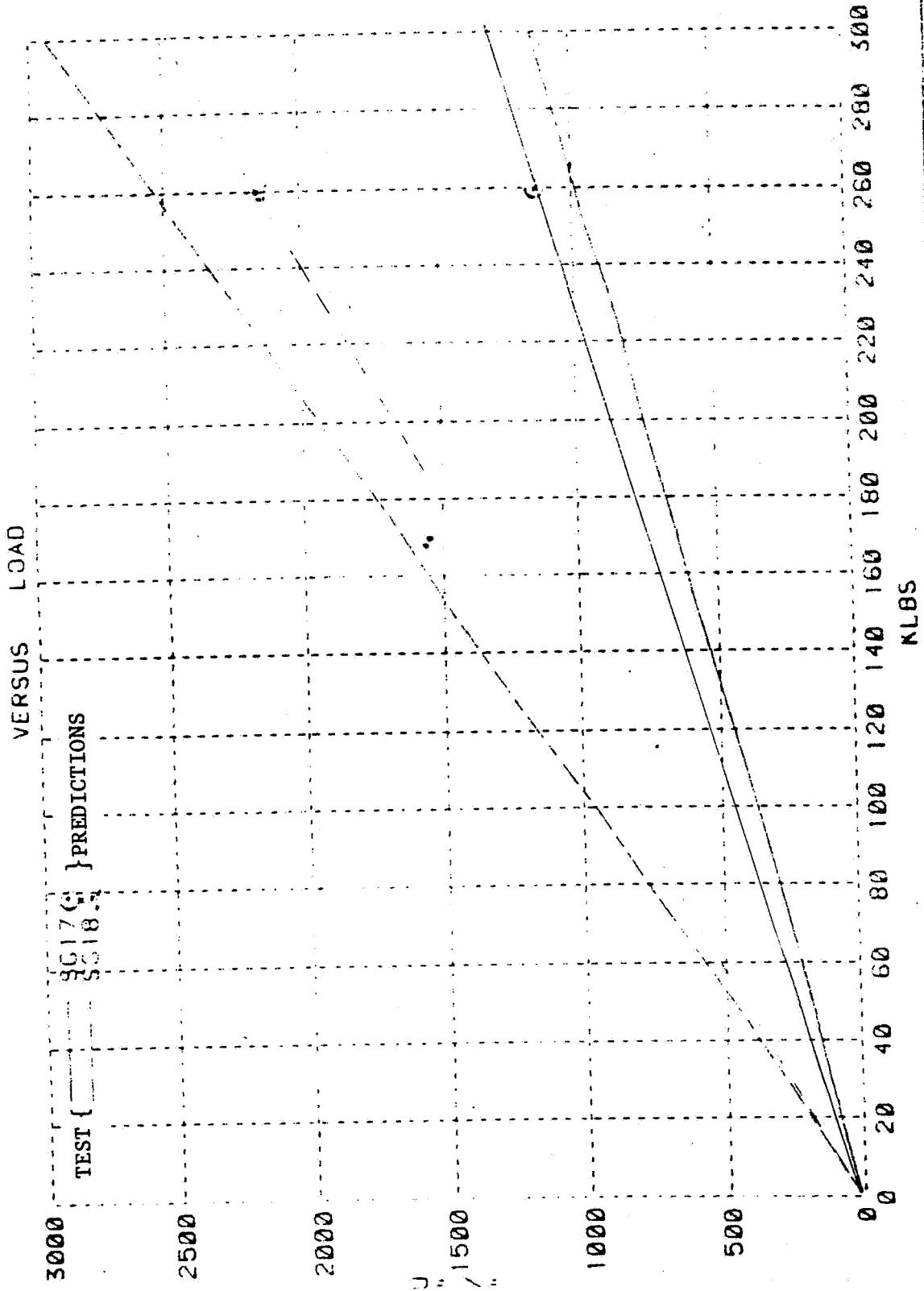
COMPOSITE CRITICAL JOINT DEMONSTRATION TEST
AUG 9, 1984 - BLDG 41 - LIMIT LOAD SURVEY



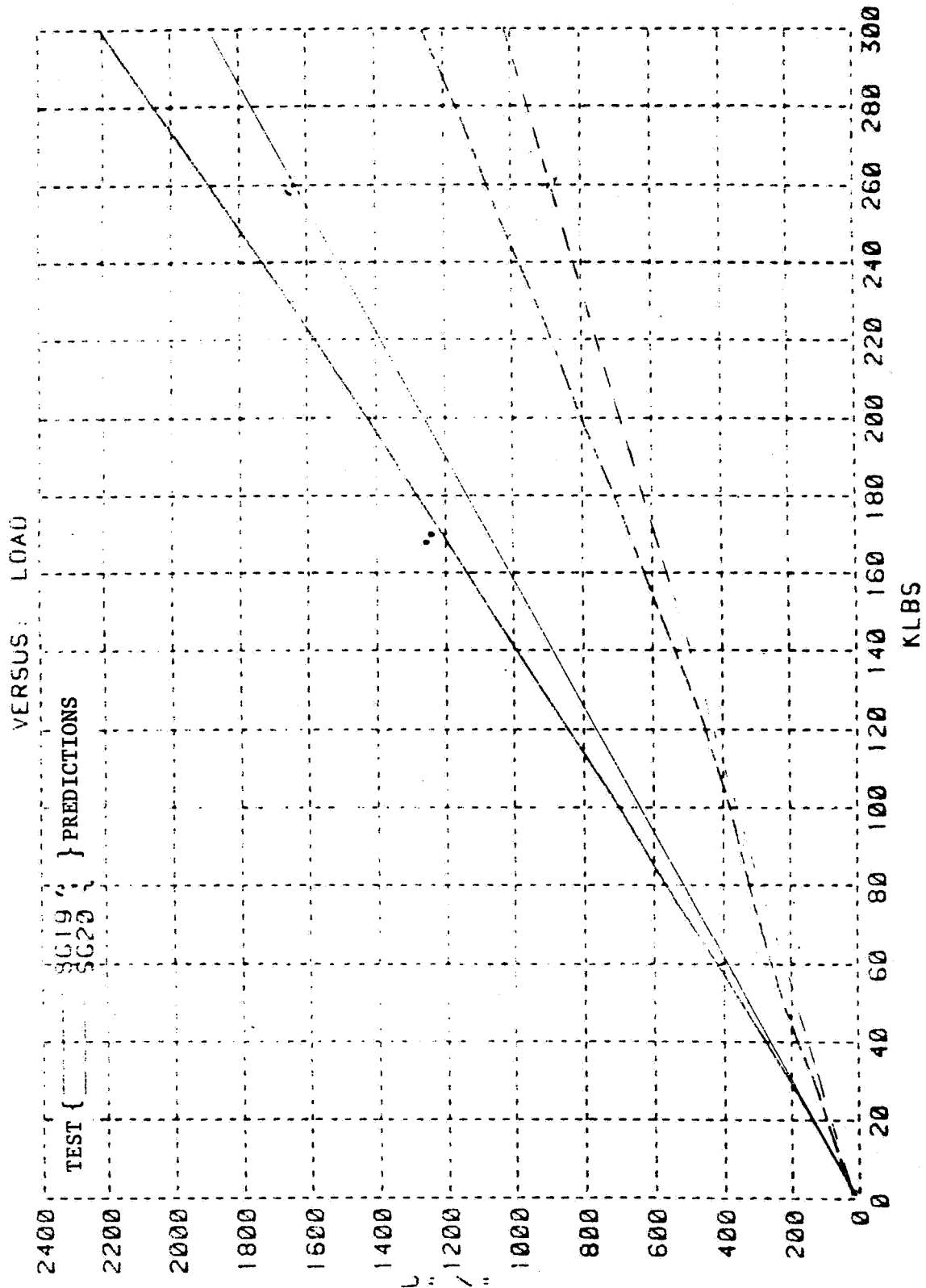
COMPOSITE CRITICAL JOINT DEMONSTRATION TEST
AUG 9, 1984 - BLDG 41 - LIMIT LOAD SURVEY



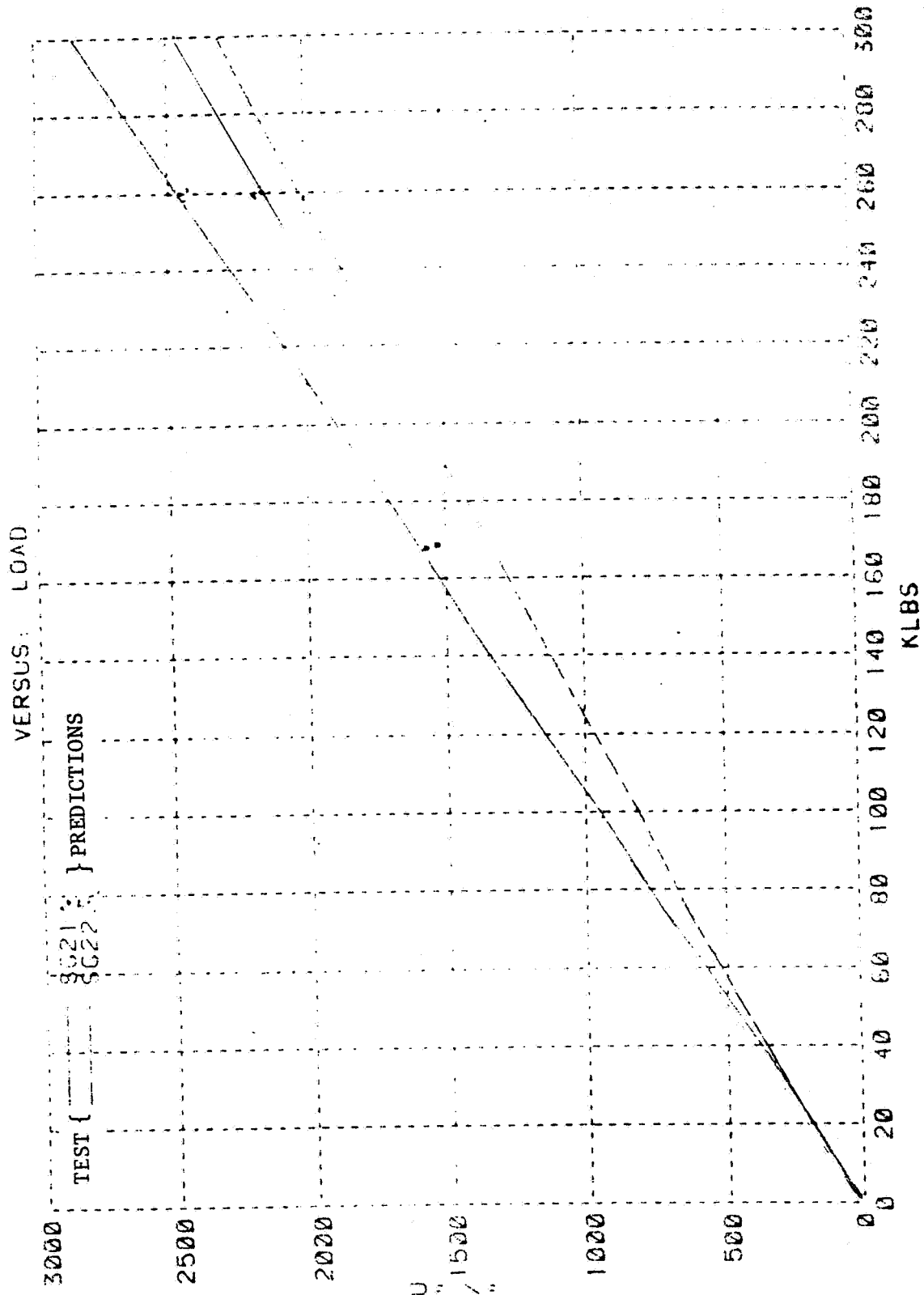
COMPOSITE CRITICAL JOINT DEMONSTRATION TEST
AUG 9, 1984 - BLDC 41 - LIMIT LOAD SURVEY



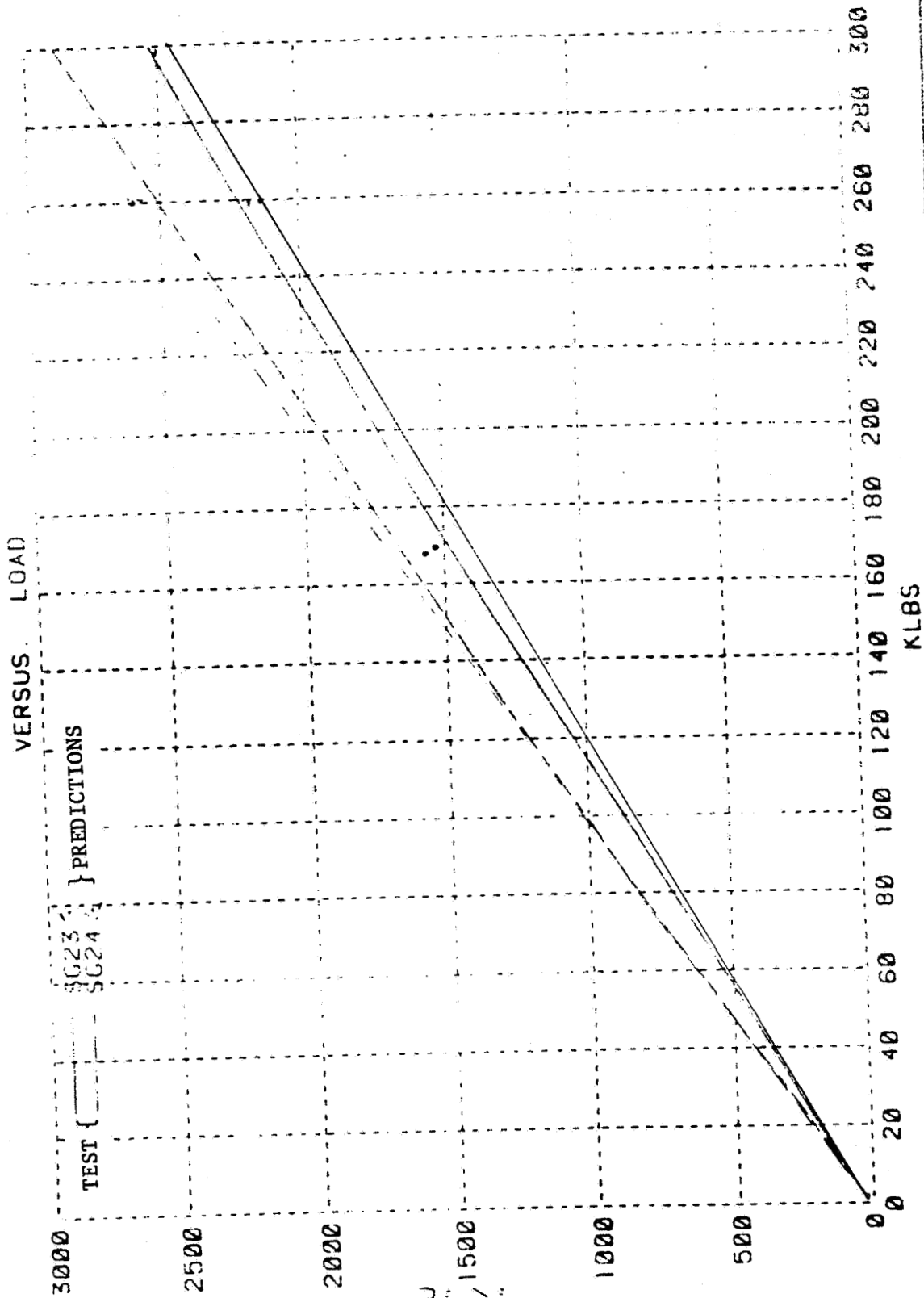
COMPOSITE CRITICAL JOINT DEMONSTRATION TEST
AUG 9, 1984 - BLDG 41 - LIMIT LOAD SURVEY



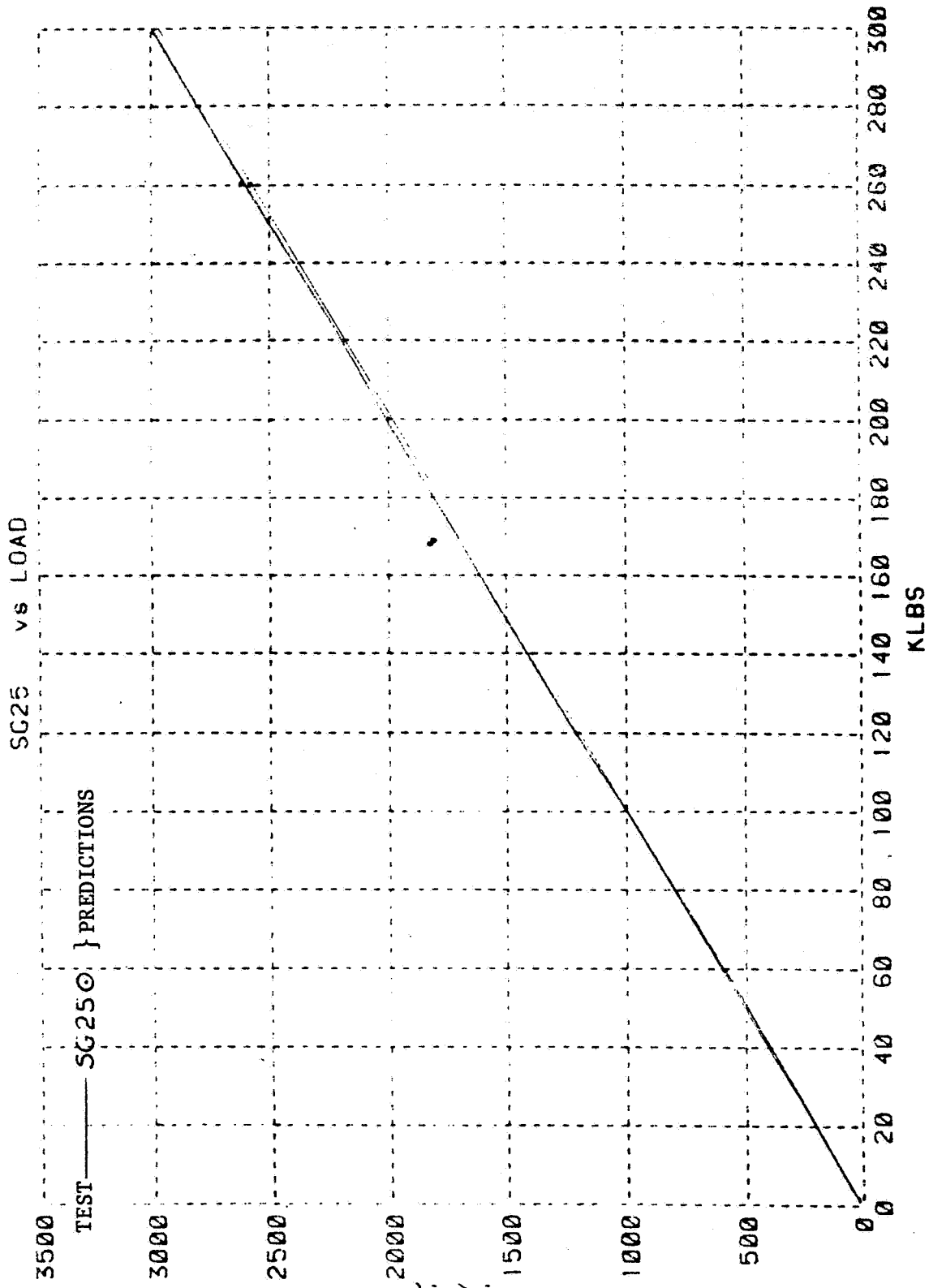
COMPOSITE CRITICAL JOINT DEMONSTRATION TEST
AUG 9, 1984 - BLDG 41 - LIMIT LOAD SURVEY



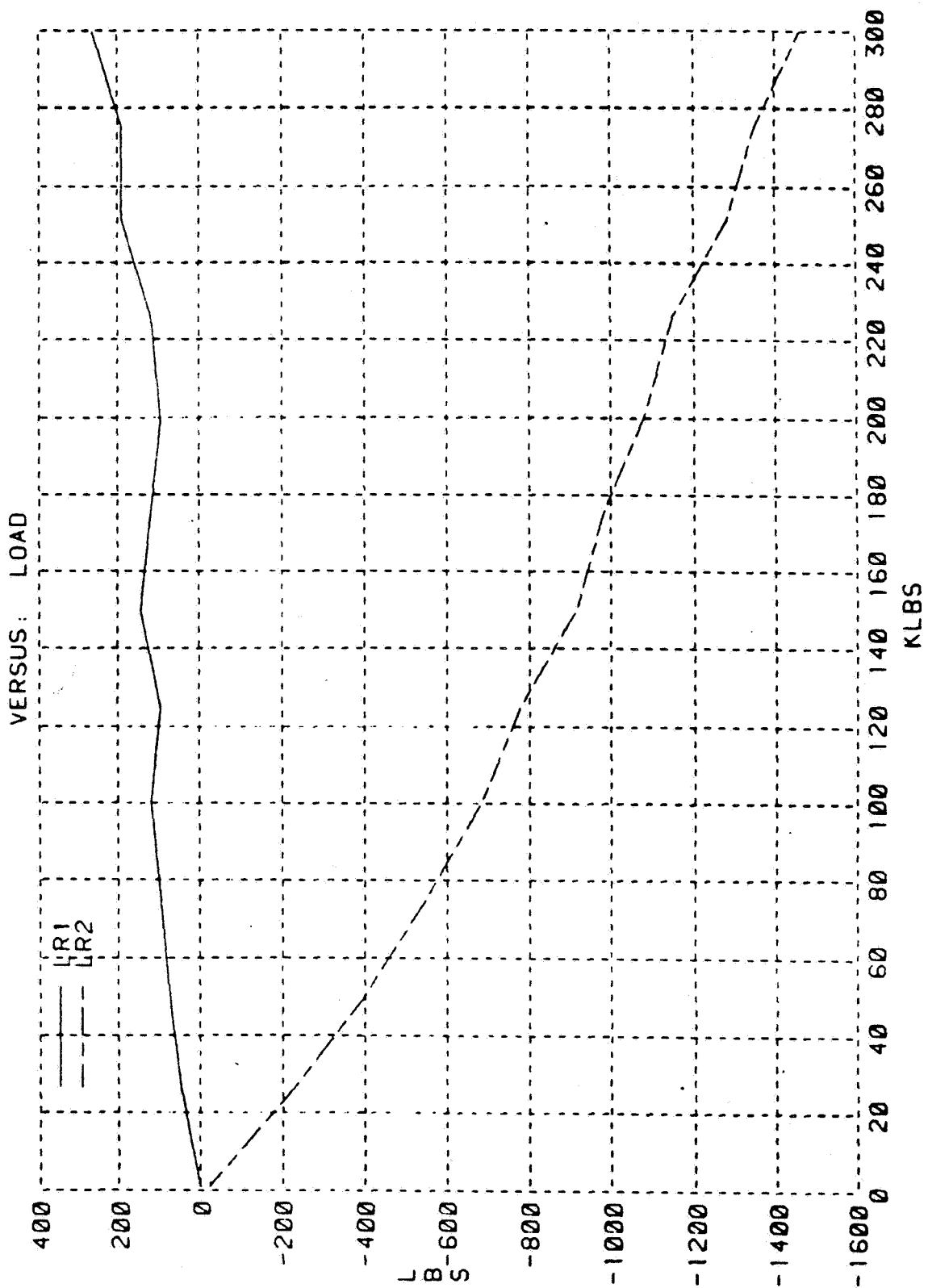
COMPOSITE CRITICAL JOINT DEMONSTRATION TEST
AUG 9, 1984 - BLDG 41 - LIMIT LOAD SURVEY



COMPOSITE CRITICAL JOINT DEMONSTRATION TEST
AUG 9, 1984 - BLDG 41 - LIMIT LOAD SURVEY

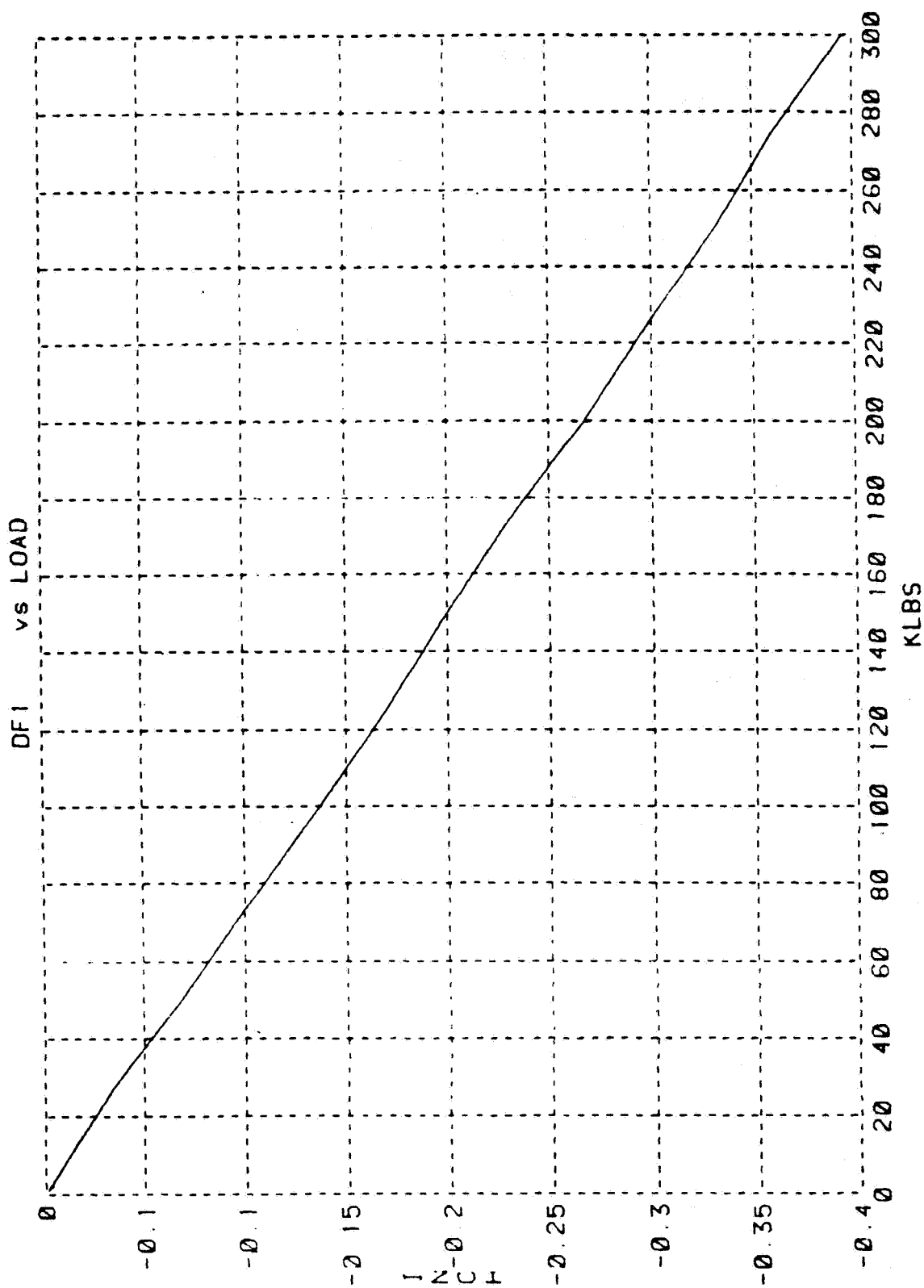


COMPOSITE CRITICAL JOINT DEMONSTRATION TEST
AUG 9, 1984 - BLDG 41 - LIMIT LOAD SURVEY



ORIGINAL PAGE IS
OF POOR QUALITY

COMPOSITE CRITICAL JOINT DEMONSTRATION TEST
AUG 9, 1984 - BLDG 41 - LIMIT LOAD SURVEY



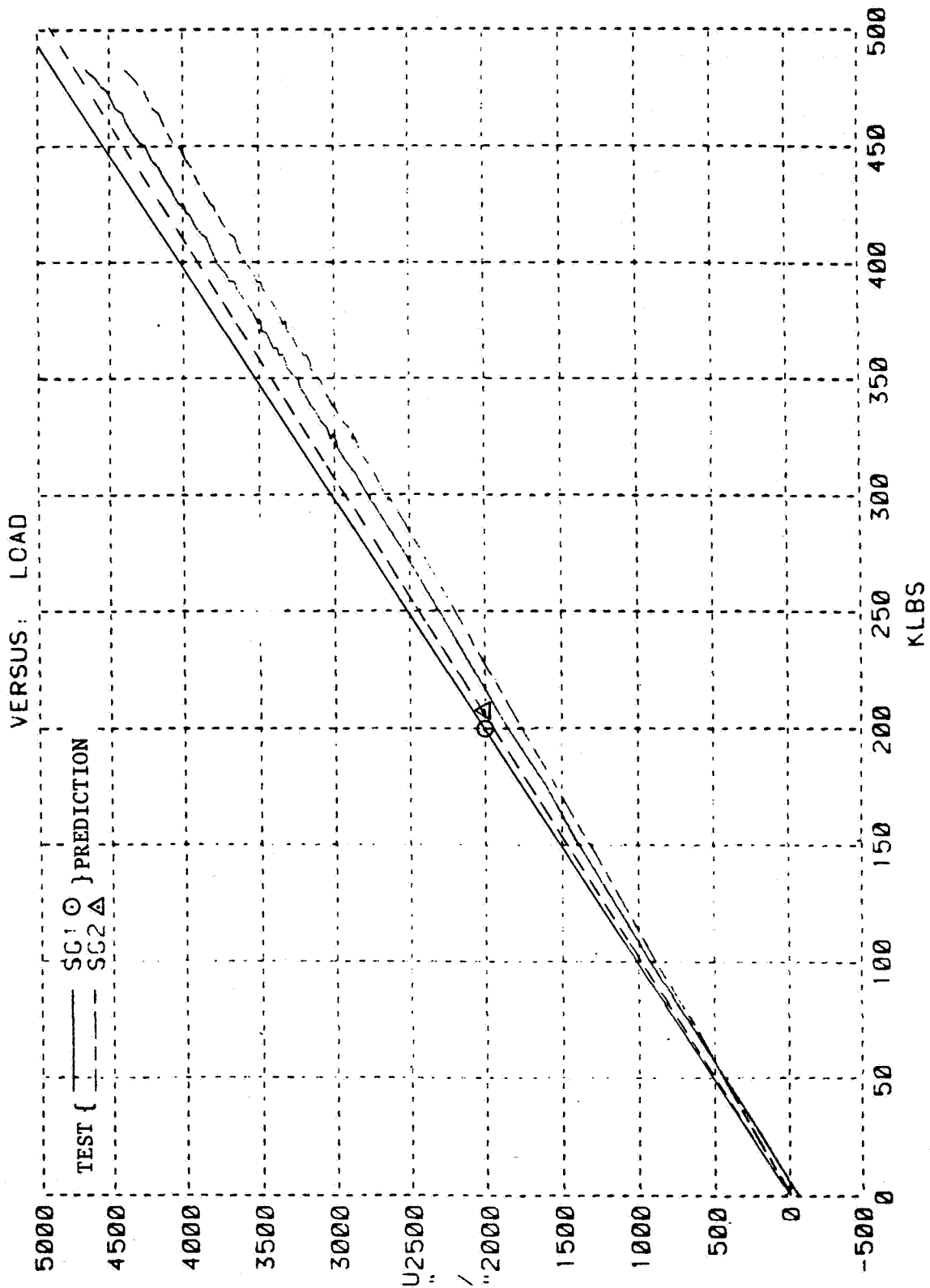
Technology Demonstration Article

Test Data to Failure (Test # 1)

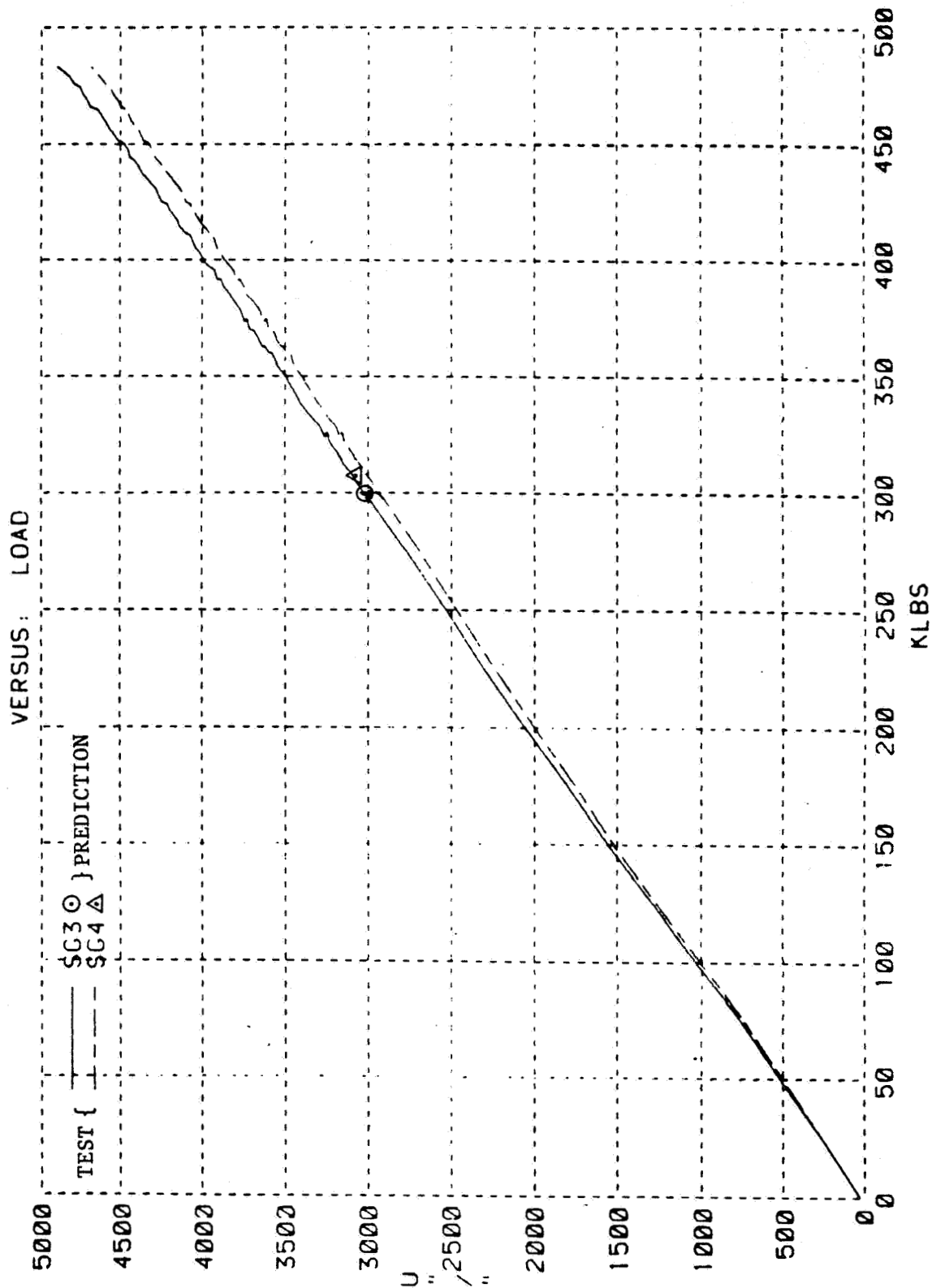
SG # - Strain Gage Number
LR # - Load Restraint Number
DF1 - Machine Head Displacement

Strain gage locations shown on page 73 .

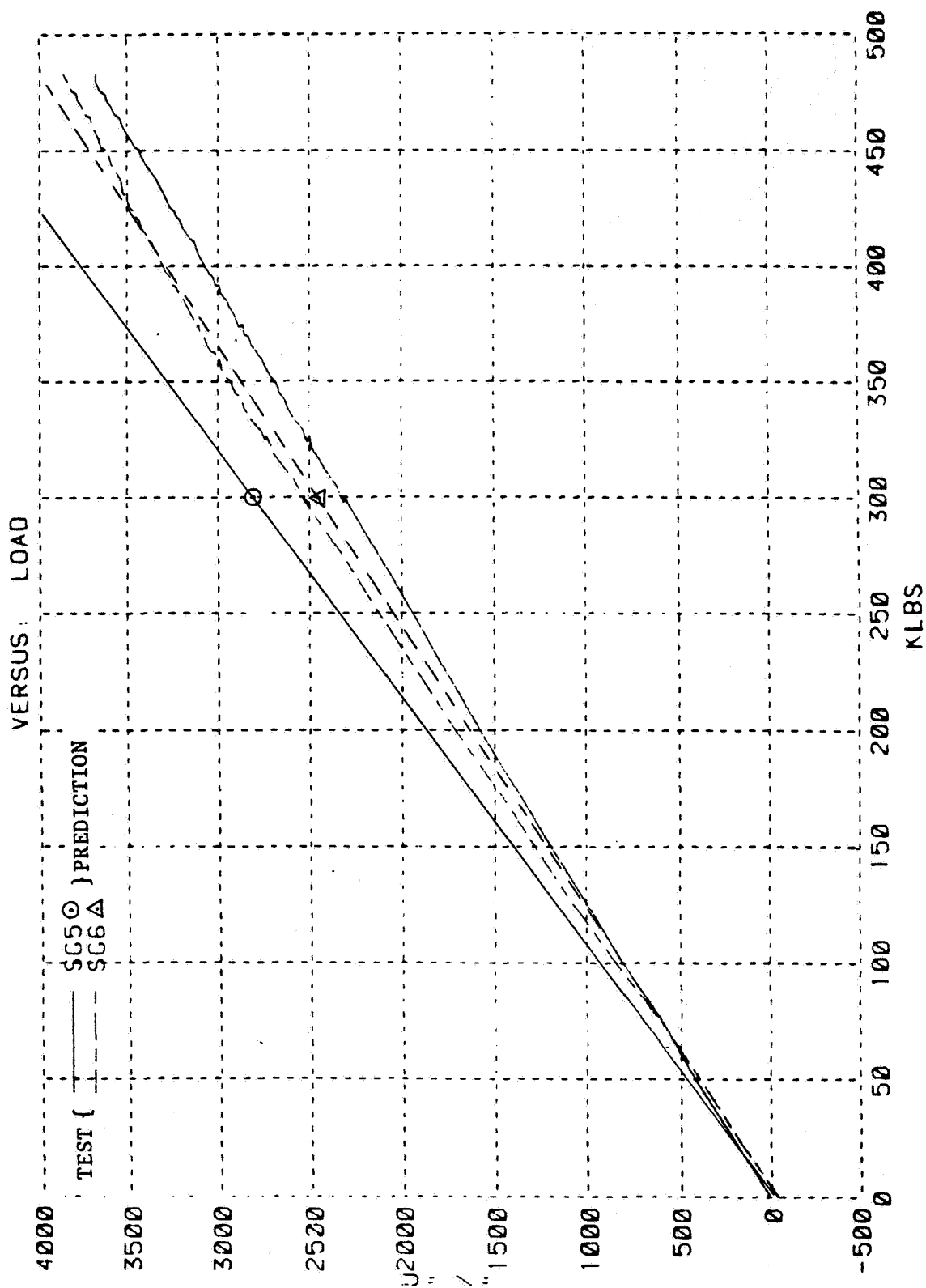
COMPOSITE CRITICAL JOINT DEMONSTRATION TEST
AUG 9, 1984 - BLDG 41 - RAMP TO FAILURE



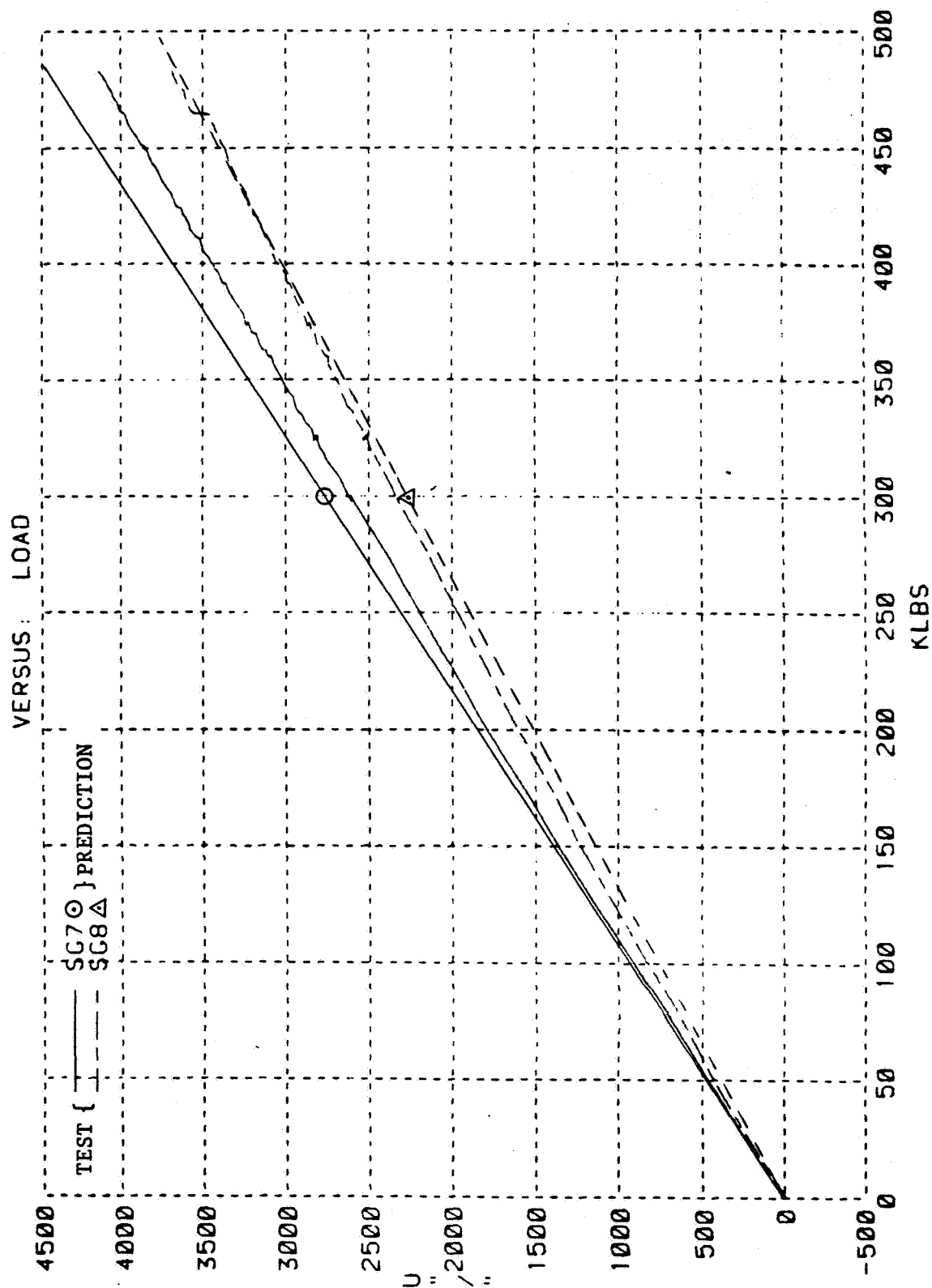
COMPOSITE CRITICAL JOINT DEMONSTRATION TEST AUG 9, 1984 - BLDC 41 - RAMP TO FAILURE



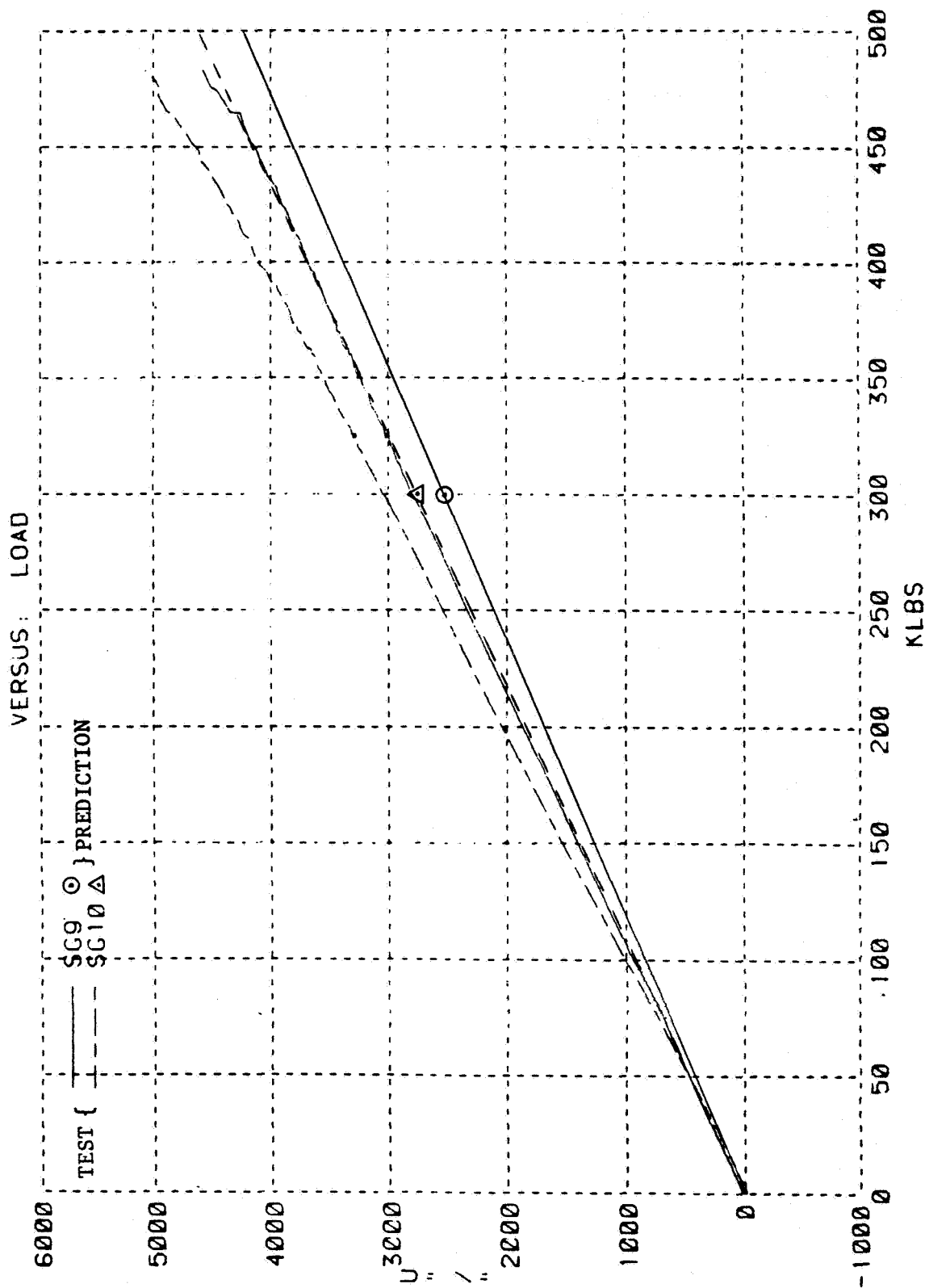
COMPOSITE CRITICAL JOINT DEMONSTRATION TEST
AUG 9, 1984 - BLDG 41 - RAMP TO FAILURE



COMPOSITE CRITICAL JOINT DEMONSTRATION TEST
AUG 9, 1984 - BLDG 41 - RAMP TO FAILURE

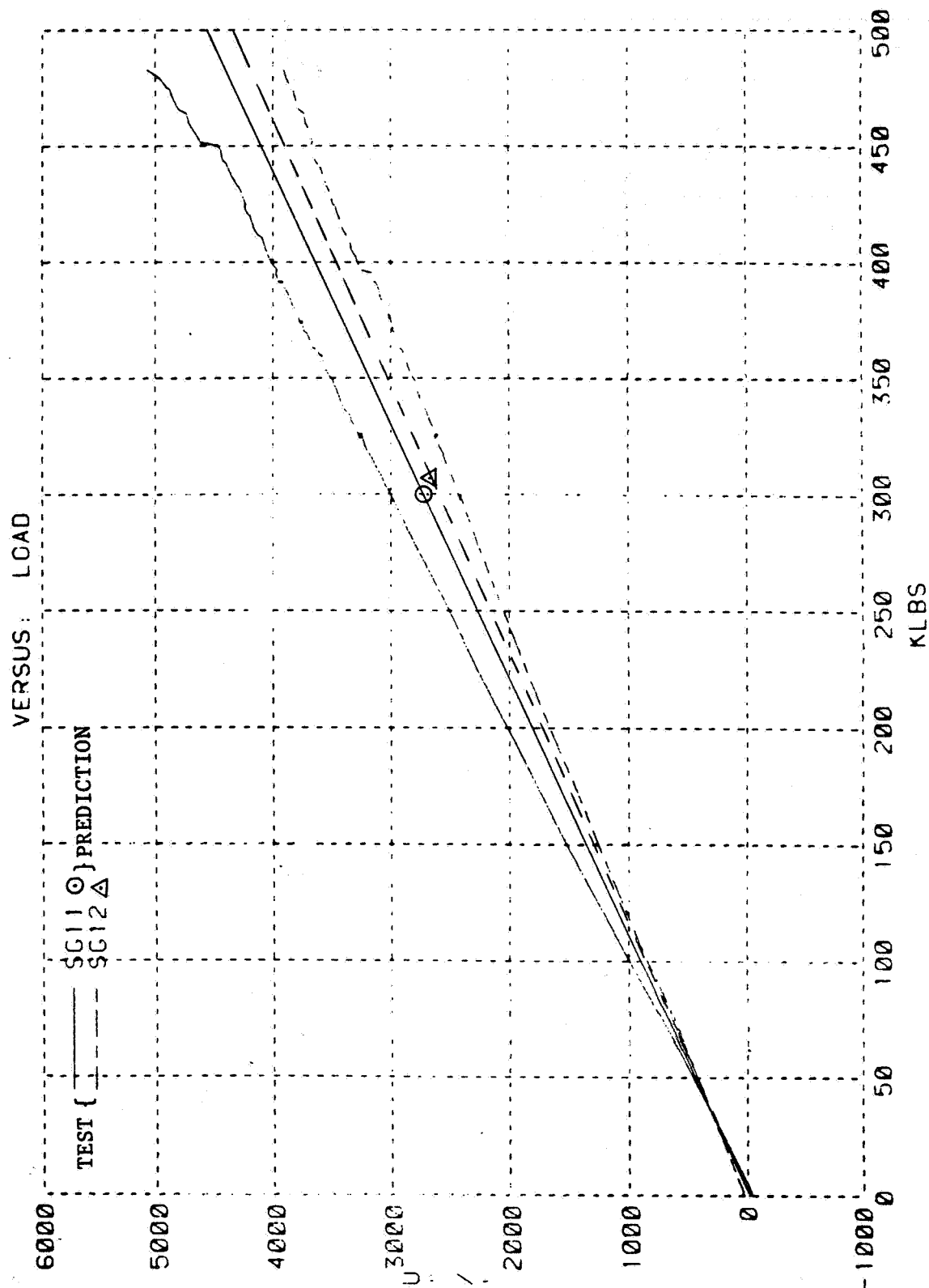


COMPOSITE CRITICAL JOINT DEMONSTRATION TEST
AUG 9, 1984 - BLDG 41 - RAMP TO FAILURE

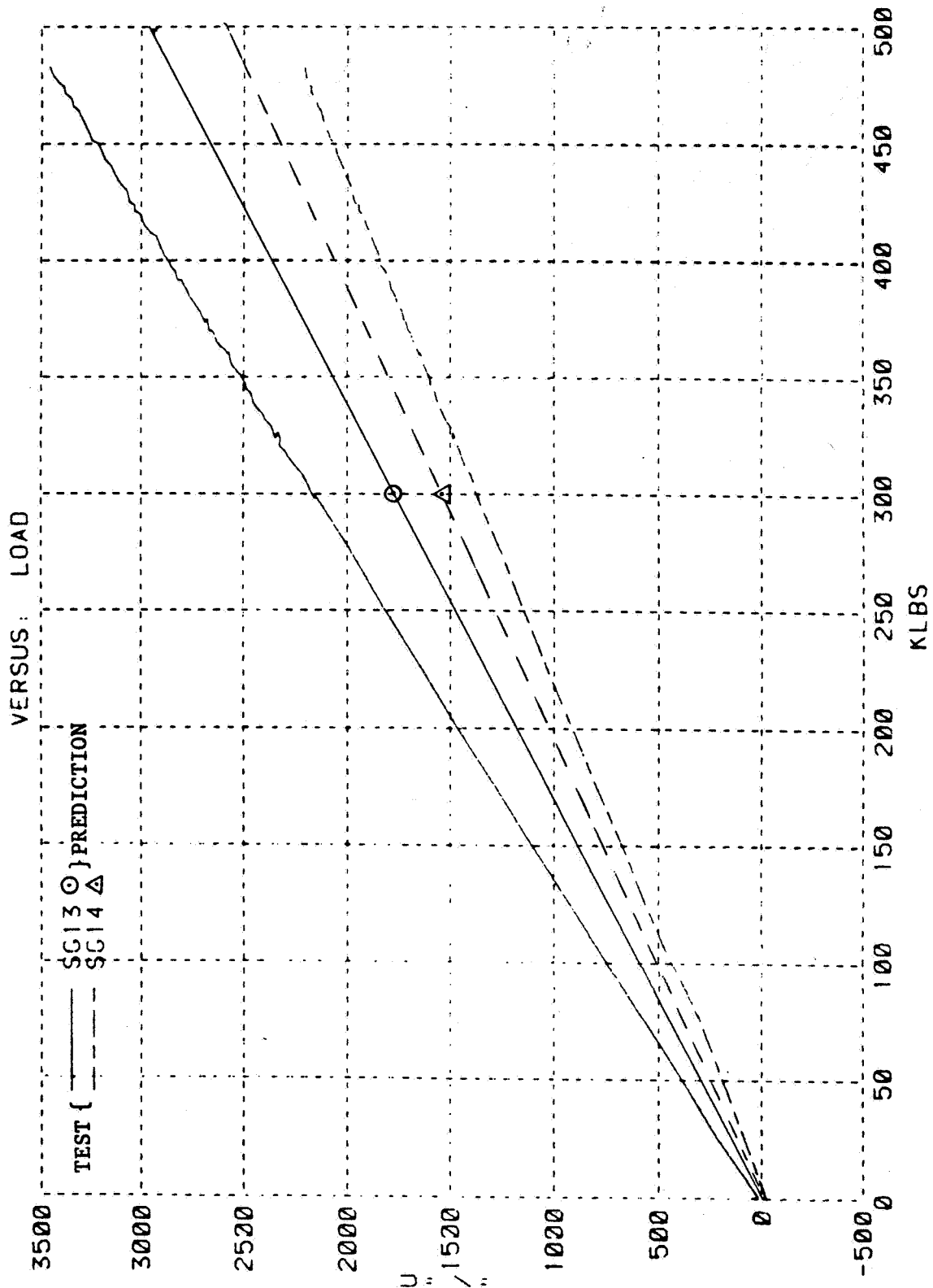


THE POOR QUALITY
OF THE ORIGINAL PAGE

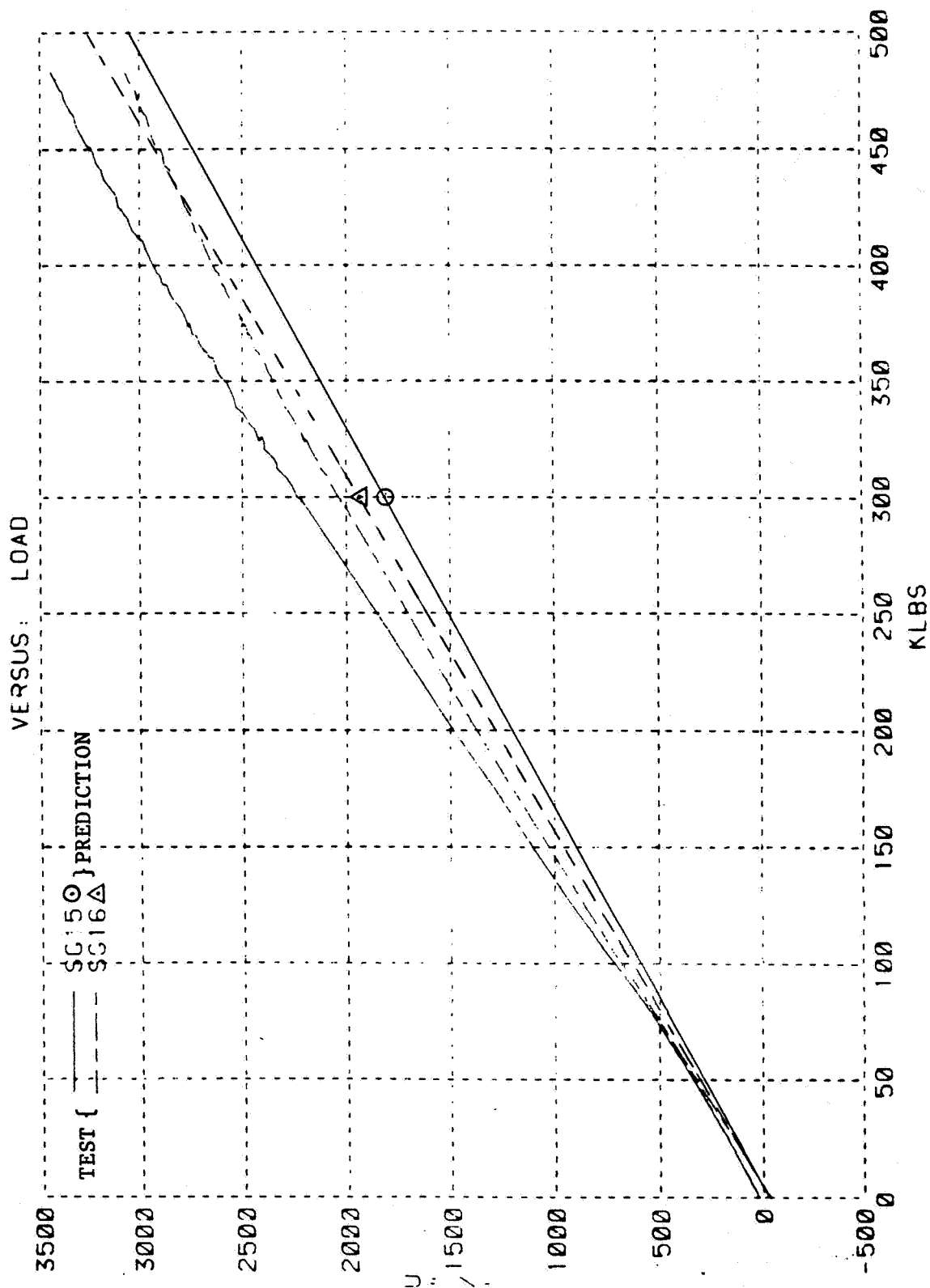
COMPOSITE CRITICAL JOINT DEMONSTRATION TEST
AUG 9, 1984 - BLDG 41 - RAMP TO FAILURE



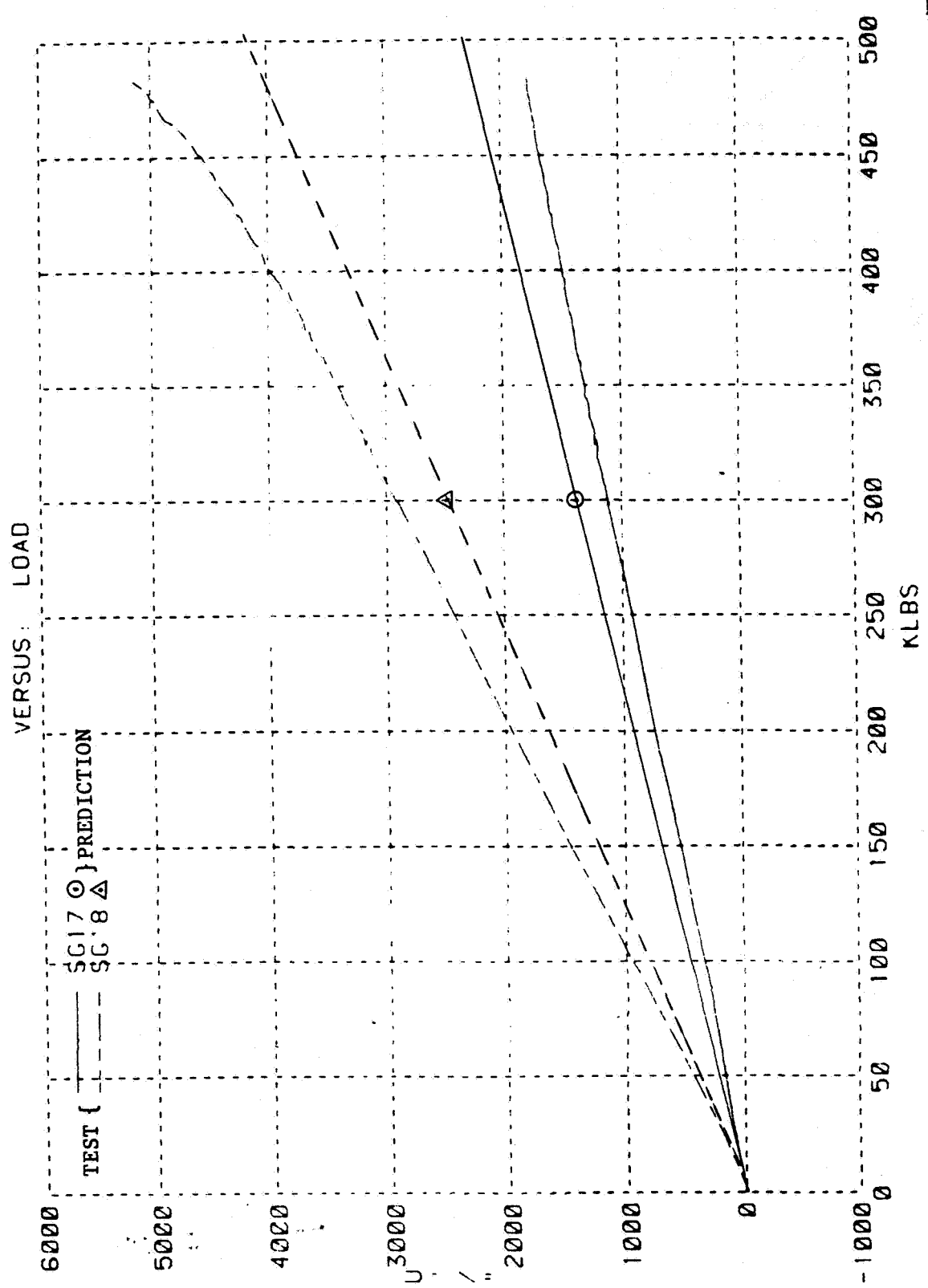
COMPOSITE CRITICAL JOINT DEMONSTRATION TEST
AUG 9, 1984 - BLOC 41 - RAMP TO FAILURE



COMPOSITE CRITICAL JOINT DEMONSTRATION TEST
AUG 9, 1984 - BLDG 41 - RAMP TO FAILURE

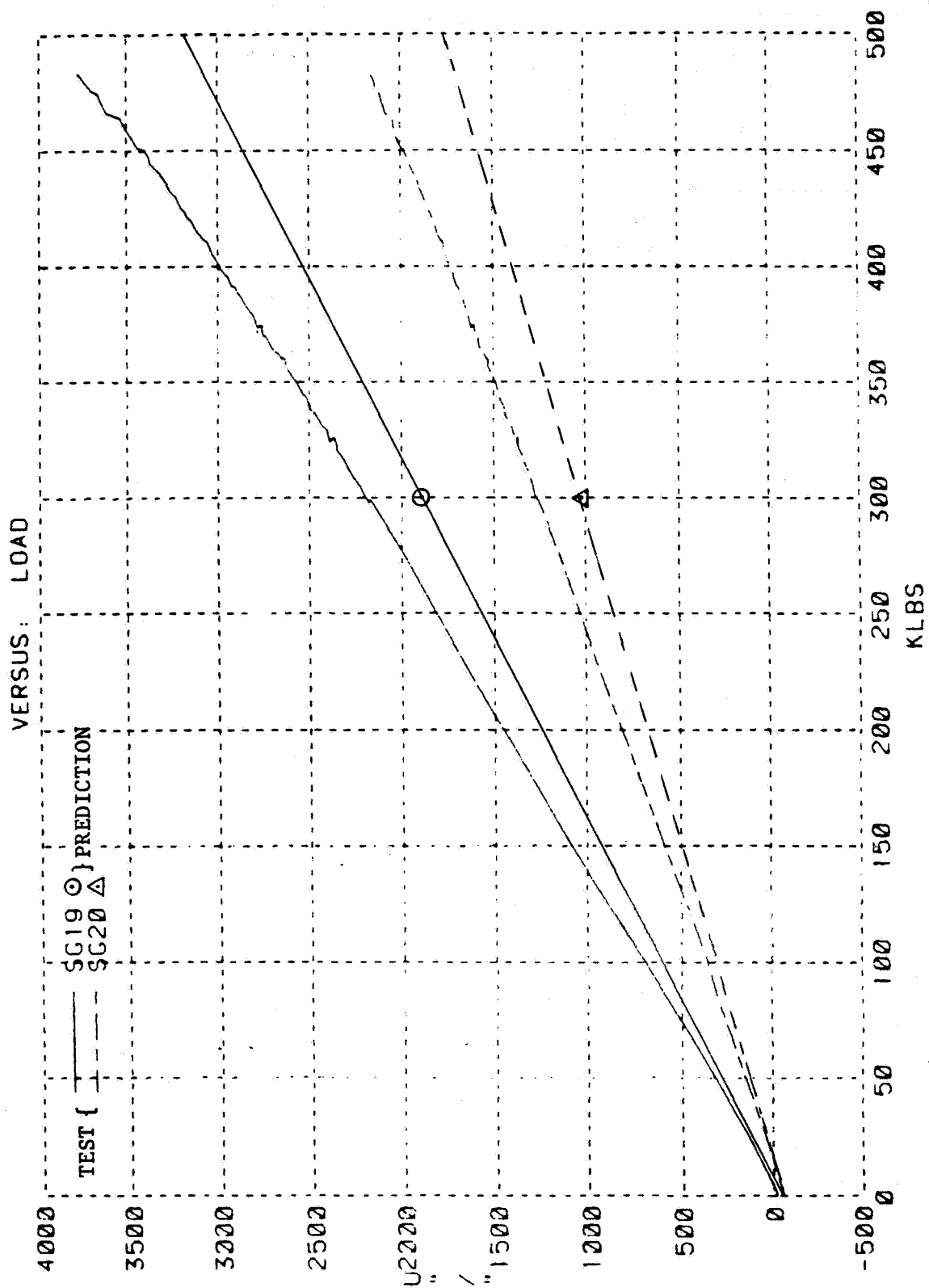


COMPOSITE CRITICAL JOINT DEMONSTRATION TEST
 AUG 9 1984 - BLOC 4: - RAMP TO FAILURE

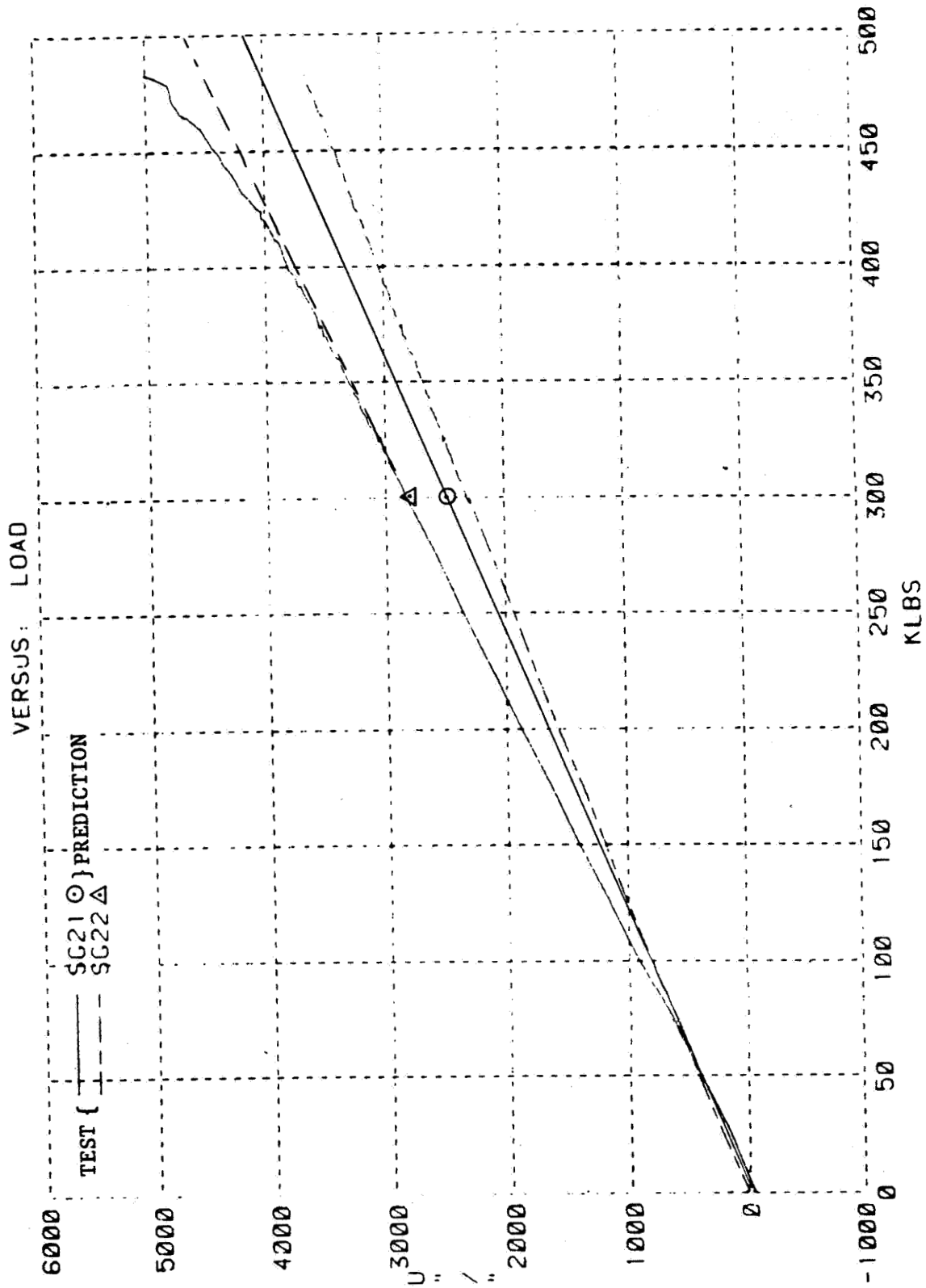


0.3

COMPOSITE CRITICAL JOINT DEMONSTRATION TEST
AUG 9, 1984 - BLDG 41 - RAMP TO FAILURE

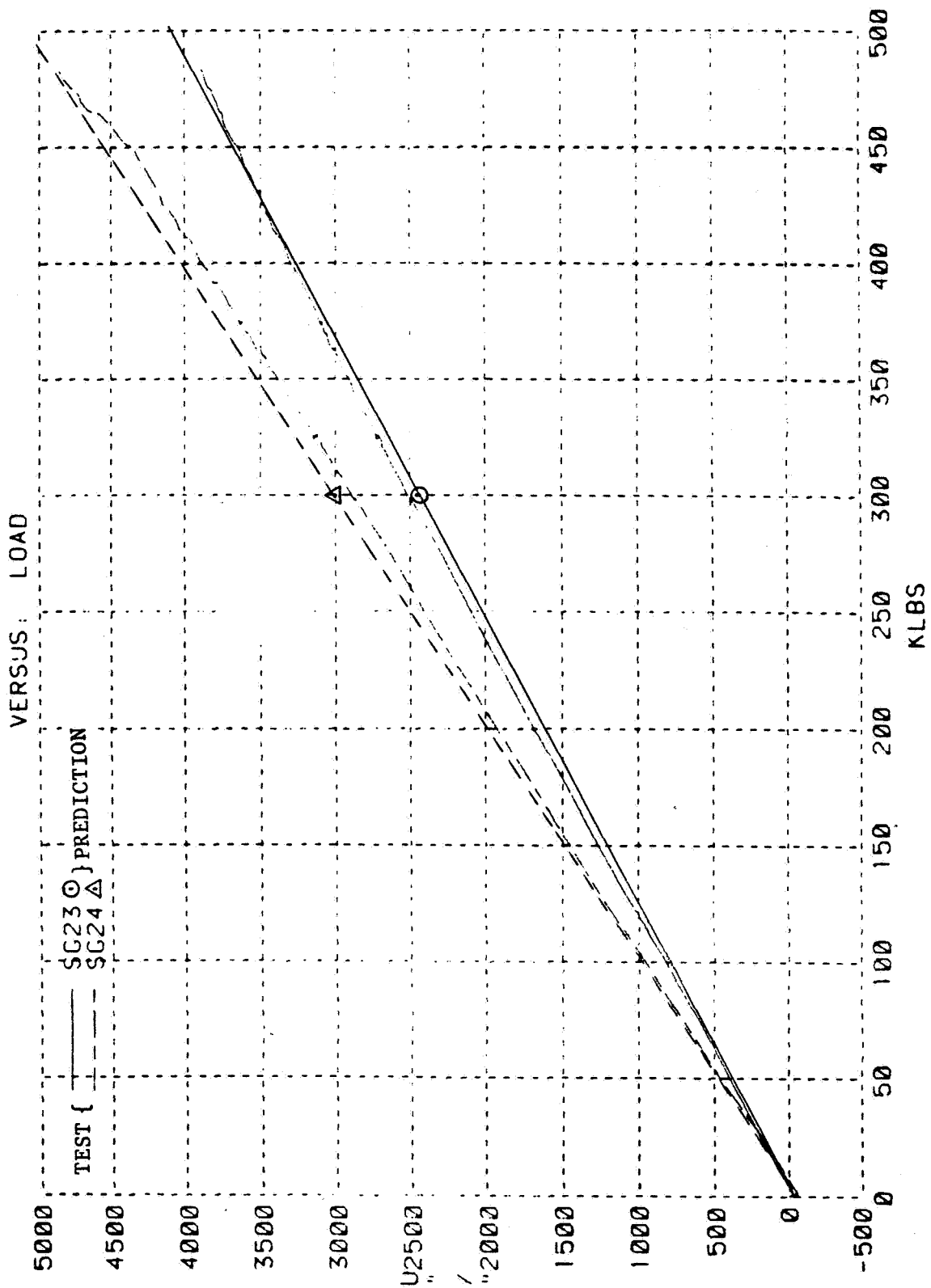


COMPOSITE CRITICAL JOINT DEMONSTRATION TEST
AUG 9, 1984 - BLDG 41 - RAMP TO FAILURE

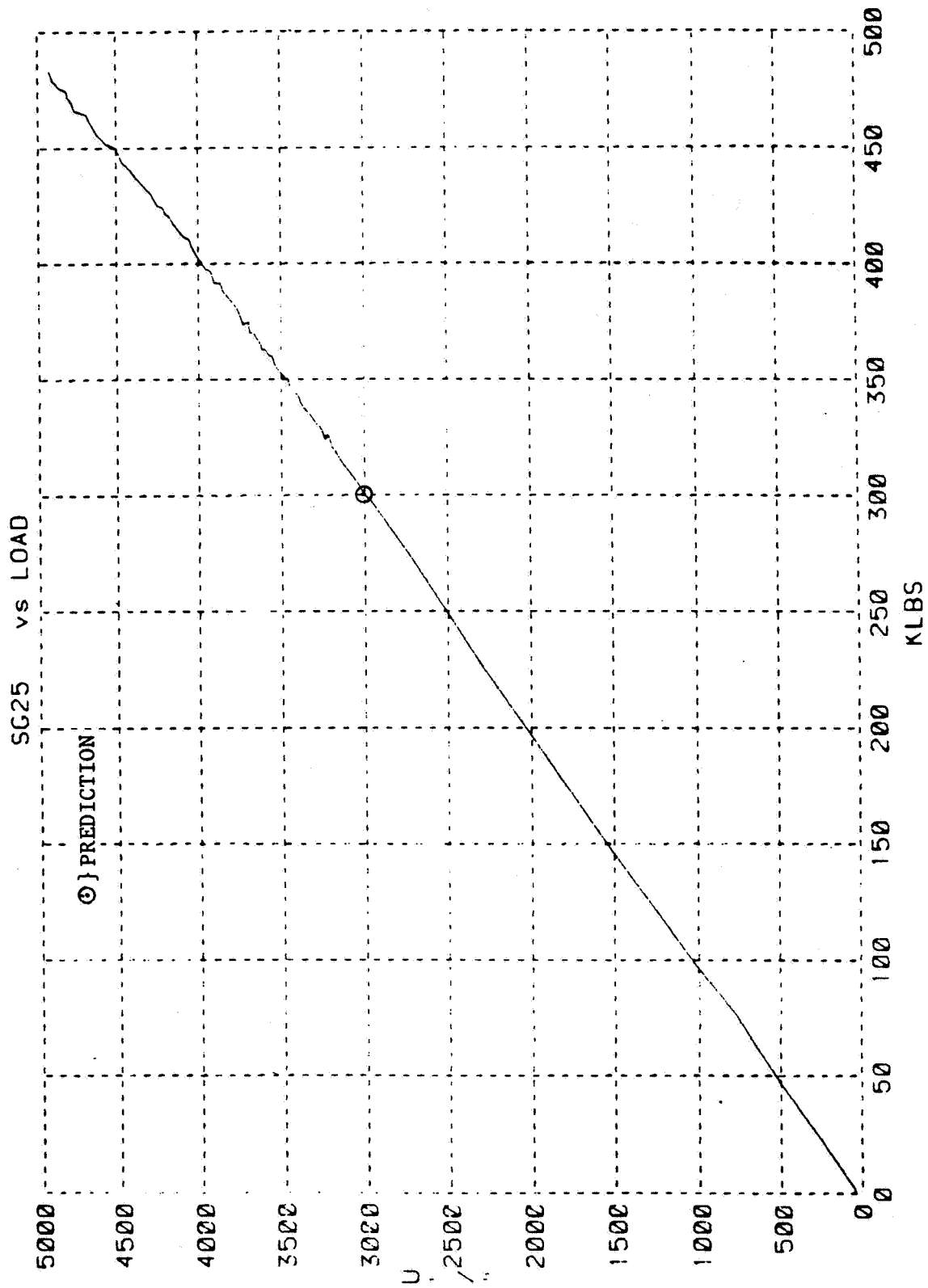


SI 1114 117 1114
YTLIAUQ 7047 70

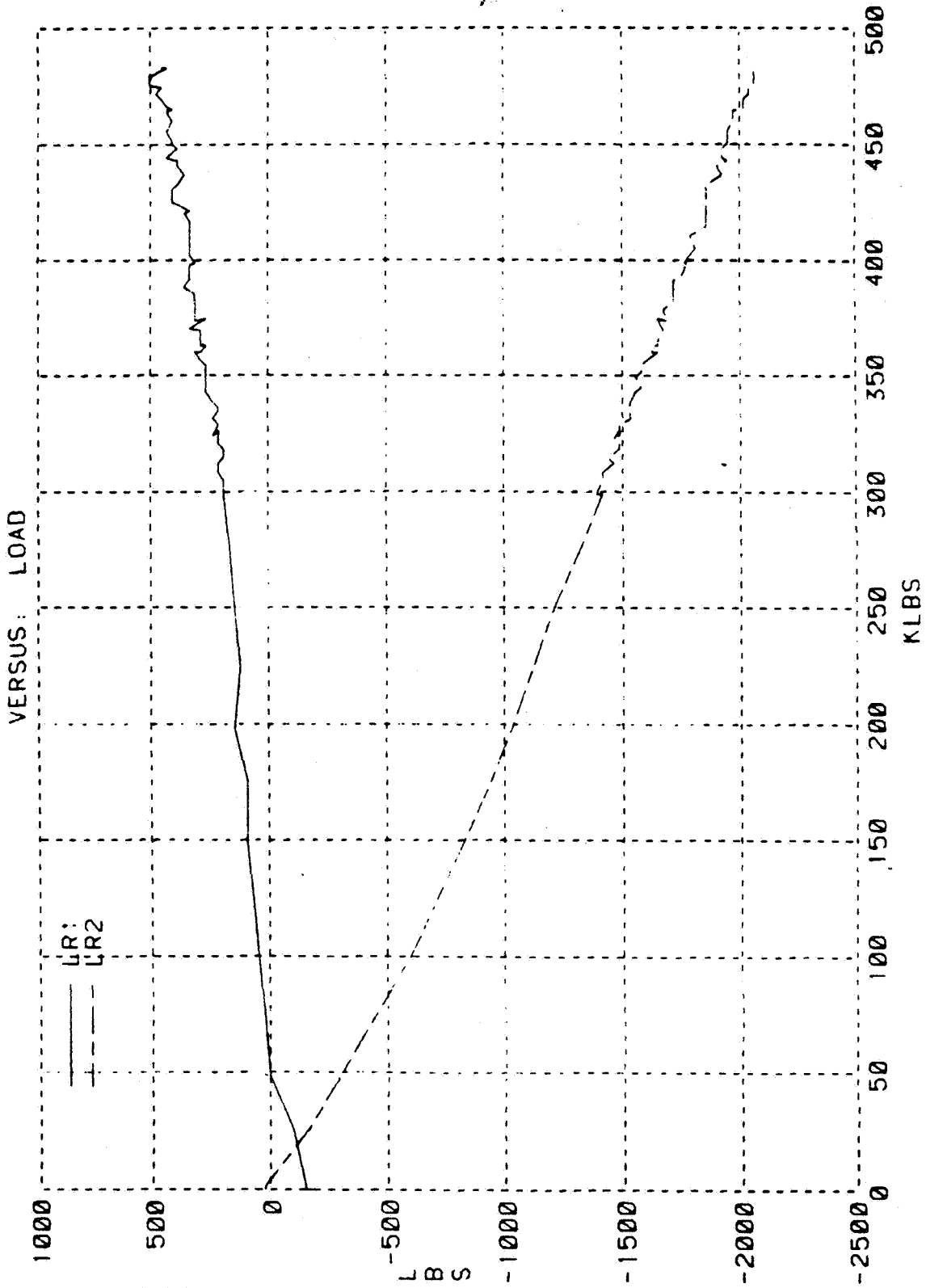
COMPOSITE CRITICAL JOINT DEMONSTRATION TEST
AUG 9, 1984 - BLDG 41 - RAMP TO FAILURE



COMPOSITE CRITICAL JOINT DEMONSTRATION TEST
AUG 9, 1984 - BLDG 41 - RAMP TO FAILURE

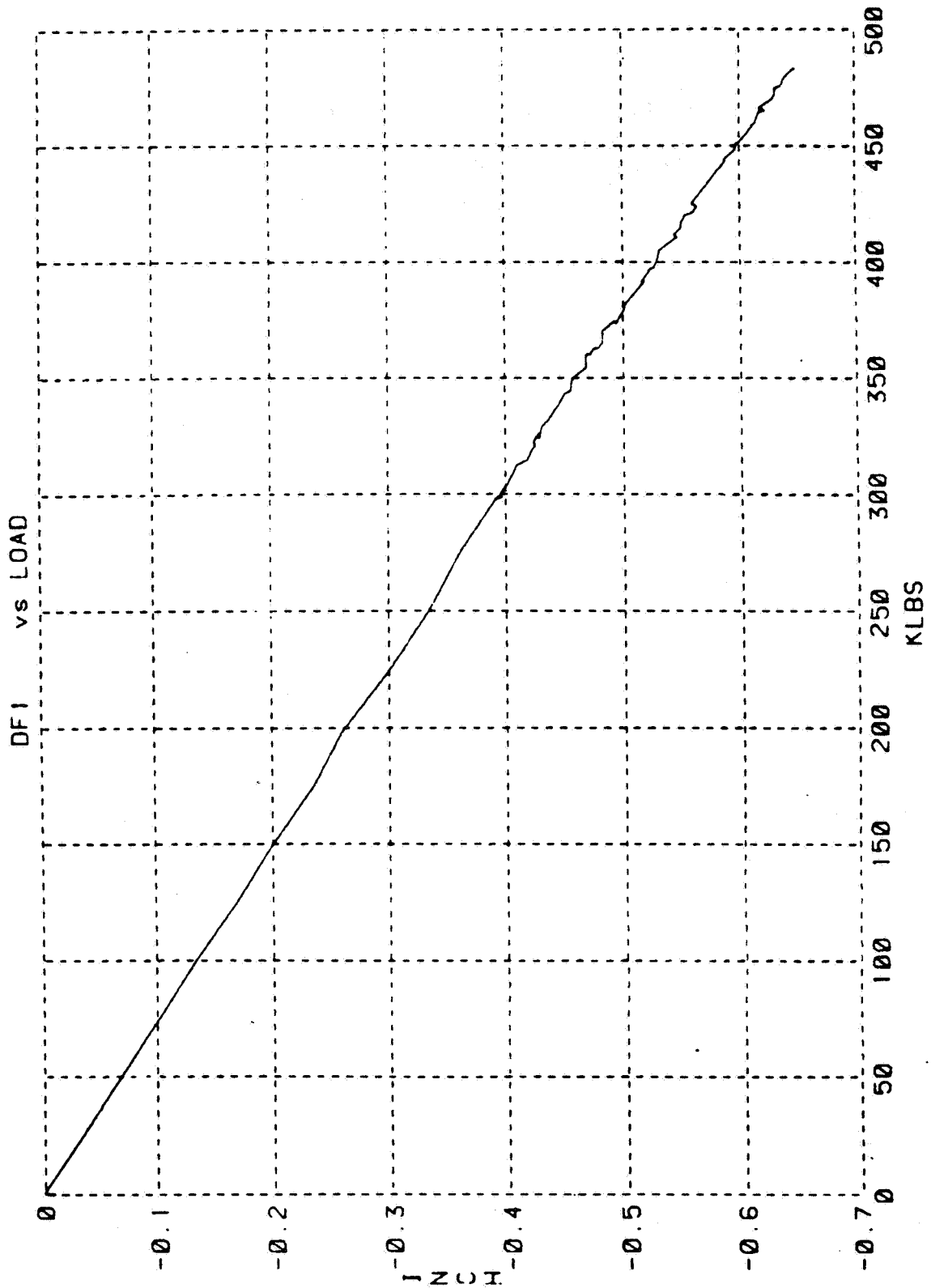


COMPOSITE CRITICAL JOINT DEMONSTRATION TEST
AUG 9, 1984 - BLDG 41 - RAMP TO FAILURE



ORIGINAL PAGE IS
OF POOR QUALITY

COMPOSITE CRITICAL JOINT DEMONSTRATION TEST
AUG 9, 1984 - BLDG 41 - RAMP TO FAILURE



Technology Demonstration Article

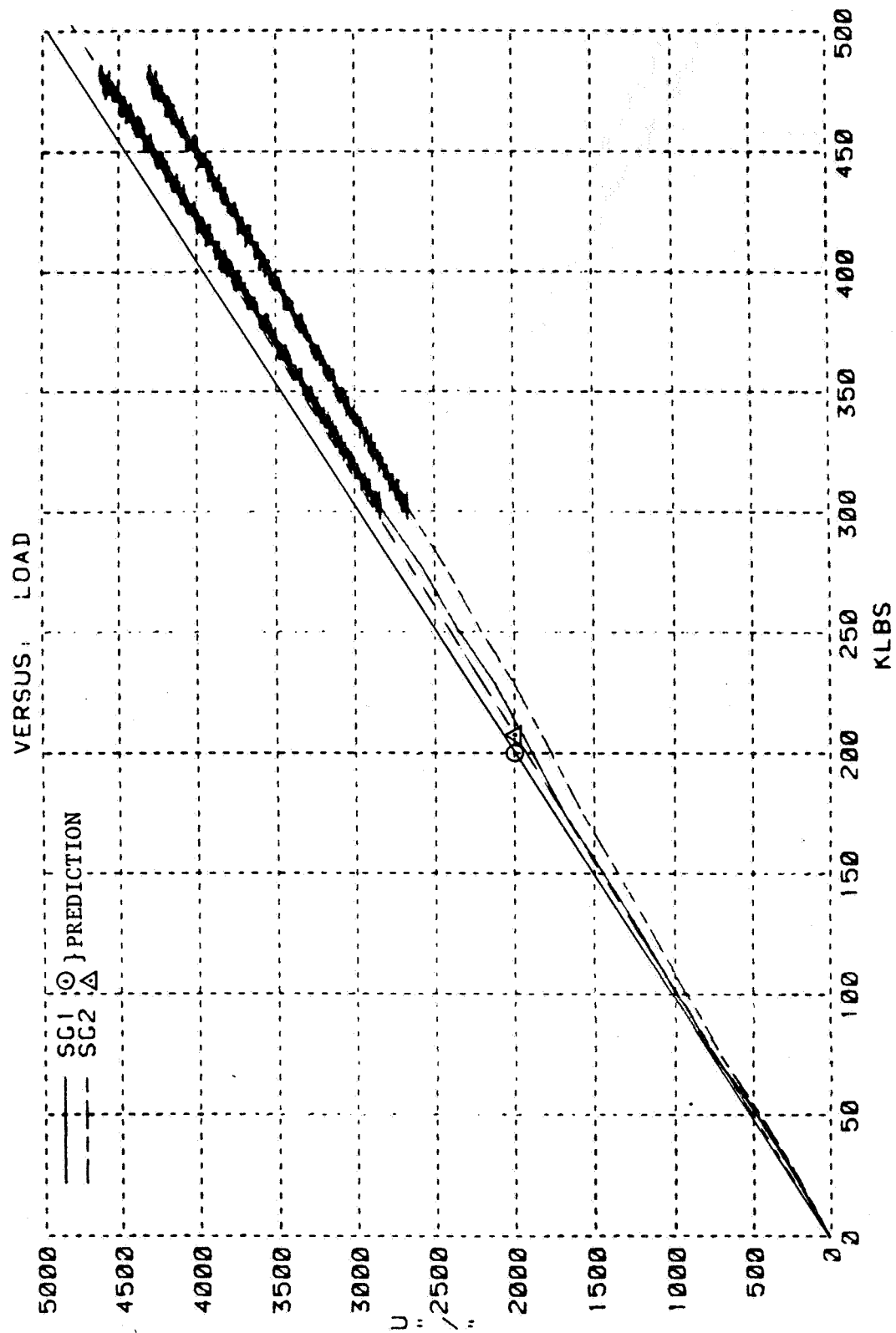
Test Data to Failure (Test #2)

SG # - Strain Gage Number
LR # - Load Restraint Number
DF1 - Machine Head Displacement

Strain gage locations shown on page

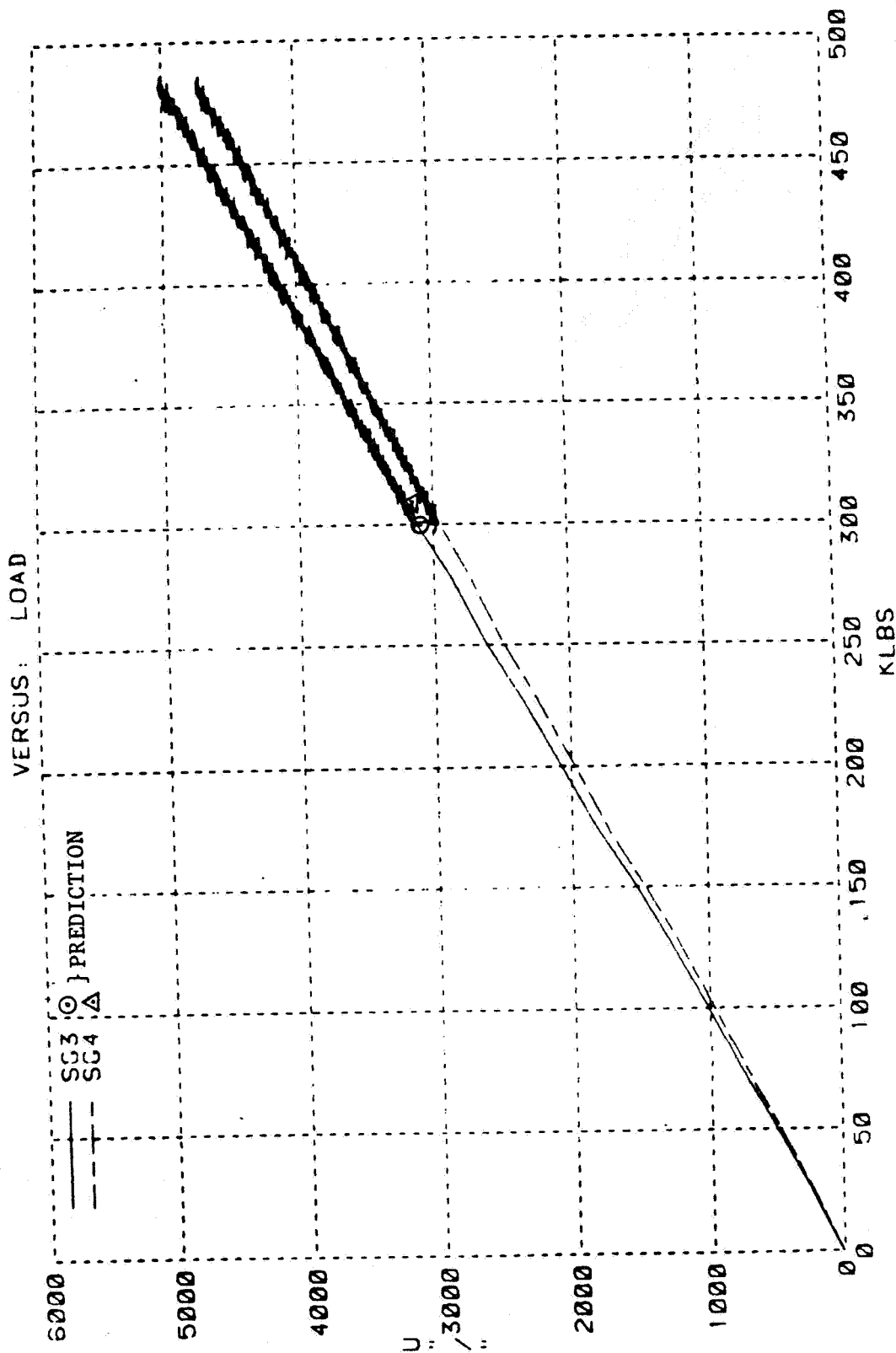
(Refer to discussion - page 73)

COMPOSITE CRITICAL JOINT DEMONSTRATION TEST #2
 NOV 29, 1984 - BLDG 41 - RAMP TO FAILURE

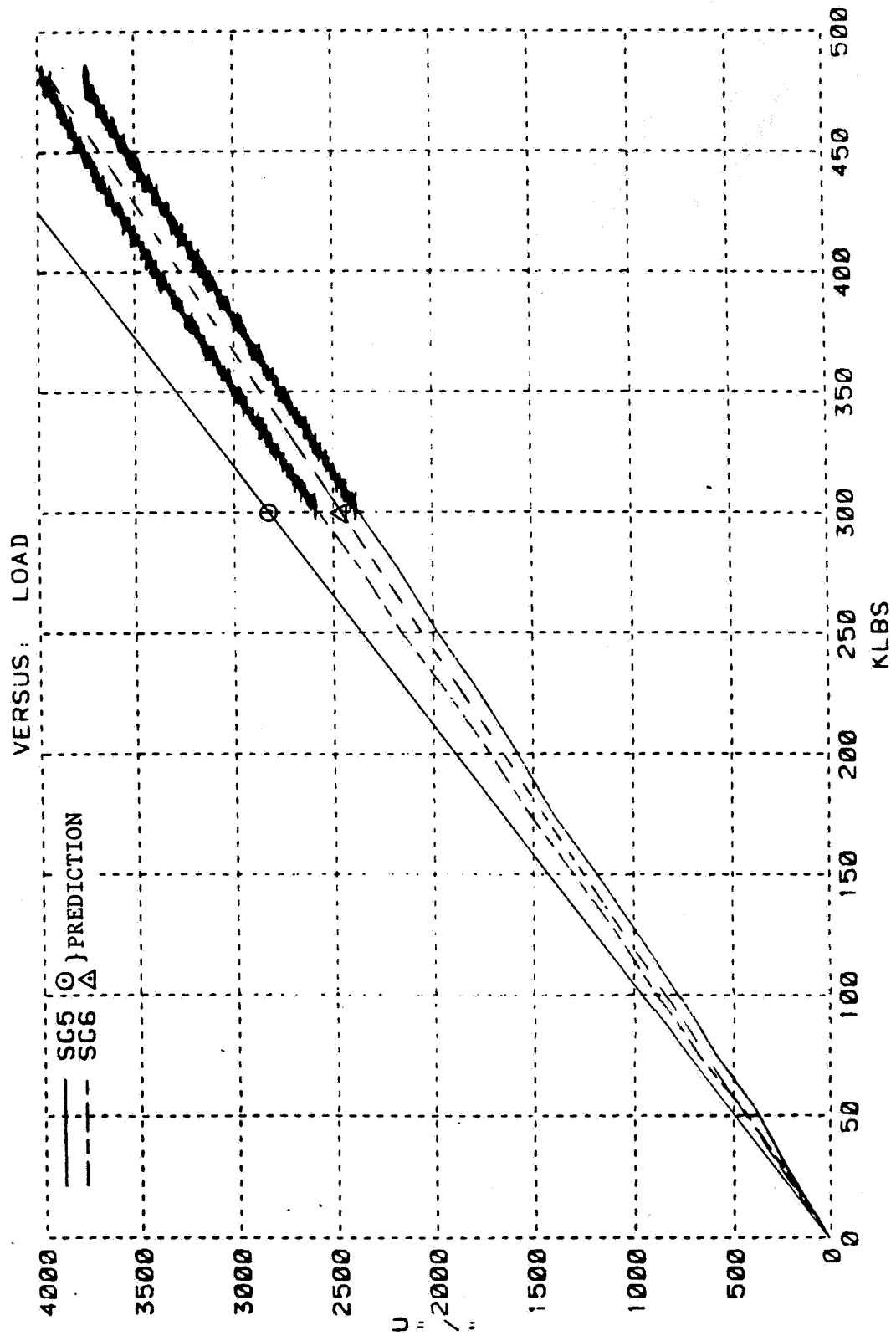


ORIGINAL PAGE IS
 OF POOR QUALITY

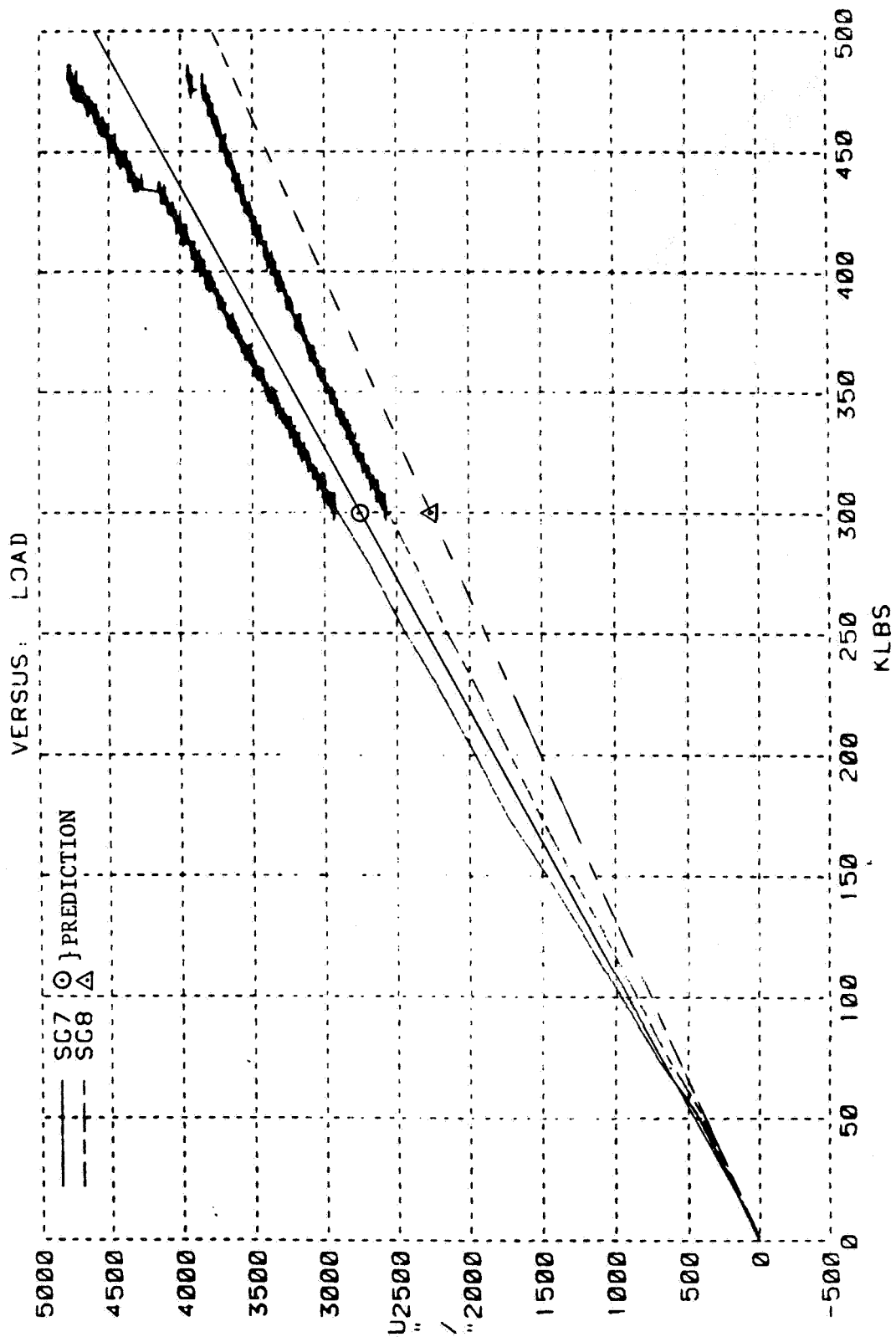
COMPOSITE CRITICAL JOINT DEMONSTRATION TEST #2
 NOV 29, 1984 - BLDG 41 - RAMP TO FAILURE

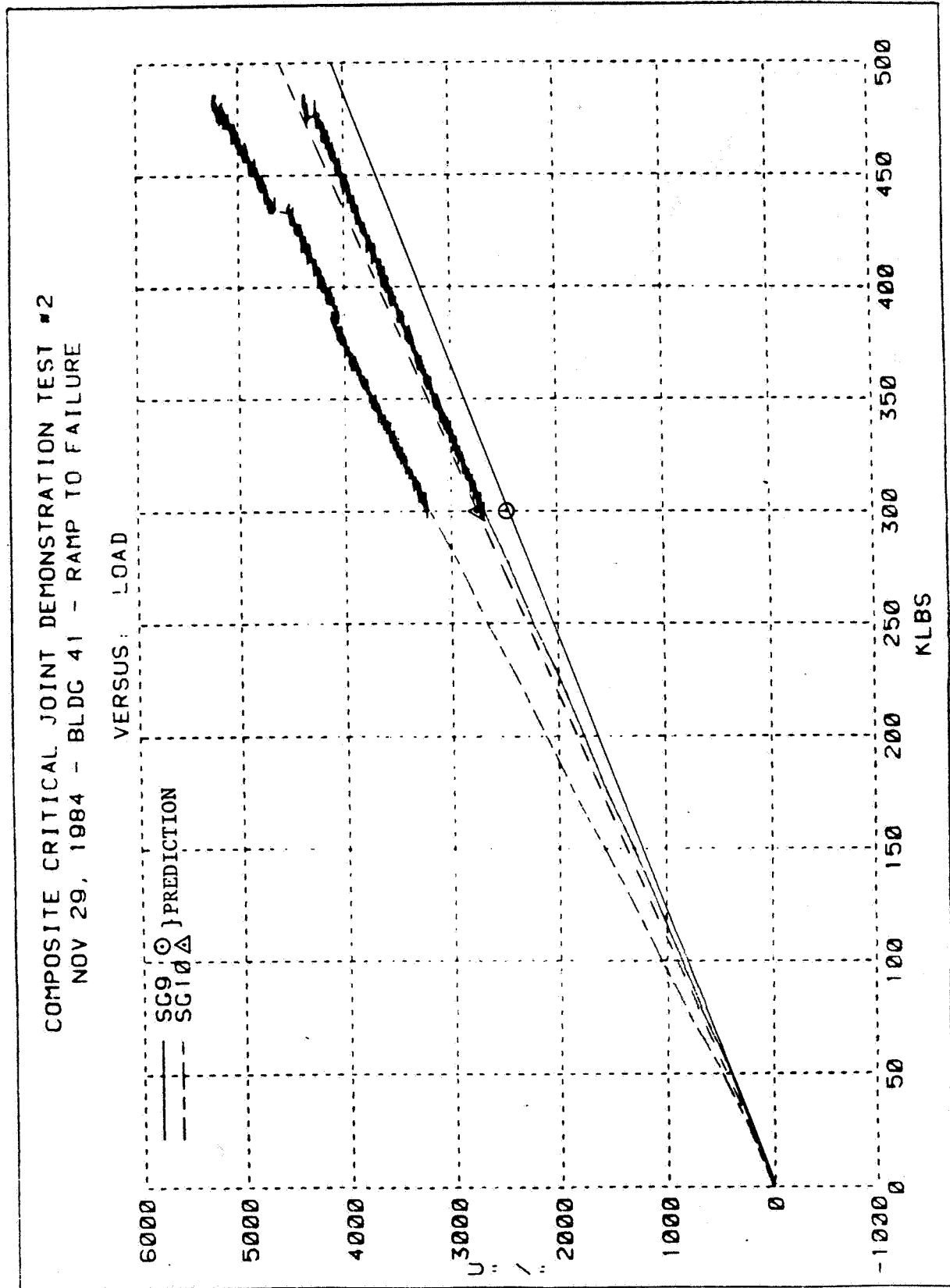


COMPOSITE CRITICAL JOINT DEMONSTRATION TEST #2
 NOV 29, 1984 - BLDG 41 - RAMP TO FAILURE

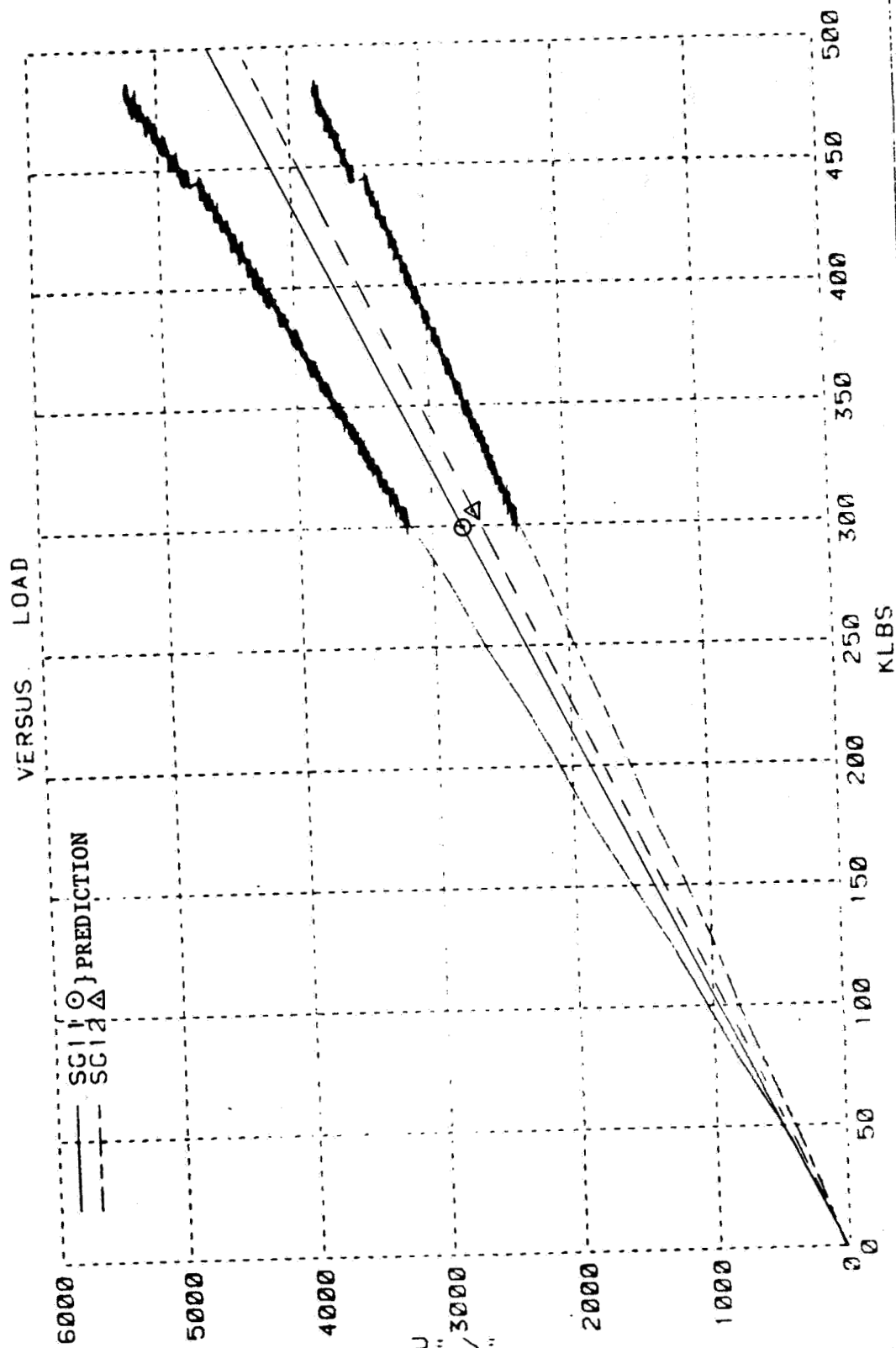


COMPOSITE CRITICAL JOINT DEMONSTRATION TEST #2
 NOV 29, 1984 - BLDG 41 - RAMP TO FAILURE

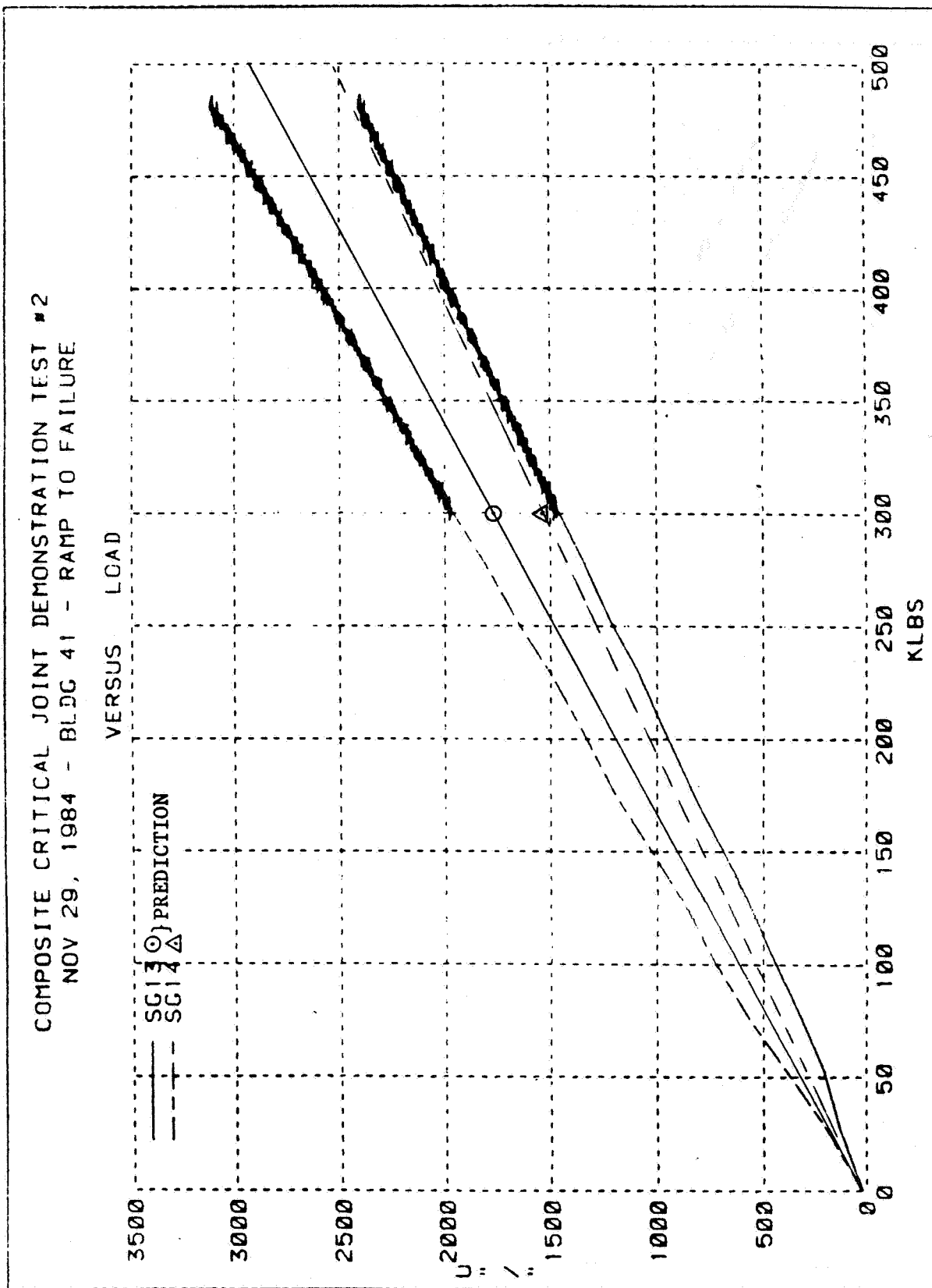




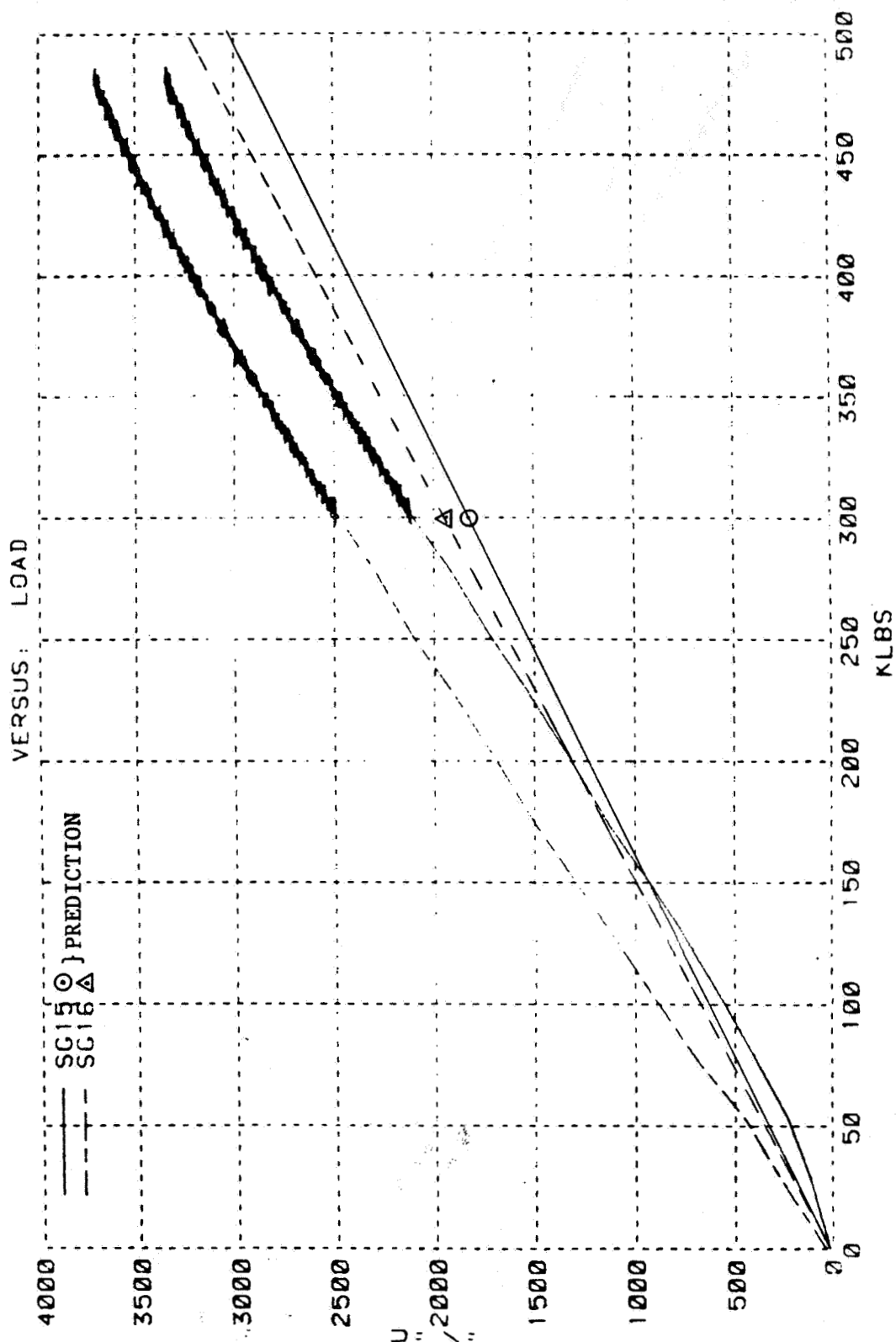
COMPOSITE CRITICAL JOINT DEMONSTRATION TEST #2
 NOV 29, 1984 - BLDG 41 - RAMP TO FAILURE



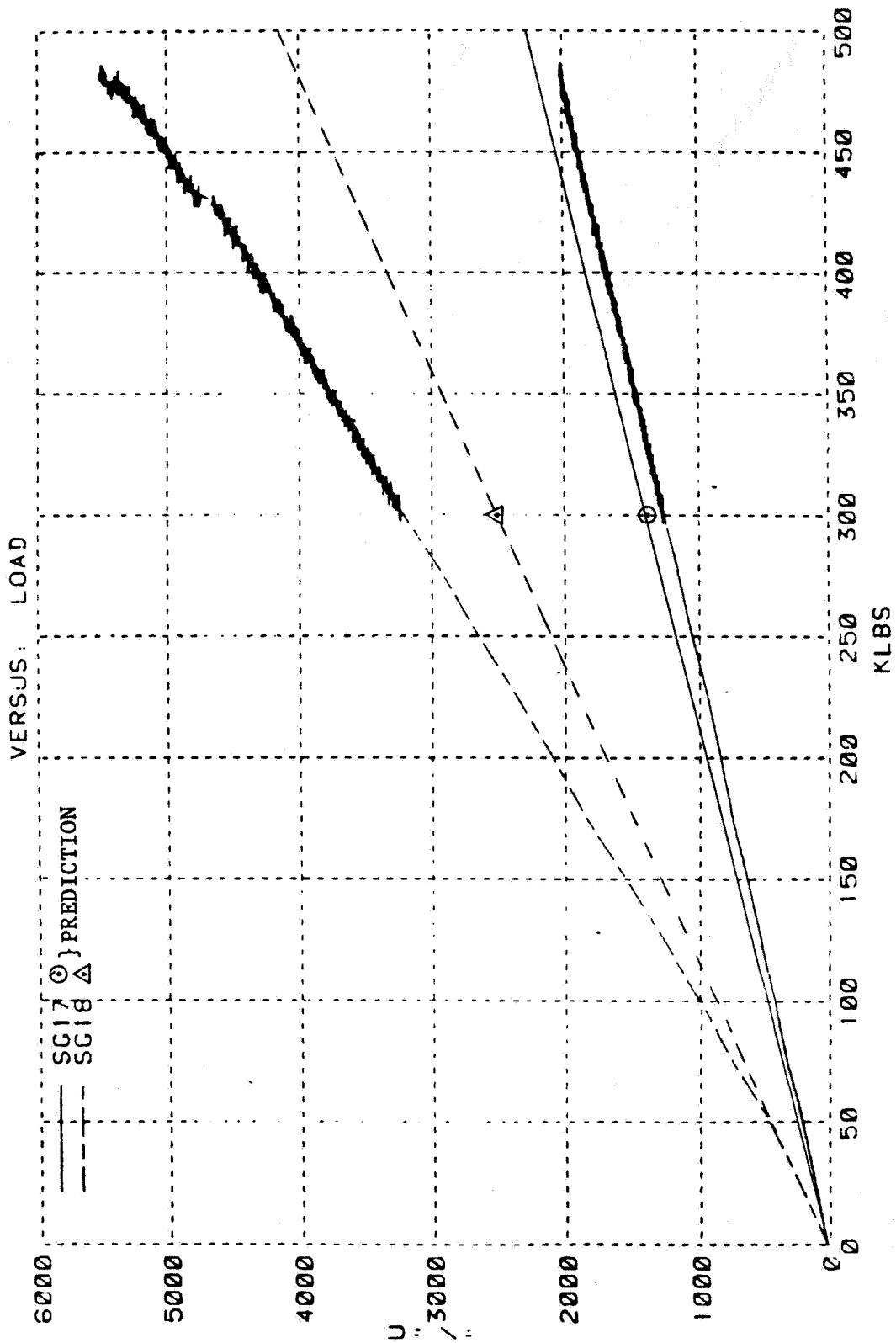
ORIGINAL PAGE IS
OF POOR QUALITY



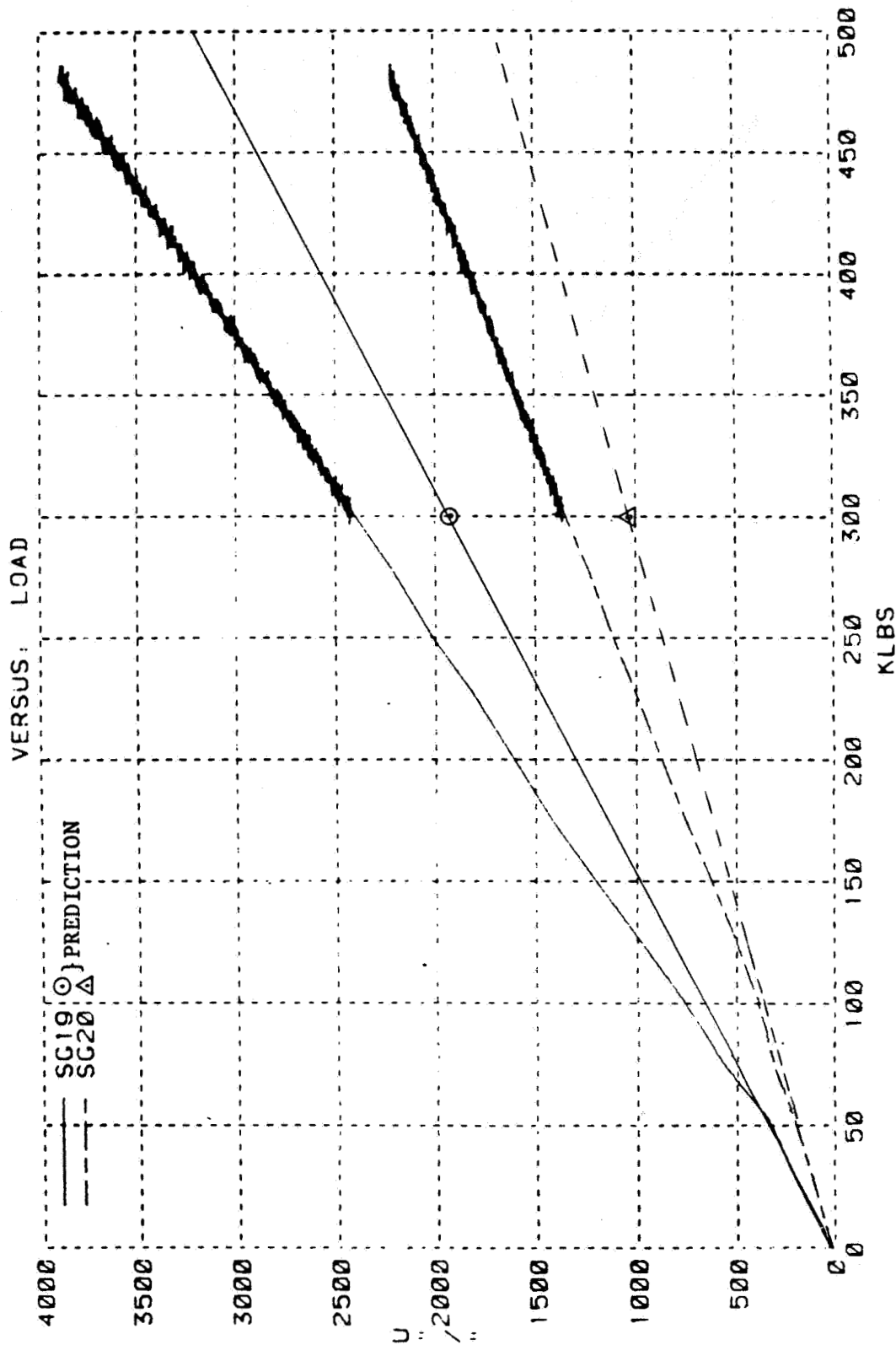
COMPOSITE CRITICAL JOINT DEMONSTRATION TEST #2
 NOV 29, 1984 - BLDG 41 - RAMP TO FAILURE



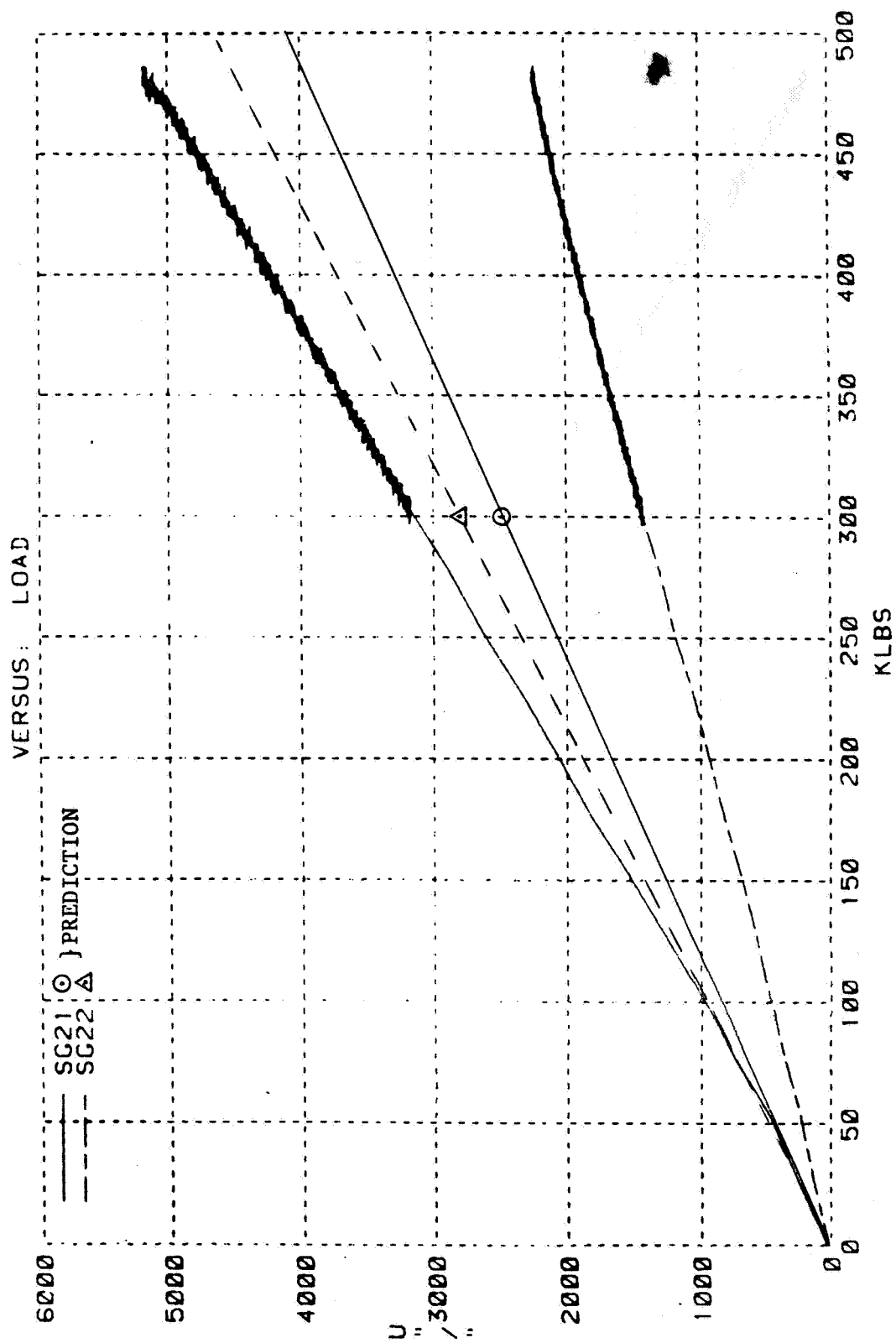
COMPOSITE CRITICAL JOINT DEMONSTRATION TEST #2
NOV 29, 1984 - BLDG 41 - RAMP TO FAILURE



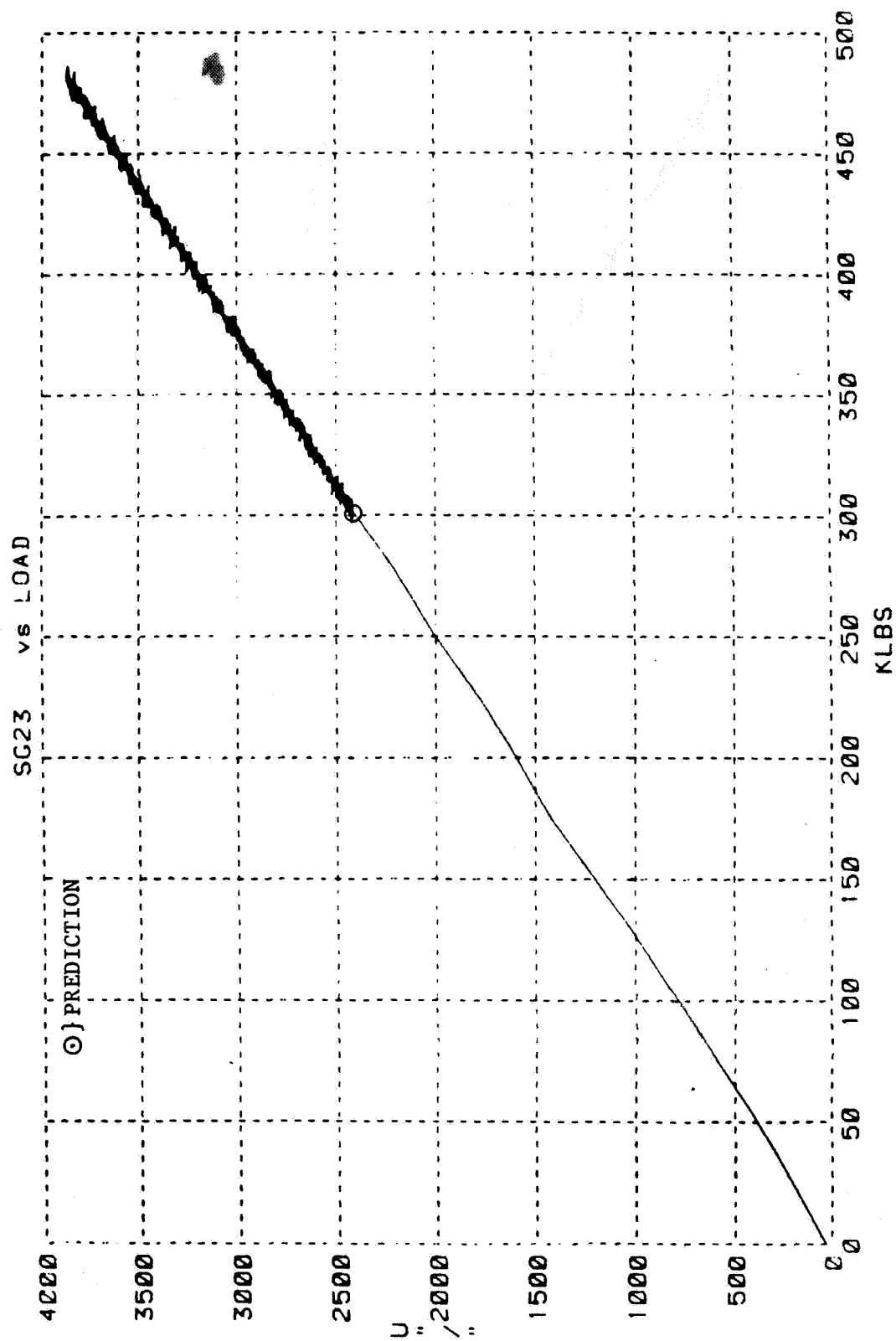
COMPOSITE CRITICAL JOINT DEMONSTRATION TEST #2
 NOV 29, 1984 - BLDG 41 - RAMP TO FAILURE



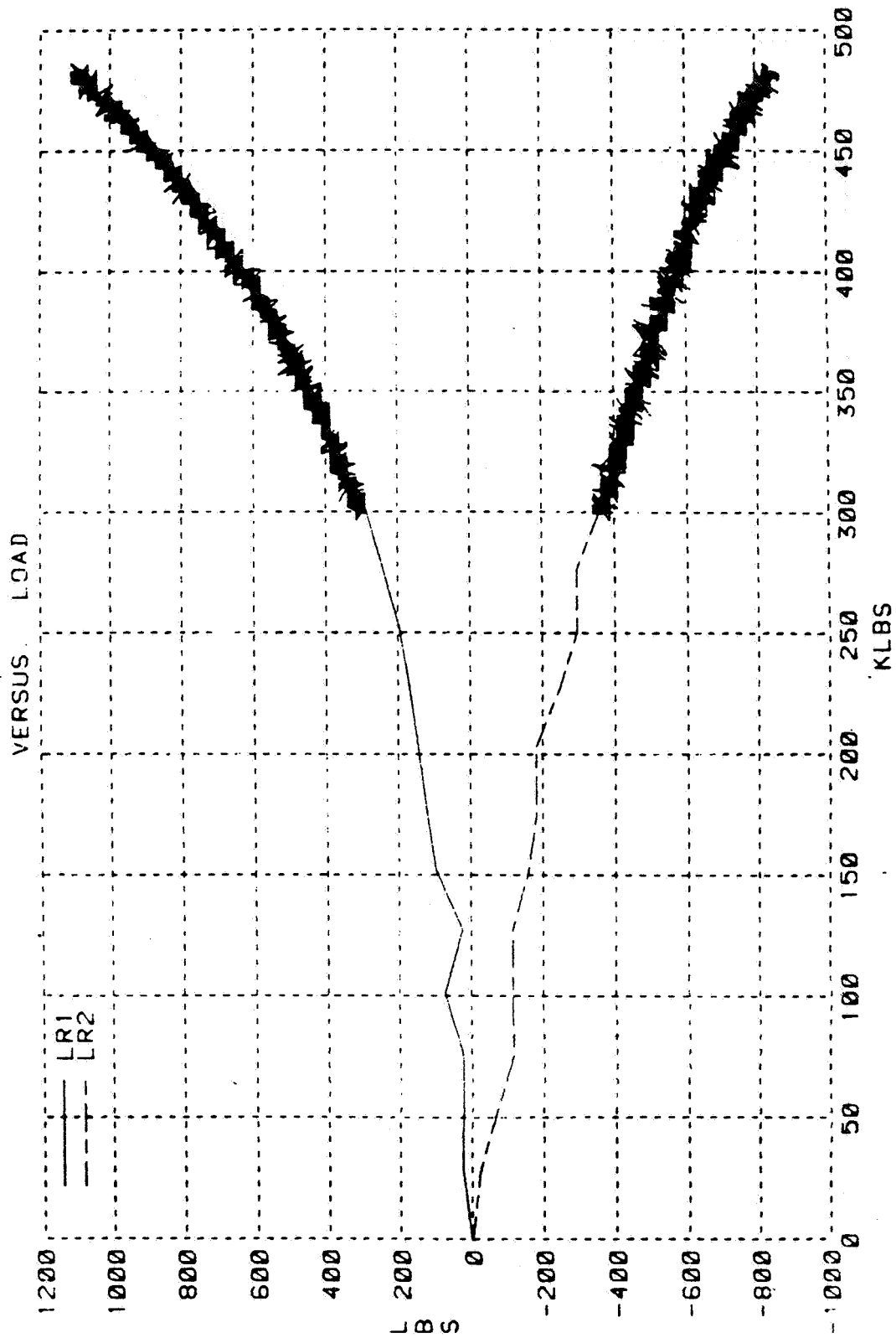
COMPOSITE CRITICAL JOINT DEMONSTRATION TEST #2
 NOV 29, 1984 - BLDG 41 - RAMP TO FAILURE



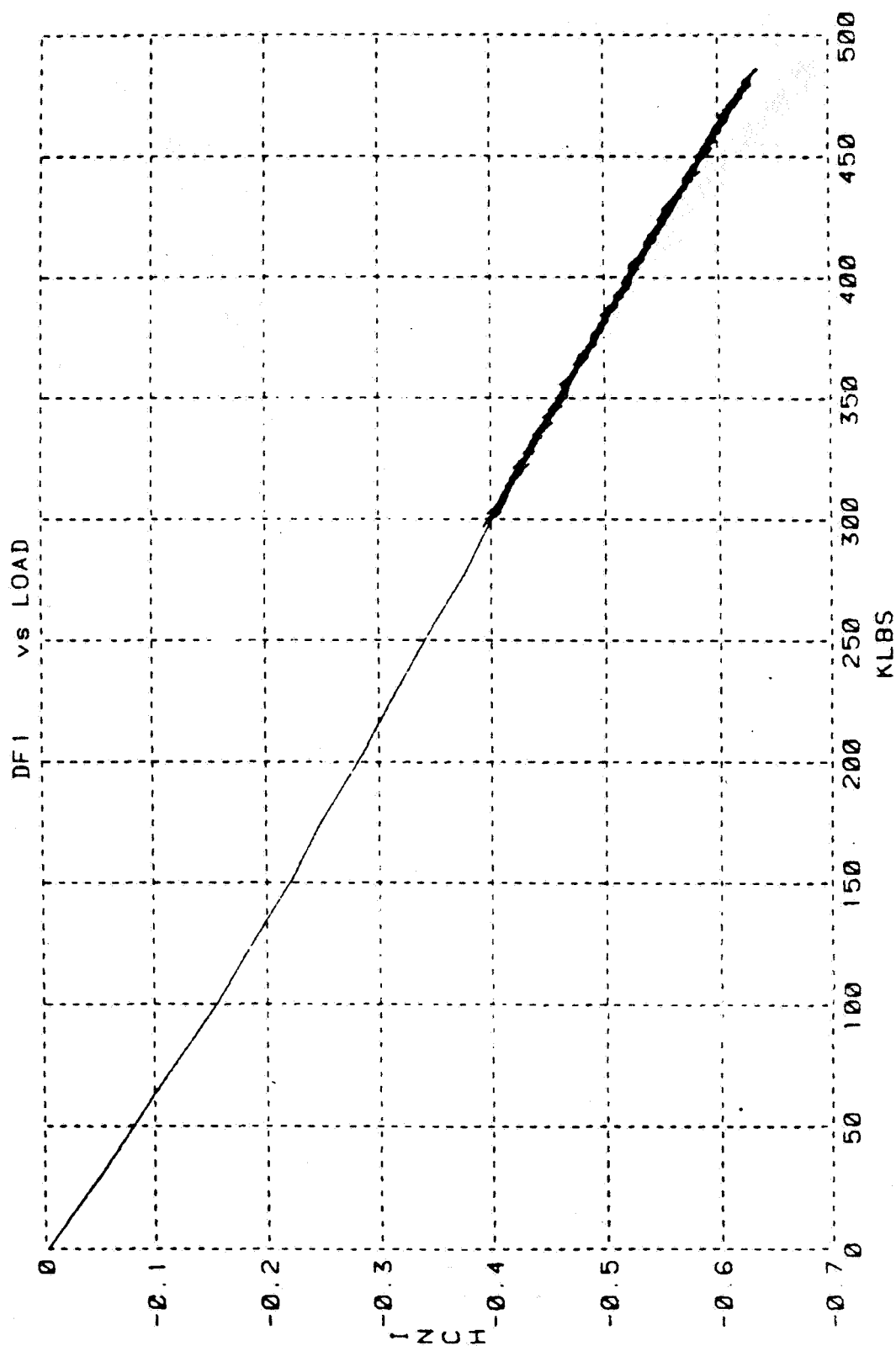
COMPOSITE CRITICAL JOINT DEMONSTRATION TEST #2
 NOV 28, 1984 - BLDG 41 - RAMP TO FAILURE




COMPOSITE CRITICAL JOINT DEMONSTRATION TEST #2
 NOV 29, 1984 - BLDG 41 - RAMP TO FAILURE



COMPOSITE CRITICAL JOINT DEMONSTRATION TEST #2
 NOV 29, 1984 - BLDG 41 - RAMP TO FAILURE



1. Report No. NASA CR-172587		2. Government Accession No.		3. Recipient's Catalog No.	
4. Title and Subtitle Critical Joints in Large Composite Primary Aircraft Structure Volume II - Technology Demonstration Test Program				5. Report Date June 1985	
				6. Performing Organization Code	
7. Author(s) B. L. Bunin				8. Performing Organization Report No. ACEE-26-TR-3478	
				10. Work Unit No.	
9. Performing Organization Name and Address Douglas Aircraft Company 3855 Lakewood Blvd. Long Beach, Ca. 90846				11. Contract or Grant No. NAS1-16857	
				13. Type of Report and Period Covered Contractor Report	
12. Sponsoring Agency Name and Address National Aeronautics & Space Administration Washington, D.C. 20546				14. Sponsoring Agency Code	
15. Supplementary Notes NASA Langley Technical Mointor: Andrew J. Chapman					
16. Abstract A program was conducted at Douglas Aircraft Company to develop the technology for critical structural joints in composite wing structure that meets all the design requirements of a 1990 commercial transport aircraft. This report contains the results of four large composite multirow bolted joint tests. The tests were conducted to demonstrate the technology for critical joints in highly loaded composite structure and to verify the analytical methods that were developed throughout the program. The first test consisted of a wing skin-stringer transition specimen representing a stringer runout and skin splice on the wing lower surface at the side of the fuselage attachment. Two specimens were tested as representative portions of the fourth and final technology demonstration test, which consisted of a large bolted joint representing the lower wing skin and rear spar joint at the side of the fuselage. All tests were static tension tests. The composite material was Toray T-300 fiber with Ciba-Geigy 914 resin in 10 mil tape form. The splice members were metallic, using combinations of aluminum and titanium. This report contains discussions of the test article, instrumentation, test setup, test procedures, and test results for each of the four specimens. Some of the analytical predictions are also included.					
17. Key Words (Suggested by Author(s)) Advanced Composite Structures Bolted Joints Composite Wing Test Results			18. Distribution Statement 		
19. Security Classif. (of this report) Unclassified	20. Security Classif. (of this page) Unclassified	21. No. of Pages 221	22. Price		